

The potential of multimodal neuroimaging to personalize transcranial magnetic stimulation treatment protocols

Citation for published version (APA):

Klooster, D. C. W. (2019). *The potential of multimodal neuroimaging to personalize transcranial magnetic stimulation treatment protocols*. [Phd Thesis 1 (Research TU/e / Graduation TU/e), Electrical Engineering, Ghent University]. Technische Universiteit Eindhoven.

Document status and date:

Published: 13/11/2019

Document Version:

Publisher's PDF, also known as Version of Record (includes final page, issue and volume numbers)

Please check the document version of this publication:

- A submitted manuscript is the version of the article upon submission and before peer-review. There can be important differences between the submitted version and the official published version of record. People interested in the research are advised to contact the author for the final version of the publication, or visit the DOI to the publisher's website.
- The final author version and the galley proof are versions of the publication after peer review.
- The final published version features the final layout of the paper including the volume, issue and page numbers.

[Link to publication](#)

General rights

Copyright and moral rights for the publications made accessible in the public portal are retained by the authors and/or other copyright owners and it is a condition of accessing publications that users recognise and abide by the legal requirements associated with these rights.

- Users may download and print one copy of any publication from the public portal for the purpose of private study or research.
- You may not further distribute the material or use it for any profit-making activity or commercial gain
- You may freely distribute the URL identifying the publication in the public portal.

If the publication is distributed under the terms of Article 25fa of the Dutch Copyright Act, indicated by the "Taverne" license above, please follow below link for the End User Agreement:

www.tue.nl/taverne

Take down policy

If you believe that this document breaches copyright please contact us at:

openaccess@tue.nl

providing details and we will investigate your claim.

The potential of multimodal neuroimaging to personalize transcranial
magnetic stimulation treatment protocols

PROEFSCHRIFT

ter verkrijging van de graad van doctor aan de Technische Universiteit
Eindhoven op gezag van de rector magnificus
prof.dr.ir. F.P.T. Baaijens, voor een commissie aangewezen door het
College voor Promoties, in het openbaar te verdedigen op woensdag
13 november 2019 om 13:30 uur

door

Deborah Cornelia Wilhelmina Klooster

geboren te Geldrop

Dit proefschrift is goedgekeurd door de promotoren en de samenstelling van de promotiecommissie is als volgt:

voorzitter:	prof.dr.ir. P.H.N. de With
1 ^e promotor:	prof.dr. A.P. Aldenkamp
2 ^{de} promotor:	prof.dr. P.A.J.M. Boon (Universiteit Gent)
copromotor:	dr. A.J.A. de Louw
leden:	prof.dr.ir. M. Breeuwer
	prof.dr. R. van Ee (Radboud Universiteit Nijmegen)
	dr. M. Arns (Brainclinics)
	prof.dr. C. Baeken (Universiteit Gent)
adviseurs:	dr.ir. R.M.H. Besseling (Demcon Advanced Mechatronics)
	dr. Evelien Carrette (Universitair Ziekenhuis Gent)

Het onderzoek of ontwerp dat in dit proefschrift wordt beschreven is uitgevoerd in overeenstemming met de TU/e Gedragscode Wetenschapsbeoefening.

The potential of multimodal neuroimaging to personalize transcranial magnetic stimulation treatment protocols

Deborah Cornelia Wilhelmina Klooster

Thesis submitted in fulfillment of the requirements for the degree of doctor (PhD) in
Medical Sciences

To my parents

The potential of multimodal neuroimaging to personalize transcranial magnetic stimulation treatment protocols

Deborah C.W. Klooster

Cover photo: iStock.com, adapted by Deborah Klooster.

Cover design: Deborah Klooster.

Printed by: Gildeprint drukkers.

ISBN 9789-46-32-3901-1

Copyright © 2019 by Deborah Klooster

All rights reserved. No part of this material may be reproduced or transmitted in any form or by any means, electronic, mechanical, including photocopying, recording or by any information storage and retrieval system, without the prior permission of the copyright owners.

Summary

The potential of multimodal neuroimaging to personalize transcranial magnetic stimulation treatment protocols

Globally, approximately 300 million people suffer from mental illness. Major depressive disorder (MDD), one of the most prevalent mental disorders, is a major contributor to the overall global burden of disease. Unfortunately, the current available treatment strategies such as psychopharmacotherapy and psychotherapy are not always efficient; approximately 30% of the MDD population can be considered as treatment-resistant. Therefore, additional treatment options to alleviate depressive symptoms should be investigated.

Transcranial magnetic stimulation (TMS) is a non-invasive brain stimulation technique that is based on the principles of electromagnetic induction. A time-varying electric current is sent through a coil that is placed tangentially to the scalp. A magnetic field is induced perpendicular to the coil and will traverse the scalp and skull into the brain. Subsequently, an electric field is induced in the superficial cortex. This field can modulate neuronal activity. The effect of repetitive application of pulses (rTMS) outlasts the actual duration of the stimulation. This makes rTMS a promising treatment option for various neurological and psychiatric disorders. rTMS is FDA approved for the treatment of MDD but the current response and remission rates remain rather modest. Also, there is a large inter-individual variability in these response and remission rates. This could partly be explained by the lack of knowledge about the exact mechanisms of action and this could also be attributed to the application of too general rTMS protocols for a broad patient-population.

Although the focus of this thesis is on TMS, it has to be noted that this is not the only brain stimulation technique. A broad overview of all invasive and non-invasive brain stimulation techniques is given in **Chapter 3**. Deep brain stimulation and vagus nerve stimulation are effective invasive stimulation techniques and TMS and transcranial direct current stimulation are the most commonly used non-invasive methods. Insight into the technical basis of brain stimulation might be a first step towards a more profound understanding of the mechanisms of action.

Standard rTMS guidelines to treat MDD typically follow a daily stimulation pattern repeated over 4-6 weeks. Accelerated intermittent theta burst stimulation (aiTBS) is a relatively new stimulation protocol, aimed to further improve clinical efficacy, in which stimuli are applied in a vast pattern (3 stimuli at 50Hz, repeated every 200ms, 2s stimulation alternated with 6 or 8s rest). Instead of single rTMS sessions over multiple days, the aiTBS protocol contains 5 daily stimulation sessions on 4 consecutive days. **Chapters 4-6** are based on a double-blind, randomized, sham-controlled, cross-over aiTBS study. Fifty MDD patients were randomized to receive first active then sham stimulation, or the other way around. Both sham and active stimulation were applied to the left dorsolateral prefrontal cortex (DLPFC) at 110% of the resting motor threshold (rMT) with a figure-of-eight shaped coil. At baseline, and after both stimulation sessions, MRI data was recorded with a 3 Tesla scanner. The MRI acquisition protocols contains anatomical scanning, resting-state functional MRI (rs-fMRI) and diffusion weighted imaging (dMRI). At similar time-points, and additionally after two weeks during follow-up, clinical well-being was tested using the 17-item Hamilton Depression Rating Scale questionnaire.

Specifically, the effects of aiTBS on resting-state functional connectivity (rsFC) on a network level by means of graph theory were studied in **Chapter 4**. The rs-fMRI data were parcellated into 264 parcels, further referred to as nodes. Graph parameters were calculated on whole brain level, including all the nodes, and within the single nodes. Baseline data and data after the first stimulation session were used such that the differences between sham and active stimulation could be investigated. Although no differences were observed between the effects of sham and active stimulation on whole brain graph parameters and changes in graph measures did not correlate with clinical response, the baseline clustering coefficient and global efficiency showed to be significantly correlated with the clinical response to aiTBS. Nodal effects were found throughout the brain. The spatial distribution of these nodal effects could not directly be linked to the rsFC map derived from group-connectome data.

The same rs-fMRI datasets were used in **Chapter 5** for a methodological study into modeling approaches of the local effects of TMS and their effects on functional connectivity analyses. Here, regressors were compared from 2 seeding methods based on a simple cone model and a more complex model derived from TMS-induced electric field (Efield) distributions. The regressors and resulting rsFC maps from both seeding methods were compared. Because of the overall high correlations between cone- and Efield-regressors, computational complexity of the TMS-induced electric field simulations, and the lack of the golden standard, the cone model was stated to be reliable to derive regressors for rsFC analyses to study the effects of TMS.

Chapter 6 describes the first attempt within the scientific world to derive parameters from dMRI data that are predictive for the clinical response to aiTBS. Because earlier work showed that the clinical effects of aiTBS treatment may have a delayed onset, the study investigated prediction of the delayed clinical response, measured two weeks after the stimulation protocol. The focus in this study was on the structural connections between the stimulation position in the left DLPFC and the cingulate cortex. The Desikan-Killiany

parcellation scheme was used to split the dMRI data into 89 nodes and compute the structural connections between pairs of nodes. An important finding was the absence of direct structural connections between the stimulation site and the cingulate cortex. However, indirect connections with up to two internodes, between the stimulation site and the right caudal and left posterior part of the cingulate cortex were significantly correlated with the clinical response to aiTBS. These findings suggest that baseline structural connectivity may be of essence for the clinical response to aiTBS in MDD patients.

A more fundamental study is described in **Chapter 7**. The propagation of TMS pulses in terms of the brain's intrinsic rsFC was investigated. Ten datasets from the Berenson-Allen Center for Noninvasive Brain Stimulation were used in which TMS was applied during EEG. Approximately 100 single TMS pulses were applied to six stimulation sites: the DLPFC, motor cortex, and parietal cortex bilaterally. EEG source imaging was performed on the TMS-evoked potentials (TEPs). The TEPs in source space were quantified by the root mean square in the time-intervals between 15 and 400 ms after the pulse. Additionally, the interval between 15 and 75 ms was separately studied since this period is thought to be less affected by sham effects. The quantified TEPs were correlated with the rsFC maps, derived from group-connectome data with the subject-specific stimulation position as seed. On the group level, significant correlations were found between the quantified TEPs and rsFC strength after stimulating motor areas, in both time-intervals. This suggests that the propagation of TMS pulses follows the pattern of the subject's intrinsic rsFC, at least when stimulating the motor cortex.

Within this thesis, we have shown various applications of neuroimaging techniques to gain more understanding about the mechanism of action of TMS. Knowledge about potential importance of structural connections (**Chapter 6**) and the propagation of effects via rsFC (**Chapter 4** and **Chapter 7**) might be translated into subject-specific optimal coil positioning. Besides the coil position, also other parameters can be subject for personalization such as the stimulation intensity and the timing and frequency of the stimulation. A potential route towards personalization of stimulation protocols is discussed in **Chapter 8** with the focus on the possible role of multimodal neuroimaging techniques.

The actual stimulation target might be a deep brain region that can only be reached indirectly via structural and functional connections. The optimal patient-specific cortical stimulation position might be derived from individual rs-fMRI and dMRI data. Electric field models, using individual head models derived from anatomical and dMRI data, can help to guide the coil position to optimally target the preferred cortical area. The stimulation intensity is derived from the rMT, since the output of motor cortex stimulation can be measured with motor evoked potentials. Intensity for stimulation at other locations beyond the motor cortex might benefit from correction methods that use the variation in coil-cortex distance. This can be derived from anatomical MRI. The response to stimulation is also dependent on the brain state during the application of stimuli. Timing of the stimulation might be optimized by using real-time EEG information, which can inform about the state of excitability. Moreover, the frequency of the stimulation could be adapted to the patient's intrinsic brain rhythms.

Using information from neuroimaging to obtain patient-specific brain stimulation protocols might decrease the inter-individual variability and potentially also increase the overall clinical effectiveness.

Samenvatting

Het potentieel van multimodale neuro-imaging om behandelprotocollen van transcraniële magneetstimulatie te personaliseren

Wereldwijd lijden ongeveer 300 miljoen mensen aan een mentale ziekte. Depressie is een van de meest voorkomende mentale ziektes en vormt daardoor een grote last voor de maatschappij. Helaas zijn huidige behandelstrategieën zoals met behulp van psychopharmacotherapie en psychotherapie niet altijd effectief. Ongeveer 30% van de depressie patiënten is behandelings-resistent. Daarom is het van belang om nieuwe behandelmethodes te onderzoeken die de depressieve symptomen kunnen verminderen.

Transcraniële magneetstimulatie (TMS) is een niet-invasieve hersenstimulatie techniek die is gebaseerd op de principes van elektromagnetische inductie. Een tijdsvariërende elektrische stroom wordt door een spoel gestuurd die tangentieel tegen het hoofd is geplaatst. Hierdoor wordt een magnetisch veld geïnduceerd, loodrecht op de spoel, wat door de schedel het brein binnen gaat. Dit veroorzaakt een kleine elektrische stroom in de oppervlakkige lagen van de cortex dat neuronale activiteit kan beïnvloeden. Het effect van het repetitief aanbieden van pulsen (rTMS) houdt langer aan dan de periode waarin gestimuleerd wordt. Hierdoor is rTMS een veelbelovende behandelmethode voor een breed scala van neurologische en psychiatrische aandoeningen. Ondanks dat rTMS een goedgekeurde behandeling is voor depressie blijft het aantal responders en remitters bescheiden. Er is een grote inter-individuele variatie in deze responder en remitter aantallen. Dit kan gedeeltelijk veroorzaakt worden door de missende kennis van de werkingsmechanismen en door het gebruiken van te algemene stimulatie protocollen voor een brede patiëntpopulatie.

Deze thesis focust op TMS, maar dit is niet de enige hersenstimulatie techniek. **Hoofdstuk 3** geeft een breed overzicht van alle invasieve en niet-invasieve stimulatie technieken. Diepe hersenstimulatie en nervus vagus stimulatie zijn effectieve invasieve hersenstimulatie technieken. TMS en transcraniële directe stroom stimulatie zijn de meest gebruikte niet-invasieve methoden. Inzicht in de technische basis van deze hersenstimulatie tech-

nieken kan een eerste stap zijn om de werkingsmechanismen beter te begrijpen.

Volgens de standaard rTMS richtlijnen voor behandeling van depressie vindt de behandeling plaats volgens een dagelijks patroon wat wordt herhaald gedurende een periode van 4 tot 6 weken. Accelerated intermittent theta burst stimulatie (aiTBS) is een relatief nieuw stimulatie protocol, bedoeld om de klinische effectiviteit te vergroten, waarin stimuli in een bepaald patroon aangeboden worden (3 stimuli op 50Hz, herhaald elke 200ms, 2s stimulatie afgewisseld met 6 of 8s rust). In plaats van een enkele dagelijkse stimulatiesessie over langere periodes, omvat aiTBS 5 dagelijkse stimulatiesessies gedurende 4 aaneengesloten dagen. **Hoofdstuk 4 - 6** zijn gebaseerd op een gerandomiseerde, geblindeerde, sham-gecontroleerde, cross-over aiTBS studie. Vijftig depressie patiënten werden gerandomiseerd om eerst actieve en dan sham stimulatie te ondergaan, of andersom. Zowel actieve als sham stimulatie werd gegeven met een intensiteit van 110% van de motor threshold tijdens rust (rMT) en stimulatie werd toegediend aan de linker dorsolaterale prefrontale cortex (DLPFC) met een figuur-8 spoel. MRI data werd opgenomen voordat de stimulatie begon, en na beide stimulatie sessies met een 3 Tesla MRI scanner. Het MRI acquisitie protocol omvatte anatomische beeldvorming, resting-state functionele MRI (rs-fMRI) en diffusie gewogen MRI (dMRI). Op dezelfde tijdstippen, en 2 weken na de stimulatie tijdens de follow-up fase, werd het klinisch welbevinden gemeten aan de hand van de 17-item Hamilton Depression Rating Scale vragenlijst.

In **Hoofdstuk 4** zijn de effecten van aiTBS op resting-state functionele connectiviteit (rsFC) op netwerk level bestudeerd met behulp van graaf-analyse. De rs-fMRI data werd gesplitst in 264 gebiedjes, ook wel nodes genoemd. Graaf-parameters werden berekend voor het volledige brein, waarbij alle nodes geïnccludeerd werden, en voor de nodes apart. Data van voor en na de eerste stimulatie sessie werden gebruikt om specifiek naar de verschillende effecten van sham and actieve stimulatie te kijken. Ondanks dat er geen verschillen gevonden werden tussen de effecten van actieve en sham stimulatie in graaf-parameters afgeleid van het volledige brein en dat veranderingen in deze graaf-parameters niet significant gecorreleerd waren met de klinische response, vonden we wel een significante correlatie tussen de cluster coëfficiënt en de globale efficiëntie en de klinische response. Verschillende effecten van sham en actieve stimulatie werden gevonden in meerdere nodes verspreid door het brein. De spatiële distributie van deze nodes kon niet direct gelinkt worden aan de rsFC maps die werden afgeleid van group-connectome data.

Dezelfde rs-fMRI datasets werden gebruikt in **Hoofdstuk 5** voor een methodologische studie naar het effect van verschillende modelleer-methoden van de locale effecten van TMS op de functionele connectiviteit. In deze studies zijn 2 *seed*-methoden vergeleken gebaseerd op het relatief gemakkelijke kegel-model en een complexer model dat afgeleid is van TMS-geïnduceerde elektrische velden (Eveld) in het brein. De regressors en resulterende rsFC maps van beide *seed*-methoden zijn vergeleken. Vanwege de hoge correlaties tussen de regressors afgeleid van beide methoden en de resulterende rsFC maps, de complexiteit van het bepalen van de TMS-geïnduceerde elektrische velden, en het ontbreken van een gouden standaard, hebben we hier geconcludeerd dat het kegel-model betrouwbaar is voor het afleiden van regressors voor rsFC analyses om het effect van TMS te bestuderen.

Een eerste poging binnen de wetenschappelijke wereld om parameters af te leiden van dMRI data die de klinische response van aiTBS kunnen voorspellen is beschreven in **Hoofdstuk 6**. Vanwege een eerdere bevinding dat klinische effecten van aiTBS een vertraging zouden hebben, is hier gekeken naar de voorspelling van het zogenaamde vertraagde klinische effect, gemeten 2 weken na het einde van de daadwerkelijke stimulatie sessies. De focus van deze studie was op de structurele verbindingen tussen de stimulatie positie in de linker DLPFC en de cingulate cortex. Het Desikan-Killiany parcellatie schema werd gebruikt om de dMRI data te splitsen in 89 nodes en om de structurele verbindingen te berekenen tussen alle node-paren. Een belangrijke bevinding was het ontbreken van directe verbindingen tussen de stimulatie positie en de cingulate cortex. Echter, indirecte verbindingen met 1 of 2 internodes tussen de stimulatie positie en het rechter caudale en linker posterieure deel van de cingulate cortex waren significant gecorreleerd met de vertraagde klinische response. Dit suggereert dat structurele verbindingen van belang zijn voor de klinische response van aiTBS in depressie patiënten.

Een meer fundamenteel onderzoek is beschreven in **Hoofdstuk 7**. Hierin wordt de propagatie van TMS pulses bestudeerd in termen van de intrinsieke rsFC binnen het brein. Tien datasets van het Berenson-Allen Center for Noninvasive Brain Stimulation zijn gebruikt waarin TMS toegediend werd tijdens EEG registratie. Ongeveer 100 enkelvoudige TMS pulsen werden gegeven op 6 posities: de DLPFC, de motor cortex, en de pariëtale cortex aan beide kanten. EEG bronlokalisatie werd toegepast op de *TMS-evoked potentials*. De TEPs in bronruimte zijn gekwantificeerd door middel van de root mean square maat in het tijdsinterval van 15 tot 400ms na de pulse. Daarnaast is het interval tussen 15 en 75ms apart bestudeerd omdat dit minder sham artefacten bevat. De gekwantificeerde TEPs werden gecorreleerd met rsFC maps, afgeleid van groep-connectome data waarbij de specifieke stimulatie locaties van elke subject gebruikt werden als *seed*. Op groepsniveau vonden we een significante correlatie tussen de gekwantificeerde TEPs en rsFC na het stimuleren van de motor cortices aan beide zijden. Dit suggereert dat de propagatie van TMS pulsen het patroon van de functionele connecties in het brein volgt.

In deze thesis zijn verschillende applicaties van neuro-imaging aan bod gekomen waarmee de huidige kennis over het werkingsmechanisme van hersenstimulatie vergroot zou kunnen worden. Kennis met betrekking tot het belang van structurele connecties (**Hoofdstuk 6**) en de propagatie van effecten van stimulatie via functionele verbindingen (**Hoofdstuk 4** en **Hoofdstuk 7**) zouden vertaald kunnen worden naar een patiënt-specifieke optimale spoel positie. Daarnaast zouden ook andere stimulatie parameters gepersonaliseerd kunnen worden zoals de intensiteit en de timing en frequentie van de pulsen. Een mogelijke weg om hersenstimulatie protocollen te personaliseren is beschreven in **Hoofdstuk 8**, waarbij gefocust wordt op de mogelijke rol van multimodale neuro-imaging.

Het daadwerkelijk te stimuleren gebied is mogelijk een dieper gelegen hersengebied dat enkel indirect bereikt kan worden via structurele of functionele verbindingen. De optimale patiënt-specifieke corticale stimulatie positie zou mogelijk afgeleid kunnen worden van individuele rs-fMRI en dMRI data. Simulaties van het door TMS-geïnduceerde elektrische veld, waarbij gebruik wordt gemaakt van individuele hoofdmodellen afgeleid van

anatomische en dMRI, dragen mogelijk bij aan het bepalen van de spoel positie op het hoofd om de corticale target optimaal te stimuleren. De stimulatie intensiteit wordt afgeleid van de rMT, omdat de response van motor cortex stimulatie direct gemeten kan worden met *motor evoked potentials*. De intensiteit voor stimulatie van andere locaties buiten de motor cortex zou voordeel kunnen hebben van correctie-methodes gebaseerd op de variaties in de afstand tussen de spoel en de cortex in verschillende hersengebieden. De spoel-cortex afstand kan bepaald worden met anatomische MRI data. Daarnaast heeft gebleken dat de response van stimulatie afhankelijk is van de status van het brein tijdens de stimulatie. De precieze timing van de stimulatie zou geoptimaliseerd kunnen worden met behulp van real-time EEG informatie, wat informatie kan verschaffen over de exciteerbaarheid van het brein. Ook zou de frequentie van de pulsen aangepast kunnen worden aan de individuele frequentie van de brein-oscillaties.

Door gebruik te maken van neuro-imaging kunnen stimulatie protocollen gepersonaliseerd worden. Dit zou mogelijk kunnen leiden tot een vermindering in de inter-individuele variabiliteit in de response op hersenstimulatie en zou ook kunnen zorgen voor een verhoging van de klinische effectiviteit.

Contents

Summary	i
Samenvatting	v
1 General introduction and outline of the thesis	1
1.1 Introduction	3
1.2 Brief historical overview	4
1.3 Basic characteristics of transcranial magnetic stimulation	4
1.4 Problem description	7
1.5 Thesis outline	8
2 Neuroimaging to predict and study the effects of TMS	11
2.1 MRI	13
2.1.1 Functional MRI	14
2.1.2 Combining fMRI and TMS	16
2.1.3 Diffusion MRI	17
2.1.4 Combining dMRI and TMS	19
2.2 EEG	20
2.2.1 EEG source imaging	21
2.2.2 Combining EEG with TMS	22
3 Technical aspects of neurostimulation: Focus on equipment, electric field modeling, and stimulation protocols	23
Abstract	24
3.1 Introduction	25
3.2 Non-invasive neurostimulation	25
3.2.1 Transcranial magnetic stimulation (TMS)	26
3.3 Summary of technical aspects of TMS	40
3.3.1 Transcranial direct current stimulation (tDCS)	41
3.3.2 Summary of technical aspects of tDCS	45
3.4 Invasive neurostimulation	46
3.4.1 Vagus nerve stimulation (VNS)	46
3.4.2 Deep brain stimulation (DBS)	50
3.4.3 Alternative stimulation techniques	58

3.4.4	Discussion on neurostimulation	60
4	Focal application of accelerated iTBS results in global changes in graph measures	65
	Abstract	66
4.1	Introduction	67
4.2	Methods	69
4.2.1	Inclusion criteria	69
4.2.2	Data acquisition	70
4.2.3	Graph analysis	71
4.2.4	Statistical analysis	73
4.2.5	Spatial distribution	73
4.2.6	Biomarker investigation	73
4.3	Results	73
4.3.1	Whole brain network topology changes	74
4.3.2	Changes in nodal graph measures	74
4.3.3	Propagation of effect via functional connections	75
4.3.4	Potential of graph measures as biomarker	76
4.4	Discussion	79
4.4.1	The effect of aiTBS on graph measures	80
4.4.2	Spatial distribution of aiTBS effects	81
4.4.3	Graph measures as biomarker	82
4.4.4	General limitations	83
4.5	Conclusion	83
4.6	Appendices	84
4.6.1	Additional information on preprocessing	84
4.6.2	Graph parameter overview	85
4.6.3	Full overview of correlations between changes in graph measures and changes in clinical well-being in nodes showing significant effects of stimulation	88
5	Modeling local effects of transcranial magnetic stimulation for functional connectivity analyses	89
	Abstract	90
5.1	Introduction	91
5.2	Methods	92
5.2.1	Study protocol	92
5.2.2	MRI data acquisition	93
5.2.3	Data analysis	93
5.2.4	Regressor derivation	93
5.2.5	Effects of seeding method on FC	94
5.2.6	The effect of the exact stimulation location	95
5.3	Results	96
5.3.1	Correlation between different regressors	96
5.3.2	Whole brain FC	97
5.3.3	FC between the DLPFC and the sgACC	97
5.3.4	Effect of stimulation position	97
5.4	Discussion	99
5.4.1	Potentials and pitfalls of using electric field modeling	100
5.4.2	The cone model	100
5.4.3	Cone versus electric field simulations	101
5.4.4	Knowledge of the exact stimulation position	101
5.5	Conclusion	102

6	Indirect frontocingulate structural connectivity predicts clinical response to accelerated rTMS in major depressive disorder	103
	Abstract	104
6.1	Introduction	105
6.2	Methods	106
6.2.1	Patient inclusion	106
6.2.2	Study protocol	106
6.2.3	Analysis pipeline	107
6.2.4	Fiber paths of interest	108
6.2.5	Quantification of structural connectivity	110
6.2.6	Specificity to frontocingulate structural connectivity	110
6.2.7	Group analysis	111
6.2.8	Statistics	111
6.3	Results	112
6.3.1	Structural pathways between the left DLPFC and the cingulate cortices	112
6.3.2	Significant correlations between structural connectivity and clinical response	112
6.3.3	Clinical response prediction based on whole brain and nodal structural connectivity metrics	113
6.3.4	Results using group depression connectome	113
6.4	Discussion	114
6.4.1	Biomarkers derived from individual data vs group connectome data	116
6.4.2	Study limitations	116
6.5	Conclusion	118
6.6	Supplementary materials	119
6.6.1	Group connectome generation	119
6.6.2	Distribution of internodes connecting the stimulation position in the left DLPFC to any of the ROIs in the cingulate cortex	119
6.6.3	Direct versus indirect structural connections between the stimulated area in the left DLPFC and the cingulate cortex	122
6.6.4	Prediction of the immediate clinical effects	123
6.6.5	Specificity to frontocingulate structural connectivity	126
7	Stimulation propagation versus functional connectivity	129
	Abstract	130
7.1	Introduction	131
7.2	Methods	133
7.2.1	TMS-EEG protocol	133
7.2.2	rsFC maps	134
7.2.3	Brain parcellation	135
7.2.4	Statistics	136
7.3	Results	136
7.3.1	EEG source localization	138
7.4	Discussion	140
7.4.1	Clinical interpretation	141
7.4.2	Inter-individual variability	141
7.4.3	Methodological considerations	142
7.5	Conclusion	142
8	General discussion: The route towards personalized rTMS protocols for depression	145
8.1	General discussion	147
8.1.1	TMS targeting	148

CONTENTS

8.1.2	Stimulation intensity	152
8.1.3	Stimulation timing and frequency	153
8.2	Personalized brain stimulation protocols	154
8.2.1	Future efficient TMS treatment	155
8.3	Conclusion	158
Bibliography		159
Publication List		187
Acknowledgements		191
Curriculum Vitae		197

*"We have little idea at present of the importance
they may have ten or twenty years hence."
Michael Faraday*

CHAPTER **1**

General introduction and outline of the thesis

1.1 Introduction

Globally, over 300 million people suffer from mental health disorders according to the World Health Organization (WHO) (*WHO factsheet: Depression* 2018). Amongst these disorders is depression; one of the oldest, well-recognized medical disorders. Depression is diagnosed according to the Diagnostic and Statistical Manual of Mental Disorders (DSM) 5, when at least 5 out of 9 symptoms are present for more than two weeks. These symptoms include abnormalities in mood, anhedonia, weight gain or loss without clear cause, abnormal sleep patterns, psychomotor hyperactivity or retardation, tiredness, persistent feelings of worthlessness, loss of focus, and suicidal thoughts. Classic severe states of depression have no external precipitating cause (Belmaker and Agam, 2008). Since a patient should report at least 5 out of 9 symptoms this allows for several hundred unique combinations of clinical symptoms, making depression a very heterogeneous disorder. Moreover, depression is a disorders that affects people from all ages. Patients who have the first depression episode during childhood or adolescence typically continue to suffer from episodes during adulthood as well. Depression is often a life-long disorder with multiple recurrences (Fava and Kendler, 2000). It is a major contributor to the overall global burden of disease.

There are treatment options for moderate and severe depression such as psychotherapy and pharmacotherapy by means of anti-depressant medication. Psychotherapy consists of talking sessions with a trained mental health care professional, i.e. psychologist or psychiatrist, who helps the patient to identify and work through factors that may trigger the depression symptoms. Currently, numerous anti-depressants are available. The most optimal medication for an individual patient is not known so often several sequential treatment steps are tried in order to obtain remission. The acute and longer term outcomes of depression treatment by means of anti-depressant medication were investigated in the Sequenced Treatment Alternatives to Relieve Depression (STAR*D) trial (Rush et al., 2006). The Hamilton Depression Rating Scale (HDRS) (Hamilton, 1967) can be used to determine a patient's level of depression, before, during, and after treatment. A Hamilton-score higher than 7 indicates depressed state. Remission from depression is therefore often classified by a Hamilton score smaller than or equal to 7. The most currently used definition of responder is a minimum change of 50% of the initial HDRS score. The STAR*D trial showed that first two treatment attempts led to remission rates of 36.8% and 30.6%. Remission rates after two additional treatment attempts was only 13.7% and 13%. So even after 4 treatment attempts, 33% of the subjects did not respond to consecutive anti-depressant medication trials. Greater illness burden was furthermore characteristic of those who required more treatment steps.

Given these limitations of pharmacotherapy and psychotherapy, transcranial magnetic stimulation (TMS) might be an important additional treatment arm to increase remission rates in patients with medication resistant depression (MDD), but also for a broader variety of mental health disorders.

1.2 Brief historical overview

The discovery of bioelectricity already dates back to the late eighteenth century. The link between nervous tissue and electricity was found by the Italian physician Luigi Galvani. He observed muscle twitches in the leg of a dead frog during dissection when struck with an electric spark. Probably the most important and crucial finding in the history that led to the invention of the current TMS systems is the discovery of electromagnetic induction by the English physicist Michael Faraday in 1831. Electromagnetic induction is a process in which electricity converts into magnetism and vice versa. Thirty years later, in 1861, the Scottish physicist and mathematician James Clerk Maxwell provided the unifying proof for the reciprocal relation between electricity and magnetism. The first attempts to use Faraday's principles to alter brain activity were performed by Arsenne d'Arsonval in 1896 and Silvano Thompson in 1910. Both physicists independently reported about the induction of phosphenes, a sensation of a ring or spot of light produced by stimulation of the visual system other than by light, in subjects who placed their head into a coil through which alternating currents were sent.

The technical problems of generating the large-peak magnetic field strengths and rates of change of magnetic field necessary to cause stimulation became apparent. It was not until 1976 that Anthony Barker and his group at the University of Sheffield solved many of the earlier technical problems and developed a device capable of generating peak fields of 2 Tesla with an approximate rise time of 100 μ s. With this device the velocity selective stimulation of peripheral nerves could be performed, which led to publication in 1979 (Barker, Brown, and Freeston, 1979). Later in 1982, Polson, Barker, and Freeston described the design of a stimulator proven to be effective for peripheral nerve stimulation (Polson, Barker, and Freeston, 1982). Subsequently, in 1985 TMS was introduced for the first time by Barker and colleagues, as a non-invasive brain stimulation technique that uses the principles of electromagnetic induction to focus currents in the brain and modulate the function of the cortex (Barker, Jalinous, and Freeston, 1985).

1.3 Basic characteristics of transcranial magnetic stimulation

The introduction of the TMS system in 1985 by Barker et al. (1985) has led to various commercially available systems through various companies. TMS was the new tool to unravel unknown brain behaviour. The basic characteristics can be seen in Figure 1.1. In short, a magnetic stimulator stores electrical current and discharges this into a TMS coil which is placed tangentially to the subject's scalp. This excitation current can reach values up to 8 kA. The discharge time, also called pulse duration, is usually less than 1 ms. The time-varying current in the coil induces a strong, but also very brief and rapidly changing magnetic field. Since this magnetic field is perpendicular to the coil and is able to traverse the scalp and skull without impedance, an electric field is induced in the underlying brain tissue. The maximum TMS-induced electric field strengths in the brain are typically around 100 V/m. Note that even though TMS is named after the magnetic field, it is the induced electric field that leads to actual neuronal stimulation.

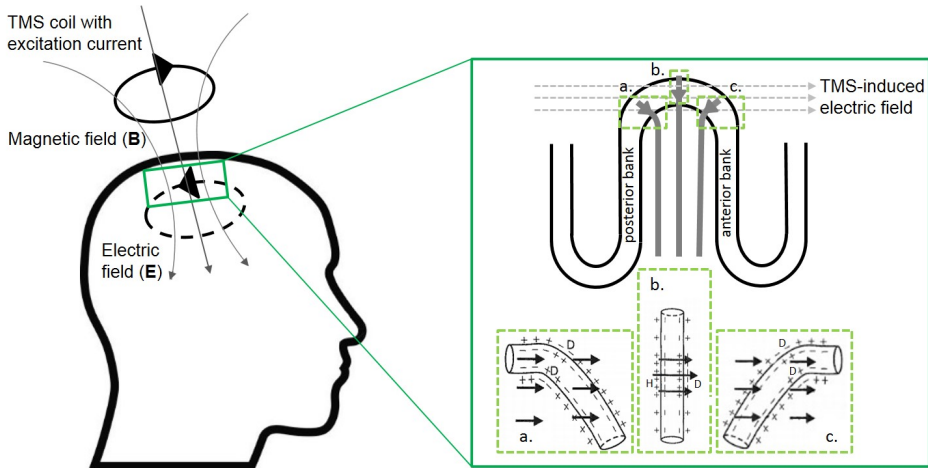


Figure 1.1 — The basic characteristics of TMS. A time-varying current is sent through a coil that is placed tangentially to a subject's scalp. According to Faraday's law, a magnetic field is induced perpendicular to the coil and traverses the scalp and skull without impedance. Subsequently, a small electric field is induced in the superficial layers of the cortex that interfere with the neuronal activity. The activation function states that induced neuronal activity depends on the spatial gradient of the electric field along the neuron. Therefore, it is thought that mostly the pyramidal neurons in the sulcal walls that bend within the electric field (a. and c.), and therewith cause a transmembrane potential, are the responders to TMS. The pyramidal neurons in the gyral crown are mostly perpendicular to the TMS-induced electric field. Only a gradient in the electric field along the neuron would induce neuronal activation.

The magnetic field strength decreases quadratically with distance. Therefore, the TMS-induced electric field mostly interferes with neurons in the superficial regions of the cortex. To produce neuronal activity, the electric field must differ across the cell membrane. If the field is uniform with respect to the cell membrane, no current will be induced. The activation function is the spatial derivative of the electric field along the nerve membrane (Walsch and Pascual-Leone, 2003). The axon must either be bent across a uniform electric field or a non-uniform field must traverse an unbent axon. Considering the well-established knowledge about the columnar neuronal orientation and functional organization of the cerebral cortex, it can be assumed that the axons in the sulcal wall are subject of stimulation. An example of the interference between neurons and TMS-induced electric fields can be seen in Figure 1.1. In the top of the gyral crowns, the pyramidal neurons are perpendicular to the electric field. If the field is constant in that area, these neurons will not be activated. Only if there is a gradient in the electric field along with the direction of the neuron, neuronal activation can be induced (Figure 1.1b.). However, a great preponderance of pyramidal neurons is located in the sulcal walls, aligned with the TMS-induced electric fields but deep within the brain. The bending neurons in the sulcal wall (shown in Figure 1.1a and c) cause a change in transmembrane potential. The direction of the induced current is often defined to be perpendicular to the gyrus (for example 45° with the anteroposterior plane in case of motor cortex stimulation) and defines if pyramidal neurons in the anterior or posterior bank are mostly activated (orthodromic vs antidromic

activation). Note that there also exist horizontal interneurons and collaterals of pyramidal neurons in the gyrus crown which align perfectly with the TMS-induced electric field. Initially, they were thought to be the main responders to TMS (Day et al., 1989). However, these neurons are isotropically distributed and could therefore not explain the orientation dependent effects of TMS (Brasil-Neto et al., 1992).

The shape of the TMS-induced electric fields in the brain highly depends on the type of stimulation coil that is used and the interaction of the fields with the underlying brain geometry. TMS coils are usually made of tightly wound concentric turns of copper wire, which are adequately insulated and housed in plastic covers. In clinical practice, a round coil and a figure-of-eight coil are the most commonly used coil shapes (Figure 1.2). As the name implies, the round coil consists of circular wiring and the TMS-induced electric field within the brain is located under the coil winding. In contrast to the round coil, the figure-of-eight coil is assumed to be a focal (though still in the order of cm) stimulation coil. Two round coils are connected so that the current in one coil runs opposite to the current in the other coil. The advantage of this configuration is that the electric field from the two windings add up at the crossing. This results in an electric field under the centre of the figure-of-eight coil. Therefore, stimulation is more likely to occur at the center of the coil.

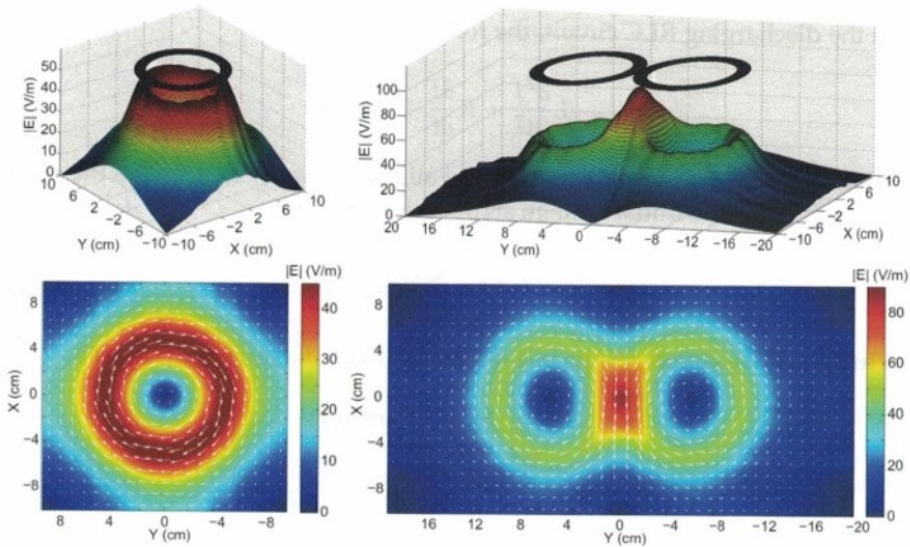


Figure 1.2 — Simulation of the TMS-induced electric field distributions by a round coil and a figure-of-eight coil (shown in black in the upper plots), by De Geeter (De Geeter, 2015). As can be seen, the figure-of-eight coil induces a more focal and stronger electric field under the crossing of the two windings.

TMS can be applied as one stimulus at a time (single pulse stimulation) or as trains of repetitive stimuli (rTMS) delivered at a fixed frequency or according to a certain

paradigm. Especially with single pulse paradigms (also including paired-pulse studies) brain functioning can be studied (Klomjai, Katz, and Lackmy-Vallée, 2015). The effects of rTMS showed to outlast the actual duration of the stimulation, thereby making rTMS a potential treatment option for a broad variety of neuropsychiatric disorders (Klooster et al., 2016). TMS is considered safe in humans and there are guidelines for appropriate application of stimulation protocols (Rossi et al., 2009). However up till now, rTMS is only FDA and CE approved as treatment for medication resistant MDD and obsessive compulsive disorder (OCD).

1.4 Problem description

The first rTMS trials in MDD showed promising decreases in HDRS (Pascual-Leone et al., 1996; Nahas et al., 2003). However, Nahas et al. (2003) also found clinical improvement after sham stimulation. Results are often reported on the group level. On the individual level, rTMS has shown to be beneficial in some patients, for others it does not help. There is a high inter-, but also intra-, individual variability in clinical responses which causes the overall clinical efficacy of rTMS to remain rather modest (Jannati et al., 2017; Guerra et al., 2018; López-Alonso et al., 2014; Sommer et al., 2002). According to a meta-analysis by Berlim et al. (2014), 29.3% and 18.6% of depression subjects who received TMS responded or remitted respectively. The obvious question that arises is which factors cause these inter-individual differences. It was hypothesized that these differences might, at least partly, be explained by subject-specific brain wirings and brain connections. Because the mechanism of action of (r)TMS is not exactly known yet, also the optimal stimulation parameters, such as the stimulation position, duration, and intensity (Klooster et al., 2016) are not known. To state it boldly, patients that show clinical improvement might have been treated according to a stimulation protocol that *accidentally* is optimal for them. Optimal stimulation parameters might be subject-specific because of the individual differences in brain architecture. Therefore, it is important to investigate the potential of personalized brain stimulation protocols.

In Figure 1.3, an overview of the route towards personalized brain stimulation protocols is depicted. The horizontal axis depicts the time whereas the vertical axis represents the obtrusiveness of TMS treatment. The time starts at 1985, since that year Anthony Barker presented the first human brain simulator. Note that the stimulation procedure itself will not become more complex. The obtrusiveness here refers to the amount of additional procedures that need to be performed. The figure can be split in two steps. The first step is to learn more about the mechanism of action of brain stimulation techniques. Brain imaging techniques such as magnetic resonance imaging (MRI) and electroencephalography (EEG) (see Chapter 2 for a detailed description) can be used to study the effects of stimulation by comparing before and after measurements. Moreover, baseline measurements can be used to predict the effects of stimulation. In the second step, this knowledge can be used to personalize the stimulation protocols and thereby optimizing the clinical efficacy of brain stimulation techniques.

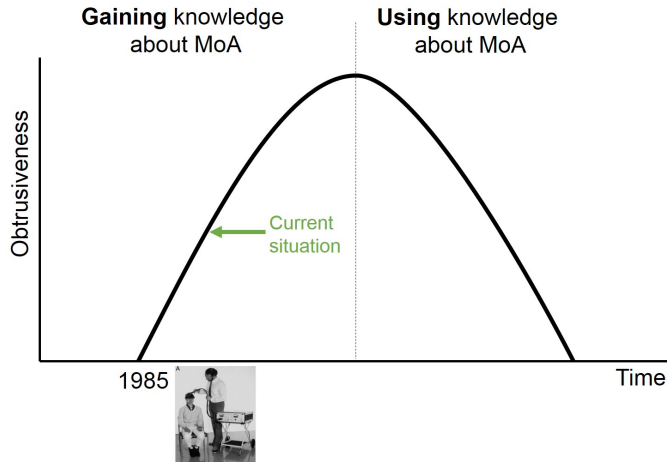


Figure 1.3 — Evolution of the obtrusiveness of TMS experiments over time, starting from 1985 since that year Anthony Barker presented the first human brain stimulator. Firstly, the obtrusiveness will increase because the knowledge about the actual mechanism of action of TMS is not yet fully understood. Therefore, additional recordings are needed to be able to study the effect of TMS on the brain and vice versa. Secondly, the knowledge about the mechanism of action can be used in clinical practice. This will in turn decrease the obtrusiveness of brain stimulation procedures. MoA = mechanism of action.

1.5 Thesis outline

This thesis is a modest contribution to the current knowledge about the mechanism of action of TMS. Even though the focus on this thesis is on TMS, this is not the only brain stimulation technique. **Chapter 3** provides an extensive overview of non-invasive and invasive brain stimulation techniques.

The research, as described in **Chapter 4** until **6** is based on a clinical trial performed at the psychiatry department of the University Hospital Ghent (Belgium). Fifty medication resistant MDD patients were enrolled in a randomized, double-blind, sham-controlled, cross-over accelerated intermittent theta burst stimulation (aiTBS) study design. **Chapter 4** and **Chapter 5** are based on the resting-state functional MRI (rs-fMRI) data. **Chapter 4** describes the effects of stimulation on graph measures. **Chapter 5** is a methodological paper in which two different seeding methods are compared. Biomarkers that can predict the response of rTMS treatment might prospectively exclude patients who are less likely to benefit from treatment, thereby increasing overall clinical efficacy. Therefore in **Chapter 6**, the focus is solely on the prediction of clinical responses to aiTBS based on the baseline diffusion MRI (dMRI) data.

Chapter 7 describes the most fundamental study of this thesis and is based on a dataset from the Berenson-Allen Center for Noninvasive Brain Stimulation (Boston, US). Here, the propagation of single TMS pulses is quantified using EEG data and linked to the brain's intrinsic functional connectivity.

The research in this thesis is discussed in **Chapter 8**. There, focus is more on the bigger picture. Specifically, possible improvements are highlighted and potential recommendations for incorporating knowledge about the mechanism of action of TMS in the development of future personalized brain stimulation protocols are given.

"I have been absolutely amazed by the results. My life has been completely transformed. After around three weeks of daily treatment, I finally saw a crack of light in the dark and suddenly something inside me told me I was going to get better."

Depression patient after TMS treatment

CHAPTER 2

Neuroimaging to predict and study the effects of TMS

Neuroimaging is a broad term that encompasses multiple techniques to visualize anatomy or function within the central nervous system in vivo. In this chapter, an introduction of two neuroimaging techniques, namely magnetic resonance imaging (MRI) and electroencephalography (EEG) will be given, with a specific emphasis on how these techniques can be used to gain more knowledge about the mechanism of action of TMS.

2.1 MRI

The human body consists for approximately 70% of water (H_2O). MRI relies on the magnetic properties of a hydrogen atom (^1H) to produce an image. These hydrogen atoms have a magnetic property called spin; a characteristic that represents the intrinsic angular momentum. These spins induce small magnetic field. So every proton in the body acts like a tiny magnet. Note that every nucleus with an odd number of protons has a net magnetic moment and is therefore amenable for magnetic imaging. Hydrogen is by far the most abundant in the human body.

Normally, these atoms are orientated randomly, so there is no net magnetic field. An MRI scanner is basically a long tube, also called bore, that contains powerful magnets. A strong static magnetic field (B_0 , in the order of 1.5-7 Tesla for human use) exists in the direction of the bore. If a subject enters the scanner, the spins in the body align with this static magnetic field, either in parallel or anti-parallel direction. Because there is a small extend in spins that align in the parallel, low-energy, direction with B_0 , there is a main magnetic dipole moment in the direction of the subject. This is also referred to as longitudinal magnetisation. The presence of the magnetic field causes the spins to precess around the long axis of their primary magnetic field. The frequency of the precession is called Larmor frequency and is proportional to the strength of B_0 .

The bore of the MRI scanner contains radiofrequency (RF) coils. These coils can emit RF pulses and can also record the energy that is released. The application of a RF pulse, at a certain precession frequency, has two effects. Firstly, the low energy parallel protons flip towards the transverse plane, thereby decreasing the longitudinal magnetization. Secondly, protons synchronize and start precessing in phase. As a result, the net magnetization vector turns towards the transverse plane (transverse magnetization). This flipped magnetisation gradually returns to the original state, or equilibrium in a process called relaxation. The magnetization in the transverse plane (T_2 relaxation) decreases whereas the longitudinal magnetization will increase (T_1 relaxation). In reality, the spins dephase much quicker than T_2 because of inhomogeneities in B_0 . The combination between T_2 relaxation and the field inhomogeneities is termed T_2^* . The relaxation times depend on the tissue type.

The RF coils can also record the net magnetic vector (the sum of the longitudinal and transversal magnetization) in the transverse plane. After excitation, the protons fall back to the initial low energy state, parallel to the direction of B_0 . This change in magnetic moment results in a free-induction decay (FID) signal. The electrical signals that are emitted by the protons when they transfer back to the lower energy state can be picked up by the RF coils. A computer receives this signal and performs an analog to digital conversion.

Then the information is stored in k-space, also called image space. Applying a Fourier transformation to the information in the k-space can result in the final MR image.

Without spatial encoding the RF coils would only pick up one signal averaged over the whole brain. However, gradient coils in the bore of the MRI scanner can create secondary magnetic fields that allow the spatial encoding. Basically, gradient magnets change the strength of the primary magnetic field, thereby making the precession frequency dependent on the location in the direction of the gradient. Note that the RF pulses only act on the spins that precess with the frequency of the RF pulse. By smart combinations of the gradient the MR signals can be localized in 3D space (slice selection in z-direction, phase encoding in y-direction, frequency encoding in x-direction).

Besides anatomical information, MRI can be sensitized to various body processes. Even though there are many more MR sequences, the remaining of this chapter focusses on functional MRI and diffusion MRI.

2.1.1 Functional MRI

As the name implies, functional MRI (fMRI) can reveal information about brain function. It provides an indirect measure of neuronal activity by measuring the changes in metabolic requirements related to neuronal activity. The most commonly used fMRI contrast is blood-oxygenated level-dependent (BOLD) fMRI, which is based on the ratio between oxygenated and deoxygenated blood. Deoxyhemoglobin has paramagnetic properties and can, therefore, act as an endogenous contrast agent. Paramagnetic substances produce macroscopic magnetic field inhomogeneities, which can accelerate transverse relaxation, i.e. shorten T_2 and T_2^* .

During neuronal activity, there are three parameters that change the ratio between oxygenated and deoxygenated blood (Figure 2.1a and b) and therefore play an important role in the occurrence of the BOLD contrast; the cerebral metabolic rate of oxygen ($CMRO_2$), cerebral blood flow (CBF), and the cerebral blood volume (CBV). After neuronal activation, first the $CMRO_2$ increases. The consumption of oxygen leads to a higher concentration of deoxyhemoglobin which causes an initial signal dip. Quickly thereafter, both the CBF and the CBV tend to go up. The increased CBF causes more oxyhemoglobin to enter the site of activation, thereby increasing the BOLD signal. Increased CBV causes opposite effects on oxyhemoglobin concentration. However, the effect of the CBF increase outpaces the signal reduction caused by the higher $CMRO_2$ and CBV (Deichmann, Nöth, and Weiskopf, 2010). An overview of these steps can be seen in Figure 2.1c.

Echo planar imaging (EPI) is the most commonly used acquisition scheme to collect fMRI data (Deichmann, Nöth, and Weiskopf, 2010). EPI is an efficient way of T_2^* -weighted scanning. The typical repetition time (TR) is between 0.5 and 3 seconds. The temporal resolution of fMRI is therefore relatively low. However, because the hemodynamic response function is much slower (peak about 5 seconds after the onset of neuronal activity, see Figure 2.1c.) than neuronal activity, a very high temporal resolution cannot be achieved with fMRI.

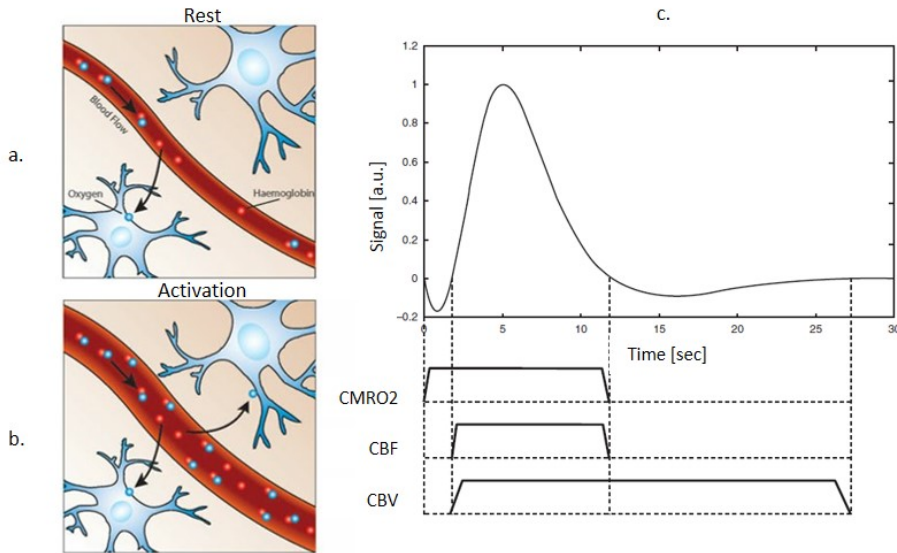


Figure 2.1 — The occurrence of the BOLD contrast is related to the ratio between oxygenated and deoxygenated blood. During rest (a)), there is a low amount of oxygenated hemoglobin, which increases after neuronal activity (b, Figure adapted from (www.oxfordsparks.ox.ac.uk/mr)). The changes in $CMRO_2$, CBF, and CBV, as a result of neuronal activity, induce the final BOLD contrast (Figure c, adapted from (Deichmann, Nöth, and Weiskopf, 2010)).

. 1 Paradigm-driven versus resting-state fMRI

Initially, studying a particular brain function required the presentation of a certain task or stimulus to trigger the phenomena under investigation. In these so-called paradigm driven designs, stimuli are presented in repeated blocks, typically in the order of tens of seconds. The analysis of paradigm-driven fMRI is based on the difference in BOLD signal between activation and baseline conditions. This contrast is typically formulated in a general linear model (GLM). The GLM results in a functional connectivity map that shows which regions in the brain are linked to the task or stimulus, i.e. have the same functional properties.

In 1995, Biswal et al. (1995) performed the first so-called resting-state fMRI (rs-fMRI) experiment. In contrast to paradigm-driven fMRI studies, resting-state functional connectivity studies examine BOLD fluctuations in the absence of any explicit input or output, i.e. study the spontaneous brain activity. Regions with similar functional properties exhibit coherent BOLD fluctuations even in the absence of a specific task (Biswal et al., 1995). Since the aim of rs-fMRI is to study neuronal activity that is intrinsically generated by the brain, subjects are usually instructed to lie still and refrain from falling asleep (Fox and Raichle, 2007). Functional connectivity can be calculated from resting-state data based on correlations between the BOLD data of an a priori defined region of interest with other brain regions (see Figure 2.2) or by means of a data-driven approach such as spatial independent component analysis (ICA) (Beckmann and Smith, 2004). ICA has

shown the presence of consistent resting-state networks (Damoiseaux et al., 2006) which seemed to correspond with the networks during activation (Smith et al., 2009). One specific resting-state networks showed clear anti-correlations with task-related network. This default-mode network (DMN) has shown to be active during the brain's resting condition and becomes more silent during activation (Fox et al., 2005; Fox et al., 2009).

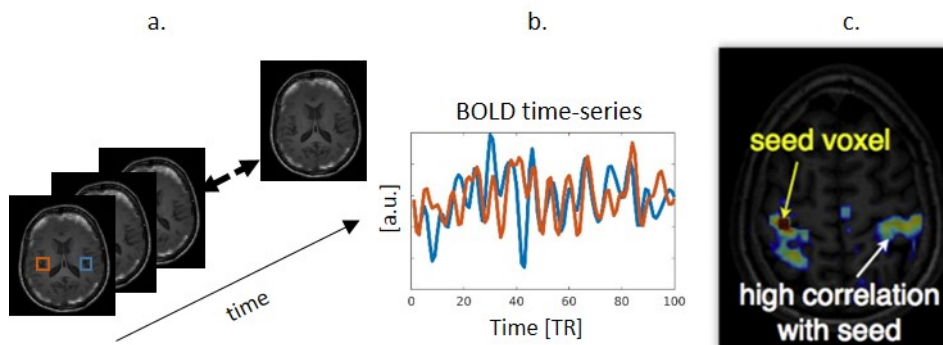


Figure 2.2 — Example of the determination of a resting-state functional connectivity map. First (a), multiple BOLD volumes are acquired. Examples can be seen in (a), overlaid on an anatomical template. An a priori seed region, also called region of interest, is defined within the motor cortex, represented with the red box in Figure a. Figure b shows BOLD time-series of this a priori defined ROI and another region in the brain (blue box in a). Correlations between the BOLD time-series of the a priori ROI and all other brain regions lead to the final resting-state functional connectivity map (c). Figure adapted from Van den Heuvel and Hulshoff Pol (Heuvel and Hulshoff Pol, 2010).

Rs-fMRI has several practical and theoretical advantages over task-based fMRI for clinical applications, including improved signal to noise, reduced need for patient compliance, avoidance of task performance confounds, and expanded patient populations (Fox and Michael Greicius, 2010). Significant rs-fMRI abnormalities have been identified across almost every major neurological and psychiatric disorder (Fox and Michael Greicius, 2010). Specifically in depression, Greicius et al. (2007) was the first to show increased activity in the subgenual cingulate and the thalamus in depressed patients compared to healthy subjects. On network level, increased connectivity within the anterior DMN, increased connectivity between the salience network and the anterior DMN, changed connectivity between the anterior and posterior DMN, and decreased connectivity between the posterior DMN and the central executive network were reported (Mulders et al., 2015).

2.1.2 Combining fMRI and TMS

TMS and neuroimaging are complementary tools that can be combined to optimally study brain connectivity and manipulate distributed brain networks (Fox et al., 2012b). TMS can temporally disrupt ongoing neural activity permitting to study causal relationship between the stimulated cortical area and the underlying brain function. Globally, TMS can be combined with fMRI in two ways; TMS can be applied online during MRI (concurrent TMS-fMRI (Bohning et al., 1997; Bestmann, Baudewig, and Frahm, 2003; Bestmann et

al., 2005)), or offline. Since concurrent TMS-fMRI was not used in this thesis, the remainder of this section focuses on offline TMS-fMRI. With offline TMS-fMRI either the baseline (before stimulation) data is used to investigate the possibilities to predict the clinical response to TMS or a combination of fMRI datasets (before and after a stimulation protocol) are compared to study the effects of TMS on the brain.

There are many example studies that aimed to use rs-fMRI data to predict the clinical outcome to various rTMS protocols as treatment for MDD. In 2012, Fox et al. (2012) showed that clinical efficacy of rTMS treatment for depression was linked to the functional anti-correlation between the subgenual cingulate cortex and the stimulated left DLPFC. These findings have later been confirmed by Weigand et al. (2017). Besides the specific functional connectivity between the subgenual cingulate and the DLPFC, also the functional connection between the subgenual and parts of the superior medial frontal cortex were stronger in responders to 10Hz left DLPFC rTMS (Baeken et al., 2014). Moreover, positive functional connections between the subgenual cingulate cortex and the medial orbitofrontal cortex could distinguish aiTBS responders from non-responders (Baeken et al., 2017a). Successful aiTBS treatment furthermore strengthened the connectivity between the subgenual and the medial orbitofrontal cortex. Beyond single functional connections, this thesis showed that whole-brain graph parameters derived from baseline rs-fMRI data were also correlated with the clinical outcome of aiTBS (chapter 4, (Klooster et al., 2019)).

Instead of functional connectivities, Cash et al. (2019) showed that response to high frequency left DLPFC stimulation was linked to low BOLD power in the caudate, prefrontal cortex, and thalamus (Cash et al., 2019). Additionally, this information was used to train a support vector machine and it was shown that binary therapeutic outcome (response vs non-response) to left DLPFC rTMS could be predicted with a 85-95% accuracy.

Prediction of the clinical outcome of stimulation of the dorsomedial prefrontal cortex (DMPFC) could also be predicted based on resting-state functional connectivity. Higher baseline cortico-cortical connectivity between DMPFC and subgenual cingulate and between subgenual cingulate and DLPFC and lower cortico-thalamic, cortico-striatal, and cortico-limbic connectivity were associated with better treatment outcomes (Salomons et al., 2014). Instead of investigating single functional connectivity characteristics, Drysdale et al. (2017) clustered resting state fMRI data and showed that there are 4 depression subtypes. Especially subjects within 2 of these biotypes, derived from reduced connectivity in frontoamygdala networks and in anterior cingulate and orbitofrontal areas in one subtype, or hyperconnectivity in thalamic and frontostriatal networks in another subtype, seemed to respond to DMPFC rTMS. Even though these results were promising, an attempt to replicate these findings failed (Dinga et al., 2019).

2.1.3 Diffusion MRI

Information on white matter networks of the brain can be obtained with diffusion weighted MRI (dMRI). Diffusion is the microscopic movement of atoms and molecules in a solution or gass, also called Brownian motion. Specifically in dMRI, the diffusion of the

protons (^1H) of water molecules (H_2O) is measured. The MR signal can be sensitized to molecular motions, i.e. diffusion, if a pair of opposite gradients is used (Mori, 2014a). After the initial RF pulse, the protons start to precess at the same frequency in the transverse plane. During the first so-called dephasing gradient, protons start to resonate at different frequencies depending on their location. The application of a second (rephasing) gradient, would lead to perfect rephasing if the gradient has opposite polarity and if no diffusion occurred. However, if the protons moved position between the two gradients they will not experience an equal but opposite magnetic gradient. As such, at the end of the dephasing and rephasing, the protons will remain out of phase. This results in a signal attenuation.

If the water molecules are in a restricted environment, such as is the case in the white matter in the brain, the displacement will be anisotropic with the preferred diffusion direction along the white matter axis. To capture this anisotropy, the diffusion needs to be measured in multiple directions. Field gradients along any arbitrary orientation can be created by combining the x, y, and z gradients. The diffusion tensor model is based on the fact that 6 parameters are needed to uniquely define the ellipsoid shape that represents anisotropic diffusion (Mori, 2014b; Jones, 2010) (Figure 2.3a). In 2000, Basser et al. (2000) was the first to describe tractography based on this diffusion tensor model. Tractography allows the reconstruction of anatomical (structural) connections between different areas in the brain and makes use of the assumption that the fiber orientation is parallel to the direction of the principal eigenvector (λ_1 , Figure 2.3b) (Mori, 2014c). A disadvantage of this diffusion tensor model is the inability to resolve multiple fiber directions within a voxel, i.e. crossing fibers. Jeurissen et al. (2013) showed a very high prevalence of multi-direction voxels which limits the accuracy of the diffusion tensor model in the majority of white matter regions. More advanced higher order algorithms have been proposed that can also capture more complex diffusion processes within a voxel. High angular resolution diffusion imaging (HARDI) is an extension of the diffusion tensor imaging protocol; instead of 6 diffusion directions, diffusion is measured along multiple directions. Since the results need to be rotationally invariant because of the variation of the neurons within the white matter the gradients need to be uniformly distributed. Multiple techniques, such as constrained spherical deconvolution (CSD) (Tournier et al., 2008), can be used to accurately estimate the white matter fiber orientations in every voxel.

Diffusion information can be quantified with voxel-based metrics or metrics can be derived from the whole-brain tractography result. Common metrics are the fractional anisotropy (FA) and the mean diffusivity (MD) (Basser and Pierpaoli, 1996). The FA characterizes the extend in which the diffusion varies along the orientations ($\lambda_1, \lambda_2, \lambda_3$). The MD is the average diffusion along the orientations. Specifically in depression, a meta-analysis showed decreased FA in the superior longitudinal fasciculus and increased FA values in the fronto-occipital fasciculus as compared to controls (Murphy and Frodl, 2011). Furthermore, negative correlation was reported between the FA and the duration of the depression episodes in both the right anterior cingulate and the left frontal white matter parts (Abe et al., 2010).

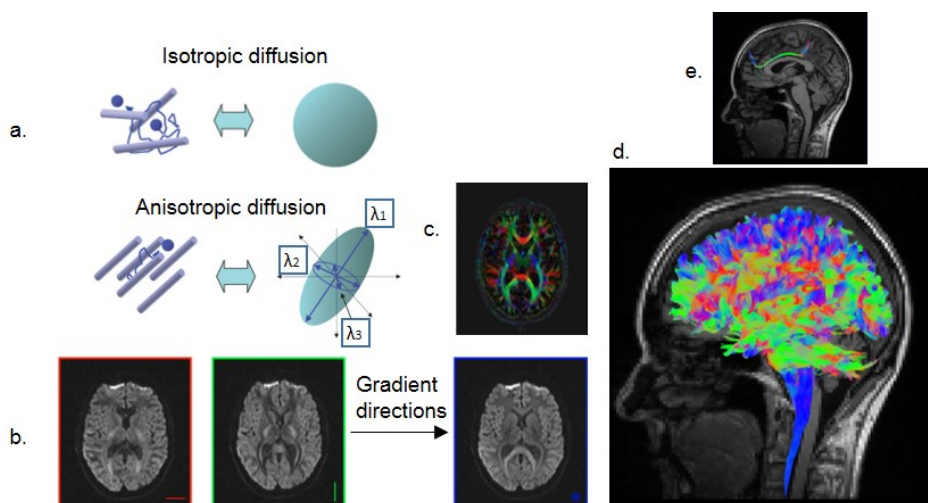


Figure 2.3 — Figure a represents the difference of isotropic versus anisotropic diffusion. If the diffusion is measured along 6 gradient directions, the ellipsoid shape of the diffusion can be calculated in every voxel, with λ_1 , λ_2 , and λ_3 the principal diffusion directions. Figure b shows diffusion weighted images, with the gradients applied in the left-right direction, anterior-posterior direction, and top-down direction. Signal attenuation can be seen of the structures that align with the gradient direction. A color coded FA map is shown in Figure c. Combining the information about the diffusion direction in every voxel, whole brain tractography can be performed (d). Specific fiber bundles can be studied by selecting specific parts of the whole brain tractogram. Figure e. shows an example of the fiber bundle between the left superiorfrontal cortex and the left precuneus. Different colors represent different directions of neuronal pathways: green = anterior-posterior; red = left-right, blue = inferior-superior. ExploreDTI was used for visualization (Leemans et al., 2009).

2.1.4 Combining dMRI and TMS

The first studies combining dMRI and TMS aimed to prove the safety of rTMS treatment. No reduced FA values (linked to brain damage) were found in the DLPFC after applying 10 Hz rTMS (Kozel et al., 2011). Instead, daily rTMS at the left DLPFC induced a positive effect on the white matter organization for the side of the brain stimulated, as shown by increased FA. This might represent an improvement in structural integrity between the left DLPFC and deeper limbic structures and might suggest the hypothesis that the mechanism of action of rTMS is linked to the structural brain connections. A more recent study showed that application of accelerated iTBS also affects whole brain graph measures, derived from structural brain connectivity (Caeyenberghs et al., 2018).

Few studies investigated the potential of dMRI to predict the clinical effects of rTMS. The delineation ratio of the corticospinal and the thalamocortical tracts had predictive value of rTMS treatment for central post-stroke pain (Goto et al., 2008). In the field of depression, Klooster et al. (see Chapter 6) was the first to investigate this biomarker potential of dMRI data to predict the effects of aiTBS. Based on a priori hypotheses that the cingulate cortex is involved in the release of depression symptoms, indirect structural connections

between the stimulated left DLPFC and the cingulate cortex were significantly correlated with the clinical response to aiTBS.

DMRI might furthermore have added value for the accurate derivation of the TMS-induced electric fields within the brain (Opitz et al., 2011). Firstly, the directional dependency of conductivity values can be derived from diffusion information under the assumption that the motion of water molecules is linearly dependent on the ionic movement in membranes (Schmidt and Rienen, 2012b; Tuch et al., 2001). Secondly, combining TMS-induced electric field distributions with tractography results might lead to effective electric field distributions (Nummenmaa et al., 2014). Neuronal activation requires a component of the electric field gradient along the neuronal tract that exceeds a threshold for activation. Combining TMS-induced electric fields with the spatial distribution of neuronal tracts might ameliorate the insights of the deeper brain structures that can indirectly be reached with TMS (De Geeter et al., 2012).

2.2 EEG

The electrical activity within the brain can be recorded with the electroencephalogram (EEG). EEG has an excellent temporal resolution, in the order of ms, allowing studies of fast neuronal dynamics (Baillet, Mosher, and Leahy, 2001). The EEG is measured with electrodes either glued to the scalp or embedded in a cap or a net that is tied around the subject's head. The electrode positions are arranged according to the 10-20 system (Klem et al., 1999). An electrolytic gel or solution is used to minimize the impedance between the electrodes and the skin. In clinical practice, approximately up to 64 electrodes are used. For research purposes, also caps and nets with more electrodes exist (128 or even 256). Because of the relatively low number of electrodes, the spatial resolution of EEG is limited.

The main generators of the EEG are the pyramidal neurons. The pyramidal cells are organized in such a way that the neighboring dendritic trees lie parallel to each other and orthogonal to the cortical surface. There are two types of electrical activity within these cells: action potentials and postsynaptic potentials. An action potential is induced when the transmembrane potential exceeds a threshold. Action potentials can travel along the neurons so that communication is possible. Communication between neurons requires the propagation of the action potentials via synapses, small gap junctions between two neurons. When an action potential arrives at a synapse a postsynaptic potential is generated if a threshold is exceeded. The action potential is then transferred to the postsynaptic neuron. Action potentials take approximately 1 ms and do not fire synchronously in a large number of neurons (Figure 2.4a). On the contrary, because of the longer duration of the postsynaptic potentials (~ 10 ms), synchronous generation of postsynaptic potentials can occur in a large number of neurons (Figure 2.4b). Even though the action potentials are stronger than the postsynaptic potentials, summation of the latter can produce unidirectional current flow that is large enough to be picked up with electrodes outside the brain. These currents can propagate to the scalp because the brain acts as a volume conductor with anisotropic and heterogeneous electrical properties. The resulting EEG signal in every electrode is in the order of $100\mu\text{V}$ and is therefore the summation of underlying

sources, weighted by volume conduction factors (Figure 2.4c).

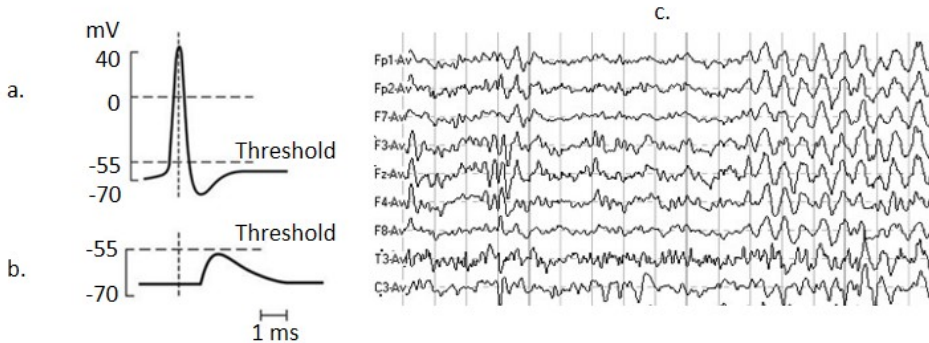


Figure 2.4 — Figure a and b show an action potential and a postsynaptic potential. As can be seen, the action potentials are stronger (~ 100 mV versus ~ 10 mV) but shorter (~ 1 ms versus ~ 10 ms) compared to the postsynaptic potential. Figure c. shows an example of EEG data measured in 9 electrodes attached to the scalp.

EEG can be used to identify normal and pathological brain rhythms based on their amplitude and frequency. EEG is most commonly, but not exclusively, used in the field of epilepsy, since it represents (interictal) epileptiform activity (Noachtar and Rémi, 2009).

2.2.1 EEG source imaging

As stated before, the EEG sources within the brain project to many EEG electrodes because of volume conduction. EEG source imaging (ESI) estimates the electrical source distribution inside the brain that corresponds most likely to the recorded scalp potentials. This allows 3D visualization of the EEG data. ESI consists of 2 main parts: the forward model and the inverse solution.

The forward model estimates for every EEG electrode the contribution of all sources. It requires the positions of the scalp EEG electrodes, a head model, and a source model. For accurate ESI, head models can be derived from subject-specific anatomical MRI data. This data can be segmented in different tissue types and specific electrical properties (i.e. conductivity values) can be assigned to these different tissue types. Since the neuronal activity can be macroscopically modelled with a current dipole parallel to the neurons, a current dipole is often used as source model. The source space is built from many of these source models. Since the pyramidal neurons are located in the cortex, source space is often restricted to the cortical gray matter regions. Subcortical gray matter regions such as the thalamus and basal ganglia are often excluded since these are not assumed to be generators of the EEG signals.

Subsequently, the inverse solution uses the forward model to estimate the underlying sources of the measured EEG. The inverse problem is ill-posed, which means that there

is no unique solution. The activity of millions of neurons is distributed through the brain and head and is then sampled with a limited amount of electrodes. Inverse solutions can be made based on different assumptions on how the brain works. The inverse solution leads to a current distribution within the brain corrected for the volume conduction effects which are present in the scalp EEG.

2.2.2 Combining EEG with TMS

When combining EEG with TMS, the effect of a pulse applied to the cortex can be assessed by measuring the neuronal response in the EEG. The EEG response obtained after averaging the response over multiple single TMS pulses is called the TMS-evoked potential (TEP). A TEP is a complex waveform time-locked to the TMS pulse, composed of a series of peaks and troughs at specific latencies (Hill et al., 2016; Tremblay et al., 2019). TEPs offer a measure of cortical excitability. Combining TMS with EEG instead of electromyography (EMG) greatly expands the amount of neurophysiological information that can be derived. TMS-EMG is restricted to stimulation of the motor cortex since it depends on the motor output.

The main challenge of combining EEG and TMS is related to a large EEG artefact that is produced by the electromagnetic field generated by the TMS coil (Farzan et al., 2016). To avoid saturation of the amplifier, a sample-and-hold amplifier or a DC amplifier should be used. TMS-compatible EEG electrodes should be used to prevent the electrodes from heating (Veniero, Bortoletto, and Miniussi, 2009). Besides the artefact generated by the TMS pulse, also scalp-muscle activity can be induced by TMS causing additional muscle artefacts in the EEG. Moreover, the loud coil-click sound, produced by the TMS when the energy is released into the coil, produces an auditory artefact, auditory-evoked potential. Advanced artefact removal techniques have been proposed (Rogasch et al., 2014). Still, overall multisensory effects might contribute to TEPs. Therefore, appropriate sham TMS-EEG is of importance to extract the real neuronal response of TMS (Conde et al., 2019).

Information derived from TEPs has shown to be valuable in the distinction of several pathologies (Tremblay et al., 2019). In this thesis, simultaneous TMS-EEG data from healthy volunteers was used in a more fundamental way, to study the propagation of TMS pulses in terms of the intrinsic MR resting-state functional connectivity (chapter 7).

*"There has never been a better time to be a
cognitive neuroscientist."*

*Prof. Vincent Walsch and Prof. Alvaro
Pascual-Leone*

CHAPTER 3

Technical aspects of neurostimulation: Focus on equipment, electric field modeling, and stimulation protocols

D.C.W. Klooster, A.J.A. de Louw, A.P. Aldenkamp, R.M.H. Besseling, R.M.C. Mestrom,
S. Carrette, S. Zinger, J.W.M. Bergmans, W.H. Mess, K. Vonck, E. Carrette, L.E.M.
Breuer, A. Bernas, A.G. Tijhuis, P.A.J.M. Boon

Neuroscience and Biobehavioral Reviews, 2016, 65:113-41
doi: 10.1016/j.neubiorev.2016.02.016

Abstract

Neuromodulation is a field of science, medicine, and bioengineering that encompasses implantable and non-implantable technologies for the purpose of improving quality of life and functioning of humans. Brain neuromodulation involves different neurostimulation techniques: transcranial magnetic stimulation (TMS), transcranial direct current stimulation (tDCS), vagus nerve stimulation (VNS), and deep brain stimulation (DBS), which are being used both to study their effects on cognitive brain functions and to treat neuropsychiatric disorders. The mechanisms of action of neurostimulation remain incompletely understood. Insight into the technical basis of neurostimulation might be a first step towards a more profound understanding of these mechanisms, which might lead to improved clinical outcome and therapeutic potential. This review provides an overview of the technical basis of neurostimulation focusing on the equipment, the present understanding of induced electric fields, and the stimulation protocols. The review is written from a technical perspective aimed at supporting the use of neurostimulation in clinical practice.

3.1 Introduction

Neuromodulation is defined as a field of science, medicine, and bioengineering that encompasses implantable and non-implantable technologies, electrical or chemical, for the purpose of improving quality of life and functioning of humans, by the international neuromodulation society (Krames, Peckham, and Rezai, 2009). Brain neuromodulation involves different neurostimulation techniques that can activate parts of the nervous system. Neurostimulation can be applied invasively by means of deep brain stimulation (DBS) or non-invasively by transcranial magnetic stimulation (TMS) or transcranial direct current stimulation (tDCS). Vagus nerve stimulation (VNS) allows both invasive and non-invasive stimulation. Stimulation techniques can be used as therapeutic tool in psychiatry and neurology and are also applied in cognitive neuroscience to study the functioning of the brain.

Various studies have demonstrated successful clinical outcomes of neurostimulation in multiple disorders. Relief of tremor in patients with Parkinson's disease is the most common and longstanding indication for DBS. However, not all patients respond optimally to a neurostimulation therapy. In clinical practice, neither the type of neurostimulation that is most suitable for an individual patient, nor the optimal stimulation parameters, such as the frequency, intensity, pulse shape, and electrode combinations are evidence-based. Also, the optimal target within the nervous system for various disorders remains to be identified.

The clinical application of neurostimulation has preceded the elucidation of the different mechanisms of action. Improved understanding of these mechanisms is crucial to ameliorate the outcome of neurostimulation therapies in clinical practice and expand their therapeutic potential. Understanding the technical basis of neurostimulation is a prerequisite to elucidate the effects of neurostimulation on neuronal tissue.

In this review we focus on the technical basis of the currently available stimulation techniques in clinical practice: TMS, tDCS, VNS, and DBS. The stimulation equipment, the current knowledge of electric field modeling, and the effects of stimulation protocols will be described. The last part of the review will elaborate on alternative stimulation methods, that are not standardized in clinical practice or that are under development and might be used in the future. Finally, future perspectives will be described.

The review is written from a technical perspective and aimed to support the use of neurostimulation in clinical practice. The review can be read to retrieve a more global overview of neurostimulation techniques but more importantly, it will give clinicians ideas what protocols can be used in certain cases and how the stimulation parameters can be chosen. Moreover, an increased insight in the technical background will increase the insight in the interpretation of the results of different neurostimulation studies.

3.2 Non-invasive neurostimulation

In this section, TMS and tDCS are extensively described whereas external trigeminal nerve stimulation (eTNS) and transcutaneous vagus nerve stimulation (tVNS) will be de-

scribed briefly, later in this review. The stimulation coil used for TMS and the electrodes used for tDCS, eTNS, or tVNS are located outside the brain on the patient's head. This means that neuronal tissue is reached via several additional tissue layers. Figure 3.1 gives an overview of the non-invasive neurostimulation techniques.

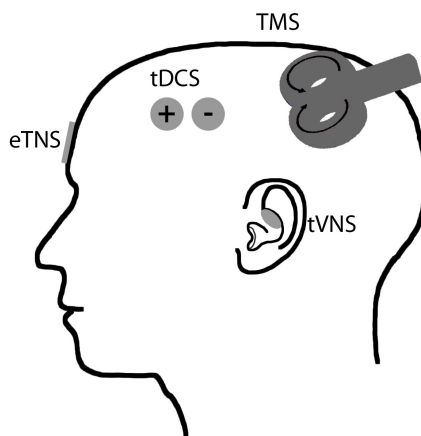


Figure 3.1 — *Non-invasive brain stimulation. Overview of non-invasive stimulation techniques: TMS, tDCS, tVNS and eTNS.*

3.2.1 Transcranial magnetic stimulation (TMS)

TMS is a non-invasive stimulation method based on magnetic induction. A coil is placed over the head to locally apply a rapidly fluctuating magnetic field that generates electric current in the underlying brain tissue (Hallet, 2000; Kobayashi and Pascual-leone, 2003). Since the currents fall off rapidly with the distance to the magnetic stimulator coil, stimulation seems to be restricted to the cortex (Barker, Jalinous, and Freeston, 1985; Barker, 1991).

TMS can be applied as single pulse stimulation (spTMS) to depolarize neurons and evoke measurable effects, such as motor evoked potentials (MEPs) after stimulating the motor cortex or phosphenes (visual sensations) after stimulating the visual cortex. Paired pulse stimulation (ppTMS), a combination of a so-called conditioning stimulus (CS) and test stimulus (TS), with varying inter stimulus intervals to the same or different brain regions, is mainly used to assess cortical excitability. Table 3.1 provides an overview of the different ppTMS protocols (Pascual-Leone et al., 2002).

Repetitive TMS (rTMS) consists of trains of stimuli with a certain frequency and intensity. In contrast to spTMS and ppTMS, the effects of rTMS exceed the duration of the stimulation. rTMS might therefore be useful as a therapeutic tool for a broad spectrum of neurological and psychological disorders (Lefaucheur et al., 2014). Repetitive stimulation is nowadays approved by the Food and Drug Administration (FDA) for the treatment

Table 3.1 — *Different paired pulse TMS protocols.*

Protocol	What is examined	Intensity	Inhibition ISI	Facilitation ISI
Two equal suprathreshold stimuli at long ISI (10-250ms)	Paired pulse facilitation and inhibition which are primarily due to intracortical facilitatory and inhibitory mechanisms operating at long ISI	120-160% RMT	10-30ms	50-200ms
Subthreshold CS and suprathreshold TS at short ISI (1-20ms)	Excitability of separate inhibitory and excitatory neural circuits of the motor cortex	CS 80% RMT, TS should be adjusted to produce reasonable MEP	1-5ms	8-25ms
Suprathreshold CS and subthreshold TS at very short ISI (0.5-6 ms)	Excitability of motor cortical circuits	CS should produce MEP of about 1 mV, TS should be 90% RMT		1.1-1.5ms 2.3-2.9ms 4.1-4.4ms

ISI = inter stimulus interval, CS = conditioning stimulus, TS = test stimulus

of migraine and depression.

The mechanism of action by which TMS deploys a long-lasting therapeutic effect is thought to originate from changes in synaptic plasticity. Long-term potentiation (LTP) is a long-lasting increase in synaptic strength whereas long-term depression (LTD) means a long-lasting decrease. Post-synaptic N-methyl-D-aspartate (NMDA) plays an important role in LTP and LTD. TMS has also shown to have effect on neurotransmitter γ -aminobutyric acid (GABA), as show in a magnetic resonance spectroscopy study by Stagg et al. (2009). Even though it is strongly suggested that synaptic plasticity is involved in the therapeutic effect, there has not been a clear direct link up to date (Hoogendam, Ramakers, and Di Lazzaro, 2010).

In general, TMS is considered to be a safe technique, when it is performed according to the TMS guidelines (Rossi et al., 2009). The most serious concern when applying TMS is the possible induction of epileptic seizures. Schrader et al. (2004) showed that the crude risk of seizure induction is 0.0 - 2.8% after spTMS and 0.0 - 3.6% after ppTMS in epilepsy patients. Bae et al. (Bae et al., 2007) showed a crude-risk of 1.4% for epilepsy subjects undergoing rTMS. Important to note is that because of the random occurrence of seizures, no direct causal relation between TMS and seizures was proven (Bae et al., 2007; Krishnan et al., 2015; Oberman et al., 2011; Schrader et al., 2004). The application of TMS in non-epilepsy patients induced seizure in few subjects (see Rossi et al. (2009) for overview of these cases to 2009), of whom some had a pre-existing neurological disorder and in some cases the stimulation protocol was not according to the guidelines (Loo, McFarquhar, and Mitchell, 2008). None of these seizures induced long-term sequelae and they all ended spontaneously. Pre-screening of potential risk-factors is very important.

Even though in general adverse events related to rTMS were reported to be mild, the exact numbers differ between treatments of various pathologies. Overall, 17.1% of the epilepsy patients included in the review of Bae et al. (2007) reported on adverse events of which headache was most often found (9.6%). In the sham-controlled rTMS studies in depression, reviewed by Loo et al. (2008), approximately 28% of the patients experienced headache and 39% reported about pain or discomfort during stimulation. These numbers were higher compared to sham-stimulation (16% and 15% respectively).

A. Equipment: TMS coils

TMS equipment consists of two main components: a high-current charge-discharge system and a magnetic stimulation coil. In the charge-discharge system, a capacitor is charged to a high voltage and discharged into the stimulating coil (Walsch and Pascual-Leone, 2003). The TMS stimulation coil is the key component of the equipment since it transfers the magnetic energy to the neuronal tissue and it determines the shape of the induced electric field.

TMS coils are constructed from tightly wound copper wires, which are adequately insulated and housed in plastic covers (Wagner, Valero-Cabre, and Pascual-Leone, 2007). The induced electric field, and thus the site of stimulation, depends largely on the shape of the TMS coil used. A circular coil induces a non-focal ring-shaped electric field. With a figure-of-eight coil, consisting of a pair of adjacent loops, with the current flowing in opposite directions, a relatively focal electric field is generated at the point where the two circles meet (Deng, Lisanby, and Peterchev, 2013; Liu, Yin, and Guan, 2003; Roth, Pell, and Zangen, 2013). Using figure-of-eight coils, negative stimulation is induced under the twain edges of the coil (Liu, Yin, and Guan, 2003).

Besides the circular and figure-of-eight coils, also the use of double-cone coils and H-coils, aiming at stimulation of deeper targets in the brain, has been investigated (Fadini et al., 2009; Roth, Zangen, and Hallett, 2002; Roth et al., 2007; Roth, Pell, and Zangen, 2010; Roth et al., 2014). In general it was concluded that both double-cone coils and H-coils indeed can effectively stimulate deeper targets, with the H-coil being most efficient (Roth, Zangen, and Hallett, 2002). Deeper stimulation comes at the cost of a wider electric field distribution, so less focality. Deng et al. (2013) investigated the depth-focality trade-off in fifty TMS coils with different geometries. In all coils, a trade-off between depth and focality of the stimulation was shown. Rotem et al. (2014) introduced a coil that superimposes the electric fields from two figure-of-eight coils, orthogonal to each other, that operate with relative phase shift in time, to overcome the directional sensitivity of TMS. This coil may be useful to target brain regions in which the optimal coil orientation cannot be determined.

Since only $1/10^8$ of the magnetic energy in the coil is efficiently transmitted to the nervous tissue (Ravazzani et al., 2002), the power requirement of TMS is high. High frequency TMS protocols with conventional coils can quickly result in coil heating. Coil heating depends on the geometry of the TMS coil, the current and the pulse width (Ruohonen, Virtanen, and Ilmoniemi, 1997; Ruohonen, Ravazzani, and Grandori, 1998). Cooling systems for TMS coils have been developed in which moving air or liquid is transferred along the coil to prevent heating. Most coils contain a heat sensor that automatically blocks the stimulation coil when the temperature exceeds approximately 41 degrees centigrade (Wassermann et al., 2008). The optimal coil design depends greatly on the application and there is no globally optimal solution (Ravazzani et al., 2002).

B. Electric field modeling

As stated before in this review, the mechanisms of action of neurostimulation techniques are not yet fully understood. Since it remains impossible to visualize the current distribution in the brain *in situ*, multiple studies have been performed to model the electric fields induced by stimulation. Firstly, knowledge of the electric field distribution in the brain can provide a link with the induced physiological stimulation effects. Secondly, modeling the fields as a function of different stimulation parameters will increase the knowledge about the effect of these parameters. Here, a short introduction on electric field modeling is given, followed by an overview of previous modeling studies. The TMS modeling studies in this review cover three main topics: the importance of incorporating tissue anisotropies in the model; the effect of incorporating coil geometry in the model; and the spatial distribution of the electric field as a function of coil orientation.

The first models that were used to assess the stimulation induced electric fields were simple, spherical head models assuming homogeneity in the brain and isotropic conductivity. Conductivity is a measure of the ability of a material to conduct electric current. Different tissue types in the brain have different conductivity values, and will therefore cause the electric field to propagate differently. So these simple spherical head models needed to be extended into models taking into account the anisotropic and heterogeneous properties of the brain. The head can be segmented into different layers: white matter (WM), gray matter (GM), cerebrospinal fluid (CSF), skull, and scalp, each with its own conductivity value (Figure 3.2a - e). Nowadays, also patient-specific models are used incorporating anatomical information derived from magnetic resonance imaging (MRI) data. Mathematically, the electric field resulting from TMS can be described as the sum of two terms: the primary electric field and the secondary electric field. The primary field is a direct result of the coil's rapidly changing current. A secondary field exists because of charge accumulations at surfaces with different electrical conductivities (Salinas, 2009). From the numerical side, several methods can be used to solve the mathematical equations for the electric field inside the brain. For most of these methods, the brain is first discretized into small elements. Next, a solution technique is applied such as the finite element method (FEM) (Laakso and Hirata, 2012; Miranda, Hallett, and Basser, 2003; Opitz et al., 2013; Opitz et al., 2011; Pu et al., 2010; Thielscher, Opitz, and Windhoff, 2011; Windhoff, Opitz, and Thielscher, 2013; Zheng, Li, and Huo, 2005), finite difference method (FDM) (Roth et al., 1991), the boundary element method (BEM) (Salinas, 2009) or the impedance method (Tachas and Samaras, 2014; De Geeter, Guillaume, and Luc, 2011; De Geeter, Crevecoeur, and Dupre, 2011; De Geeter et al., 2012). An example of the discretization can be seen in Figure 3.2f and Figure g shows an example of the resulting electric field calculation.

The effect of incorporating specific conductivities within the brain was investigated. On the one hand, Davey et al. (2003) assumed a homogeneous brain since no large differences were found between the calculated electric fields using models with different conductivities versus homogeneous models. On the other hand, Miranda et al. (2003) showed a significantly increased electric field in the outer low conductivity region when using a concentric two layer model, with high and low conductivity. The latter study stated that detailed models provide better insight of the location of possible stimulation

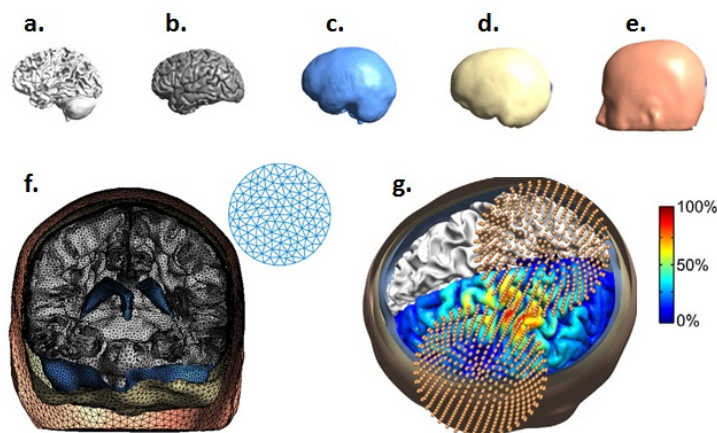


Figure 3.2 — *Electric field modeling. The head can be segmented into different layers (SimNIBS software, www.simnibs.de): white matter (a), gray matter (b), CSF (c), skull (d) and scalp (e) based on information obtained from MRI. These various tissue types have different properties concerning electric field propagation. By using models, such as for example FEM, BEM, the brain is split into small elements (f). Giving every area specific parameters, the electric field can be determined mathematically. An example is shown in (g) (Opitz et al. (2011), with permission). Here, the yellow dots represent the TMS coil, positioned above the left motor area. The modeled electric field is depicted in color (in the online version), scaled to the maximum.*

sites in the brain.

Conductivity values can be derived for every tissue type. Nowadays, it is possible to derive accurate conductivity values, as a function of position and direction within a tissue type. A geometrically accurate model of an individual head to calculate the electric field, based on high-resolution diffusion tensor imaging (DTI) for conductivity mapping, was used by Opitz and Thielscher (Opitz et al., 2011; Thielscher, Opitz, and Windhoff, 2011). In DTI, the fact that diffusion of water molecules primarily takes place along the direction of the white matter tracts is used to visualize these tracts. It is assumed that the motion of water molecules is linearly dependent on the ionic movement in membranes (Schmidt and Rienen, 2012b). This allows the position- and direction-specific conductivities to be derived by solving a linear transformation of the DTI tensor (Tuch et al., 1999; Tuch et al., 2001). It was assumed that the gyral folding patterns and the anisotropy of the brain tissue can have a strong effect on the field. Using position- and direction-specific conductivity values, more reliable calculations could be made for the induced electric fields in the GM and WM.

The fact that the patient-specific gyral folding patterns influence the electric field can be linked to the finding that the orientation of the coil has an influence on the primary electric field (Jung et al., 2012; Kaneko et al., 1996; Thielscher, Opitz, and Windhoff, 2011). Thielscher et al. (2011) found the highest field strength occurring at the parts of the gyral crowns that are oriented perpendicularly to the induced field. Opitz et al. (2013) showed

that rotating the coil has a larger effect on the calculated field compared to tilting the coil. The preferred coil orientation was different among people. This study furthermore focused on the impact of the gyrus folding on the induced electric field. An effect of the current direction on the electric field distribution in the GM was found, with higher field strengths when the induced currents were perpendicular to the local gyrus orientation.

Orientation selectivity of TMS was investigated in more detail by Fox et al. (2004). Since most of the times TMS coils are flat and placed tangential to the scalp during stimulation, the resulting current in the brain is also tangential to the scalp. Day et al. (1989) hypothesized that TMS must be exciting the tangentially oriented neural elements at the gyrus crown, such as horizontal interneurons or horizontal collaterals of pyramidal track axons. However, since horizontal fibers are isotropic, this cannot explain the preferred orientation for TMS. Mills et al. (1992) also found a clear orientation preference in TMS. In this study, it was speculated that horizontal fibers might have an anatomic orientation preference which tends to lie at right angles to the central sulcus. Laakso et al. (2014) showed the importance of the coil orientation on the electric field, both the strength and the depth of the penetration, when stimulating the hand motor area. The study of Fox et al. (2004) also showed excitation of the sulcal cortical surface, not on the gyrus crown, in contrast to the hypothesis of Day et al.

The shape of the TMS coil has a major influence on the electric field distribution. Salinas et al. (Salinas, Lancaster, and Fox, 2007) incorporated the coil geometry in the model. It was shown that modeling the electric field induced by TMS based on the wire width, height, shape and number of turns of the coil, clearly improved the fit of calculated-to-measured field near the coil body. Later (Salinas, 2009), the BEM was used to emphasize the importance of the secondary electric field, and it was shown that the direction of the secondary field was generally opposite to the primary field.

C. TMS stimulation protocol

A stimulation protocol has several parameters: the stimulation frequency, and its intensity, pulse shape, and duty cycle. Also the stimulation position is of major importance. A schematic overview is provided in Figure 3.3. This section elaborates on the different parameters that influence the outcome of TMS. Furthermore, the differences between sp, pp, and rTMS are described, as well as the possibility to extend the TMS protocol by priming.

TMS can be applied according to different protocols: sp, pp, and rTMS. Different TMS protocols, and variations of these protocols, have been compared by Mochizuki et al. (2005), Thomson et al. (2011), Hamada et al. (2007), and Sacco et al. (2009). Comparison of reaction times resulting from ppTMS and theta burst stimulation (TBS) (Huang et al., 2005). Mochizuki et al. (2005) revealed that TBS leads to widespread changes in activity and more complex effects on behavior than pp sequences. Thomson et al. (2011) used near infra-red spectroscopy to compare the hemoglobin concentration after sp- and ppTMS over the left prefrontal cortex. The significant, initial, drop in hemoglobin level was not significantly different in different protocols. However, the pp protocol with inter stimulus interval of 15 msec showed significant shorter time for hemoglobin levels to re-

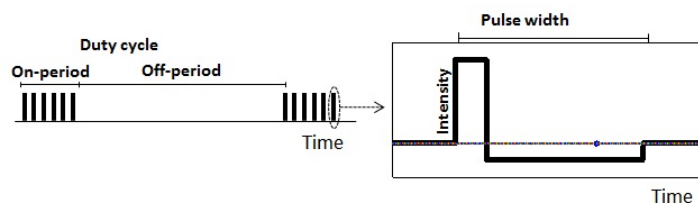


Figure 3.3 — *Stimulation protocol. Overview of a stimulation protocol with the different stimulation parameters; the duty cycle determined by the on- and off-period, the amplitude and the width of the pulse, and the frequency.*

turn back to baseline values. Sewerin et al. (2011) furthermore showed that the efficiency of ppTMS paradigms can be optimized by using patient-specific values of the inter stimulus interval, derived from the response to single pulse stimulation.

Variations of the pp paradigms, triple pulse (Sacco et al., 2009) and quadro pulse stimulation (Hamada et al., 2007), have shown promising for enhancing motor cortical excitability. Triple pulse stimulation showed larger MEP responses than ppTMS (Sacco et al., 2009) and repetitive quadro pulse stimulation led to an even greater enhancement of motor cortical excitability (Hamada et al., 2007), suggesting a summation effect of additional pulses. However, because the inter stimulus intervals of the two studies differ (msec versus sec), it cannot be concluded that the addition of a pulse in a pp protocol further enhances cortical excitability.

Stimulation protocols can be extended by priming. Priming is the application of brief pre-treatment stimulation that might increase the effect of the subsequent stimulation. Silvanto and Pascual-Leone (2008) stated that external stimulation interacts with the ongoing cortical excitability state so the rationale of priming is to optimize this state before stimulation. The cortical excitability state at the particular moment of stimulation will have an effect on, or even determine, the response to stimulation. The outcomes of different priming studies are ambiguous. On the one hand, significant improvements of the clinical effects on depression, after priming, were reported by Fitzgerald et al. (2008) and Iyer et al. (2003). On the other hand, 6 Hz priming before low-frequency (1 Hz) rTMS in a tinnitus population did not show clinical improvements (Langguth et al., 2008), neither did priming of an inhibitory continuous TBS (cTBS) protocol lead to significant changes in MEP sizes in healthy subjects (Todd, Flavel, and Ridding, 2009). Priming cTBS protocols with intermittent TBS (iTBS) showed further inhibition of the cTBS protocol (Doeltgen and Ridding, 2011; Todd, Flavel, and Ridding, 2009). The above mentioned priming studies all use a subthreshold intensity (90% resting motor threshold), but the number of stimuli differs (600 - 1200 pulses), and different outcome measures are used. Appropriate priming protocols still have to be determined and might depend on the pathology. 6 Hz priming seems to work to improve rTMS treatment for depression patients but not for tinnitus and no effect is seen in healthy subjects. To improve and extend the use of priming in clinical practice, more knowledge should be gained about the mechanism of action. To date, this mechanism of priming is believed to be closely related to a phe-

nomenon called metaplasticity: the response of a synapse, the induction of LTP or LTD by for example TMS, depends on the history of the synapse, also sometimes referred to as activity-dependent plasticity (Abraham and Bear, 1996; Todd, Flavel, and Ridding, 2009).

Garry and Thomson (2009) compared the effect of pp paradigms during different excitability states: rest and isometric abduction of the left or right index finger. Effects were shown to depend on the intensity of the test stimulus, but not on the excitability state. Conte (2008) furthermore showed the lack of effect of attention in pp protocols. These findings contradict with the earlier mentioned, general, phenomenon that the outcome of TMS depends on the excitability state. A more refined definition of the excitability state might help to interpret these findings.

Transcranial magnetic stimulators can produce two types of pulses: monophasic and biphasic. Monophasic TMS pulses peak at around 100 μ sec and decay within approximately 1 msec. Biphasic pulses consist of two phases, together lasting for approximately 300 μ sec in which the current of the second pulse flows in opposite direction. Biphasic pulses are energy-efficient compared to monophasic pulses, since up to 60% of the energy needed to produce the pulse can be restored in the stimulator, for example for a next pulse (Pascual-Leone, Davey, and Wasserman, 2001). Arai et al. (2007; 2005) investigated the differences in after-effects between monophasic and biphasic high-frequency rTMS. The main finding of the latter study was that monophasic subthreshold rTMS has stronger, and longer-lasting (in the order of minutes), after-effects on MEPs than biphasic stimulation. This is probably because monophasic pulses preferentially activate one population of neurons oriented in the same direction, causing summation of the effect. This phenomenon only holds for rTMS. In case of single pulses, biphasic pulses are thought to be more powerful because the higher peak-to-peak amplitude between the two phases of the pulse and the longer duration (Arai et al., 2005). Antal et al. (2002) compared static contrast sensitivities before, during, and ten minutes after monophasic and biphasic low frequency (1 Hz) rTMS applied to the occipital cortex at an intensity of the phosphene threshold (PT). Significant loss of contrast was found during, and after 10 min of monophasic stimulation, while biphasic stimulation resulted in no significant effect. The effect of stimulation significantly depended on the current waveform and direction. Niehaus et al. (2000) added that current direction has a higher influence in monophasic stimulation. Delvendahl et al. (2014) furthermore showed a stronger influence of current orientation for monophasic compared to half-sine shaped pulses.

An effective treatment should have long-lasting effects. Thut and Pascual-Leone (2010) reviewed combined TMS-EEG studies to characterize these lasting effects. They suggested that TBS protocols (Huang et al., 2005) show longer after-effects compared to conventional low and high frequency repetitive stimulation protocols (70 minutes versus 31 and 28 minutes). Several factors were suggested to extend the duration of the after-effects such as repeating sessions over days. A recent study by Quan et al. (2015) for example, showed a significant improvement of the negative symptoms in schizophrenia patients six weeks after applying rTMS sessions over a two week period. However, the exact relation between the number of stimulation days and the extension of the after-effects in time, is not known.

Stimulation intensity in TMS protocols is usually defined as a percentage of a subject's individual motor threshold (MT). An international committee defined the MT as the minimal stimulation intensity that induces a reliable MEP of minimal amplitude in the targeted muscle (Rossini et al., 2015). Often, MEPs are recorded from the first dorsal interosseous (FDI) or the abductor pollicis brevis (APB), since these muscles are well represented in the motor hand knob and can be easily stimulated. Thresholds can be determined while the muscle is at rest (resting motor threshold, RMT) or when the muscle is contracted (active motor threshold, AMT). The AMT is lower than the RMT. Besides the MT, the PT is often used in protocols investigating visual responses with TMS (Fierro et al., 2005). A study that assessed the variability in peak intensities of the stimulator, showed that after intensity change, the first stimulus induces a higher peak intensity (Reutens, Macdonnell, and Berkovic, 1993). This might slightly influence the determination of the MT.

MTs vary between and also within subjects (Conforto et al., 2004; Thordstein et al., 2013). Danner et al. (2008) showed that this variation can be reduced by using neuronavigation during stimulation, since neuronavigation can guarantee stimulation of a specific position. Julkunen et al. (2012) mentioned that the MT is highly dependent on the distance between the coil and the cortex. The distance between the scalp and the cortex was not found to have a significant influence (Danner et al., 2012). Janssen et al. (2014) confirmed this finding and stated that the use of MT might be suboptimal when stimulating other areas than the motor areas in the brain because of the large intra-individual differences in coil-target distance and target site anatomy. For this reason, some studies have used a percentage of the maximum stimulation output as stimulation intensity measure (Sparing et al., 2001). Others proposed the use of an adjusted threshold, with a correction for the distance between the motor area and the stimulation location (Stokes et al., 2013). Additionally, Kozel et al. (2000) showed that the distance from the stimulation coil to the cortex in the prefrontal cortex was greater than in the motor cortex in most subjects, with the difference increasing with age. Nahas et al. (2001) showed that subjects with the smallest distance from the coil to the outer cortex showed greater increase in brain activity under the TMS coil.

Table 3.2-3.4 provide an overview of the studies that have been performed to investigate the influence of different stimulation parameters in TMS research: frequency, stimulation position and intensity. Tables 3.5 and 3.6 show an overview of the studies performed to investigate pp paradigms and combinations of parameters.

A general finding is that stimulation above a frequency of 5 Hz increases the excitability whereas stimulation below 1 Hz causes a decreased excitability (Gorsler et al., 2003; Hallet, 2000; Knoch, Brugger, and Regard, 2005; Loo et al., 2003; Sparing et al., 2001). However, this does not always hold since Lin et al. (2014) showed an increase in anti-convulsant properties when frequency increases from 1 to 5 Hz, followed by a decreased effect after increasing the frequency to 10 Hz. A comparable trend in the effect of frequency, however in different frequency ranges, was found by Yadollahpour et al. (2014) in a rat study and by Luber et al. (2007) in healthy subjects. Speer et al. (2000) reported increases in regional cerebral blood flow (rCBF) when stimulating at 20 Hz. In contrast,

Table 3.2 — Overview of rTMS-studies investigating the influence of stimulation parameter: frequency.

Animal/human	Position	Investigate effect on	Frequencies [Hz]	Parameter of interest	Outcome	Source
Depression						
Human	Left and right DLPFC	Treatment of major depression (HF left rTMS versus LF right rTMS)	Low, high	HAMD	No significant difference in responder rate was found	Rossini et al. (2010)
Human	Prefrontal cortex (left and right)	Treatment of major depression (HF left rTMS versus LF right rTMS)	Low, high	MADRS, BDI, HAMD, BPRS, CORE, GAF	HF left rTMS is as effective as LF right rTMS	Fitzgerald et al. (2009)
Human	Left and right DLPFC	Anti-depressant effects	1, 10	HAMD	Left 10 Hz and right 1 Hz showed similar significant anti-depressant effects	Stern et al. (2007)
Human	Left and right DLPFC	Treatment of major depression	1, 20	HAMD, BDI, CGIC	rTMS given at LF over the right frontal cortex appears to be as effective as HF treatment to the left frontal cortex for treatment of depression	Isenberg (2005)
Human	Left prefrontal cortex	Mechanism of action	1, 15	rCBF extracted from SPECT	HF rTMS led to an overall increase, whereas LF rTMS produced a slight decrease in the mean relative rCBF in the left DLPFC	Loo et al. (2003)
Human	Left prefrontal cortex	Anti-depressant effect of daily rTMS	1, 20	rCBF extracted from PET	20 Hz rTMS over the left prefrontal cortex was only associated with increases in rCBF, recorded 72h after the last treatment session. 1 Hz rTMS showed only decreases in rCBF	Speer et al. (2000)
Epilepsy						
Rats	Right motor cortex	Penicillin-induced seizures	1, 5, 10	Density spectral array trend-graphs, iEEG parameters	1 and 5 Hz showed anti-convulsive properties in iEEG seizure profiles. 5 Hz outperformed 1 Hz in seizure suppression. Data from 10 Hz rTMS suggested facilitative characteristics	Lin et al. (2014)
Healthy subjects						
Human	M1	Modulation induced on M1	1, 5	Amplitude of CNV, motor reaction time	Inhibition of motor cortex due to 1 Hz rTMS stimulation, resulted in an amplitude increase of early and late components of CNV, and a slight reducing effect on motor reaction times, while 5 Hz stimulation did not change CNV amplitude	DeTommaso et al. (2012)
Human	M1	ISP	3, 5, 10	ISP derived from EMG of FDI	rTMS of 10 Hz increased the area of ISP. At 3 and 5 Hz, the ISP remained unchanged	Cincotta et al. (2006)
Human	Left or right DLPFC	Inhibition of well-learned routines, relying on frontal lobe functioning	1, 10	RNG performance	Counting bias was significantly reduced after the 1 Hz stimulation compared with baseline, but significantly exaggerated after 10 Hz stimulation	Knoch et al. (2005)
Human	Right motor cortex	Excitability of the unstimulated left motor cortex by stimulating right site	0.5, 5	MEP induced by single pulse TMS	HF right motor rTMS can increase left motor cortex excitability whereas LF right motor rTMS can decrease it	Gorsler et al. (2003)
Schizophrenia						
Human	DLPFC	Schizophrenia outcome	Patient specific peak alpha frequency, 3, 20	PANSS	Individual alpha-TMS demonstrated a significantly larger therapeutic effect than the other conditions	Jin et al. (2006)

BDI = Beck Depression Inventory, BPRS = Brief Psychiatric Rating Scale, CGIC = clinical global impression of change, CNV = contingent negative variation, CORE = rating of psychomotor disturbance, DLPFC = dorsolateral prefrontal cortex, EMG = electromyography, FDI = first dorsal interosseous, GAF = global assessment of function, HAMD = Hamilton Depression Rating Scale, HF = high frequency, HV = healthy volunteers, iEEG = intracranial EEG, ISP = ipsilateral silent period, LF = low frequency, MADRS = Montgomery-Asberg Depression Rating Scale, MEP = motor evoked potential, PANSS = positive and negative syndrome scale, PET = positron emission tomography, rCBF = regional cerebral blood flow, RNG = random number generation, SPECT = single photon emission computed tomography.

a decrease in rCBF was found at 10 Hz. The application of high frequency left rTMS and

Table 3.3 — *Overview of rTMS-studies investigating the influence of stimulation parameter: stimulation position.*

Position	To investigate the effect of	Parameter of interest	Outcome	Source
Depression				
Left and right DLPFC	A single rTMS session on a go/no-go task	Task performance	Performance significantly improved after right DLPFC rTMS	Bermppohl et al. (2006)
Healthy subjects				
Primary motor cortex and primary visual cortex	Stimulation on the TEPs in different locations	TEPs	1 Hz rTMS over the motor cortex appears to increase the amount of inhibition following a TMS pulse. No effect was found after stimulation of the visual cortex.	Casula et al. (2014)
DLPFC and MPFC	Prefrontal 1 Hz rTMS by stimulating the generators of ERPs in the prefrontal cortex	N2 amplitude in a go/no-go task	After 1 Hz rTMS of the left DLPFC (but not of the MPFC) in inhibitory effect on the N2 amplitude was observed. After 1 Hz rTMS of the MPFC, a trend towards an increased P3 amplitude was found.	Grossheinrich et al. (2013)

DLPFC = dorsolateral prefrontal cortex, ERP = event related potential, HV = healthy volunteers, MPFC = medial prefrontal cortex, TEP = TMS evoked potential.

low frequency right rTMS has comparable anti-depressive effects which might suggest that the effect of frequency depends on the stimulation position (Fitzgerald et al., 2009a; Isenberg et al., 2005; Rossini et al., 2010; Stern et al., 2007). However, when the knowledge about the pathology, in this case depression, is taken into account, this effect might also be explained by the imbalance between left and right hemispheres in patients with depression (Grimm et al., 2008). The effect of frequency might also be patient-specific, as shown by Jin et al. (2006).

The direction of the effect of TMS, inhibitory or excitatory, might also depend on the number of stimuli and the spacing, the period between stimulation trains, as was shown in TBS studies performed at intensities derived from the AMT (Gamboa et al., 2010; Gamboa et al., 2011). Conventional inhibitory cTBS and excitatory iTBS protocols (Huang et al., 2005) were compared to prolonged protocols, containing twice as many pulses. The prolonged continuous protocols showed excitatory effects and the prolonged intermittent protocol showed inhibitory effects (Gamboa et al., 2010). A later study showed that different spacing might enhance or decrease the effect of a single stimulation train (Gamboa et al., 2011). Voluntary motor activation, necessary for AMT determination, has also been shown to influence the effect of TBS (Gentner et al., 2008).

The choice of the stimulation target and positioning of the TMS coil on the scalp depends on knowledge of the pathology to be treated. For example in depression, the left dorsolateral prefrontal cortex (DLPFC) is known to be hypoactive (Koenigs and Grafman, 2009). Therefore, a facilitating TMS protocol targeted at this position is deemed relevant to improve depression symptoms. Compared to depression, the variability of the expression of epilepsy is larger: in case of focal epilepsy, the focus can be located in different parts of the brain resulting in various patient-specific stimulation positions. Superficial foci, such as for example in epilepsy patients with focal cortical dysplasia, can be stimulated directly. The hyperexcitable characteristics of epilepsy aim for an inhibiting, low frequency, stimulation protocol (Sun et al., 2012). Deeper foci might be stimulated indirectly, by stimulating cortical areas that are known to be functionally connected to the

Table 3.4 — Overview of TMS studies in healthy volunteers investigating the influence of stimulation parameter: stimulation intensity.

TMS	Animal/human	Position	Investigate effect on	Intensity	Parameter of interest	Outcome	Source
sp	Human	Hotspot for ADM MEP	TEPs	60, 80, 100, 120% RMT	TEPs in the EEG (GMFA and peak amplitudes)	Also low intensities (60% RMT) were able to induce TMS evoked brain responses. The peak amplitudes depend nonlinearly on the intensity.	Komssi et al. (2004)
r	Human	Primary motor cortex (M1)	Local and distant effects on brain activity	80, 90, 100, 110, and 120% of twitch threshold	rCBF extracted from PET	1 Hz rTMS delivered to the primary motor cortex (M1) produces intensity-dependent increases in brain activity locally and has associated effects in distant sites with known connections to M1.	Speer et al. (2003)
r	Human	Left PFC	Intensity-related changes in brain	80, 90, 100, 110, and 120% of twitch threshold	rCBF extracted from PET	Stimulation intensity was found to be inversely correlated with the rCBF in the stimulated and contralateral PFC and other areas	Speer et al. (2003)
r	Rats	Rat's head	LTP in the rat hippocampal CA1	0.75T (<RMT) and 1.00T (>RMT)	LTP recorded after stimulating brain slices	LTP was enhanced only in the 0.75 T rTMS group, while no change was observed in the 1.00 T rTMS group	Ogiue-Ikeda et al. (2003)
r	Human	Hotspot for APB muscle activation	Inhibitory function and cortical excitability	85, 115% RMT	Inhibitory function, RMT and MEP size	rTMS at both intensities produced an increase in the RMT but only 115% stimulation reduced the size of MEPs. rTMS had no effects on the cortical silent period or cortical inhibition measured with pp TMS	Fitzgerald et al. (2002)
r	Human	Left PFC	Bilateral effects as measured by interleaved BOLD fMRI	80, 100, 120% RMT	BOLD fMRI activation maps	All intensities activated auditory cortex, with 80% RMT having no other area of significant activation. 100% MT showed contralateral activation and 120% MT showed bilateral prefrontal activation	Nahas et al. (2001)

APB = abductor pollicis brevis, ADM = abductor digiti minimi, BOLD = blood oxygen level dependent, GMFA = global mean field amplitude, LTP = long-term potentiation, MEP = motor evoked potential, PET = positron emission tomography, PFC = prefrontal cortex, rCBF = regional cerebral blood flow, RMT = resting motor threshold, TEP = TMS evoked potential.

foci or by the use of coils designed to stimulate deeper structures. Table 3.3 lists some findings about the influence of the stimulation position on the outcome of TMS. For example, the performance of a go/no-go task improved after rTMS of the right DLPFC, but not after stimulation of the left DLPFC (Bermppohl et al., 2006). Also, differences between stimulation of the DLPFC and the medial prefrontal cortex (Grossheinrich et al., 2013) and the primary visual cortex were listed (Casula et al., 2014).

The effects of the stimulation position might be linked to the effect of the stimulation intensity. The two studies by Speer et al. (2003; 2003) showed opposite intensity-dependent effects of the stimulation when stimulating the primary motor cortex and the left prefrontal cortex using the same stimulation protocol. Komssi et al. (2004) found a non-linear relation between the peak amplitudes of TMS evoked brain responses and the intensity. Imaging studies showed that higher intensity TMS in general produced more activity under the coil as well as in contralateral brain regions (Fitzgerald et al., 2002). Also intensities below the MT were able to induce brain responses (Table 3.4).

In pp studies, Vucic et al. (2009) and Schäfer et al. (1997) found maximum short-interval

Table 3.5 — *Overview of research into stimulation parameters for paired-pulse TMS studies in healthy volunteers.*

Position	Goal	Parameter of interest	Outcome	Source
Hotspot of tongue motor cortex	To investigate the influence of multiple parameters on SICI and ICF	1. Body position (recline and supine), inter-stimulus intervals (ISI, 2, 10, 15 ms) between the TS (120, 140, 160% RMT) and CS (80% RMT) 2. ppTMS ISI (2, 2.5, 3 ms), CS (70, 80% RMT), TS (120% RMT)	1. Significant effect of body position, TS intensities and ISIs and interaction between intensity and ISIs, 2. Significant effect of ISI but not CS intensity on MEP amplitude	Kothari et al. (2014)
APB hotspot	To investigate SICI at three different CS intensities (40, 70, 90% RMT)	CMCT	Maximum SICI developed with CS set to 70% RMT	Vucic et al. (2009)
Motor cortex	To investigate the variability in cortical excitability by comparing sub-and suprathereshold intensity of CS (80% versus 120% of individual RMT)	EMG response in ADM	Reductions in EMG response in the ADM after CS in one hemisphere and TS in the opposite hemisphere (in a range of 12 ms) were found after CS of 120%	DeGennaro et al. (2004)
Vertex	To investigate the influence of the intensity of the CS on ICI and ICF with different ISI (3 versus 13 ms)	Latencies and areas of motor evoked potentials in right extensor carpi radialis muscle	MEP areas of 3 ms and 13 ms showed a different dependency on the intensity of the CS. Changes in MEP latencies were comparable	Koshev et al. (2003)
Left motor cortex	To investigate the influence of stimulus parameters (intensity of the CS varying from 0 to 100% RMT and ISI of 1, 3, and 5 ms)	CMAP	Maximal reduction of the amplitude of the MEPs was found at a CS intensity of 65% RMT and ISI of 1 ms	Schafer et al. (1997)

ADM = abductor digiti minimi, APB = abductor pollicis brevis, CMAP = compound muscle action potential, CMCT = central motor conduction time, ICF = intracortical facilitation, ICI = intracortical inhibition, ISI = inter-stimulus interval, MEP = motor evoked potential, RMT = resting motor threshold, SICI = short-interval intracortical inhibition.

intracortical inhibition (SICI) and maximum MEP reduction at 70% and 65% of RMT respectively. Both studies investigated a range of intensities for the CS, suggesting that the intensities below around 70% RMT cause an increase in inhibiting effect and higher intensities attenuate the effect. A contrasting finding was reported by De Gennaro et al. (2004), who only showed a reduction in EMG response, measured in the abductor digiti minimi in the hand, using a CS of 120% RMT.

Table 3.6 — *Overview of research into combination of parameters in rTMS studies.*

Animal/ human	Position	Investigate	Parameters and values	Parameter of interest	Outcome	Source
Depression						
Human	Prefrontal cortex	the regional blood flow after SPECT	Frequency (5, 20 Hz) and coil- cortex distance	rCBF	20 Hz rTMS caused more relative flow below the TMS coil, compared to 5 Hz rTMS. Patients with smallest distance from coil to outer cortex showed greatest increase in brain activity at the site of stimulation	Nahas et al. (2001)
Human	Left pre- frontal cortex	Response rate of left sided stimulation (at 5 and 10 Hz) after failed response on right sided stimulation	Frequency (5 and 10 Hz) and position (left versus right prefrontal cortex)	HAMD, MADRS	Small but significant response was found to left sided stimulation, independent of the frequency	Fitz- gerald et al. (2009)
Epilepsy						
Rats	Spot with the maximum resultant electric field in kindling focus	the anti-epileptic effect	Frequency (0.5, 1, 2 Hz) and coil shape (figure- of-eight versus round)	ADD, progression of kindling (cumulated)	rTMS had anti-epileptogenic effects at all frequencies. The inhibitory, anti-epileptic, effect was higher at 1 Hz compared to 0.5 and 2 Hz. Application of rTMS 1 Hz by circular coil imposed a weaker inhibitory action compared with the figure-of-eight coil	Yadol- lah- pour et al. (2014)
Human	Epileptic focus or central ver- tex (in case nonfocal/- multifocal epilepsy)	the anti-epileptic effect	Stimulation duration (3000 versus 1500 pulses) and position (see po- sition)	Seizure fre- quency	Longer stimulation subgroup tended to have fewer seizures (not statistically significant). TMS stimulation site and structural brain lesions did not influence seizure outcome. Interictal spikes decreased significantly	Joo et al. (2007)
Healthy volunteers						
Human (and model)	Primary motor cortex	MEP sizes	Stimulation intensity (85%, 100% and 115% RMT) and number of pulses (up to 1800)	MEPs	Results showed that more pulses and stronger intensities lead to a larger decrease in MEP amplitude at 1 Hz stimulation	Nojima et al. (2013)
Human	V5/MT	to test the effects on MAE	Intensity (20% versus 90% PT), stimulation hemisphere	MAE	No main effects were reported. No effect of motion direction, stimulation location, stimulation intensity or side was found	Murd et al. (2012)
Human	SMG	P300 latencies of the ERP	Frequency (0.25, 0.5, 0.75, 1 Hz) and hemisphere	P300 latency	P300 is only altered when stimulating left SMG at 1 Hz (lengthened 15 msec) or 0.75 Hz (shortened 15 msec)	Torii et al. (2012; 2012)
Human	M1/PMC	excitability of the FDI corticospinal pathway	frequency (1, 20 Hz) and intensity (90, 115% RMT)	Input- output curve (in- tensity versus MEP threshold)	LF115 over M1 increased the slope of the FDI input-output curve but did not change the S50 and plateau value. HF90 led to a more complex effect with an increase in the slope and a decrease in the S50 and plateau value	Hou- dayer et al. (2008)
Human	Precuneus on working memory	Frequency (1, 5, 20 Hz) and timing (presentation versus retention phase)	RT	Only 5 Hz stimulation to the parietal site resulted in a significant decrease in RT.	Significant speeding of RT occurred in the retention phase but not the probe phase	Luber et al. (2007)
Human	Left pri- mary motor cortex (M1)	on inhibitory after-effects	Stimulation intensity (10% below or 15% above RMT), two different figure-of-eight shape coils	TMS in- duced MEPs from FDI	Suprathreshold 1 Hz rTMS has bigger effect on suppression of corticospinal excitability. Coil manufacturer also has influence	Lang et al. (2006)

Continued on next page

Table 3.6 — *Overview of research into combination of parameters in rTMS studies.*

Animal/ human	Position	Investigate	Parameters and values	Parameter of interest	Outcome	Source
Cats	Occipital cortex	on VEPs and EEG	Stimulation frequency (1, 3, and 10 Hz) and duration of the protocol (1, 5, 20 min)	VEP and EEG recordings	Short high-frequency trains seem to be more effective than longer trains, and low-frequency rTMS requires longer application. Changes in the spectral composition of the EEG were not correlated to changes in VEP size	Aydin-Abidin et al. (2006)
Human	Left or right DLPFC	lateralized and frequency- dependent effects	Frequency (1, 10 Hz) and hemisphere	rCBF changes recorded by PET	Right prefrontal rTMS induces a different pattern of rCBF changes than left prefrontal rTMS	Knoch et al. (2006)
Human	Wernicke's area	picture naming	Frequency (1, 20 Hz), intensity (35, 45, 55% MSO)	Naming latency	Naming latency could be facilitated only immediately after Wernicke's area stimulation at a frequency of 20 Hz and at an intensity of 55% MSO, which is more than the motor threshold	Sparing et al. (2001)
Rats	Rat's head	Effect of TMS compared to those produced by other anti-depressant treatments, in particular to repeated ECS	Stimulation frequency (20 versus 30 Hz) and number of sessions (9 versus 18 days)	Porsolt's forced swimming test	Standard ECS reduced the immobility by 50%, effects of rTMS were smaller (significant though). The stimulation at 20 Hz required 18 treatment sessions to produce a significant effect, while only 9 sessions with stimulation at 30 Hz were necessary	Zyss et al. (1999)
Human	APB hotspot	MEP size	Intensity, coil orientation (360 degrees in steps of 45 degrees), 2 different coils	MEP size	Orientation of maximum MEP size depend on coil type. Influence of the stimulation frequency also depends on coil type	Brasil-Neto et al. (1992)

ADD = after-discharge duration, APB = abductor pollicis brevis, DLPFC = dorsolateral prefrontal cortex, ECS = electroconvulsive shock, ERP = event related potential, FDI = first dorsal interosseus, HAMD = Hamilton Depression Rating Scale, HF = high frequency, HV = healthy volunteers, LF = low frequency, MEP = motor evoked potential, MADRS = Montgomery-Asberg Depression Rating Scale, MAE = motor after-effects, MSO = maximum stimulator output, MT = motor threshold, PET = positron emission tomography, PMC = premotor cortex, PT = phosphene threshold, rCBF = regional cerebral blood flow, RMT = resting motor threshold, RT = reaction time, SMG = supramarginal gyrus, SPECT = single photon emission computed tomography, VEP = visual evoked potential.

When investigating rTMS as treatment option for epilepsy, the anti-epileptic effect was more pronounced when a figure-of-eight coil was used, and was shown to depend on the frequency of the stimulation and the duration of the protocol (Joo et al., 2007; Yadollahpour et al., 2014). Studies in healthy animals show a relation between the duration of the protocol and the frequency: higher frequencies require shorter protocols (Aydin-Abidin et al., 2006; Zyss, Mamczarz, and Vetulani, 1999).

According to Nojima et al. (2013) the combination of long protocols and high intensities can also emphasize the effect of TMS: a larger decrease in MEP amplitude was found with increasing intensities and duration of a 1 Hz stimulation protocol. An extensive review by Pell et al. (2011) stated that there is quite some dependency among the different stimulation parameters.

3.3 Summary of technical aspects of TMS

In clinical practice, figure-of-eight coils are mostly used to perform relatively focal TMS. Single- and paired-pulse protocols can be used if one wants to study the functioning of the brain whereas repetitive stimulation protocols are necessary to obtain a long-lasting, therapeutic effect. In rTMS studies, monophasic pulses have shown to have longer-lasting

effects on MEPs compared to biphasic pulses. However, because of efficient energy consumption in the stimulator, biphasic pulses are mostly used in rTMS protocols. In single pulse protocols, biphasic pulses are more effective.

The transfer from simple head models, assuming homogeneous and isotropic brain properties, to more complex models including position- and direction-specific properties probably leads to more accurate calculations of the electric field induced by TMS. The shape of the TMS coil, the position, and more specifically, the orientation have a major influence on the electric field distribution. The preferred coil orientation differs between people, indicating the importance of incorporating patient-specific anatomical information in the models. Various pathologies require different stimulation protocols. For example, the hyperexcitable characteristics of epilepsy make inhibiting protocols, so low frequency protocols or continuous TBS protocols, suitable. Depression requires facilitating, high frequency or intermittent TBS protocols when stimulating the left DLPFC.

The stimulation intensities are often defined as a percentage of a subject's individual motor threshold. It is not sure if this percentage is also representative for stimulation outside the motor cortex. Correction methods, e.g. for the distance between stimulation position and motor cortex, can be used.

Higher stimulation intensities and longer protocols have been suggested to enhance the strength and duration of the therapeutic outcome. The effect of TMS might be reversed after extending protocols beyond a certain duration. In determining the final stimulation protocol, the burden on the patient should also be taken into account. The guidelines for the use of TMS are published (Rossi et al., 2009).

3.3.1 Transcranial direct current stimulation (tDCS)

tDCS is another non-invasive brain stimulation method in which a weak current is applied to the brain via a pair of large, spongy, electrodes. Generally, positioning the positively charged electrode (the anode) over the stimulation target causes enhancement of neural activity, whereas positioning the negatively charged electrode (the cathode) over the target reduces excitability (motor cortex stimulation at 1 mA) (Nitsche et al., 2008; Paulus, 2011). An important difference between tDCS and other brain stimulation techniques is that tDCS does not induce direct activation by neural action potentials because the tDCS static fields, in the range of approximately 0.5 - 2 mA, are not strong enough (Nitsche et al., 2008). It is believed that tDCS modifies the transmembrane neural potential and thus influences the level of excitability (Wagner et al., 2007). tDCS is therefore often referred to as a brain modulation technique instead of a brain stimulation technique (Parazzini et al., 2011).

Common adverse events of tDCS were reviewed by Brunoni et al. (2011). The occurrence of adverse events was compared between an active stimulation group and a sham group. Itching was the most commonly reported adverse event (39.3% versus 32.9%), followed by tingling (22.2% versus 18.3%), headache (14.8% versus 16.2%), burning sensation (8.7% versus 10%), and discomfort (10.4% versus 13.4%). Although tDCS is presently

not approved for any indication, the FDA has cleared some tDCS devices as having a non-significant risk. The rules for using tDCS vary from country to country (Fregni et al., 2014). tDCS is currently being investigated in clinical trials to treat depression, anxiety, attention deficit hyperactivity disorder (ADHD), epilepsy, and tinnitus (Brunoni et al., 2013).

Besides tDCS, also transcranial alternating current stimulation (tACS) or transcranial random noise stimulation (tRNS) are investigated to modulate cortical excitability. An oscillating electric field with either a specific frequency, or white noise in the range of 0.1 - 640 Hz, is used for tACS and tRNS respectively (Antal and Paulus, 2013; Paulus, 2011; Terney et al., 2008). Where tDCS used a constant field to induce membrane polarization to change the spiking rate of neurons, tACS uses an oscillating field aiming to induce network synchrony and changes in the phases of the spiking (Antal and Paulus, 2013; Zaghi et al., 2010). Brain oscillations are closely related to multiple cognitive functions (Herrmann et al., 2013). With these techniques directional sensitivity of standard tDCS can be avoided. The main characteristics of tDCS, tACS, and tRNS are shown in Table 3.7 (adapted from Kadosh (2014)). However, the remainder of the review will focus on tDCS.

Table 3.7 — Overview of the main characteristics of tDCS, tACS, and tRNS, adapted from Kadosh (2014).

	tDCS	tACS	tRNS
Current delivered	Small direct, constant current (0.5-2 mA)	Bidirectional, biphasic current in sinusoidal waves (0.25-mA), frequency 1, 10, 15, 30, 45 Hz, voltage 5-15 mV	Alternating current with random amplitude and frequency (0.1-640 Hz), intensity between -500 and 500 μ A, sampling rate 1280 Hz, current of 1 mA
Typical stimulation time	20 min	2 and 5 min	10 min
Effect on cortical excitability	Increased excitability with anodal stimulation, decreased excitability with cathodal stimulation	No effects found	Unambiguous findings: tRNS might enhance cortical excitability, potentially with reduction of rCBF without affecting regional cerebral metabolic rate of oxygen consumption
Mechanism of action	Membrane polarization	Interfere with ongoing brain oscillations by entraining or synchronizing neuronal networks	Not known

rCBF = regional cerebral blood flow

A. Equipment: tDCS electrodes

In tDCS, constant currents are applied via patch electrodes with surface areas ranging from 16 - 100 cm² (e.g. Kuo et al. (2013) and Martin et al. (2014)). In its simplest form, the DC source is placed in series with the scalp electrodes and a potentiometer, which is used to adjust the constant current. The configuration and the shape of the tDCS electrodes determine which part of the brain is actually stimulated.

Datta et al. (2008; 2009) investigated the influence of different tDCS electrode configurations. The degree of shunting, the loss of effective current through the scalp because of the relatively high resistivity of the skull, depends on the configuration of the electrodes. Decreasing the distance between the electrodes results in an increased amount of shunting

and more current is necessary to obtain an equivalent peak cortical electric field. In case the reference electrode is placed over the scalp, anodal stimulation of one cortical area is combined with cathodal stimulation and vice versa. Increasing the size of the reference electrode was shown to result in a decreased effect of the functionally efficient reference electrode (Nitsche and Doemkes, 2007). To prevent unwanted excitability changes under the reference electrode, the efficacy of various montages using cranial and extracranial reference electrode positions for tDCS was investigated (Moliadze, Antal, and Paulus, 2010). The distance between the electrodes correlated negatively with the duration and size of the induced after-effects suggesting that stimulation intensity should be adapted to compensate for the inter electrode distance, which is relatively large when using an extracranial reference electrode.

The low spatial focality is considered to be a limitation of tDCS. Focality can be increased by reducing the size of the stimulation electrode (Nitsche and Doemkes, 2007) or by using ring electrode configurations, containing a cathodal ring electrode surrounding an anodal inner disc electrode. In this case, the focality also depends on the distance between the anodal and cathodal part of the electrode. Increasing the ring diameter decreases the fraction of shunting but also decreases focality (Datta et al., 2008; Datta et al., 2009).

B. Electric field modeling

The electric field in the brain after tDCS is comparable to the secondary field induced by TMS (see Section 3.2.1.B) because there is no rapidly changing current in case of tDCS. The skull strongly affects the electric field resulting from tDCS because of its high resistivity to electrical current. Studies modeling the electric field have been performed (Eaton, 1992; Kim et al., 2014; Metwally et al., 2012; Parazzini et al., 2014; Ravazzani et al., 1996; Roth and Basser, 1990; Ruohonen, 1995; Salvador et al., 2010; Salvador et al., 2012; Shahid, Wen, and Ahfock, 2013; Tofts and Branston, 1991) and showed that the induced electric field is not restricted to the area close to the stimulation electrodes. This section describes the electric field distributions resulting from models that incorporate between five and forty tissue types. Also the effects of skull composition and different electrode configurations are mentioned.

Salvador et al. (2010) discovered, by using high resolution FEM in a five-layer head model, that the maxima of the current densities do not appear on the gyri under the electrodes but in localized hotspots at the bottom of the sulci. In a later study, Salvador et al. (2012) further emphasized the importance of the conductivity values in the modeling studies. In isotropic models, it was shown that decreasing the conductivity of the skin resulted in increased maximum values of all field components, on both the CSF-GM and the GM-WM interface. The distribution of the electric field, however, remained almost unaltered. Decreasing the conductivity of the skull led to an expected decrease of electric field values. In this case, also the distribution of the field was affected significantly. According to Salvador, the skull is the tissue whose conductivity mostly influences the electric field distribution. Parazzini et al. (2011; 2012; 2014) used 40 different tissue types for the head models. It was shown that the region with the maximum induced field is usually below or close to the anode. Variations in the size of the anodal or cathodal electrodes resulted in different electric field distributions. It was furthermore shown that

variations in the injected current are linearly correlated with the field amplitudes.

Shahid et al. (2013) and Wagner et al. (2014) explicitly investigated the effect of adding more compartments to electric field models. Shahid et al. (2013) focused on the estimation of the contribution of regional anisotropic conductivity to the spatial distribution of an electric field across GM, WM, and subcortical regions. Four models were analyzed in this study. The first model contained average isotropic conductivity values assigned to 19 segmented tissues. Three additional models were derived from the base model by assigning different conductivity values to the cortical and subcortical regions and taking into account the anisotropies. By comparing the different models, it was shown that anisotropy causes variations in the strength of electric field hotspots across the cortex. The formation of active zones away from regions directly under the electrodes is attributed to the location of electrodes, geometry of the cortex, and a highly conductive CSF layer, which also acted as a region of high current density. Wagner et al. (2014) started with a three compartment model and extended this model to six compartments in a step by step process. A new method was used to model the anisotropy in white matter conductivity, based on a reversed gradient approach. Incorporation of the specific conductivity values for spongiosa and compacta bone in the skull (conductivity of the spongiosa areas being approximately 3.5 times higher) resulted in a change in electric field, depending on the position of the electrodes. The closer the electrodes are to the spongiosa, the more current is shunted through the spongiosa resulting in decreased brain current density. Incorporation of the CSF in the model also leads to a more inhomogeneous current distribution in the brain, mainly because of the high conductivity of CSF. Modeling the white matter regions turned out to be mostly important when considering deeper target regions in the brain. Also, Metwally et al. (2012) emphasized the importance of incorporating the anisotropic characteristics of the skull and white matter in the brain models used for electric field modeling in tDCS. Incorporation of tissue anisotropies resulted in more diffused electric field in the white matter.

The impact of skull thickness and composition was recently investigated by Opitz et al. (2015). Different correlations were found between the electric field strengths resulting from the full model, including the distinction between spongiosa and compacta areas in the skull, and from the reduced model, in which the conductivity values of spongiosa and compacta areas were modelled equally. In general, thinner skull regions lead to higher electric field strengths. However, this is not a linear effect since the thicker parts of the skull contain more spongiosa areas with higher conductivities.

Besides the different models used by Shahid et al. (2013), four different electrode configurations were investigated. Different configurations resulted in distinct field patterns with noticeable variations in their strengths. The hotspots across the cortex were mostly located between and in the proximity of electrodes. Generally, it is expected that an increase in the distance between the electrodes would enhance the strength of the electric field in the brain. But it appeared that the distance between the electrodes is not as important as their relative locations. The skull thickness and composition also affect the electric field distribution in the brain (Opitz et al., 2015a). FEM can be used to derive the optimal electrode position for tDCS (Im et al., 2008; Rampersad, Stegeman, and Oost-

endorp, 2013). By simulating the electric fields induced by tDCS for different electrode configurations, it was shown that the optimized configurations do not coincide with the configurations that are commonly used (Rampersad, Stegeman, and Oostendorp, 2013).

C. tDCS stimulation protocol

Positioning of the electrode patches, the distance between the patches, stimulation duration, and stimulation intensity are the most important parameters in a tDCS stimulation protocol. Studies investigating the effect of these parameters on the outcome of tDCS studies are described in this section. Batsikadze et al. (2013) investigated the effect of stimulation intensity after applying tDCS to healthy volunteers. Whereas both anodal and cathodal 2 mA stimulation of the left primary motor cortex were found to induce a significant increase in MEP amplitudes, as recorded from the FDI, 1 mA cathodal tDCS decreased the corticospinal excitability, suggesting an intensity-dependent effect on polarity. Shekhawat et al. (2013) investigated the influence of stimulation intensity and duration on the response effect for suppression of tinnitus. Twenty minutes of 2 mA stimulation was found to be most effective. An interaction was found between duration and intensity of the stimulus on the change in rated loudness of tinnitus and clinical global improvement score. The general tendency, that longer stimulation induces longer after-effects (in the order of minutes and sometimes even hours), is expected to hold only for cathodal tDCS (Paulus, 2011). An anodal tDCS study has shown that the excitatory after-effects finally resulted in inhibition after applying 26 min of anodal tDCS, suggesting an upper limit for excitatory after-effects (Monte-Silva et al., 2013; Paulus, 2011). Dieckhofer et al. (2006) compared anodal with cathodal stimulation by recording low and high frequency components of somatosensory evoked potentials. Cathodal tDCS induces a significant reduction of the N20 (the negative evoked potential after 20 ms) component while there was no effect after anodal stimulation. No changes in source activity were found for the N30 (the negative evoked potential after 30 ms) component or high frequency oscillations, suggesting distinct generators of the low and high frequency sources. Two different montages were furthermore compared in a patient with tinnitus (Parazzini, Fiocchi, and Ravazzani, 2012). It was shown that tDCS of the left temporoparietal cortex resulted in a widespread distribution of the electric field whereas tDCS of the DLPFC showed a concentrated field.

3.3.2 Summary of technical aspects of tDCS

In tDCS, low current is applied via patch electrodes. Generally, anodal stimulation causes neuronal excitation whereas cathodal stimulation causes inhibition. However, the direction of the effect also depends on the stimulation intensity and the stimulus duration: excitatory effects might become inhibitory when the duration of stimulation is extended beyond approximately 20 minutes. The stimulation intensity depends on the distance between the electrodes. The distance between the electrode patches affects the electric field strength, because decreasing the distance results in an increased amount of shunting and more current is necessary to obtain an effect. Positioning of the tDCS electrodes highly depends on the stimulation target. The electric field is not confined to the proximity of the stimulation electrodes, but also occurs distant from regions under the electrodes. One of the possible causes is the highly conductive layer of CSF. The anisotropic properties and

even also the composition of the skull affect the electric field distribution. Incorporation of the white matter properties is most important when the focus is on the electric fields deeper in the brain.

3.4 Invasive neurostimulation

In invasive neurostimulation techniques, electrodes are placed in direct contact with excitable tissue during a surgical procedure. Figure 3.4 provides an overview of the positioning of the electrodes and pulse generators for VNS, DBS and responsive neurostimulation (RNS).

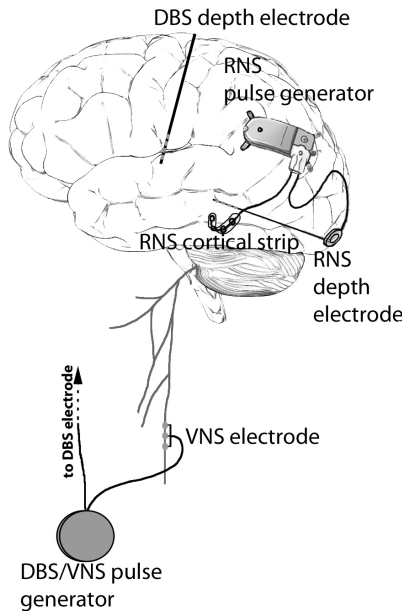


Figure 3.4 — *Invasive brain stimulation. Overview of invasive stimulation techniques. An example of the positioning of the electrodes of DBS and RNS within the brain and the VNS electrodes in the cervical region. Also the position of the pulse generators are shown for the different stimulation modalities.*

3.4.1 Vagus nerve stimulation (VNS)

VNS is a stimulation technique in which the vagus nerve, the tenth cranial nerve, is stimulated. The technique was developed in the eighties and was approved for the treatment of partial-onset epilepsy by the European Union in 1994 (Ben-menachem, 2002) and by the FDA in 1997. For depression, VNS gained CE approval in 2001, and FDA approval in 2005 (Amar et al., 2008). Over 100,000 patients have been implanted with the Neurocybernetic Prosthesis System (Cyberonics Inc., Houston, Texas), a device that is implanted under the skin in the left pectoral area and delivers stimulation through a bipolar lead that

is wound around the vagus nerve in the cervical region.

Stimulation is performed on the left vagus nerve, since the right vagus nerve has more dense projections to the atria of the heart which could theoretically result in negative adverse events during stimulation. The most prevailing side effect of VNS is hoarseness with or without voice alterations (55% (Sackeim et al., 2001), 60 - 62% (Ben-Menachem, 2001)). Also, the occurrence of dyspnea (16%, 23%), pain (17%, 27%), headache (20%, 30%), and infection (4%, 3%) was reported in an epilepsy study (Handforth et al., 1998) and a depression study (Rush et al., 2000) respectively. The side effects are usually related to periods in which the stimulation is on and seemed to diminish over time (Ben-Menachem, 2001; Boon et al., 2001b; Boon et al., 2007a; Vonck et al., 2001; Vonck et al., 2012). Important structures in the mechanism of action of VNS are the locus coeruleus (LC), the nucleus tractus solitaries (NTS), the thalamus, and the limbic structures (Krahl and Clark, 2012; Woodbury and Woodbury, 1990). The NTS, located in the brainstem, is bilaterally innervated by afferents of the vagus nerve during unilateral stimulation. So unilateral VNS can influence both hemispheres. Neurotransmitter release possibly plays a role in the mechanism of VNS. The LC is a noradrenergic nucleus which is known to have for example anti-epileptic effects (Boon et al., 2001b; Vonck et al., 2008; Vonck et al., 2003; Vonck et al., 2001).

Typically, the stimulation is automatically provided according to a certain duty cycle which does not require any intervention from the patient. In addition, the VNS device can be triggered to deliver one stimulation train by means of a handheld magnet when patients experience an aura or by caregivers who witness seizures. Boon et al. (2001) and Tatum and Helmers (2009) investigated the efficacy of the magnet. Even though, in most cases, an intervention from caregivers was required, the magnet was considered an added value in controlling seizures (Boon et al., 2001a).

Based on the promising results obtained with the magnet, responsive VNS (rVNS) is being investigated for epilepsy. Responsive stimulation means that stimulation is only provided after a trigger is detected. In case of rVNS, the trigger can be extracted from the patient's electrocardiogram. Seizure-related cardiac changes, such as ictal tachycardia or increase in heart rate, occur in over 70% of the epileptic seizures. A case study using this novel VNS device reported a decreased seizure duration in a patient with refractory epilepsy (Hampel et al., 2015). A large prospective randomized trial has been performed in the European Union, demonstrating that the cardiac based seizure detection algorithm, incorporated in the device, has a high sensitivity. Long-term results on seizure duration and severity are pending (Boon et al., 2014).

Even though this review focuses on invasive VNS, recently also non-invasive transcutaneous VNS (tVNS) has been developed which involves unilateral external transcutaneous stimulation of the auricular branch of the vagus nerve using an external pulse generator (Stefan et al., 2012) (see Figure 3.1). tVNS has demonstrated initial efficacy in epilepsy (Ellrich, 2011; He et al., 2013; Stefan et al., 2012) and depression (Rong et al., 2012). These results should be interpreted with caution since they were obtained in small pilot studies.

A. VNS electrodes

Per definition, so independent of the pathology, VNS stimulates the vagus nerve using a specially designed electrode that surrounds this nerve. Compared to other stimulation techniques, the variation of electrode position and shape of the electrode is limited.

The VNS lead contains helical cuffs that contain one positive and one negative electrode and one anchor tether that surround the vagus nerve. Two sizes are available for clinical practice, with a helical inner diameter of 2 or 3 mm. Materials typically used are platinum, iridium and stainless steel as conductors and silicone rubber, polytetrafluorethylene and polyimide as insulating carriers (Rodriguez et al., 2000). Cuff-electrodes may have several advantages compared to intramuscular, epymisial and surface electrodes. Firstly, these electrodes reduce the stimulus intensity required for nerve activation minimizing hazardous electro-chemical processes secondary to charge delivery and diminishing the power consumption of the stimulator system. Secondly, cuff-electrodes are more flexible with respect to the positioning of the electrode which minimizes mechanical distortion and the probability of lead failure (Rodriguez et al., 2000).

B. Electric field modeling

The vagus nerve contains multiple fiber types of which some are known to be important for VNS to be effective (Krahl, Senanayake, and Handforth, 2001). Electric field modeling in VNS might be helpful in steering the field towards the important fibers. To the best of our knowledge, only one study has been performed in which computational models were used to investigate the effect of stimulation parameters, output current and pulse width, and tissue encapsulation at the site of electrode placement, in VNS (Helmers et al., 2012). A 3D digital representation of the geometry of the vagus nerve and VNS electrodes was created and a FEM was constructed to determine the voltage distribution in the vagus nerve, as a function of output current and pulse width. Two cases, with and without encapsulation layer, were compared. While the model showed activation in 99.5% of the fiber types that are important for vagus nerve activation without an encapsulation layer, this was reduced to 55% when the encapsulation layer was taken into account. In both cases, stimulation intensity was set to 1.5 mA and pulse width to 500 μ s. The optimal combination of stimulation parameters was derived from strength-duration curves, illustrating the non-linear relation between output current and pulse width. The optimal intensity was concluded to be between 0.75 and 1.75 mA and the optimal pulse width between 250 and 500 μ s.

C. VNS stimulation protocol

Even though there is hardly variation in the stimulation position and the electrode type used for VNS, the remaining stimulation parameters, such as the frequency, pulse width, the duty cycle, and the intensity, can still create various stimulation protocols. The stimulation parameters may influence the outcome of VNS. The choice of the duty cycle can for example determine whether a patient responds to VNS or not (Scherrmann et al., 2001).

Mu et al. (2004) and Lomarev et al. (2002) investigated the effects of respectively pulse width and frequency on functional MRI (fMRI) activation maps in patients with depression. Mu et al. (2004) showed that, compared to 250 and 500 μ s, a pulse width of 130 μ s produced significantly less overall activation and 500 μ s produced more deactivation compared to 130 and 250 μ s. Both regional overlap and differences in fMRI activation maps were seen with the various pulse widths. Moreover, Lomarev et al. (2002) showed that 20 Hz produced more acute activity changes compared to 5 Hz stimulation. Besides the frequency of the stimuli, also the frequency of the stimulation trains: the duty cycle, can influence the outcome of VNS (Heck, Helmers, and DeGiorgio, 2002). A duty cycle of 30 s stimulation on, 180 min off, 1 Hz and 130 μ s pulse width, is often considered to be the condition control. The standard therapeutic protocol, that is clinically used is 30 s stimulation on, 5 min off, 30 Hz, 500 μ s pulse width (DeGiorgio et al., 2000), has shown to be significantly more effective than the control condition. DeGiorgio et al. (2005) investigated the influence of the duty cycle in patients with epilepsy. Neither the output current, nor the duty cycle turned out to correlate with the clinical outcome in terms of seizure reduction and responder rate. In case of initial non-responders to the standard protocol, increasing the current or the frequency of the duty cycle might improve the clinical outcome. However in general, the standard clinical stimulation protocol showed a better outcome compared to a protocol with a rapid duty cycle: 7 s on, 30 s off (Scherrmann et al., 2001).

Another study in an epileptic rat model (Mollet et al., 2013) showed that 0.25 mA is sufficient to decrease cortical excitability. This study also showed that VNS does not have a long-lasting effect since the MT one hour after stimulation did not differ from the baseline MT, before stimulation. The influence of the current intensity was investigated by Bunch et al. (2007) in a group of 61 patients. Higher output-currents are needed to generate vagus nerve action potentials when the pulse width is reduced to less than 200 μ s. Koo et al. (2001) investigated the threshold current intensity to produce nerve action potentials as a function of pulse width and age. Also, the conduction velocity of the vagus nerve was investigated. Longer pulse widths required lower current intensities to produce action potentials. The necessary current to generate action potentials furthermore decreased with increasing age. This suggests age-related adjustments of the stimulation parameters. The conduction velocity was lower in children below age 12.

D. Summary of the technical aspects of VNS

VNS on the left vagus nerve, is an approved treatment method for epilepsy and depression. The most common clinically used VNS protocol consists of 30 s stimulation, 5 min no stimulation, 30 Hz stimulation frequency, and a pulse width of 500 μ s. Electric field modeling is not often performed for VNS but might be helpful to steer the electric field towards the important fibers and to investigate the effect of stimulation parameters. Initial non-responders might become responders after increasing the current or the frequency of the duty cycle.

3.4.2 Deep brain stimulation (DBS)

In DBS, electricity is directly delivered to specific brain areas through stereotactically implanted electrodes. During an MRI-guided stereotactic procedure under local anaesthesia (Villeger et al., 2006), DBS electrodes are implanted through burr holes (Gigante and Goodman, 2011; Pereira et al., 2012). The pulse generator is implanted under the left clavicle or in the abdominal cavity (Hassan and Al-Quliti, 2014).

DBS has gained FDA approval for the treatment of movement disorders such as essential tremor (ET), Parkinson's disease, dystonia, and obsessive compulsive disorder (OCD). In Europe, the method is also approved for movement disorders and refractory epilepsy (Al-Otaibi, Hamani, and Lozano, 2011; Labar and Dean, 2002; Sallet et al., 2009; Sprengers et al., 2014; Vonck et al., 2012). Furthermore, DBS is investigated as a treatment option for depression, chronic pain, Tourette syndrome, Huntington's disease, Alzheimer's disease, obesity, addictions, and consciousness disorders (Chen et al., 2012). Depending on the pathology, different brain regions are targeted. The ventral intermediate nucleus of the thalamus (VIM) and the globus pallidus internus (GPi) are the most widely used targets for dystonia (Ostrem and Starr, 2008). In case of Parkinson's disease, the subthalamic nucleus (STN) and the GPi are the most commonly used targets (Benabid, 2003). For ET, besides the VIM, also the posterior subthalamic area (PSA) is now used as a target (Fyttagoridis et al., 2013). Many targets have been investigated for OCD (Greenberg et al., 2006; Mallet, Polosan, and Jaafari, 2008; Sturm et al., 2003). The most widely used, and only approved, target for epilepsy is the anterior nucleus of the thalamus (ANT) (Fisher et al., 2010; Fisher and Velasco, 2014). Besides the ANT, also the centromedian nucleus of the thalamus (Velasco, Velasco, and Velasco, 2001) and the cerebellum (Velasco et al., 2005), have been investigated as targets for epilepsy in randomized clinical trials (Sprengers et al., 2014). Moreover, promising results have been obtained when the hippocampus is targeted (Boon et al., 2007b; Vonck et al., 2005; Vonck et al., 2002).

For a long time, it was hypothesized that DBS merely works either via functional ablation by suppressing or inhibiting the structure being stimulated or via activation of the stimulated structure (McIntyre et al., 2004c). Nowadays, the mechanism of action is thought to be more related to large neuronal networks in the brain since widespread changes in neuronal activity were found in networks comprising the DBS target (McIntyre and Hahn, 2010; Okun and Oyama, 2013). These changes in firing patterns of neuronal activity are probably linked to mechanisms of synaptic plasticity (Ganguly and Poo, 2013; Okun and Oyama, 2013; Van Hartevelt et al., 2014). The exact mechanism of DBS still remains to be elucidated.

Although DBS has provided remarkable therapeutic benefits for patients with several pathologies, side effects can occur related to surgery or the hardware. Zrinzo et al. (2012) showed that intracranial hemorrhage is the most prevalent side effect in DBS (0.9% in the study by Zrinzo et al. but overall literature suggested a prevalence of 5% (Zrinzo et al., 2012)). The occurrence of hemorrhage is a risk factor for the occurrence of seizures after DBS. According to Coley et al. (2009), the seizure risk after DBS is 2.4%. Most seizures occur within 48 h after the surgical implantation of the electrodes. Besides that,

implant site infections, electrode migrations or misplacement, wire fractures, skin erosion or device malfunctions can occur. The exact numbers vary between different centers. In a meta-analysis, Appleby et al. (2007) showed some cases in which significant psychiatric side effects occurred. The rates of depression, cognitive impairment, and mania are low, but also a relatively high rate of suicide (0.16 - 0.32% in DBS versus 0.02% in the normal population in the United States) was found in patients treated with DBS, depending on the stimulation target. It was suggested that patients should be pre-screened for suicide risk-factors before DBS and should be closely monitored afterwards.

DBS can also be administered by means of RNS that only provides stimulation after a trigger is detected by a so-called closed-loop algorithm (Kent and Grill, 2014; Stanslaski et al., 2012). The RNS neurostimulator (NeuroPace, Inc., Mountain View, California) is cranially implanted under the skull and is connected to one or two depth leads and/or cortical strips. RNS can also be connected to cortical strips only. Strictly speaking, in that case it is cortical stimulation rather than DBS. RNS has been studied extensively in epilepsy (Asconapé, 2013; Carrette et al., 2015; DeGiorgio et al., 2013; Gigante and Goodman, 2011; Liu et al., 2013; Morrell, 2006; Raghunathan et al., 2009; Skarpaas and Morrell, 2009; Sun, Morrell, and Wharen, 2008). In this case, the pulse generator continuously analyzes the electrocorticogram, recorded with a cortical strip lead, and automatically triggers electrical stimulation when specific characteristics are detected (Morrell, 2006). A recent study (Berger et al., 2015) showed significant seizure reduction after long-term follow-up of RNS in patients with medically refractory epilepsy. Besides use in epilepsy, different triggers, such as the typical rhythms in the beta frequency band, are being investigated for use of RNS in Parkinson's disease (Basu et al., 2013; Beuter, Lefaucheur, and Modolo, 2014; Gorzelic, Schiff, and Sinha, 2013; Modolo et al., 2012; Shukla et al., 2012).

A. Equipment: DBS electrodes

The electrodes used for DBS are surgically implanted in the brain. Depth electrodes contain multiple contact points such that the electric field can be steered to optimally stimulate the target. This section mentions the research that is performed to improve the electrode design, for example to diminish surgical complications or to perform directional steering.

Presently used DBS depth electrodes (Models 3387, 3389, Medtronic Inc., Minnesota, USA), as well as depth electrodes from the RNS system (NeuroPace, Inc., Mountain View, California), have a linear array of four cylindrical electrode contacts, consisting of platinum and iridium, that can be individually switched on or off depending on the placement of the electrode with respect to the target area in the brain (Wei and Grill, 2005). The depth electrodes have a diameter of 1.27 mm, ring-shaped contacts, and inter-contact distances ranging from 0.5 to 10 mm (Medtronic, 1998; Neuropace, 2013). Lai et al. (2012) have worked on an improved design of the electrode probes used for DBS. Based on the rationale that a lower electrode impedance increases the signal-to-noise ratio, a probe was developed with a rough three-dimensional microstructure on the electrode surface. The electric field generated by the probe was experimentally validated, using a FEM.

Parittotokkaporn et al. (2012) and Ben-Haim et al. (2009) also focused on the electrode design but aimed at decreasing the risk of adverse effects during or after DBS. Lead migration is one of the possible risks of DBS. Parittotokkaporn et al. (2012) added microtextured features to DBS probes to reduce probe mobility and showed that the lead migration in ex-vivo porcine brain was reduced without additional tissue damage. It was not investigated whether this microtexture can be used in platinum iridium electrodes (Turner, 2012) or whether it changes the physical characteristics of the electrodes. Hemorrhage is another possible complication of DBS surgery. Ben-Haim et al. (2009) showed decreased occurrence of hemorrhages using a modified microelectrode, with a decreased diameter.

Martens et al. (2011) presented a novel design of a high-resolution DBS lead that enables directional steering of the electric field. The DBS-array lead carries 64 disc-shaped electrodes, which are arranged in 16 equally spaced rows, covering a total length equivalent to the state-of-the-art DBS electrode arrangements (Toader, Decre, and Martens, 2010). By tracking the iso-fieldlines of the electric field and thresholding at a certain level, a volume of tissue activated (VTA) could be determined. It was shown that the new DBS array is capable of generating VTAs equivalent to currently used DBS electrodes but is also able to smoothly steer those in a preferential direction with 1 - 2 mm increments. Optimal overlap between the VTA and the stimulation target increases the effectiveness of the stimulation. Furthermore, the induction of adverse events by stimulating tissue beyond the stimulation target is diminished. The VTA was also investigated by Butson and McIntyre (2006) as a function of electrode design. In this study, a FEM of the electrodes and surrounding medium was coupled to models of myelinated axons to predict the VTA. The relation between the aspect ratio (diameter/height) of the electrode, and the VTA was investigated. A low aspect ratio maximized the VTA by providing greater spread of the stimulation parallel to the electrode shaft without sacrificing lateral spread. The results of this study furthermore showed that modified electrode designs can be used to customize the VTA to specific target nuclei.

B. Electric field modeling

Because the brain consists of conductive media, it acts as a volume conductor: the electric fields from an electric source are transmitted through biological tissue. Volume conduction plays an important role in DBS. Knowledge of the anatomical distribution of the electric field is of paramount importance to maximize the therapeutic effect of neurostimulation and to get a deeper insight into the underlying mechanism of action of DBS. Multiple studies using the FDM (Vasques et al., 2009) or the FEM were performed to model the electric field induced in the brain during DBS (Aström, Lemaire, and Wårdell, 2012; Butson et al., 2006; Chaturvedi et al., 2006; Grant and Lowery, 2009; McIntyre et al., 2004a; McIntyre et al., 2004b; Miocinovic et al., 2009; Pedoto et al., 2012; Schmidt and Rienen, 2012b; Schmidt and Rienen, 2012a; Wårdell et al., 2014; Wei and Grill, 2005). The main focus of these studies is the importance of incorporating specific conductivity values or encapsulation layers, and steering towards the stimulation target. Butson et al. (2006) emphasized the importance of incorporating DTI information in the model, to derive position- and direction-specific conductivity values. This was confirmed by showing significant differences in VTAs between homogeneous, isotropic models and heteroge-

neous, anisotropic tissue models, during DBS of the STN for Parkinson's disease (Butson et al., 2006).

Schmidt and van Rienen (2012; 2012) also investigated the influence of anisotropic conductivity on the field distribution in STN DBS. The maximum differences between the electric fields derived from the isotropic and anisotropic models occurred in the proximity of the active electrode contact in the unipolar stimulation cases and additionally in the proximity of the ground electrode in bipolar cases. Investigating the influence of the electrode position by moving the electrode around the primary position resulted in differences in the electric field distributions, mainly observable within the surroundings of the stimulating electrode contact.

The model used by Schmidt and van Rienen (2012) was extended with an encapsulation layer surrounding the DBS electrode body. The influence of the encapsulation layer can be described in different stages after implantation. In the acute stage, the peri-electrode space is filled with extracellular fluid. Due to the high conductivity of extracellular fluid, a path of low resistance is created enabling the current to spread further. So neglecting the peri-electrode fluid layer may lead to an underestimation of the field strength during the acute stage. Approximately two weeks after implantation, giant cells with low conductivity start to occur at the electrode surface. The spread of current into the surrounding tissue is restricted, which may cause an overestimation of the actual electric field (Yousif and Liu, 2007).

The effect of the encapsulation layer was furthermore investigated by Chaturvedi et al. (2006). Clinical measurements of the corticospinal tract activation, MEPs of various muscles, were used to address the level of model complexity necessary to accurately predict neural activation generated by STN DBS. Based on the comparison of the electric fields with the anatomy of one dataset, it was suggested that estimation of the neural response to DBS requires a model that incorporates electrode capacitance, electrode impedance, electrode location and orientation in the brain and 3D tissue conductivity values.

Other studies have focused on spatially steering the electric field towards the morphology of the stimulation target, such as the STN or the GPi, based on iso-potential fieldlines or iso-electric fieldlines (Hemm et al., 2005; McIntyre et al., 2004b; Vasques et al., 2010; Vasques et al., 2009; Wårdell et al., 2014). Wårdell et al. (2014) showed that incorporating patient-specific information, retrieved from DTI, can improve the electric field calculations in Tourette patients. McIntyre et al. (2004) developed a quantitative understanding of the VTA by DBS of the STN. It was shown that the VTA extends beyond the actual borders of the STN, using clinically effective stimulation parameters. Furthermore, it was shown that slight (~ 1 mm) deviations of the electrode positions can substantially alter the VTA. Vasques et al. (2010; 2009) showed that, compared to state-of-the-art DBS electrodes, a double contact with a height of 2.5 mm, induced a more homogeneous field and less voltage was needed for GPi stimulation.

Miocinovic et al. (2009) performed a validation study of the methods used to model the electric fields by comparing the electric field induced by DBS electrodes implanted in a

rhesus monkey in the thalamus and the STN to a theoretical field, calculated with microelectrodes positioned in a saline bath with a DBS electrode. Three important findings have been reported. Again, the importance of the inhomogeneities and anisotropies was emphasized. Furthermore, it was shown that DBS electrode impedance is primarily dictated by a voltage drop at the electrode-electrolyte interface and the conductivity of the tissue medium, and the stimulus waveform recorded in saline or brain tissue was modified from the stimulus waveform generated by the pulse generator.

Walckiers et al. (2010) investigated the influence of the neurostimulator when modeling the electric field after DBS with FEM. Using a model for the reference electrode, a reduction of VTA was shown. Grant and Lowery (2009) also showed that incorporating the reference electrode in the model changes the VTA.

C. DBS stimulation protocols

Even after implantation of the DBS electrode lead, electrical steering can be applied by selecting the electrodes that are actually used for stimulation. Multiple choices have to be made to obtain a DBS protocol: monopolar or bipolar, unilateral or bilateral, synchronous or asynchronous stimulation. This section describes the current knowledge about these options. Besides that, also the knowledge about the influence of different pulse shapes and frequencies are listed.

In DBS, stimulation must be delivered by at least one positive (anodal) or negative (cathodal) stimulation electrode. Cathodal stimulation causes positively charged ions to flow towards the electrode, causing depolarization in nearby neurons. The opposite holds for anodal stimulation. DBS can be performed in a monopolar or bipolar way. In monopolar DBS, the metal housing of the neurostimulator serves as the anode (Denys, Feenstra, and Schuurman, 2012). In general, monopolar stimulation results in a larger current spread than bipolar stimulation for a given stimulation intensity. Hemm et al. (2005) showed, based on a simple model, that monopolar stimulation causes a more homogeneous electric field. The larger spread of the electric field causes a higher number of side effects in monopolar stimulation. During bipolar stimulation, higher stimulation intensities are necessary to obtain similar clinical effects as with monopolar stimulation (Deli et al., 2011).

Unilateral versus bilateral stimulation studies were performed by Hamani et al. (2010) and Van Nieuwenhuijse et al. (2015). Hamani et al. (2010) showed that left unilateral stimulation of the subcallosal cingulate gyrus was equally effective as bilateral DBS in treating major depression. In contrast, Van Nieuwenhuijse et al. (2015) found bilateral stimulation to be more effective in a DBS study in the hippocampus of rats, for the treatment of epilepsy.

In rats, Cymerblit-Sabba et al. (2013) compared synchronous stimulation, stimulation with two electrodes that were simultaneously activated, to asynchronous stimulation, using different stimulation frequencies. The asynchronous protocol was more efficient in terminating and shortening induced hippocampal seizures. Wyckhuys et al. (2010) investigated whether Poisson-distributed stimulation, stimulation with the interstimulus inter-

vals varying according to a Poisson distribution, was more effective compared to standard high frequency stimulation in a kainate rat model. The Poisson-distribution stimulation showed a slightly increased number of rats with a significant reduction in seizure frequency. Also the reduction in seizure frequency was higher in rats treated with the Poisson protocol compared to high frequency stimulation (67% versus 50%).

Simulation studies have been performed aiming at modifying the stimulation pulse shape to optimize the efficiency of the stimulation (Grill and Mortimer, 1996; Hofmann et al., 2011; Wongsarnpigoon and Grill, 2011). The underlying thought is that the frequency of battery-replacement surgeries could be decreased by improving the energy efficiency of the stimulation. An older study by Grill and Mortimer (1996) determined the effect of rectangular stimulus pulse widths on the selectivity of peripheral nerve stimulation. Better spatially selective stimulation was observed when applying shorter pulses. Later, Wongsarnpigoon and Grill (2011) used a generic algorithm to determine the optimal waveform shape. The resulting waveforms resembled truncated Gauss-shaped pulses. The optimized waveforms turned out to be more energy- and charge-efficient than several conventional waveforms used in neural stimulation. Hofmann et al. (2011) showed a further increase in efficiency with the introduction of a pause within a biphasic pulse, with specific and optimized duration. An evaluation to compare the actual waveforms from different manufacturers showed that the actual stimulation waveforms differed from the intended ones, as prescribed by the manufacturers (Butson and McIntyre, 2007).

Table 3.8 and 3.9 provide an overview of the research that is performed to gain insight into the influence of stimulation frequency as well as studies that investigated the effect of combinations of parameters in DBS.

As can be seen in Table 3.8, the optimal stimulation frequency depends on the pathology. In dystonia and epilepsy, 130 Hz stimulation has shown to be an optimal frequency (Kupsch et al., 2003; Ostrem et al., 2014), whereas in ET, no additional benefit was found above 100 Hz (Ushe et al., 2004). In Parkinson's disease, the stimulation frequency is often set to 130 Hz. Some studies showed that stimulation at 60 Hz can decrease the number of freezing episodes, compared to 130 Hz stimulation (Moreau et al., 2008; Xie, Kang, and Warnke, 2012). However, Phibbs et al. (2013) could not confirm this finding and Brozova et al. (2009) commented that a decrease in freezing of gait (FOG) may be accompanied by worsening of other types of gait problems. Different phenotypes within a certain pathology seem to respond differently to stimulation. This was also confirmed by Yamamoto et al. (2004), who showed that stimulation parameters, such as the effective stimulation sites and intensities varied between different kinds of tremor.

An imaging study in animals, performed by Paek et al. (2015), showed that combinations of frequency and intensity influence the activated brain regions differently. A negative fMRI response was generated with 130 Hz stimulation while 10 Hz stimulation generated a positive response in the same area. Moreover, an increase of the stimulation intensity had an effect on the size of the affected brain areas.

Vercueil et al. (2007) investigated the effect of different pulse widths; 60, 120 and 450

Table 3.8 — Overview of studies investigating the effect of frequency in DBS studies in human.

Position	Investigate effect on	Frequencies [Hz]	Parameter of interest	Outcome	Source
Dystonia					
STN	Dystonia severity	60, 130	BFMDRS-M and TWSTRS-S	130 Hz stimulation is more effective than 60 Hz stimulation.	Ostrem et al. (2014)
GPi	Dystonia severity	0, 5, 50, 130, 180, 250	European Profile of QOL and BFMDRS	Original frequency of 130 Hz resulted in clinical improvement. At higher frequencies, higher improvements were found whereas at lower frequencies significant deterioration was found.	Kupsch et al. (2003)
Essential Tremor					
VIM	Tremor suppression	0, 30, 45, 60, 75, 90, 100, 130, 145, 185	RMS of tremor (measured by accelerometer)	Highly significant inverse sigmoidal relationship between stimulation frequency and normalized tremor acceleration. Tremor acceleration had a nearly linear response to stimulation frequencies between 45 and 100 Hz, with little additional benefit above 100 Hz.	Ushe et al. (2004)
Parkinson's Disease					
STN	Bradykinesia	all stimulation frequencies available to the subject's neurostimulator	Amplitude and frequency of hand opening-closing task	Multiple frequencies resulted in increased movement amplitudes. No clear relationship between stimulation frequency and movement frequency was discovered.	Huang et al. (2014)
STN	FOG	60, 130	Measure of stride length	Not able to demonstrate improved gait at either frequency.	Phibbs et al. (2013)
STN	FOG	60, 130	FOG measures	130 Hz stimulation induced severe FOG in 2 patients. Lower frequency (60 Hz) could improve FOG, without change in contacts, voltages and pulse widths.	Xie et al. (2012)
STN	Motor performance	0, 10, 20, 30	Voluntary tapping	20 Hz stimulation appeared to reduce the kinesia time relative to no stimulation compared to 10 and 30 Hz stimulation.	Kühn et al. (2009)
STN	Finger tapping task	0, 5, 10, 20	Repetitive depression of a keyboard task and extensions of the index finger	The range of frequencies investigated can slow distal upper limb movements in patients with PD. 5 and 20 Hz stimulation reduced the tapping rate and increased the coefficient of variation of tap intervals.	Eusebio et al. (2008)
STN	Kinesia time	0, 5, 10, 15, 20, 25, 30, 130	Kinesia time in a tapping task	The effects of stimulation do not simply increase with increasing frequencies. There are relative deteriorations in the 5-10 and 20-25 Hz range.	Fogelson et al. (2005)

BFMDRS-M = Burke Fahn Marsden Dystonia Rating Scale Movement score, ET = essential tremor, FOG = freezing of gait, GPi = globus pallidus internus, PD = Parkinson's Disease, QOL = quality of life, RMS = root mean square, STN = subthalamic nucleus, TWSTRS-S = Toronto Western Spasmodic Torticollis Rating Scale severity, VIM = ventral intermediate nucleus of the thalamus.

μ sec, on the clinical improvement in primary generalized dystonia. No significant differences were found. Another study investigating the effect of different combinations of pulse widths and frequencies on the intensities required to measure a positive clinical outcome in patients with Parkinson's disease (Rizzone et al., 2001). A hyperbolic intensity-pulse width curve was obtained, indicating that at higher pulse widths, lower intensities are sufficient to induce a clinical effect. Furthermore, for a certain pulse width, increasing the frequency led to decreased intensity required to obtain any effect.

Liu et al. (2012), Pedrosa et al. (2013), and Earhart et al. (2007) investigated different protocols with and without prior high frequency stimulation respectively in intentional and postural tremor. The varying results suggest that the effect of neurostimulation might be enhanced or attenuated by the cortical excitability state. Based on this thought, Zhang et al. (2012) investigated the effect of timing of high frequency DBS in the ANT on amygdala-kindled seizures in rats and showed that bilateral post-kindling stimulation has

Table 3.9 — Overview of studies investigating the effects of combinations of stimulation parameters in DBS studies.

Animal/human	Position	Investigate effect on	Parameters and values	Parameter of interest	Outcome	Source
Parkinson's Disease						
Human	STN	FOG	Voltage (3, 3.7 V) and frequency (60, 130 Hz)	Number of freezing episodes and UPDRS	Number of freezing episodes was significantly lower at 60 Hz and 3.7 V. Improvement in the UPDRS was not significant.	Moreau et al. (2008)
Human	STN	Clinical effectiveness in PD	Frequency (10, 50, 90, 130, 170 Hz) and pulse width (60, 120, 210, 450 μ sec)	Intensity necessary to obtain the disappearance of contralateral wrist rigidity and side effect threshold	Impossible to obtain required clinical effect at 10 and 50 Hz (no matter of the pulse width). Intensity-pulse width curves showed a hyperbolic trend.	Rizzone et al. (2001)
Depression						
Rats	SCG	Anti-depressant response	Stimulation intensity (100, 200, 300, 400 μ A), frequency (20, 130 Hz)	Forced swim test	Strongest response was observed with a current intensity of 200 μ A, followed by 100 μ A and 300 μ A. 400 μ A did not produce any effect. Using 200 μ A, a frequency of 130 Hz was more effective than 20 Hz.	Hamani et al. (2010)
Dystonia						
Human	GPI	Neural firing with and without prior high frequency stimulation	Microstimulation frequencies (1-100 Hz) and train lengths (0.5-20 sec)	Neural firing rate and evoked field potentials	Post-HFS, overall firing was reduced compared with pre-HFS and the firing and evoked field potential amplitudes were enhanced at low frequencies	Liu et al. (2012)
Epilepsy						
Rats	Piriform cortex	Piriform cortex kindled seizures	Intensity (0.25, 1, 3 ADT), pulse width (0.01, 0.1, 1, 10 msec), train duration (1, 15 min), state of the rat (fully kindled, during kindling acquisition)	ADT	There is a complex relation between stimulation patterns and effect on kindled seizures.	Ghorbani et al. (2007)
HV	Swine	Thalamus	Neural network activation. Frequency (10, 130 Hz) and intensity (3, 5, 7 V)	BOLD activation maps	Stimulation frequency and voltage combinations modulated the brain network activity differently in the sensorimotor cortex, the basal ganglia and the cerebellum in a parameter dependent manner. 130 Hz generated a negative BOLD response in the motor cortex, while 10 Hz increased the positive BOLD response.	Paek et al. (2015)
Tremor						
Human	Thalamus	Intentional tremor	Frequency (0, 10, 120-150 Hz), tremor type (intentional versus postural), electrode position	TRS and ultrasound-based tremor-amplitude measurements	Lowest scores for TRS were achieved under 120-150 Hz stimulation, while 10 Hz showed the highest scores. Ratio of tremor amplitude between 0 and 10 Hz stimulation was lower for intentional tremor compared to postural tremor. The more ventral the electrodes were placed, the higher the influence on the intentional tremor amplitude during 10 Hz stimulation. No influence was found on the postural tremor.	Pedrosa et al. (2013)
Human	VIM	Tremor suppression	Frequency (0, 30, 45, 60, 75, 90, 100, 130, 145, 185 Hz) and tremor type (intentional versus postural)	Tremor frequency and amplitude	130 Hz is the optimal stimulation frequency. Tremor frequency did not change with stimulation frequency. The amplitude however, decreased with increasing frequency (for postural tremor only until 130 Hz). The effect on postural tremor was bigger than on intentional tremor.	Earhart et al. (2007)

ADT = after discharge threshold, BOLD = blood oxygen level dependent, FOG = freezing of gait, GPI = globus pallidus internus, HFS = high-frequency stimulation, LFS = low-frequency stimulation, PD = Parkinson's disease, SCG = subcallosal cingulate gyrus, STN = subthalamic nucleus, TRS = tremor rating scale, UPDRS = Unified Parkinson's Disease Rating Scale, VIM = ventral intermediate nucleus of the thalamus.

a stronger effect compared to pre-kindling stimulation. This finding suggests that RNS is more appropriate for clinical anti-epileptic treatment than scheduled stimulation.

It is not yet known whether neurostimulation induces a long-lasting effect. On the one hand, Cif et al. (2013) suggested the induction of long-lasting effects by showing that no difference between symptom evolution was found in dystonia patients during DBS administration and after DBS discontinuation. On the other hand, the study by Van Nieuwenhuyse et al. (2015) showed that after discontinuation of 10 days of unilateral or bilateral DBS, the electrographic seizure rate returned to baseline. Because stimulation in the study of Cif et al. (2013) was in the order of years, and the study of Van Nieuwenhuyse et al. (2015) in the order of days, these findings might suggest that a long-lasting effect might not occur before a certain amount of stimulation time is reached.

D. Summary of the technical aspects of DBS

In DBS, the cathode causes the neuronal enhancement. In case of monopolar stimulation, the housing of the neurostimulator serves as the anode. Monopolar stimulation causes larger, more homogeneous current spread. This larger spread might also induce more side effects. Bipolar stimulation requires higher stimulation amplitudes to achieve equal effects. Accurate models to perform electric field calculations should incorporate position- and direction-specific conductivity values and also the encapsulation layer needs to be modeled. Models can be used to predict the optimal stimulation position, such that the spatial overlap between the volume of tissue activated and the target is maximized. The effectiveness of unilateral versus bilateral DBS probably depends on the pathology. In case of bilateral stimulation, the clinical effects might increase using an asynchronous or Poisson-distributed stimulation protocol. Currently, a pulse with a pause between the two Gauss-shaped phases (one positive and one negative) is considered to be optimal. No direct effect of the pulse width was found, but there is a relation between pulse width and stimulation intensity. The optimal stimulation frequency for DBS might depend on the pathology.

3.4.3 Alternative stimulation techniques

Besides the techniques mentioned earlier in this review, other stimulation techniques exist that are not standardized in clinical practice or that are under development and might be used in the future. These stimulation techniques try to overcome drawbacks of the methods mentioned before, such as the invasiveness of DBS and VNS and the relative non-focality of non-invasive techniques. Although an extensive explanation of these techniques is beyond the scope of this review, we would like to briefly mention some of them.

In trigeminal nerve stimulation (TNS) one of the two upper branches of the trigeminal nerve, the fifth cranial nerve is stimulated (DeGiorgio, Shewmon, and Whitehurst, 2003; DeGiorgio and Krahl, 2013; Fisher, 2011). TNS can be delivered either transcutaneously with external electrodes and an external pulse generator (eTNS, Monarch system by NeuroSigma or Cefaly system by Roxon) (see Figure 3.1), or subcutaneously with implanted electrodes and an implanted generator (sTNS, Monarch system by NeuroSigma, under development). eTNS received CE mark in September 2012 and is approved for subjects aged 9 and above as an adjunctive therapy for either epilepsy (DeGiorgio et al., 2013; DeGiorgio and Krahl, 2013; DeGiorgio et al., 2009; DeGiorgio et al., 2006; DeGiorgio,

Shewmon, and Whitehurst, 2003; Moseley and DeGiorgio, 2014; Pop et al., 2011) or depression (Cook et al., 2013; Schrader et al., 2011). The system has further received a Humanitarian Use Device from the FDA for the treatment of Lennox-Gastaut syndrome in children. eTNS has also been shown to have a positive effect on mood (Schrader et al., 2011). A trial in ADHD has recently been published (McGough et al., 2015). The eTNS system by NeuroSigma contains a 1.25 inch disposable, hypoallergenic, silver-gel, self-adhesive stimulation electrode (DeGiorgio et al., 2006). To the best of our knowledge, no research on the optimization of equipment or stimulation parameters has been published and eTNS has not been used in routine clinical practice. The hypothesized mechanism of action seems to overlap with that of VNS: the trigeminal nerve projects towards important structures in the brain such as the NTS and the LC (Moseley and DeGiorgio, 2014).

Electroconvulsive therapy (ECT) and magnetic seizure therapy (MST) are both old stimulation techniques that are considered as a 'last resort' treatment possibility in severe clinical depression refractory to other treatments. During ECT and MST generalized seizures are induced under anaesthesia using high-intensity electrical stimulation or rTMS respectively. Both approaches are based on the idea that seizures might have a potential therapeutic effect: they might reset the brain by possible release of norepinephrine and other neurotransmitters (Deng, McClintock, and Lisanby, 2015; Keltner and Boschini, 2009). Compared to ECT, MST is not restricted by the high electrical impedance of the skull. Kayser et al. (2011) showed comparable anti-depressant effects of ECT and MST and did not report any side effects, even though cognitive side effects are often associated with the treatment. ECT is highly efficacious in treatment-resistant depression. A meta-analysis showed superior results of ECT compared to placebo stimulation, placebo medication, and different types of anti-depressants (Pagnin et al., 2004).

Even though propagation of ultrasound through the skull is non-trivial, it is nowadays possible to direct ultrasound to focal areas deeper in the brain by using specially designed transducers. Two types of focused ultrasound (FUS) are nowadays investigated. High-intensity focused ultrasound (HIFU) has been used to irreversibly ablate tissue whereas low intensity focused ultrasound pulsations (LIFUP) can induce reversible neural excitation and inhibition. One of the major advantages of ultrasound is that it can be combined with fMRI, as ultrasound is MRI compatible. Combined with MR techniques, HIFU is increasingly used to treat various types of extracranial soft tissue tumors (Coluccia et al., 2014; Jagannathan et al., 2009) and LIFUP can be used as a neurostimulation device. The influence of stimulation parameters has been investigated (King et al., 2013), but the optimal settings are not known yet.

Another technique that can be used for neurostimulation: optogenetics, was reviewed by LaLumiere (LaLumiere, 2011). Optogenetics uses light to control the activity of neurons which have been modified to express light-sensitive proteins. Because the light influences only the neurons expressing light-sensitive ion channels, the non-specific effects of electrical stimulation or admission of medication can be overcome. The viral delivery of opsin genes, to generate the light-sensitive neurons, is a hurdle for this technique's clinical use. The light, with particular wavelength, is often administered employing laser techniques combined with a fiber-optic cable that is inserted in the brain region of interest.

Optogenetics was defined as 'Method of the year 2010', by Nature Methods (Pastrana, 2011).

3.4.4 Discussion on neurostimulation

In this review, the technical aspects of different neurostimulation techniques, which are currently applied in clinical practice, were described with the focus on equipment, electric field modeling, and stimulation protocols. Also a short overview of alternative stimulation techniques was provided.

A. Comparison of the different stimulation methods

Neurostimulation techniques aim to become a treatment option for various neurological and psychiatric disorders. Figure 3.5 shows a schematic overview of the invasiveness versus the focality of the different stimulation techniques treated in this review.

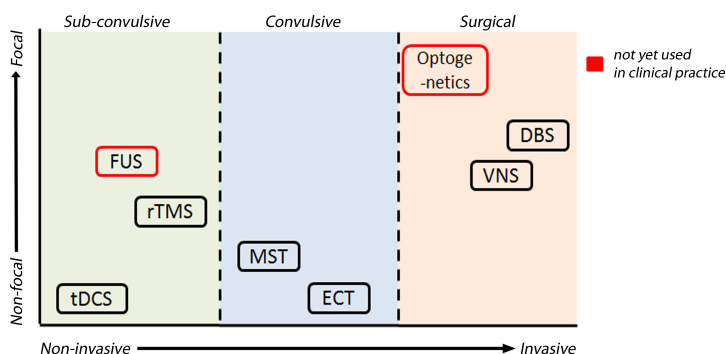


Figure 3.5 — *Invasiveness versus spatial resolution of different neurostimulation techniques. Invasiveness versus spatial resolution for the different stimulation techniques described in this review. The techniques in the red boxes are not yet used in clinical practice. This plot is adapted from Deng et al. (2015).*

On the one hand, the non-invasiveness of TMS and tDCS might be beneficial, especially from a patient's perspective. On the other hand, invasive stimulation techniques require only a single surgical procedure, though with a relatively high burden, whereafter the stimulation will continue for the duration of the battery life-time without additional interventions for the patient. A battery replacement surgery is necessary every couple of years. Battery lifetime depends on the type of neurostimulator and the stimulation protocol, with more stimuli and higher intensities decreasing the battery lifetime. The average

battery life for VNS is now 8-10 years (Ben-Menachem, 2012) and for DBS in for example epilepsy approximately 2.5 years. RNS will be even more battery efficient, since in this case stimuli are only applied if necessary (Vonck and Boon, 2015).

The invasive neurostimulation techniques DBS and VNS outperform the less invasive techniques in terms of spatial resolution. New stimulation techniques, such as FUS and optogenetics are investigated to improve the focality of the stimulation even further. VNS is the technique that is performed with the least variability when it comes to choices of stimulation parameters: the position of stimulation is fixed and a standard protocol is often used. TMS, tDCS, and DBS are performed along a broader range of stimulation parameters. Table 3.10 gives an overview of the characteristics of the neurostimulation techniques TMS, tDCS, DBS, and VNS.

Table 3.10 — *Overview of the characteristics of TMS, tDCS, DBS, and VNS.*

	TMS	tDCS	DBS	VNS
Invasiveness	Non-invasive	Non-invasive	Invasive	Invasive or non-invasive
Administration	In hospital/healthcare center	Mostly in hospital/healthcare center. Portable tDCS devices are currently available.	Implantation in hospital, then stimulation according to duty cycle.	Implantation in hospital, then according to duty cycle
Patient-interference possible	No	No	No	Yes, with a magnet.
Device	Coil	Electrode patches	Depth electrode	Cuff-electrode
Stimulation types	spTMS and ppTMS to study brain behavior, rTMS for therapeutics	tDCS, tACS, tRNS (see Table 3.7)	Not applicable	Not applicable
Stimulation frequency	Depends on pathology: <1 Hz assumed to be inhibitory, >5 Hz excitatory stimulation.	Not applicable, constant current for approximately 20 min	Most often 130 Hz but sometimes 60 Hz	20-50 Hz
Duty cycle	Not applicable	Not applicable	Standard 5 min off, 30 sec on	Standard 5 min off, 30 sec on
Duration of the stimulation protocol	Multiple days, optimal number of sessions per day and duration per session not known.	Multiple days, optimal number of sessions per day not known, duration of session approximately 20 min.	Battery lifetime	Battery lifetime
Sustainability therapeutic effect	Not known	Not known	Battery lifetime, might extend beyond the battery lifetime	Battery lifetime
Stimulation intensity	Percentage of patient-specific MT	0.5-2 mA	1-5 V	0.25-3.5 mA
Mechanism of action	Neuroplasticity	see Table 7	Neuroplasticity	Branches of vagus nerve project to important brain structures.

An extensive description of the current knowledge of the mechanisms of action was beyond the scope of this review. Although the mechanisms of action differ, there is overlap in the clinical effects of different stimulation techniques. Both DBS and VNS are used as a treatment for epilepsy and nowadays also TMS and tDCS are investigated for that pathology. Fox et al. (2014) investigated diseases treated with both invasive and non-invasive neurostimulation techniques. An important finding was that sites where DBS was effective were functionally connected to sites where non-invasive brain stimulation was effective. This suggests that the effect of non-invasive stimulation extends in the brain along the functional network comprising the stimulation position. In this way, it should in principle be possible to also, indirectly, target deeper brain regions with non-invasive stimulation techniques. Whether it is possible to achieve similar results with invasive and

non-invasive stimulation techniques in the future remains to be resolved. In line with the above mentioned findings, it might be possible to predict the outcome of invasive neurostimulation with non-invasive stimulation techniques. However, to be able to quantify this prediction, more information about the individual mechanisms should be available.

B. Current clinical practice

As can be seen in the Tables concerning the stimulation parameters (Tables 3.2-3.6, 3.8 and 3.9), a lot of research is dedicated towards pathologies such as Parkinson's disease, depression, migraine and epilepsy. Not only the information about the type of neurostimulation is important, but also the information about the pathology to be treated. Connectivity analysis can provide insight into networks that might be disturbed in certain pathologies (Besseling et al., 2013; Vaessen, 2012; Veer et al., 2010). Also, combined TMS-EEG recordings can provide additional information about pathologies and the cortical excitability (e.g. Shafi et al. (2015)). The optimal stimulation position can be determined by the location in the brain that is affected, for example the DLPFC in depression, or as a position that is involved in a specific pathology, such as the ANT in epilepsy. Because the effect of the different stimulation parameters are not known yet, optimization of the stimulation protocol per patient is currently performed based on trial-and-error (McIntyre et al., 2004a).

If a patient is eligible for neurostimulation, the first choice is the neurostimulation method: for example TMS, tDCS, VNS, or DBS. The type of neurostimulation that fits best to an individual patient is not known. Important to emphasize is that there is not a single neurostimulation method that is optimal. The optimal method depends on the specific factors, such as the patient's pathology. The choice of neurostimulation method is currently often driven by the treating hospital, which is often specialized in certain techniques.

In TMS, the exact positioning of the stimulation coil can be determined during the performance of the protocol by means of neuronavigation (Bashir, Edwards, and Pascual-Leone, 2011). It is, however, important, that clinicians are able to interpret the depicted fields by neuronavigation systems correctly. The current navigation systems show the electric field induced by the TMS coil overlaid on the patient's MRI using simple models. No patient-specific geometry is taken into account, so the neuronavigation only provides a global idea of the real stimulation position. Another important point that needs attention is that neuronavigation only shows the estimated electric fields in the brain. Due to the fact that the orientation of neurons with respect to the electric field plays an important role for stimulation, the modeled electric field is not necessarily the same as the region of the brain that is really activated. A recent study by De Geeter et al. (2015) embedded realistic models of neuron tracts in the model, computed from DTI. Moreover, activation of axons during extracellular stimulation is rather complex. The threshold for activation varies with axon diameter, orientation and curvature, and it is not known what sizes of axons are responsible for therapeutic effects and side effects during stimulation (Åström et al., 2014). So at this point, the use of neuronavigation is mostly important to get a global idea of the affected location in the brain and to guarantee stimulation of a particular position during a long or longitudinal stimulation protocol.

C. The future of neurostimulation

It can be concluded that much research is going on in all directions within the field of neuromodulation. To really make a big step forward into the clinical implementation of neurostimulation, the research focus should be on exploring the mechanisms of action, the effect of the different stimulation parameters, and the effect of external factors such as the cortical excitability state. There is a lot of debate about which scale is the most appropriate to investigate this issue. Some state that a very small, neuron-size, resolution should be used. Patch clamp techniques can be used to measure neurophysiology on single cell level (Beurrier et al., 2014; Loddenkemper et al., 2001). Patching of connected pairs can nowadays also be used to investigate synaptic behavior. Others state that brain function is not encoded in single neurons and propose the use of larger scale analyses. The concept that the brain is organized in networks is nowadays generally accepted (Bassett and Bullmore, 2009; Bullmore and Sporns, 2009).

More detailed knowledge about the mechanisms of action might be helpful to predict best candidates for specific types of neurostimulation and to predict their responses (Vonck and Boon, 2015). Even though neurostimulation is only offered in case of medication resistivity, it might be possible that a combination of pharmacological interventions with neurostimulation will become able to treat various patients (Vonck and Boon, 2015). Up till now, electric field modeling is used for research purposes to gain a better understanding of the mechanisms of action. In the future, modeling might become helpful in determining the optimal stimulation parameters. For example now, the intensity in TMS protocols is most commonly derived from the patient's specific MT. In the future, it might become possible to delineate a target in the brain and derive the appropriate stimulation intensity, and the coil position, more accurately from subject-specific simulations.

SimNIBS (simulation of non-invasive brain stimulation, www.simnibs.org, (Thielscher, Antunes, and Saturnino, 2015)), is an example of an easy to use, linux-based, free downloadable tool to simulate electric fields induced by TMS and tDCS. Many coil types that are often used in clinical practice are included in SimNIBS, such that the user only needs the MR images, the coil position and orientation, and the stimulation intensity as input. The accurate calculation of the electric field is time consuming, with the longest step being the calculation of the patient-specific head mesh. To our knowledge, there are no existing easy to use toolboxes that can be used to simulate the electric fields induced by DBS. FEMLAB (Comsol, Inc., Burlington, MA) might be used to perform finite element calculations. However, the implementation of the electric field calculations require detailed knowledge about the stimulation device and the brain and is a highly challenging technical task.

Modeling studies are hard to validate since it is impossible to measure the electric fields in situ so a gold standard is not available. One way to quantify the accuracy of the models is to stimulate parts of the brain that evoke a response that can directly be measured, such as the corticospinal tract. Presumably, the addition of the position- and direction-specific conductivity values to the models will improve the accuracy of the spatial distribution of the electric field in the brain. However, there are still uncertainties in the models for ex-

ample concerning the exact values of the conductivity and permittivity of different brain regions, and also their dependence on the stimulation frequency (Thielscher, Antunes, and Saturnino, 2015). Important to note is that the electric field models are currently only used for research purposes. So even though electric field models can improve the insights of brain stimulation, they cannot be used in clinical practice yet.

The sustainability of the therapeutic effects of TMS and tDCS need further exploration. Since these two types of neurostimulation are mainly applied in hospitals or healthcare environments, it is important that the therapeutic effects are long-lasting. In the future, self-delivery of non-invasive stimulation by the patient in a home environment, ideally according to a patient-specific stimulation protocol, may be a crucial step to really use TMS or tDCS as a therapeutic tool. Even if there is a sustainable effect of TMS or tDCS, these effects will not last forever so in both cases repeated sessions are necessary to keep the therapeutic outcome. A home-based, portable, device should incorporate features that make sure the stimulation is applied to the right position in the brain, for example a patient-specific cap positioning the TMS coil to the right position, or including the tDCS electrodes at the right spot (Wagner, Valero-Cabre, and Pascual-Leone, 2007). In migraine, a portable TMS system has already been tested with positive results (Lipton and Pearlman, 2010). tDCS equipment is simpler and smaller compared to TMS equipment. Portable tDCS equipment is commercially available (for example by Magstim Company Limited, Wales, UK).

So in conclusion, it is challenging to predict the future of neurostimulation. The answers to many remaining questions will eventually determine what different stimulation techniques will mean in a couple of years and how they will be implemented in clinical practice. The positive outcome of neurostimulation in some cases is actually a major motivation to investigate stimulation in more detail to hopefully increase the knowledge about what is really happening after neurostimulation, to fine-tune the protocols, and to increase the number of positive outcomes.

"Success is not about how much money you make: it is about the difference you make in people's lives."

Michelle Obama

CHAPTER 4

Focal application of accelerated iTBS results in global changes in graph measures

D.C.W. Klooster, S.L. Franklin, R.M.H. Besseling, J.F.A. Janssen, K. Caeyenberghs, R. Duprat, A.P. Aldenkamp, A.J.A. de Louw, P.A.J.M. Boon, C. Baeken

Human Brain Mapping, 2019, 40:432-450
doi:10.1002/hbm.24384

Abstract

Graph analysis was used to study the effects of accelerated intermittent theta burst stimulation (aiTBS) on the brain's network topology in medication resistant depressed patients.

Anatomical and resting-state functional MRI (rs-fMRI) was recorded at baseline and after sham and verum stimulation. Depression severity was assessed using the Hamilton Depression Rating Scale (HDRS). Using various graph measures, the different effects of sham and verum aiTBS were calculated. It was also investigated whether changes in graph measures were correlated to clinical responses. Furthermore, by correlating baseline graph measures with the changes in HDRS in terms of percentage the potential of graph measures as biomarker was studied.

Although no differences were observed between the effects of verum and sham stimulation on whole brain graph measures and changes in graph measures did not correlate with clinical response, the baseline values of clustering coefficient and global efficiency showed to be predictive of the clinical response to verum aiTBS. Nodal effects were found throughout the whole brain. The distribution of these effects could not be linked to the strength of the functional connectivity between the stimulation site and the node.

This study showed that the effects of aiTBS on graph measures distribute beyond the actual stimulation site. However, additional research into the complex interactions between different areas in the brain is necessary to understand the effects of aiTBS in more detail.

4.1 Introduction

Transcranial magnetic stimulation (TMS) is a well-established non-invasive neurostimulation technique used in a variety of experimental and clinical applications. A time-varying current is sent through a coil placed tangential to the scalp. The magnetic field, induced by this time-varying current, induces an electric field within the neural tissue in the brain, which is parallel to the current in the coil but has opposite direction. This electric field within the brain is able to modulate the activity of cortical neurons (Wagner, Valero-Cabre, and Pascual-Leone, 2007).

The effects of the repetitive application of TMS (rTMS) endure beyond the actual period of stimulation, affecting larger networks in the brain, which makes rTMS a potential treatment for various neuropsychiatric disorders (Klooster et al., 2016). The application of high-frequency rTMS, delivering pulses at a frequency higher than 5 Hz, is currently FDA approved as treatment for patients with medication resistant major depressive disorder (MDD), which is approximately one third of all MDD patients. Left prefrontal high-frequency rTMS has shown to be an effective and safe treatment in adult MDD patients documented as medication resistant (Pascual-Leone et al., 1996; George, 2010; George, Taylor, and Short, 2013; Padberg and George, 2009; Baeken et al., 2013; Loo and Mitchell, 2005). The rationale to stimulate these parts of the cortex is based on earlier studies showing clear involvement of the prefrontal cortex (PFC) in the pathophysiology of MDD (Koenigs and Grafman, 2009). More specifically, the ventromedial PFC (VMPFC) shows hyperactivity whereas the dorsolateral PFC (DLPFC) shows hypoactivity, as demonstrated by multiple imaging studies (Mulders et al., 2015). Reversing these effects - decreasing the activity of the VMPFC or increasing the activity of the DLPFC - has been proposed as a possible mechanism by which rTMS treatment can achieve response and remission from depressive symptoms (Seminowicz et al., 2004; George, 2010).

Standard rTMS guidelines to treat depression follow mostly a daily pattern, with applied frequencies from 1-20 Hz, repeated for 4-6 weeks (Perera et al., 2016). With such protocols, clinical effectiveness remains however rather modest. To improve clinical outcome, new treatment parameters are currently under investigation. One new approach is *accelerated rTMS*, where a similar amount of stimulation sessions is concentrated over a couple of days instead of the more conventional daily sessions, spread over multiple weeks. Another line of research focuses on theta burst stimulation (TBS)(Huang et al., 2005), where a particular set of parameter deliverables applies bursts of 3 stimuli at 50 Hz and is repeated every 200 ms (5 Hz, theta range). TBS has shown comparable clinical efficacy compared to rTMS but stimuli are delivered during a shorter period and usually with a lower intensity (Blumberger et al., 2018). Intermittent TBS (iTBS), the administration of 2 seconds of TBS alternated with 8 seconds rest, has been investigated for treatment of MDD (Li et al., 2014; Bakker et al., 2015; Chistyakov et al., 2010), based on the excitatory character of the standard iTBS protocol (600 stimuli at 80% active motor threshold) (Huang et al., 2005).

In order to maximize clinical efficacy within a shorter time period, an intensive acceler-

ated iTBS (aiTBS) protocol, consisting of multiple iTBS sessions per day, was recently tested as possible treatment for depression in our group. Here, Duprat et al. (2016) showed a rapid significant decrease after 4 days of stimulation in depression severity symptoms assessed with the 17-item Hamilton Depression Rating Scale (HDRS) (Hamilton, 1967). Although clinical effects were found both after sham and verum aiTBS, the most meaningful clinical outcomes regarding response and remission were observed two weeks after the aiTBS protocol, during follow-up. While only 28% of the patients showed a 50% reduction of their initial HDRS score at the end of the stimulation procedure, response rates mounted up to 38% two weeks later, indicating delayed clinical effects. Furthermore, 30% of the responders were considered in clinical remission.

How aiTBS has the potential to improve depression symptoms over such a limited period in medication resistant MDD patients remains to be elucidated. Because it is known that the effects of stimulation are propagated through the brain via anatomical and functional connections (Amico et al., 2017; Fox et al., 2014), the effect of aiTBS might occur on a network level. In this study, the effect of this aiTBS protocol on the brain's network topology is investigated by means of graph analysis derived from resting-state functional MRI (rs-fMRI) data of a group of MDD patients. Graph analysis is a mathematical concept to quantify networks, e.g. brain networks, according to various neurobiologically meaningful properties such as integration and segregation (Rubinov and Sporns, 2010; Bortoletto et al., 2015). Combining rs-fMRI datasets before and after a brain stimulation protocol with graph analysis allows one to map the network changes throughout the whole brain induced by TMS, instead of just looking at single connections at a time, as it is done in many functional connectivity studies.

Previous studies have investigated the brain's network topology in patients with MDD. Graph analyses were performed based on cortical thickness (Mak et al., 2016), voxel based morphometry measures (Lim, Jung, and Aizenstein, 2013), structural connectivity using diffusion MRI data (Chen et al., 2016; Korgaonkar et al., 2014; Ajilore et al., 2014; Singh et al., 2013), or functional connections using rs-fMRI datasets (Bohr et al., 2013; Li et al., 2015). The reported differences in graph measures between healthy volunteers and MDD patients were ambiguous. On the one hand some studies did not find differences, and on the other hand increases in clustering coefficient, local efficiency, and path lengths were reported.

To study the effects of stimulation on network level, only few studies have been performed combining brain stimulation and graph theory: e.g. Shafi et al. (2014) and Deng et al. (2015) used resting EEG data to examine the effects of continuous TBS and rTMS respectively. Shafi et al. (2014) showed frequency band dependent effects of stimulation on clustering coefficient and local efficiency: the beta band showed increases in clustering coefficient after cTBS whereas alpha band showed decreases in clustering coefficient along with increased path length. Deng et al. (2015) showed reduced small-worldness in the beta frequency band after stimulation. Vecchio et al. (2018) performed source localization on EEG data recorded before and after transcranial direct current stimulation (tDCS) and showed that anodal tDCS over the motor cortex reduces small-worldness. Park et al. (2014), Polania et al. (2011), and Cocchi et al. (2015) studied the effects of

various stimulation techniques using task-fMRI and rs-fMRI data. Park observed a correlation between the motor performance change and the increase and decrease in global and local efficiency respectively, induced by 10 Hz rTMS (Park et al., 2014). Cocchi showed different effects of continuous versus inhibitory TBS represented by modularity, out-degree participation index, and within-module degree (Cocchi et al., 2015). Polania et al. (2011) combined anodal tDCS over the motor cortex with rs-fMRI derived graph measures and found increases in path length in the somatomotor areas after stimulation.

Besides the effect of aiTBS on graph measures, it will clinically be relevant to investigate if graph measures can be used as biomarkers to predict the outcome of this stimulation protocol. Previously, it has been shown that rs-fMRI connectivities can be used for this purpose. Drysdale et al. (2017) derived four depression subtypes that seem to respond differently to rTMS treatment. And Fox et al. (2012; 2013) suggested that the stimulation position for optimal clinical response might be linked to the anti-correlation between the subgenual anterior cingulate cortex (sgACC) and the stimulation spot in the left DLPFC. This anti-correlation between the sgACC and parts of the left superior medial prefrontal cortex was also suggested to have predictive value for the outcome of accelerated rTMS in a cohort of MDD patients (Baeken et al., 2014), although in another accelerated iTBS this was not found to be that straightforward (Baeken et al., 2017b). Nevertheless, Downar et al. (2014) showed in a cohort of MDD patients that the graph measure betweenness centrality can be used to distinguish responders from non-responders to rTMS to the dorsomedial prefrontal cortex.

Specifically, this is the first study using graph analysis to investigate the clinical effects of the relatively new aiTBS treatment protocol. Graph analysis was performed on the whole brain level, using the clustering coefficient, global efficiency, small-worldness, and modularity, and on the nodal level, using the degree and the betweenness centrality as graph measures. Due to the presumably excitatory character of iTBS, we hypothesized that aiTBS would increase all four whole brain graph measures. On nodal level, we expected to find mostly increases in degree and betweenness centrality in nodes related to the pathophysiology of MDD. Furthermore, we expected that changes in graph measures would be linked to the clinical response. We also hypothesized that changes in functional connectivity, expressed by graph measures, would not only occur in the stimulated area (the left DLPFC), but will also be present in functionally connected regions.

4.2 Methods

This study (<http://clinicaltrials.gov/show/NCT01832805>) was approved by the local Ghent University Hospital ethics committee and is in accordance with the declaration of Helsinki (2004). All patients gave written informed consent.

4.2.1 Inclusion criteria

Fifty right-handed MDD patients were included in this study. MDD was diagnosed using the structured Mini-International Neuropsychiatric Interview (MINI, Sheehan et al. (1998)). All patients were at least stage I treatment resistant according to the Rush crite-

ria (Rush, Thase, and Dube, 2003). They had a minimum of one unsuccessful treatment trial with selective serotonin reuptake inhibitors/serotonin and norepinephrine reuptake inhibitors (SSRI/SNRI). Medication was tapered off before the aiTBS treatment period, so all were medication-free for at least two weeks before the start of the first stimulation session. More extensive information about the patients and clinical outcome can be found in Duprat et al. (2016).

4.2.2 Data acquisition

The overall design of this randomized, sham controlled, double-blind, cross-over trial is shown in Figure 4.1. Patients were randomized to receive first sham aiTBS followed by verum aiTBS (A in Figure 4.1) or the other way around (B in Figure 4.1). All patients first underwent baseline MRI (3T Siemens TrioTim, Erlangen, Germany) on day 1 (T1) with anatomical imaging (MPRAGE, TR=2530ms, TE=2.58ms, FA=7deg, FOV=220x220mm², resolution=0.9x0.9x0.9mm³, 176 slices) and rs-fMRI (EPI, TR=2000ms, TE=29ms, FA=90deg, FOV=192x192mm², resolution= 3x3x3mm³, slice thickness/gap=3/1mm, 40 slices, 300 volumes, TA = 10.12min). During the resting state measurement, patients were asked to stay awake with their eyes closed. On day 2 to 5, and day 9 to 12, verum or sham aiTBS was applied depending on the randomization order. A Magstim Rapid² Plus¹ magnetic stimulator (Magstim Company Limited, Wales, UK) connected to a verum or sham figure-of-eight shaped coil (Magstim 70mm double air film (sham) coil) was used to apply the verum and sham stimulation respectively. On the 8th day (T2) and on the 15th day (T3), so 3 days after the stimulation, the imaging protocol was repeated. At the same days when imaging was performed (T1, T2, and T3) and additionally 2 weeks after the last stimulation (T4), depression severity symptoms were assessed using the 17-item HDRS questionnaire (Hamilton, 1967).

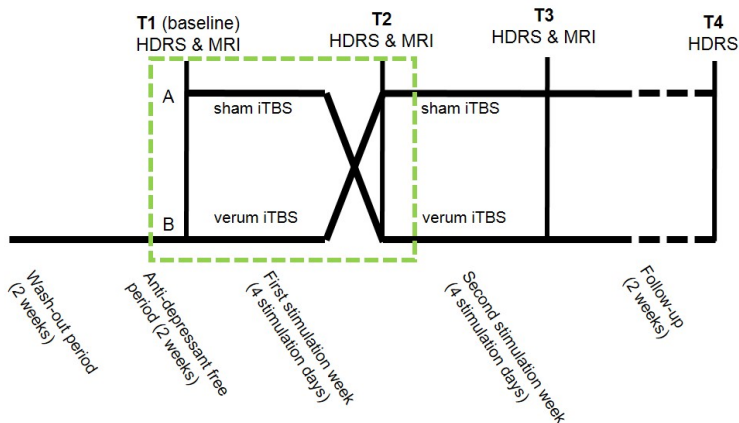


Figure 4.1 — Design of the accelerated iTBS treatment procedure. After a wash-out period, all patients were at least 2 weeks anti-depressant free before they were randomized to receive verum and sham accelerated iTBS treatment. Scheme adapted from Duprat et al. (2016).

Before the first stimulation session, the resting motor threshold (rMT) was determined based on motor evoked potentials (MEPs) induced in the right abductor pollicis brevis (APB) after applying single pulses to the hotspot. During four consecutive days, five daily sessions of iTBS were applied at 110% rMT to the left DLPFC: the center part of the midprefrontal gyrus (Brodmann area 9/46) based on structural MRI of each individual (Peleman et al., 2010). Positioning of the coil was maintained with the BrainSight neuronavigation system (BrainsightTM, Rogue Resolutions, Inc). One iTBS session consisted of 54 trains of 10 bursts of 3 stimuli. Two seconds of stimulation were given in an 8 second cycling period. This adds up to 1620 stimuli per session with a total number of 32,400 stimuli during the four-day treatment. There were breaks of approximately 15 minutes between the stimulation sessions. During the stimulation, patients were blindfolded, wore earplugs, and were kept unaware of the type of stimulation (sham or verum) they received.

4.2.3 Graph analysis

Functional connectivity analyses were performed using the rs-fMRI data from T1 and T2. In this first week of the study design, patients received either sham or verum aiTBS depending on the order of randomization. The second part of the study protocol, the period between T2 and T3 after the cross-over, was not used in order to be able to study the pure effects of sham and verum aiTBS. The duration of the after-effect of four days aiTBS is not yet known and since there was only a weekend between the stimulation weeks, effects of verum and sham might be crossed over into the second week.

Data were preprocessed with Matlab 2015b (The Mathworks Inc., Natick, MA, US) and SPM12 (Wellcome Trust Centre for Neuroimaging, London, UK) according to standard steps. After realignment, volumes with excessive motion, quantified as >0.3 mm framewise displacement, were discarded for further analysis. Complete datasets were excluded if more than 100 volumes had to be removed (based on the datasets, see Appendix 4.6.1.A). Six motion regressors, and additionally a white-matter and cerebrospinal fluid regressor were used to correct the data using SPM's REST toolbox (Song et al., 2011). The latter two regressors were defined as the mean of the time-series within the eroded white-matter and cerebrospinal fluid masks respectively. Temporal bandpass filtering was applied with cut-off frequencies of 0.1 and 0.01 Hz.

The brain datasets were parcellated using the parcellation scheme from Drysdale et al. (2017), using the 264 parcels, further referred to as nodes, from Power et al. (2011) and additionally 13 sub-cortical gray matter structures (see Appendix Table 4.8 for additional information). For all nodes, the mean time-series was computed by averaging all the voxel time-series belonging to that node. The temporal signal to noise ratio (tSNR) criterion was used to remove nodes with unreliable time-series from further analyses. Nodes were discarded if $tSNR < 40$ in more than 10% of the datasets (Liston et al., 2014). Furthermore, if more than 10% of the nodes within one dataset had $tSNR < 40$, the dataset (both T1 and T2) was removed from further analysis (Appendix 4.6.1.C).

For every patient and for both time points (T1 and T2), a connectivity matrix was calculated as the Pearson correlation between all the node time-series, herewith rejecting the first ten volumes to ensure scanner stability. The connections in this connectivity matrix are further referred to as edges. All edges are scaled to be in the range between zero and one (Schwarz and McGonigle, 2011) in a three step process. Firstly, the range of the connectivity matrix was defined by subtracting the minimum value from the maximum value. Secondly, all edge-values were divided by the range. Lastly, the minimum value of the new matrix was added which results in a scaled matrix between zero and one. This method was repeated for every subject and for every time-point separately.

The Matlab-based Brain Connectivity Toolbox (Rubinov and Sporns, 2010) and the Graph Analysis Toolbox (Hosseini, Hoeft, and Kesler, 2012) were used to calculate a range of graph measures that quantify the brain's network organization (Bullmore and Sporns, 2009; Bullmore and Sporns, 2012; Rubinov and Sporns, 2010). On whole brain level, four weighted graph parameters were calculated from every connectivity matrix: clustering coefficient, global efficiency, small-worldness, and modularity. Here, high clustering coefficients are associated with high local efficiency regarding information transfer and robustness (Bullmore and Sporns, 2009). The modularity measure represents the way in which a network can be subdivided into modules: groups of nodes with a high number of within-group links and a low number of between-group connections (Girvan and Newman, 2002; Newman, 2004). Functional integration can be described by path length and efficiencies. High functional connectivity values can be translated to short path lengths and high efficiencies. The path length is the average of the shortest routes of information flow between pairs of nodes. Global efficiency can be calculated by inverting the path lengths. Moreover, the small-worldness was calculated. Small-world networks are assumed to be efficient, both locally and globally (Rubinov and Sporns, 2010). To calculate the small-worldness, the clustering coefficient and path length were normalized by dividing them by their equivalents derived from random networks. Random networks were obtained using twenty randomization steps, leaving the degree of the connectivity matrix unchanged.

On the nodal level, two graph measures were calculated: the betweenness centrality and the degree. The betweenness centrality represents the fraction of shortest paths that pass through a certain node. Degree is a measure of interaction and can be calculated as the summation of all functional connections per node.

In general, graph measures are known to depend on the number of nodes and the average degree within a network (Wijk et al., 2010). Therefore, to obtain robust measures, every graph measure was calculated for a range of densities. The lowest density was set to 28% to prevent disconnected networks. The full density range comprises densities between 28 and 50% (in steps of 2%). Above 50%, connections are thought not to be physiologically meaningful (Hosseini, Hoeft, and Kesler, 2012; Kaiser and Hilgetag, 2006). The area under the curve was calculated over this whole density range to obtain one robust, representative value for the graph measure per patient, per time-point, and in case of the nodal analysis also per node.

4.2.4 Statistical analysis

In this study, functional connectivity, represented by various graph measures, was compared between T1 and T2 (see Figure 4.1). Here, ΔGM is the change in graph measure ($GM_{T2} - GM_{T1}$), and referred to as the effect size. Because of non-normality of the graph parameters (see Appendix 4.6.2), non-parametric permutation tests using 1000 permutations were performed to investigate the difference between sham and verum stimulation on graph measures (ΔGM_{sham} versus ΔGM_{verum}).

Significance level was set to $p < 0.05$ for the whole brain analysis. On the nodal level, additional multiple comparison correction was applied via the Holm-Bonferroni method, using the number of nodes for correction, but all findings with $p < 0.05$ were reported. Post-hoc t-tests were used to investigate the direction of the effects.

4.2.5 Spatial distribution

To study the assumption that the effect of aiTBS distributes via functional connections, the functional connectivity between the stimulation position in the left DLPFC and all the nodes showing an effect of verum stimulation over sham stimulation were calculated and correlated with the effect size. A circular region of interest (ROI), with a diameter of 1 cm, was positioned at the average stimulation position and a time-series was derived by averaging all the time-series of the gray-matter voxels within the ROI.

4.2.6 Biomarker investigation

To investigate the predictive value of graph parameters on the clinical response to aiTBS, the baseline graph measures were correlated with the change in HDRS in terms of percentage (T2 with respect to T1 in the subgroup of patients receiving verum stimulation). Here, this means the lower the scores on HDRS changes in terms of percentage, the better the clinical response. Only significant correlations ($p < 0.05$) were reported.

4.3 Results

Given five drop-out patients (due to a different diagnosis retrospectively, clinical improvement before the stimulation, or incomplete or wrongly timed MRI datasets), exclusion of seven patients (due to excessive motion in the MRI dataset at either T1 or T2), exclusion of three subjects based on the tSNR criterion, and three subjects did not have connected graphs within the density range, data from 32 patients were used for analysis. Of these patients, 14 received sham stimulation between T1 and T2 (arm A in Figure 4.1), and 18 received verum stimulation (arm B in Figure 4.1). Patient details and results on the clinical outcome of this stimulation protocol can be found in Duprat et al. (2016). Based on the tSNR criteria, 18 nodes (represented in red in Figure 4.2), were removed. Detailed information about the excluded nodes can be found in Appendix 4.6.1.B.

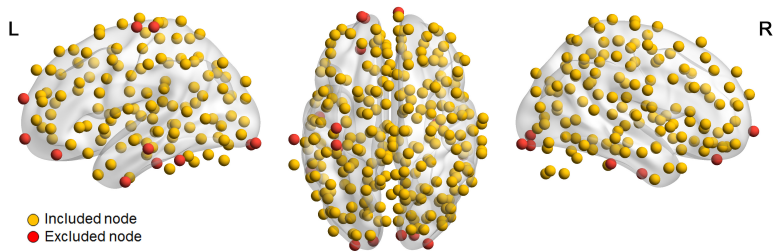


Figure 4.2 — Overview of nodes used for graph analysis. After applying a *t*SNR criterion (at least 90% of the nodes should have *t*SNR >40), 18 nodes were excluded from the graph analysis (marked in red).

4.3.1 Whole brain network topology changes

On the whole brain level, stimulation caused a significant effect on clustering coefficient and global efficiency (*p*-values <0.01, <0.01, 0.072, 0.607 for clustering coefficient, global efficiency, modularity, and small-worldness respectively) (Appendix 4.6.2). However, the effects did not differ between the subgroups receiving sham and verum stimulation. An overview can be found in Table 4.1.

Table 4.1 — Statistical overview of *p*-values (permutation test with 1,000 permutations) representing the effect of stimulation type (verum vs sham) on whole-brain graph measures.

Graph measure	<i>p</i> -value (tail = 1)	<i>p</i> -value (tail = 0)	<i>p</i> -value (tail = 1)
Clustering coefficient	0.656	0.688	0.344
Global efficiency	0.94	0.12	0.06
Modularity	0.199	0.378	0.801
Small-worldness	0.528	0.944	0.472

As can be seen in Table 4.2, changes in graph measures were not significantly correlated with changes in clinical outcome.

Table 4.2 — Correlation between the changes in whole-brain graph measures versus the changes in clinical well-being (after vs before stimulation).

	All subjects		Sham stimulated subjects		Verum stimulated subjects	
	Correlation coefficient	<i>p</i> -value	Correlation coefficient	<i>p</i> -value	Correlation coefficient	<i>p</i> -value
Clustering coefficient	-0.21	0.242	-0.35	0.227	-0.20	0.437
Global efficiency	-0.21	0.254	-0.43	0.125	-0.24	0.344
Modularity	-0.07	0.724	-0.03	0.918	-0.03	0.916
Small-worldness	0.11	0.551	0.21	0.474	0.07	0.796

4.3.2 Changes in nodal graph measures

Figure 4.3 and Table 4.3 provide an overview of the nodes with significantly ($p < 0.05$) different effects of sham versus verum aiTBS. Only the betweenness centrality in the right supplementary motor area survived Bonferroni correction for multiple comparisons.

Table 4.3 — Statistical overview of the node showing a significantly different effect between sham and verum aiTBS. Effects were defined as the change in graph measure (T2 - T1).

Node number	Node name	p-value	Corr with stim site	Mean effect (sham)	Mean effect (verum)
Degree					
17	L paracentral lobule	0.034	<0.01	1.921	-1.507
29	R precentral	0.026	— <0.01	1.677	-1.885
46	R postcentral	0.027	0.07	-1.831	1.689
51	L cingulo-opercular	0.008	-0.07	-2.647	2.746
53	R supp motor area	0.038	0.01	-2.099	1.802
57	L cingulo-opercular	0.02	-0.04	3.619	-0.609
59	L cingulo-opercular (mid cingulum)	0.016	0.01	-1.514	3.643
65	L Supramarginal (auditory)	0.049	-0.10	-1.873	1.389
69	L Supramarginal (auditory)	0.03	-0.07	0.950	-2.577
112	L frontal sup medial	0.007	0.25	-1.851	2.121
113	L anterior cingulum	0.049	0.12	-0.921	1.769
119	R mid temporal	0.026	0.07	-3.112	0.448
124	L parahippocampal	0.001	-0.07	2.534	-3.512
167	L Cuneus	0.031	-0.13	-0.886	2.639
218	R Frontal Middle	0.039	0.02	0.365	3.851
233	R subcortical	0.033	0.09	1.878	-2.227
243	L Cerebellum	0.033	-0.04	1.753	-2.101
260	L Middle Occipital	0.048	-0.05	0.620	-2.632
Betweenness centrality					
7	R parahippocampal	0.034	-0.03	-0.359	15.132
16	R supp motor area	0*	-0.03	13.547	-22.387
17	L paracentral lobule	0.01	<0.01	10.903	-16.448
29	R precentral	0.039	0.03	-3.283	8.738
45	L postcentral	0.033	-0.04	6.856	-13.340
63	R temporal sup	0.012	-0.10	4.909	-15.901
64	L Rolandic oper	0.009	-0.04	-22.929	1.287
97	R frontal sup	0.003	0.16	10.439	-9.238
101	R frontal sup	0.026	0.06	7.773	-6.713
119	R temporal mid	0.003	0.07	-13.196	10.489
124	L parahippocampal	0.025	-0.07	-17.820	2.300
133	L cingulum post	0.028	0.12	15.210	2.517
154	L occipital inf	0.021	-0.12	9.576	-7.326
161	R temporal inf	0.004	-0.02	8.237	-12.659
179	R temporal inf	0.029	-<0.01	6.494	-5.580
194	R angular	0.04	0.08	6.676	-7.374
196	R frontal mid	0.045	0.16	9.377	-0.447
198	L frontal mid orb	0.024	0.14	-11.100	4.519
213	L supp motor area	0.015	-0.07	-14.444	3.072
227	L putamen	0.023	0.03	-12.493	7.018
228	L subcortical	0.011	0.08	-15.480	16.380
235	R Temporal sup	0.031	0.01	-11.220	3.228
268	L caudate	0.004	0.05	-18.123	4.126

Table 4.4 — Overview of nodes showing significant ($p < 0.05$) correlation between the changes in graph measures versus the changes in depression severity.

		All subjects		Sham stimulated subjects		Verum stimulated subjects	
Node number	Node name	Correlation coefficient	p-value	Correlation coefficient	p-value	Correlation coefficient	p-value
Degree							
124	L parahippocampal	-0.07	0.69	-0.58	0.03	-0.03	0.90
Betweenness centrality							
45	L postcentral	0.60	<0.01	0.69	0.01	0.51	0.03
213	L supp motor area	-0.33	0.06	0.04	0.90	-0.65	< 0.01

4.3.4 Potential of graph measures as biomarker

Figure 4.6 shows an overview of the baseline whole brain graph measures versus the percentage of change in HDRS score, after versus before verum stimulation. Table 4.6 shows the statistical values.

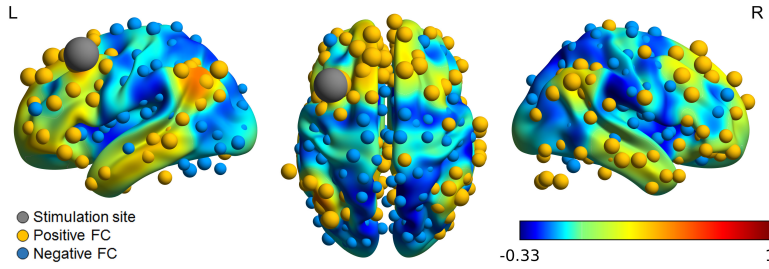


Figure 4.4 — Functional connectivity (FC) with the stimulation area in the left DLPFC (MNI [-38, 20, 54], shown in gray) as seed region. The volume shows the overall connectivity map obtained from neurosynth.org. Functional correlations with the nodes are shown in yellow and blue for positive and negative connections, respectively. The size of the nodes represents the strength of the connectivity.

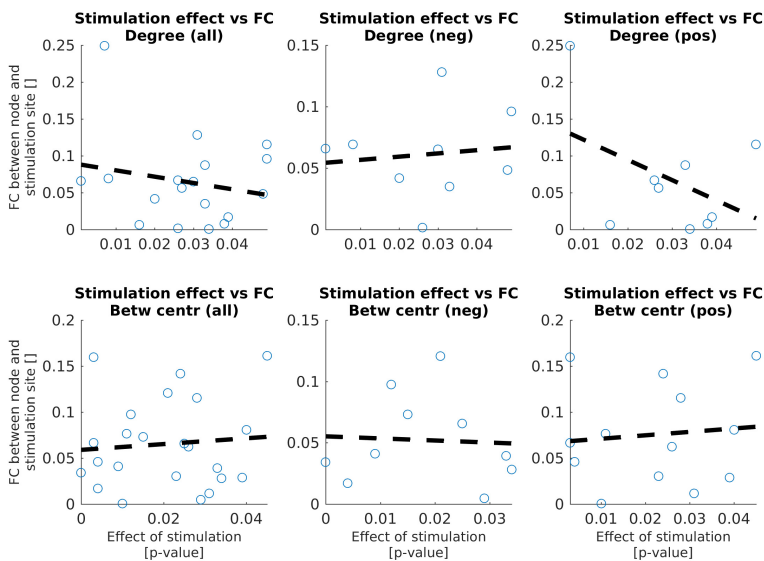


Figure 4.5 — Correlation between the functional connectivities (FC) between the stimulation site in the left DLPFC and the nodes showing effects of verum stimulation with respect to sham stimulation and the strength of the effect. Statistical details can be found in Table 4.5.

Both the clustering coefficient and the global efficiency show a significant correlation between the baseline values and the changes in clinical well-being. The negative correlation coefficient and slope indicate that higher baseline values may predict higher clinical effect of verum aiTBS.

A comparable analysis was performed on the nodal level, using the degree and the betweenness centrality as graph measures. Figure 4.7 shows an overview of the nodes

Table 4.5 — Statistical details about the correlations between the functional connectivity and the effect size (belonging to Figure 4.5).

	Correlation coefficient	Slope	<i>p</i> -value
Degree			
All	-0.20	-0.86	0.42
Negative	0.12	0.26	0.77
Positive	-0.44	-2.74	0.24
Betweenness centrality			
All	0.09	0.32	0.69
Negative	-0.06	-0.17	0.88
Positive	0.10	0.37	0.74

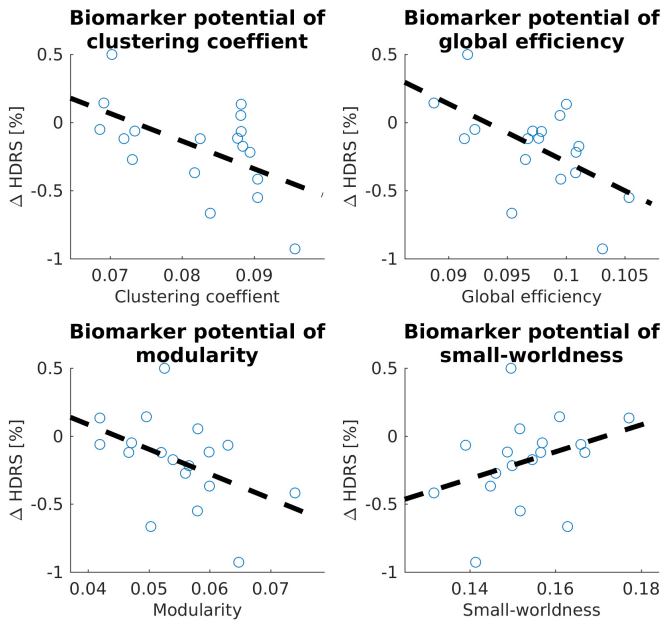


Figure 4.6 — Potential of whole-brain graph measures clustering coefficient, global efficiency, modularity, and small-worldness to predict the percentage of clinical change of verum aiTBS. Statistical details can be found in Table 4.6.

Table 4.6 — Statistical overview of the biomarker potential of the four whole-brain graph measures

Graph measure	Correlation coefficient	Slope	<i>p</i> -value
Clustering coefficient	-0.55	-20.3	0.019
Global efficiency	-0.57	-42.5	0.014
Modularity	-0.45	-18.18	0.058
Small-worldness	0.33	9.93	0.173

showing significant ($p < 0.05$) effects and the belonging statistics can be found in Table 4.7.

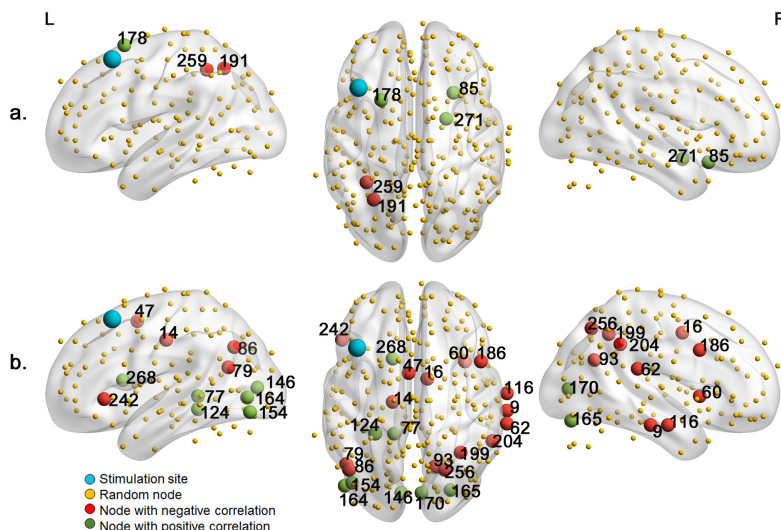


Figure 4.7 — Nodes showing a significant ($p < 0.05$) potential of degree (a) or betweenness centrality (b) to predict the effect of verum aiTBS.

Table 4.7 — Statistical information about the nodes showing significant ($p < 0.05$) biomarker potential

Node number	Node name	Correlation coefficient	Slope	p -value
Degree				
85	R insula	0.61	0.03	0.007
178	L Frontal superior	0.49	0.03	0.038
191	L inferior parietal	-0.52	-0.03	0.027
259	L inferior parietal	-0.53	-0.03	0.025
271	R amygdala	0.53	0.03	0.023
Betweenness centrality				
9	R middle temporal	-0.60	-0.01	0.008
14	L medial somatomotor	-0.52	-0.01	0.03
16	R supp motor area	-0.52	-0.01	0.03
47	L supp motor area	-0.68	-0.01	0.002
60	R cingulo-opercular	-0.69	-0.01	0.001
62	R superior temporal (auditory)	-0.62	-0.01	0.006
77	L precuneus	0.56	0.01	0.017
79	L midl temporal	-0.51	-0.01	0.03
86	L angular	-0.55	-0.01	0.018
93	R precuneus	-0.59	-0.01	0.010
116	R middle temporal	-0.57	-0.01	0.013
146	L Calcarine	0.60	0.01	0.009
154	L Occipital inferior	0.56	0.01	0.015
164	L Middle occipital	0.47	0.01	0.049
165	R Fusiform	0.52	0.02	0.029
170	R Calcarine	0.54	0.01	0.021
186	R frontoparietal	-0.56	-0.01	0.017
199	R inferior parietal	-0.56	-0.01	0.017
204	R supramarginal	-0.48	-0.01	0.017
242	L Frontal inferior	-0.49	-0.01	0.039
256	R occipital superior	-0.52	-0.01	0.028
268	L Caudate nucleus	0.50	0.01	0.036

4.4 Discussion

This study aimed to use graph theoretical analysis to investigate the effects of the relatively new accelerated stimulation protocol to treat MDD patients, namely aiTBS, on the

brain's network organization.

4.4.1 The effect of aiTBS on graph measures

A. Whole brain results

On the whole brain level, no significant differences between the effects of verum stimulation versus sham stimulation were found, and changes in graph measures did not correlate with changes in depression severity symptoms. Previous studies (Ajilore et al., 2014; Lim, Jung, and Aizenstein, 2013) found no differences between graph measures clustering coefficients, path lengths, and small-worldness in healthy subjects and patients with late-life depression on whole brain level. Clinical effectiveness might not be linked to changes in whole brain graph measures. Even though aiTBS treatment in MDD patients does not influence the whole brain's network topology, it may have effects within sub-networks. Indeed, Tik et al. (2017) recently showed in a population of healthy subjects after 10 Hz rTMS network-specific increases in functional connectivity in one specific resting-state network, containing the stimulated left DLPFC and the sgACC.

B. Nodal results

On the nodal level, some nodes showed significantly different responses to verum and sham stimulation. Because these nodes are spread throughout the whole brain, this indicates that the effects of aiTBS are not restricted to the stimulation site. The nodes in proximity to the stimulated left DLPFC did not show differences between sham and verum responses. The direction of effects varied between nodes. Some nodes displayed significantly larger increases in graph measures after verum or sham stimulation and others showed increases after sham and decreases after verum or vice versa. Previously, it was demonstrated in similar types of MDD patients that clinical improvement after an accelerated high frequency rTMS paradigm was associated with significant increases of GABA (γ -aminobutyric acid) concentrations in the stimulated area (the same left DLPFC spot that was also targeted here in this study) (Baeken et al., 2017b). These GABA increases must be primarily considered as an 'excitation' of GABAergic inhibitory neurons and pathways (Lefaucheur et al., 2006). Both Kang et al. (2016) and Liston et al. (2014) have reported reductions in connectivity after 10 Hz rTMS, which is also assumed to have excitatory effects. However, one needs to keep in mind that according to Huang et al. (2005) the standard iTBS protocol is thought to result in excitatory effects. The aiTBS protocol is a modified form of the original iTBS protocol, not only in the number of pulses but also in the number of sessions. As it is known that modifications of stimulation protocols are able to reverse the polarity of the after-effects (Gamboa et al., 2010; Gamboa et al., 2011; Gentner et al., 2008; Murakami et al., 2012), it remains to be determined whether the net effects in the stimulated and connected areas are excitatory or inhibitory.

C. Specific nodal effect

The most significant result (also the only finding that survived Bonferroni correction) was observed in the right supplementary motor area. Whereas the betweenness centrality increased after verum stimulation, it decreased after sham stimulation. This means that more shortest paths between brain regions pass the right supplementary motor area. As

TMS has been linked to changes in psychomotor performance before in the healthy as well as depressed state, this is of interest to explain to some extent the working mechanisms of this kind of stimulation. For instance, Baeken et al. (2010) found improved psychomotor performance after high frequency rTMS treatment in medication resistant depressed patients. Also Hoepfner et al. (2010) showed a trend towards reduction of psychomotor agitation in MDD after high frequency rTMS. Our current findings indicate that left DLPFC aiTBS indeed may affect cortical areas involved in (psycho)motor actions.

In addition, more exploratory analyses revealed that the aiTBS treatment protocol shows effects on several (sub)cortical areas that can be linked to the pathophysiology of depression. For example, the effects of sham and verum aiTBS on degree differ in the left cingulo-opercular nodes, which are part of the cingulo-opercular network comprising the bilateral dorsal anterior cingulate cortices (dACC), the anterior insula, anterior prefrontal cortex, and the anterior thalamus (Sylvester et al., 2012). This network integrates visceral, autonomic, and sensory data to assess the homeostatic relevance or 'salience' of internal and external stimuli, and the maintenance of tonic alertness or sustained attention (Sadaghiani and D'Esposito, 2015). The network also clears noisy information, suppresses distraction, and keeps cognitive faculties available for current processing demands (Sadaghiani and D'Esposito, 2015). Abnormalities in this network have been reported for obsessive compulsive disorder (OCD) (Vries et al., 2017), psychosis (Sheffield et al., 2017), and mood and anxiety disorders (De Witte and Mueller, 2016). Of interest, Wu et al. (2016) showed that depression symptom severity was significantly correlated with the connectivity values of this network. Indeed, increased activity in the dACC or insula during response conflict have been reported during negative mood states (Disner et al., 2011).

Furthermore, several nodes that showed significantly different effects of verum and sham aiTBS, such as for example the parahippocampal nodes, nodes within the prefrontal cortex, and the posterior cingulum node, belong to the default mode network (DMN). The DMN is found to be activated during resting-state functional imaging and de-activated when performing cognitive tasks (Fox et al., 2005; Smith et al., 2009). When the brain is not engaged in externally driven cognitive processing, self-referential processes are believed to predominate (Gusnard et al., 2001). When clinically depressed, more activity in the DMN is observed (Disner et al., 2011). Changes in DMN activation have earlier been linked to anti-depressant responses.

4.4.2 Spatial distribution of aiTBS effects

Previous studies have already shown distributed 'network-effects' of TMS (Fox et al., 2014; Fox, Liu, and Pascual-Leone, 2013). In the current study, using nodes showing significantly different effects between verum and sham stimulation, the correlation between effect sizes and functional connectivity strengths did not reach significance. This indicates that the propagation of aiTBS-effect from the stimulated node in terms of graph parameters is not directly linked to the strength of the functional connections. Considering the network-hypothesis, we hypothesize that the indirect effects of TMS occur at different levels. After the activation of brain areas connected to the stimulation site are

activated, in the following steps the brain areas connected to those areas are activated and so on and so forth. This could, at least partly, explain the occurrence of increases and decreases in graph measures in distinct areas of the brain.

4.4.3 Graph measures as biomarker

Clinical improvement was associated with higher baseline clustering coefficient or global efficiency on the whole brain level. This indicates that all nodes within the whole brain are better integrated. The effect of verum stimulation therefore seems to propagate more easily through the whole brain via functional connections, also to deeper structures involved in the deregulated neurocircuitry of depression.

On the nodal level, we found that graph measures in multiple nodes showed potential to predict the clinical effect. For example, a positive correlation between the baseline betweenness centrality and clinical effect was found in the left caudate nucleus. So lower betweenness centrality might be advantageous for clinical outcome. Given that the caudate has neural innervation from amongst others the prefrontal cortex, our left caudate nucleus findings could be linked to the application of left sided stimulation (Kang et al., 2016). Indeed, stronger connectivity between the dorsal prefrontal cortex and the (dorsal) caudate has been associated with depression severity (Furman et al., 2011; Kerestes et al., 2015). Furthermore, observations of increased connectivity with the DLPFC and the more ventral parts of the ACC in MDD was associated with heightened cognitive regulation of affect, usually problematic when clinically depressed; whereas reduced connectivity with the caudate results in worsening symptoms such as anhedonia, reduced motivation and psychomotor dysfunction (Davey et al., 2012). Of note, although the sgACC was not implicated in our findings, the structural and functional connections between the striatum (caudate) and the (sg)ACC are well known (Gabbay et al., 2013). In treatment resistant depression, the sgACC has been proposed as biomarker for response for a variety of interventions, including rTMS treatment (Fox et al., 2012a; Fox, Liu, and Pascual-Leone, 2013; Weigand et al., 2017). However, for the latter application the functional connectivity findings are not that straightforward (Baeken et al., 2014; Baeken et al., 2017b) and the aiTBS treatment delivered to the left DLPFC may have different neurobiological effects on the reward system (including the caudate), based on the level of anhedonia in the depressive state (Duprat et al., 2017). Indeed, it remains to be determined whether the left DLPFC is the best target to stimulate. Other prefrontal areas, such as the dorsomedial prefrontal cortex have been successfully stimulated in depressed patients (Downar et al., 2014), and alternatively when facing non-response, the right orbitofrontal cortex (OFC) was found to be an excellent alternative (Feffer et al., 2018). The right OFC is considered as a 'non-reward' nexus (Cheng et al., 2016) showing reduced functional connectivity in MDD patients. Together with our own findings on clinical improvement combined with baseline striatal (caudate) betweenness centrality, these observations suggest that left DLPFC aiTBS could be successful for a selected cohort of patients.

Furthermore, the degree in the right amygdala was significantly correlated with the clinical effects of verum aiTBS, suggesting that less connections to the right amygdala could be predictive for better clinical responses. Given that the amygdalae are involved in

(in)effective emotion regulation in stress-related disorders (Perlman et al., 2012; Gold and Chrousos, 2002) and in particular the right amygdala is implicated when processing negative information stressful events (Baeken et al., 2010b; Mothersill and Donohoe, 2016), it is of interest to note that increased baseline and sustained amygdala activity to antidepressant treatment is associated with clinical non-response in major depression (Fonseka, Macqueen, and Kennedy, 2018).

4.4.4 General limitations

This study has some general limitations that need to be considered. Notwithstanding that rs-fMRI is a unique and powerful tool to investigate human brain organization, it is based on an inherently ambiguous measure reflecting dynamic couplings that are not yet fully understood. Interscan rs-fMRI data has shown great variability. For example, Ning et al. (2017) aimed to derive the optimal TMS stimulation position based on functional connectivity between the DLPFC and the sgACC and showed different results using resting-state data from same subjects at different time-points. Longer rs-fMRI scans were suggested to reduce this variability. Moreover, various patient-specific factors may also influence the outcome of a stimulation protocol (Silvanto and Pascual-Leone, 2008). As referred to earlier, Drysdale et al. (2017) has shown that the sub-type of depression could be related to the response to stimulation. Furthermore, the sustainability of the effects of aiTBS, or any type of stimulation treatment, are not yet exactly known. Pascual-Leone et al. (1996) showed clinical responses in MDD patients for up to six weeks. Changes in functional connectivity are mostly reported on shorter time-scales. EEG functional connectivity showed changes up to 70 minutes after rTMS (Thut and Pascual-Leone, 2010). Also, changes might be specific over time, e.g. Tik et al. (2017) only showed increased functional connectivity after 15, but not after 30, minutes of rTMS. In this study, the effect of aiTBS was determined 3 days after the last stimulation session. Even though, aiTBS is a much more intense stimulation protocol compared to single day rTMS, changes in functional connectivity might have already faded out after three days.

4.5 Conclusion

This study showed that there are no differences between the effects of verum and sham stimulation on whole brain graph measures and that changes in graph measures are not correlated with clinical response. However, baseline values of clustering coefficient and global efficiency were found to have predictive value of the clinical response to verum aiTBS. On the nodal level, differences between sham and verum aiTBS were found throughout the whole brain, indicating that the effects of aiTBS distribute beyond the actual stimulation target. Knowledge about both functional connectivity changes and the potential use of graph measures as biomarkers could be important additions to novel neurostimulation protocols, as not only a better understanding on the underlying working mechanisms of aiTBS on the depressed brain may provide more insights, it may also guide future stimulation protocols to ameliorate treatment outcome.

4.6 Appendices

4.6.1 Additional information on preprocessing

A. Motion parameters

Overview of the number of volumes per patient after removing the ones with framewise displacement (FWD) > 0.3 . Datasets with less than 200 volumes were discarded from further analysis. Note from Figure 4.8 that 5 datasets in T1 show excessive motion versus 6 in T2. With three overlapping datasets, this led to removal of 8 datasets for further analyses.

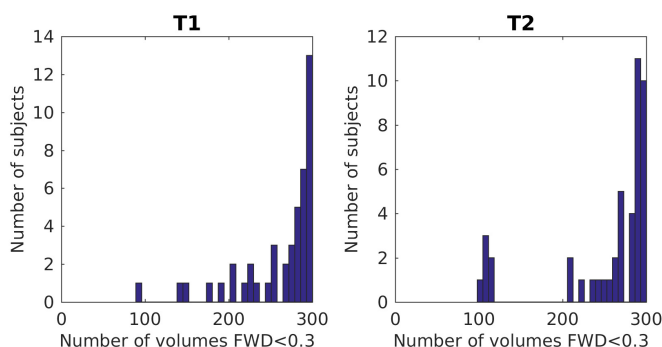


Figure 4.8 — Number of volumes included in the analysis (FWD < 0.3) for every subject, per time-point.

B. Node selection

The first 264 nodes are resulting from the Power parcellation, as described in Power et al. 2011 (Power et al., 2011). Thirteen additional nodes were appended, in accordance to Drysdale et al. 2017 (Drysdale et al., 2017). An overview can be found in Table 4.8.

Table 4.8 — Nodes that were added to the parcellation scheme proposed by Power et al. (2011), in line with Drysdale et al. (2017).

Node number	X (MNI)	Y (MNI)	Z (MNI)	Node name
265	-9	10	-10	Nucleus accumbens (L)
266	10	10	-9	Nucleus accumbens (R)
267	1	25	-11	sgACC
268	-14	-12	12	Caudate nucleus (L)
269	14	12	12	Caudate nucleus (R)
270	-20	-4	-15	Amygdala (L)
271	22	-2	-15	Amygdala (R)
272	-28	-22	-12	Ventral hippocampus (L)
273	28	-22	-12	Ventral hippocampus (R)
274	-6	-38	-30	Locus coeruleus (L)
275	6	-36	-28	Locus coeruleus (R)
276	-4	-15	-9	MTA
277	0	-32	-24	Raphe nucleus

C. tSNR

Figure 4.9 displays an overview of the mean tSNR (averaged over patients) per node. The nodes that were discarded for further analysis are listed in Table 4.9.

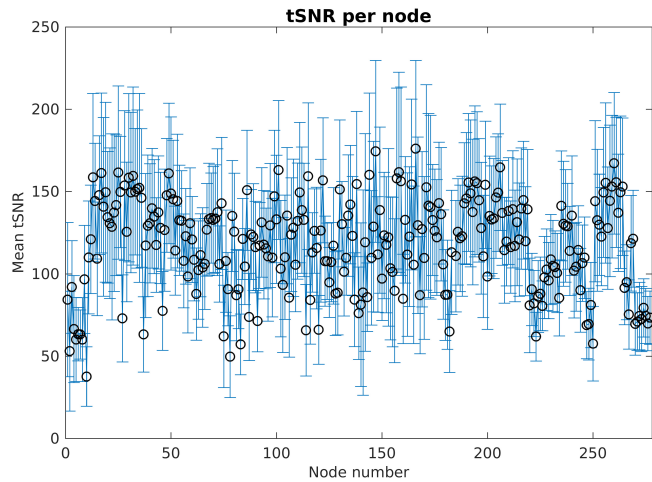


Figure 4.9 — Overview of mean tSNR and standard deviation averaged over all subjects, per node. Nineteen nodes showed tSNR < 40 in more than 10% of the datasets and were excluded for further analysis (Table 4.9).

Table 4.9 — Nodes that were removed from further analysis because the tSNR requirements were not reached.

Node number	X (MNI)	Y (MNI)	Z (MNI)	Node name
1	-25	-98	-12	Left occipital interior
2	27	-97	-13	Right occipital inferior
4	-56	-45	-24	Left temporal inferior
5	8	41	-24	Right Rectus
8	-37	-29	-26	Left fusiform
10	52	-34	-27	Right temporal inferior
27	-38	-27	69	Precentral left
37	-38	-15	69	Left somatosensory
75	6	67	-4	Right medial orbitofrontal
78	-18	63	-9	Left superior orbitofrontal
83	-68	-23	-16	Left middle temporal
114	-20	64	19	Left superior frontal
140	8	-91	-7	Right lingual
141	17	-91	-14	Right lingual
142	-12	-95	-13	Left lingual
182	-21	41	-20	Left middle orbitofrontal
247	33	-12	-34	Right temporal inferior
250	-50	-7	-39	Left temporal inferior

4.6.2 Graph parameter overview

Figure 4.10 and 4.11 show the distributions of whole brain graph measures for the subgroup of patients receiving sham and verum aiTBS respectively.

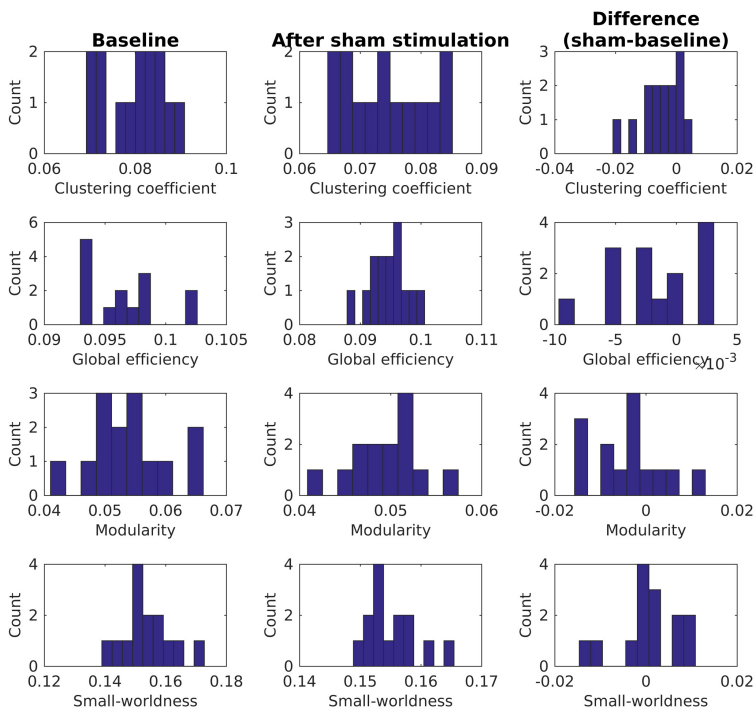


Figure 4.10 — Overview of whole-brain graph measures for subgroup of patients ($n = 14$) who received sham aiTBS during the first week of the stimulation protocol.

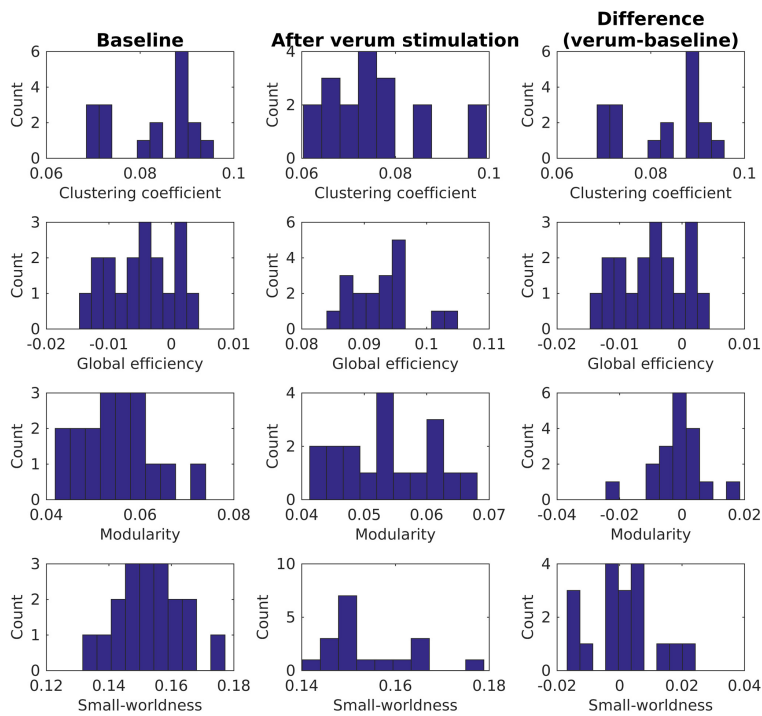


Figure 4.11 — Overview of whole-brain graph measures for subgroup of patients ($n = 18$) who received verum aiTBS during the first week of the stimulation protocol.

4.6.3 Full overview of correlations between changes in graph measures and changes in clinical well-being in nodes showing significant effects of stimulation

A full overview of correlations between changes in graph measures and changes in clinical well-being in nodes showing significant effects of stimulation can be found in Table 4.10.

Table 4.10 — Full overview of correlations between changes in graph measures and changes in clinical well-being in nodes showing significant effects of stimulation.

Node number	All subjects		Sham stimulated subjects		Verum stimulated subjects	
	Correlation coefficient	p-value	Correlation coefficient	p-value	Correlation coefficient	p-value
Degree						
17	-0,0452	0,8061	-0,0105	0,9717	-0,2375	0,3427
29	0,2749	0,1278	-0,118	0,6878	0,3886	0,111
46	-0,1538	0,4007	0,0406	0,8905	-0,1743	0,4891
51	-0,0663	0,7185	0,1236	0,6737	-0,0243	0,9237
53	0,2027	0,2659	0,2112	0,4686	0,3676	0,1334
57	0,098	0,5935	-0,1127	0,7013	0,0829	0,7437
59	0,1546	0,3982	0,308	0,2841	0,2623	0,2931
65	-0,011	0,9526	-0,2247	0,4399	0,3092	0,2119
69	-0,0686	0,7091	0,0415	0,8879	-0,3547	0,1487
112	0,0411	0,8235	0,0131	0,9645	0,2892	0,2445
113	0,1355	0,4595	0,224	0,4413	0,2288	0,3611
119	-0,2307	0,2039	0,152	0,604	-0,4557	0,0573
124	-0,0723	0,6943	-0,5791	0,03	-0,031	0,9028
167	-0,1504	0,4114	-0,3954	0,1617	0,0712	0,7788
218	-0,0583	0,7511	-0,034	0,908	0,0484	0,8489
233	0,3357	0,0603	0,3958	0,1613	0,2184	0,3839
243	-0,1695	0,3537	-0,3481	0,2227	-0,2205	0,3792
260	-0,084	0,6477	-0,2677	0,3547	-0,0759	0,7646
Betweenness centrality						
7	-0,255	0,1589	-0,0173	0,9532	-0,2897	0,2436
16	0,1441	0,4314	0,2126	0,4656	-0,1616	0,5217
17	-0,0247	0,8934	-0,024	0,9351	-0,2211	0,378
29	-0,1332	0,4674	-0,11	0,7081	-0,032	0,8997
45	0,596	0,0003	0,6874	0,0066	0,5075	0,0316
63	0,4115	0,0193	0,2543	0,3802	0,4287	0,0759
64	0,0122	0,9471	0,5075	0,064	-0,2301	0,3583
97	0,247	0,173	0,1566	0,5929	0,189	0,4525
101	0,3499	0,0497	0,3261	0,2551	0,2696	0,2794
119	-0,2289	0,2077	-0,4309	0,124	0,0293	0,908
124	0,1761	0,3349	0,2405	0,4076	0,3206	0,1946
133	-0,0752	0,6826	-0,1231	0,6751	-0,2093	0,4046
154	0,1378	0,452	-0,0042	0,9887	0,0901	0,7222
161	0,1588	0,3854	-0,25	0,3887	0,2791	0,2621
179	-0,0191	0,9175	-0,0158	0,9572	-0,1837	0,4655
196	0,1062	0,563	-0,0731	0,8039	0,1791	0,4771
198	-0,2706	0,1341	0,0539	0,8547	-0,3695	0,1313
213	-0,3315	0,0638	0,0391	0,8945	-0,6532	0,0033
227	-0,1596	0,3829	-0,1797	0,5388	0,0162	0,949
228	-0,279	0,122	-0,1476	0,6145	-0,2986	0,2287
235	-0,0431	0,8148	-0,0629	0,8307	0,1389	0,5825
268	-0,0992	0,5893	0,0465	0,8747	-0,0714	0,7784

"All models are wrong but some are useful."

George Box

CHAPTER **5**

Modeling local effects of transcranial magnetic stimulation for functional connectivity analyses

D.C.W. Klooster, R.M.H. Besseling, A.P. Aldenkamp, A. Opitz, M.D. Fox, C. Baeken
submitted

Abstract

Resting state functional connectivity MRI (rs-fcMRI) between transcranial magnetic stimulation (TMS) sites and remote brain regions can lend insight into mechanism and therapeutic response. However, these analyses depend on modeling local effects at the TMS site to generate a seed region. Modeling approaches range from simple to highly complex, with no consensus on how much complexity is required. The aim of this study is to investigate the impact of these modeling approaches on rs-fcMRI results.

Baseline anatomical and rs-fMRI data from 37 depressed patients who received TMS to the left dorsolateral prefrontal cortex (DLPFC) were used. Two different seeding methods were implemented. First, nine seeds were derived from TMS-induced electric field (Efield) simulations using SimNIBS. Regressors were defined as the weighted averaged time-series of the gray matter voxels where the electric field exceeds a patient-specific threshold (10-90% of the maximum field strength in gray matter in steps of 10%). Second, a simpler cone model was implemented (Cone).

For every patient, the cone regressor was correlated with the nine Efield-regressors. Correlation between these types of regressors depends on the threshold value used to determine the Efield seed. The FC between the stimulation position and the subgenual anterior cingulate cortex did not significantly differ when using different seeding methods ($p = 0.445$, for cone- versus Efield50-regressor). Whole brain FC maps derived from these two different regressors showed high mean correlations (0.68 and 0.69 for the gray matter and combined gray and white matter regions respectively). Knowledge of the actual stimulation position has shown to be important since the correlation between regressors becomes lower when the distance increases, both for the cone-regressors and the Efield50-regressors.

Because of the overall high correlations between cone- and Efield-regressors, computational complexity of the TMS-induced electric field simulations, and the lack of the golden standard, the cone model is currently sufficient to derive regressors for FC analyses to study the effects of TMS.

5.1 Introduction

Transcranial magnetic stimulation (TMS) is an established non-invasive brain stimulation method used in basic and clinical research and treatment (Wagner, Valero-Cabre, and Pascual-Leone, 2007; Valero-Cabré et al., 2017). Based on Faraday's Law, a small electric field can be induced in the brain that is able to depolarize neurons and elicit action potentials. The repetitive administration of TMS pulses, called repetitive TMS (rTMS), can cause physiological effects that outlast the actual period of stimulation. Therefore, rTMS is applied as treatment for a broad variety of neuropsychiatric disorders (Klooster et al., 2016).

The mechanisms of action of (r)TMS are not yet fully understood (Hoogendam, Ramackers, and Di Lazzaro, 2010). Combining (r)TMS with brain imaging can extend our insights into the underlying mechanisms (Fox et al., 2012b). Nowadays, mainly magnetic resonance imaging (MRI) techniques are used because of the superior spatial resolution. Functional MRI (fMRI) allows studying functional connectivity non-invasively. Both task-based fMRI studies, in which fluctuations in blood-oxygen-level-dependent (BOLD) time-series are caused by presenting certain tasks (e.g. visual or cognitive stimuli), and resting-state fMRI (rs-fMRI) studies, in which time-series show spontaneous fluctuations in BOLD signals, can be used to study these functional brain connections. It has been shown that resting-state fMRI time-series can be used to extract similar functional networks compared to task-based studies (Fox et al., 2012a; Fox and Raichle, 2007; Fox et al., 2005; Damoiseaux et al., 2006; Smith et al., 2009).

Functional connectivity (FC) is often defined as the correlation between time-series within a certain target brain area, also referred to as seed, and other areas in the brain (Fox and Raichle, 2007). The seed region in FC studies investigating the effects of stimulation can be described as the region in the brain that is directly affected by the stimulation. However, the exact definition is ambiguous. Multiple studies simply use circular regions of interest (ROIs), with a certain radius, positioned on MNI coordinates in the area of the stimulation coil position, not necessarily directly linked to the exact coil position (Liston et al., 2014; Philip et al., 2017).

More advanced seeding methods, incorporating the knowledge of the (r)TMS-induced electric fields, are nowadays also employed. One example is the cone model, as described by Fox et al. (2013). The linear decay of metabolic changes seen in animal TMS experiments was shown to occur within 12 mm of the stimulation site (Fox, Liu, and Pascual-Leone, 2013; Valero-Cabré et al., 2005). This distance resembles an electric field strength of approximately 75% of the peak field strength at the stimulation site, which seems to overlap with the sub-threshold conditioning pulses to induce physiological effects in human paired-pulse experiments (Kujirai et al., 1993). Therefore, the TMS induced effect in the brain could be modeled using a series of concentric spheres with different radii (2,4,7,9,12 mm). The summed overlap of these spheres generates a cone-shape, with the highest intensity at the modeled stimulation position and a gradual decrease to the sides. Based on this cone model, Fox et al. (2013; 2017) previously showed that FC between the dorsolateral prefrontal cortex (DLPFC) and the subgenual anterior cingu-

late cortex (sgACC) can provide information about the optimal stimulation position to treat patients with major depression. Furthermore, FC analyses using a cone model have been performed to show that targets deep within the brain that are used for successful invasive neurostimulation treatment of various neuropsychiatric disorders are functionally connected to superficial, cortical, areas that are used as targets for non-invasive brain stimulation techniques (Fox et al., 2014).

Also numerical electric field simulations can be used for the derivation of seed regions. Currently, realistic head models exist, incorporating subject-specific geometry, tissue parameters, and also anisotropic tissue conductivities, derived from individual diffusion MRI recordings, can be considered (Klooster et al., 2016; Opitz et al., 2011; Opitz et al., 2013). These electric field models are more complex compared to the cone model and especially generation of subject-specific head models is time-consuming. Seeds representing the TMS effects can be derived from the simulated TMS-induced electric field by thresholding this field. Opitz et al. (2016) used SimNIBS (Windhoff, Opitz, and Thielscher, 2013) to simulate TMS-induced electric fields and used a threshold of 50% of the maximum electric field strength to determine the seed region.

In this study, we investigated the effect of two different seeding methods on FC. Regressors for FC analyses were derived from the cone model and from TMS-induced electric field simulations using existing data of 50 patients that were included in a stimulation study at the University Hospital in Ghent. Besides looking at the seeding method, we also investigated the effect of the knowledge of the exact stimulation location on FC results.

5.2 Methods

For this study, baseline anatomical and rs-fMRI data were used from 50 depressed patients who were included in an accelerated intermittent theta burst stimulation (aiTBS: a particular rTMS protocol) study that was approved by the local Ghent University Hospital ethics committee (<http://clinicaltrials.gov/show/NCT01832805>). All patients gave written informed consent.

5.2.1 Study protocol

An extensive description of this randomized, double-blind, sham-controlled, cross-over study protocol is beyond the scope of this study and can be found in Duprat et al. (2016). In short: depressed patients received both sham and active aiTBS in an order depending on the randomization. The aiTBS protocol comprises 5 daily stimulation sessions on four consecutive days, at 110% of the resting motor threshold using a Magstim Rapid² Plus¹ magnetic stimulator (Magstim Company Limited, Wales, UK). According to the clinical standard, the left DLPFC position that is used as target for rTMS treatment of depression is based on the 5-cm rule. Here, stimulation was applied to the position in the left DLPFC defined as the center part of the midprefrontal gyrus on the gray-matter surface (Brodmann area 9/46) derived from anatomical MRI data of each individual (Peleman et al., 2010). The term stimulation location, as used in this paper, therefore refers to a manually

defined point at the gray-matter surface. This patient-specific information was saved and BrainSight Neuronavigation (BrainSight™, Rogue Resolutions, Inc.) was used to determine the coil position on the scalp to stimulate the predefined target on the gray-matter surface. The current study was focused only on the effect of different methods to model the stimulation position, not on clinical response (details are reported in Duprat et al. (2016)).

5.2.2 MRI data acquisition

MRI data was recorded using a 3T Siemens TrioTim scanner (Erlangen, Germany). Baseline (before stimulation commenced) anatomical imaging (MPRAGE, TR=2530ms, TE=2.58ms, FA=7deg, FOV=220x220mm², resolution=0.9x0.9x0.9mm³, 176 slices) and rs-fMRI (EPI, TR=2000ms, TE=29ms, FA=90deg, FOV=192x192mm², resolution=3x3x3-mm³, slice thickness/gap=3/1mm, 40 slices, 300 volumes, TA = 10.12min) were acquired. During the resting state measurement, patients were asked to stay awake with their eyes closed.

5.2.3 Data analysis

Data were preprocessed with Matlab 2015b (The Mathworks Inc., Natick, MA, US) and SPM12 (Wellcome Trust Centre for Neuroimaging, London, UK) according to standard steps, also described by Drysdale et al. (2017). After realignment, volumes with excessive motion, quantified as >0.3 mm framewise displacement, were discarded for further analysis. Complete datasets were excluded if more than 50% of the volumes had to be removed (leaving at least 150 volumes (Wijk et al., 2010)). Six motion parameters, a CSF and a white matter regressor, and a constant and quadratic term were used to correct the data using a regression approach (Song et al., 2011). Temporal bandpass filtering was applied as the last step with cut-off frequencies of 0.1 and 0.01 Hz.

5.2.4 Regressor derivation

A. Electric field modeling

Electric field modeling was performed with SimNIBS 2.0.1 (Saturnino et al., 2018). Patient-specific tetrahedral finite element method (FEM) meshes were generated from the anatomical MRI data and standard tissue conductivity values were assigned ($\sigma_{WM} = 0.126$ S/m, $\sigma_{GM} = 0.275$ S/m, $\sigma_{CSF} = 1.654$ S/m, $\sigma_{scalp} = 0.465$, $\sigma_{bone} = 0.010$ for white matter, gray matter, cerebrospinal fluid, scalp, and bone respectively) (Thielscher, Antunes, and Saturnino, 2015).

A TMS-induced electric field was modeled using the patient-specific stimulation location at the gray-matter surface in the left DLPFC, as saved in the neuronavigation system. The orientation of the coil was estimated to be in a 45 degree angle with respect to the anterior-posterior line, with the handle pointing backwards. The remaining coil characteristics of the Magstim coil, necessary for the simulation, are by default implemented in

SimNIBS.

After converting the headmeshes to nifti-files (msh2nii), different regressors were derived from the electric field simulations taking into account only the area in the brain above a certain threshold level. First, the electric field strength values in the gray matter were analyzed and a maximum field strength value was defined as the 99 percentile value. This was done to increase the robustness of the thresholding procedure by minimizing effects from possible numerical errors, potentially resulting into very high singular values. Second, nine regressors were computed defined as the mean of the time-series in brain areas exceeding the threshold, weighted by the electric field strengths. Threshold values between 10 and 90% of this maximum field strength value were used, in steps of 10%. An overview of the derivation of these Efield-regressors in a random subject can be found in Figure 5.1.

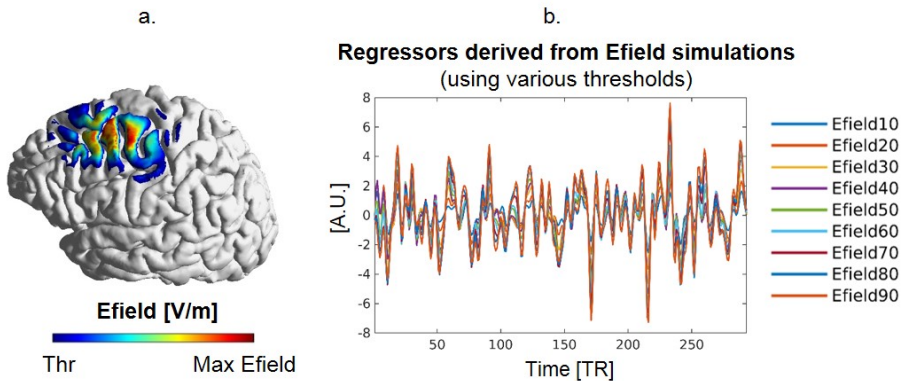


Figure 5.1 — Derivation of the Efield-regressors for a random subject. Figure a. shows the spatial distribution of the TMS-induced electric field. Only the field above a certain threshold, in this case 50% of the maximum strength of the electric field within the gray matter is shown. Figure b. shows the actual regressor time-series derived using 9 different threshold values: 10-90% (referred to as Efield10-Efield90) in steps of 10%. Regressors are computed by averaging the time-series of the gray matter voxels that exceed the electric field threshold, weighted by the electric field strength.

B. Cone modeling

A simpler, and less time-consuming method to model the TMS-induced electric field, is by means of the cone model, as described in Fox et al. (2013). A cone is created using a series of concentric spheres with radii of 12, 9, 7, 4, 2 mm centered on the stimulation location. The final cone is defined by the overlap of the cones masked with a gray and white matter mask. Figure 5.2 shows how the cone regressor can be computed.

5.2.5 Effects of seeding method on FC

To study the effect of different seeding methods on whole brain level, FC maps were computed using SPM12, using the cone-regressor and an Efield-regressor. The remain-

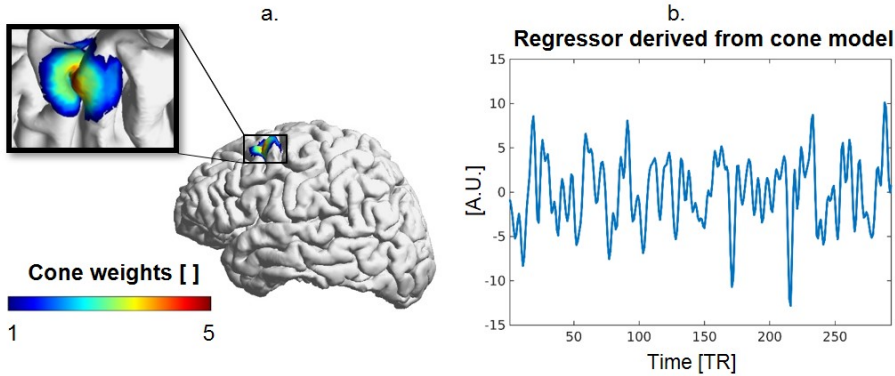


Figure 5.2 — Derivation of the cone regressor for a random subject. The cone can be seen in Figure a. A series of spheres with radii of 12, 9, 7, 4, and 2 mm are placed on the stimulation position. The regressor time-series (b) was computed by the weighted average of the gray and white matter voxels within the cone.

der of this work mainly focuses on the Efield50-regressor, which is comparable to Opitz et al. (2016) who derived thresholds from the maximum electric field strength on the pial surface at 50%. For every patient, the spatial correlation was computed between the whole brain FC maps derived from these two regressors. These spatial correlations were computed for the gray matter area, using a gray matter mask, and the whole brain area, using a gray-and-white matter mask.

Furthermore, the sgACC has shown to be an important structure in the pathophysiology of major depression (Baeken et al., 2014; Fox et al., 2012a; Fox, Liu, and Pascual-Leone, 2013; Weigand et al., 2017). Therefore, the specific connectivity between the stimulation location and the sgACC has been studied in more detail. An sgACC-regressor was derived by placing a circular ROI with diameter 15 mm at MNI coordinates [1, 11, -25] (Baeken et al., 2015). This circular ROI was masked with a gray matter mask. The regressor was defined as the mean time-series of these gray matter voxels. Since the sgACC is located deep in the brain, close to the ventricles, the rs-fMRI signal may suffer from loss-of-signal artefacts. Therefore, the temporal signal to noise ratio (tSNR) was calculated, defined as the mean of the MR signal over time divided by the standard deviation of the time-series. Datasets showing a tSNR < 40 (Liston et al., 2014) were excluded from further analyses. Connectivity was defined by the correlation between the sgACC-regressor and cone- and Efield50-regressors.

5.2.6 The effect of the exact stimulation location

The regressors also depend on the stimulation location; i.e. location in the brain that is used to place the cone or to focus the electric field simulation around. To investigate the effect of the stimulation location on the regressors, for every subject different regressors have been generated using a variety of simulated stimulation locations (note: only one location was actually stimulated). This variety of locations is derived from the different

stimulation locations of the patients included in this study (Figure 5.3a).

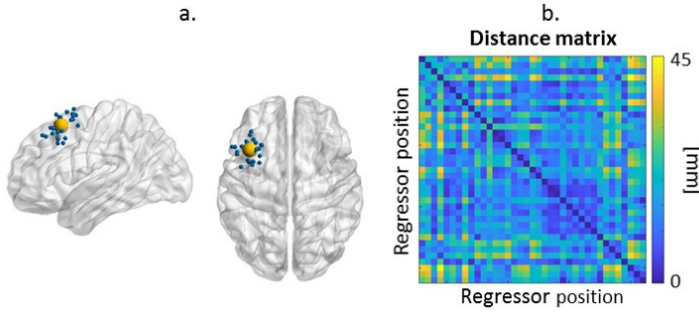


Figure 5.3 — Figure a shows an overview of the gray matter DLPFC stimulation locations in 37 patients (blue dots). The yellow dot represents the mean stimulation location (MNI: -38, 19, 55). A distance matrix containing the distances between the stimulation locations between different patients (in mm) is shown in Figure b.

In case of the cone modeling, cones have been positioned on the variety of stimulation locations over all patients. A regressor was derived for every simulated location. For every subject, correlations were computed between the regressor of the actual stimulation location and all the other regressors (resulting in an array of 1 x number of subjects correlations). Correlations between different regressors were compared to Euclidian distances between the locations (Figure 5.3b).

In case of the electric field modeling, all electric fields and the rs-fMRI time-series were normalized to MNI space using SPM12 such that a comparable strategy could be used as for the cone modeling to investigate the effect of the knowledge of the stimulation position on the Efield-regressor.

5.3 Results

Given 5 dropouts, 3 rs-fMRI datasets with excessive motion, and 5 cases in which the coil position was not saved properly in the neuronavigation system, data of 37 patients were used for analysis in this study. The mean (MNI) coil location was -37.77 (std 6.73 mm) ; 18.62 (std 7.52 mm); 54.87 (std 8.08 mm), see Figure 5.3a.

5.3.1 Correlation between different regressors

For every patient, the cone-regressor was correlated with every Efield-regressor, as can be seen in Figure 5.4. A linear fit was calculated through the means of the correlations per threshold value (as represented by the black circles and dotted line). The correlation (Corr) between regressors derived from the cone-model and the Efield-simulations could be described as a function of the Efield-threshold (Thr) that was used:

$$Corr = 0.568 + 0.003 * Thr \quad (5.1)$$

This means that the correlation between the regressors depends on the threshold used. However, the effects are small due to the low parameter value for Thr, 0.003.

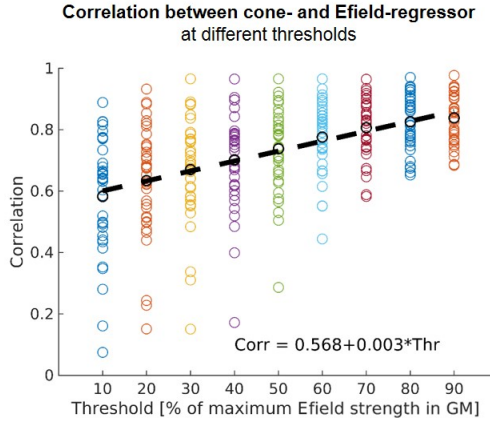


Figure 5.4 — Correlation between the cone-regressor and Efield-regressors for all patients.

5.3.2 Whole brain FC

The resulting spatial correlation values between the FC maps derived with the cone- and Efield50-regressor are shown in Figure 5.5a. Mean correlation values are 0.68 and 0.69 for the gray-matter and gray-and-white matter areas respectively. Even though the mean correlation between whole brain FC maps derived using different regressors is high, FC maps of some subjects show high variability (low spatial correlation). Figure 5.5b and c, show FC maps derived from the Efield50-regressor and the cone-regressor for a subject with high and low spatial correlation respectively.

5.3.3 FC between the DLPFC and the sgACC

Correlation between the sgACC and the stimulation site was calculated for 27 patients since ten of the datasets showed $tSNR < 40$ in the sgACC region. The results can be found in Figure 5.6. Positive and negative FC were found. A paired sample t-test did not show significant differences in FC when using the cone- or Efield50-regressors ($p = 0.445$, $t\text{-stat} = -0.776$, $dof = 26$).

5.3.4 Effect of stimulation position

For every patient, 37 regressors were derived and correlated with the regressor derived from the actual stimulation location (resulting in 37 correlation values per patient). These correlations were plotted against the distance, represented in Figure 5.7.

In case of both regressor-types, the correlation between regressors depends negatively on the distance: meaning that the further away from the actual stimulation location, the lower

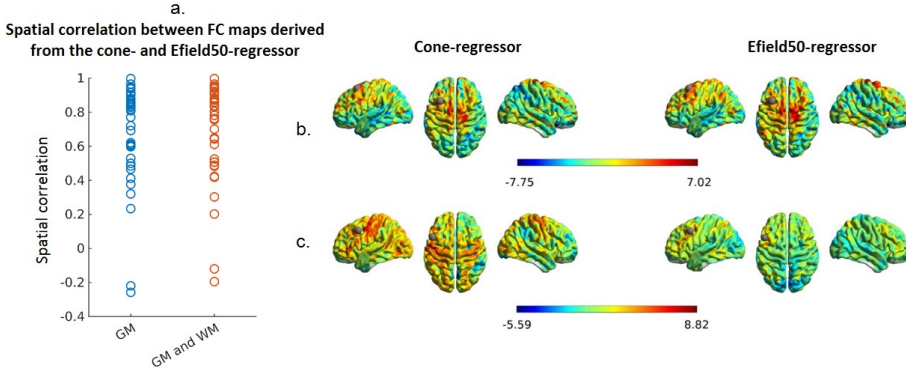


Figure 5.5 — Figure a shows the spatial correlation between FC maps in the gray matter and the combined gray and white matter regions, derived from the Efield50- and the cone-regressor. In Figure b and c, FC maps can be seen, derived from the Efield50- and the cone-regressor, from two example subjects with high and low spatial correlation respectively.

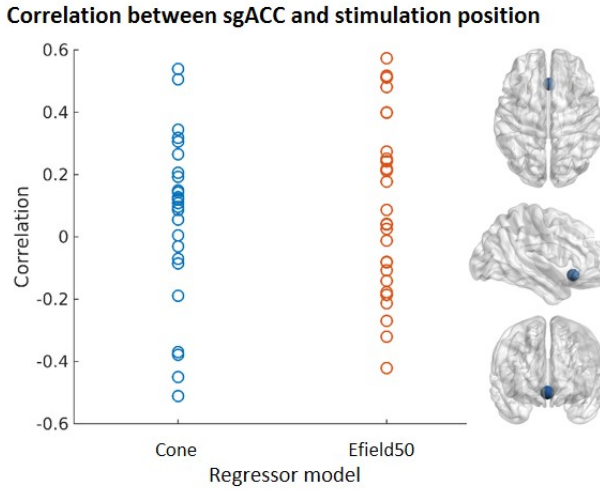


Figure 5.6 — FC between the sgACC and the stimulation site in the left DLPFC using the cone-regressor and the Efield50-regressor.

the correlation between the regressors. Specifically, based on a linear fit, the correlation between Efield50-regressors can be described by:

$$Corr_{Efield50} = 1.003 - 0.004 * Dist \quad (5.2)$$

For the correlation between cone-regressors, the following trend was found:

$$Corr_{Cone} = 1.007 - 0.022 * Dist \quad (5.3)$$

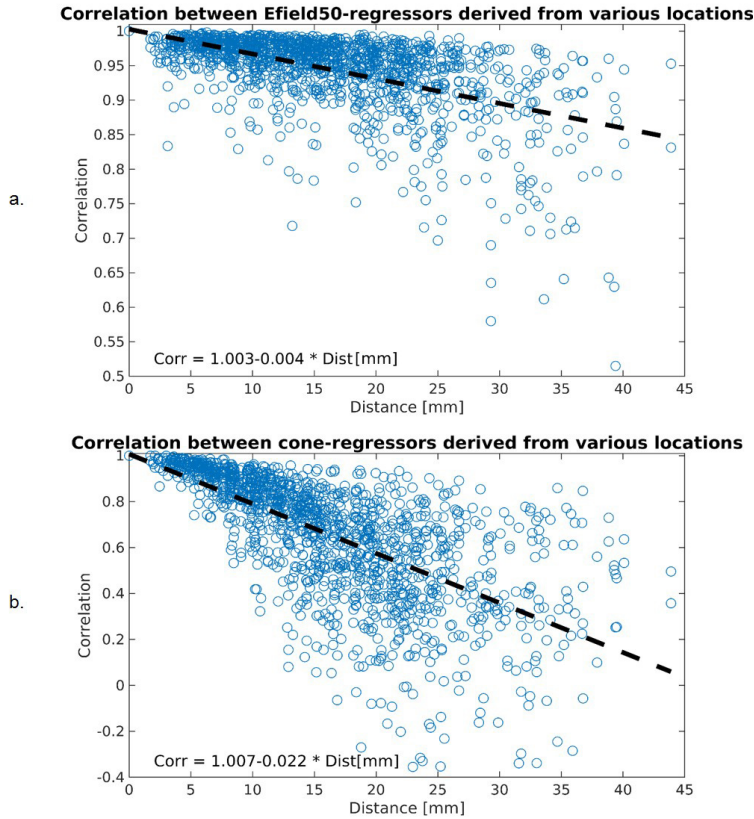


Figure 5.7 — The effect of distance on the correlation between cone- and Efield50-regressors derived at different locations. Distance refers to the Euclidean distance between the simulated stimulation location and the actual stimulation location, in mm.

The effect of distance is bigger for the cone-model compared to the Efield50-model (steeper slope: -0.022 versus -0.004).

5.4 Discussion

The main finding of this study is that both the cone model and the TMS-induced electric field simulations can be used to derive regressors for FC analyses to study the effects of rTMS. Overall, we showed high correlations between regressors. However, important to note is that on the individual subject level some subjects showed variability in FC maps using different regressors. Due to the computational complexity of the simulation of the TMS-induced electric fields compared to the cone model, our main conclusion is that the cone model is sufficient to perform FC studies. Moreover, it was shown that correlations between regressors derived at different locations were negatively correlated with the distance between locations. So knowledge about the actual stimulation position is important.

5.4.1 Potentials and pitfalls of using electric field modeling

Extensive computational models are currently used to predict the brain areas that are affected by non-invasive brain stimulation: beyond TMS, this also holds for transcranial current stimulation (tCS) (Cabral-Calderin et al., 2016; Klooster et al., 2016; Opitz et al., 2015b). Electric field simulations can be used to understand the relationship between stimulation-induced electric fields and the physiological responses to stimulation and can therefore provide valuable information for therapeutic possibilities. The effect of neurostimulation is nowadays known to spread beyond the region that is directly stimulated, supposedly via functional (Fox et al., 2014) and structural connections (Amico et al., 2017). In order to directly activate neurons, a component of the electric field should be aligned with the neurons (axons), so that the membrane potential can exceed the threshold to produce action potentials (Wagner, Valero-Cabre, and Pascual-Leone, 2007). Therefore, combining electric field simulations with structural connectivity patterns, i.e. tractography, may help to find the actual effective part of the TMS-induced electric field; i.e. the part of the induced electric field that aligns with the neuronal tracts and is therefore able to induce effects. De Geeter et al. (2012; 2015) combined TMS-induced electric field simulations with realistic neural structures derived from diffusion MRI data to obtain insight in these effective electric fields. However, the exact interaction between electric fields and the neural system are unknown yet. The strength of the TMS-induced electric field within the brain that causes actual neuronal activation is not identified. Therefore, the optimal thresholding of the electric field strengths to capture this effective electric field, is not known. Opitz et al. (2015) tested a variety of thresholds (0-90% of the highest electric field value) and showed that the overall pattern of connectivity was similar. These findings were reproduced in this study by showing overall similarity between the cone-regressor and the Efield-regressors using thresholds of 10-90%.

5.4.2 The cone model

Cone model is a rough approximation of the TMS-induced electric fields within the brain. The parameters are derived from a TMS study applied to anaesthetized cats (Valero-Cabré et al., 2005), which might underestimate the effect of stimulation on non-anaesthetized cats. Moreover, the exact translation from animal results to true effect in human is not clear yet. Differences in brain and head size will cause differences in the induced electric fields. The cone model is rotationally invariant so it cannot capture effects of coil orientation. Furthermore, it does not take tissue transitions of morphology into account, other than the fact that a white and gray matter mask was used. In this study, the cones were centered around the stimulation location which was saved in the neuronavigation system as a point on the gray matter surface. Ideally, the cone should be positioned at the coil location on the scalp since the maximum electric field strength is induced directly under the coil. Furthermore, the projection of the stimulation location to a coil position on the scalp, as also implemented in the BrainSight neuronavigation system, can induce inaccuracies caused by patient-specific gyral folding patterns (Opitz et al., 2013).

5.4.3 Cone versus electric field simulations

Regressors derived from the cone model and from electric field simulations have been generated using gray and white matter and gray matter masks. These different masks might have a slight influence on the computed regressors due to the potential influence of BOLD signal within the white matter (Gawryluk, Mazerolle, and D'Arcy, 2014). However, that is not the case in this study since the mean correlation between the regressors derived from a cone model using different masks was 0.99 (data not shown). Because different masks were used in previous literature, we decided to use these to be able to compare methods that have actually been used earlier (Fox, Liu, and Pascual-Leone, 2013; Opitz et al., 2015a).

Generally, the size of the simulated TMS-induced electric field is larger than the cone, as can for example be seen when comparing Figures 5.1 and 5.2. This explains why the correlations between regressors derived from both methods becomes higher if the Efield-threshold increases, i.e. in that case the spatial overlap between the voxels taken into account for the derivation of the cone- and Efield-regressors increases. Also, the time-series used for Efield-regressor derivation are more superficial, compared to the simpler circular cone model. This is in line with findings by Thielscher et al. (2011), who showed that highest TMS-induced electrical field strengths occur at parts of the gyral crowns. Electric field simulations are highly depending on the assigned biophysical properties, such as the conductivity and permittivity, which determine the spread of the electric field. In many cases, these values are derived from in-vitro or ex-vitro studies (Gabriel, Gabriel, and Cothout, 1996). Opitz et al. (2017), therefore studied the differences between in-vivo and ex-vivo conductivity values in non-human primates. Large changes in electric fields were found that increased with the post-mortem time. Also, body temperature showed to have a significant effect on conductivity values. Overall, post-mortem conductivity values are higher compared to in-vivo values causing an overestimation of the simulated electric fields in living subjects participating in stimulation studies. More recently, and using a frequency range that is more applicable for TMS, Koessler et al. (2017) performed in-vivo impedance measurements of healthy and pathological brain tissues using focal electrical current injection through intracerebral multicontact electrodes. Resulting conductivity values were 0.26 S/m and 0.17 S/m for gray and white matter respectively. These are slightly different compared to the ones implemented in SimNIBS.

5.4.4 Knowledge of the exact stimulation position

Standard inter-individual variability of the coil positioning was 8, 10, and 9 mm, for the x, y, and z directions respectively, using an adapted 5cm+1 rule, in a cohort of 195 patients (Johnson et al., 2013). This is slightly larger than the variability in our dataset (7, 8, 8 mm). The further away from the actual stimulation site, the lower the correlation between regressors. Proper usage of neuronavigation is helpful to keep the variation in stimulation locations, especially during multi-session protocols, as low as possible. This is in line with the knowledge about the functional architecture within the brain. Brain functions are localized and the further away from the actual stimulation position the more likely it becomes that the brain will exhibit another function (Craddock et al., 2013; Power et al., 2011), with different time-series.

5.5 Conclusion

In this study, we showed significant overlap between the regressors derived from TMS-induced electric field simulations and a simpler cone model. Together with the reduced computational complexity of the cone model, we therefore conclude that at the moment the cone model is sufficient to derive regressors for FC analyses to study the effects of TMS. Correlations between regressors derived at different positions were found to be negatively correlated with the distance from the actual stimulation, so improved spatial accuracy still delivers a net gain in accuracy. A gold standard is momentarily lacking so the optimal targeting strategy remains to be determined. Even though extensive TMS-induced electric field simulations are useful to gain more insight in the effect of TMS within the brain and the link with the physiological effects, many issues remain in the exact computation of these fields and in the translation to effective electric fields.

"Prediction is very difficult, especially when it is about the future."

Niels Bohr

CHAPTER 6

Indirect frontocingulate structural connectivity predicts clinical response to accelerated rTMS in major depressive disorder

D.C.W. Klooster, I.N. Vos, K. Caeyenberghs, A. Leemans, S. David, R.M.H. Besseling, A.P. Aldenkamp, C. Baeken

Journal of Psychiatry and Neuroscience, in press

Abstract

Although repetitive transcranial magnetic stimulation (rTMS) is an established treatment for major depressive disorder (MDD), clinical efficacy remains rather modest. One possibility could be that the propagation of the rTMS effects via structural connections from the stimulated area to deeper brain structures, such as the cingulate cortices, is sub-optimal.

We investigated whether structural connectivity, derived from diffusion MRI (dMRI) data, could serve as a biomarker to predict treatment response. We hypothesized that stronger structural connections between the subject-specific stimulation position in the left dorso-lateral prefrontal cortex (DLPFC) and the cingulate cortices would predict better clinical outcome.

Accelerated intermittent theta burst stimulation (aiTBS) was applied to the left DLPFC in 40 MDD patients. Baseline structural connectivity, quantified using various metrics (fractional anisotropy, mean diffusivity, tract density, tract volume, and number of tracts), was correlated with changes in depression severity scores after aiTBS.

Exploratory results ($p < 0.05$) show that structural connectivity between the patient-specific stimulation site and the caudal and posterior parts of the cingulate cortex have predictive potential for the clinical response to aiTBS.

The diffusion tensor was used to perform tractography. A main limitation is that multiple fiber directions within voxels cannot be resolved, which might have led to missing connections in some subjects.

Stronger structural frontocingular connections may be of essence to optimally benefit from left DLPFC rTMS treatment in MDD. Even though the results are promising, further investigation with larger patient numbers, more advanced tractography algorithms, and with the classic daily rTMS treatment paradigms is warranted.

6.1 Introduction

Excitatory repetitive transcranial magnetic stimulation (rTMS) is an FDA approved non-invasive brain stimulation technique to treat (moderate) medication resistant major depressive disorder (MDD) (George, Taylor, and Short, 2013). Most frequently applied to the left dorsolateral prefrontal cortex (DLPFC), the repetitive administration of magnetic stimuli induces brain plasticity changes that outlast the actual period of stimulation (Klooster et al., 2016). Notwithstanding that this technique has shown promising results, the overall response rate to date is rather modest with the classical daily rTMS protocols. According to a meta-analysis by Berlim et al. (2014) the rates for response and remission are 29.3 and 18.6% respectively. Accelerated rTMS treatment protocols (e.g. accelerated rTMS or accelerated intermittent theta burst stimulation (aiTBS)) have been evaluated on their potential to increase clinical responses. Instead of the application of the usual daily stimulation sessions, accelerated stimulation protocols contain multiple sessions a day, thereby significantly reducing the time-period of stimulation, and showing similar clinical outcome rates (Baeken et al., 2013; Fitzgerald et al., 2018).

A possible explanation for the modest clinical outcomes could be that for some patients the cortical stimulation region is not the best 'entrance point' to affect the underlying deregulated neurocircuitry in MDD (Baeken and De Raedt, 2011). MDD can be considered as a network disease and especially the cingulate cortex has shown to be of paramount importance when it comes to treatment response (Fox et al., 2014; Fox et al., 2012a; Lozano et al., 2008; Mayberg, 2003; Weigand et al., 2017). Even though the exact mechanism of action of brain stimulation techniques is not yet known, there is now evidence that the effects of stimulation spread throughout underlying brain networks. Fox et al. (2014) moreover supported this network theory by showing functional connections between the subgenual cingulate area and the left DLPFC. Invasive and non-invasive stimulation of these brain areas have shown clinical effects in depression patients. Furthermore, it has been stated that preserved frontocingulate neurocircuitries may be of essence to optimally benefit from left DLPFC neurostimulation (Baeken et al., 2009; Baeken and De Raedt, 2011).

So far, the potential link between structural connections and clinical response to brain stimulation has not yet been investigated. However, Amico et al. (2017) showed correlations between structural connections and TMS effects, as measured by TMS-evoked potentials in the electroencephalogram. This might suggest that the effects of stimulation propagate through the brain via structural connections. Furthermore, this might mean that structural connections can play a role in obtaining clinical efficacy (Amico et al., 2017; Baeken et al., 2009; Baeken and De Raedt, 2011).

In this study, we investigated the importance of structural connectivity, estimated with diffusion MRI (dMRI), for clinical effectiveness of aiTBS. Using various gradient directions during MR scanning, the direction in which water diffusion is least restricted can be mapped and a so-called diffusion tensor can be derived (Le Bihan et al., 2001; Le Bihan, 2006). The application of tractography algorithms allows the reconstruction of the assumed spatial orientation of anatomical (structural) connections between different

brain areas. We evaluated whether in MDD patients individual baseline structural connectivity between the stimulated area (left DLPFC) and the cingulate cortices could be of predictive value for clinical response to aiTBS (Mayberg, 2003). Specifically, we hypothesized that stronger baseline structural connections between the stimulated area and the cingulate cortex would be associated with better clinical responses.

6.2 Methods

The study (<http://clinicaltrials.gov/show/NCT01832805>) was approved by the Ghent University Hospital ethics committee and was conducted in accordance with the declaration of Helsinki (2004). All patients gave written informed consent.

6.2.1 Patient inclusion

Fifty right-handed MDD patients were included in this clinical aiTBS study. MDD was diagnosed using the structured Mini-International Neuropsychiatric Interview (MINI, (Sheehan et al., 1998)). All patients were at least stage I treatment resistant. They had a minimum of one unsuccessful treatment trial with selective serotonin reuptake inhibitors/serotonin and norepinephrine reuptake inhibitors (SSRI/SNRI). Medication was tapered off and all patients were at least 2 weeks anti-depressant free before stimulation. More extensive information about the patients and clinical outcome can be found in Duprat et al. (2016).

6.2.2 Study protocol

The overall design of this randomized, double blinded, sham-controlled, cross-over trial is shown in Figure 6.1. Patients were randomized to receive first sham aiTBS followed by active aiTBS (A in Figure 6.1) or the other way around (B in Figure 6.1). Importantly, only the baseline dMRI data (at T1) were used to investigate our hypothesis.

All patients first underwent baseline MRI (3T Siemens TrioTim, Erlangen, Germany) on day 1 (timepoint 1, T1) with anatomical imaging (MPRAGE, TR=2530ms, TE=2.58ms, FA=7deg, FOV=220x220mm², resolution=0.9x0.9x0.9mm³, 176 slices) and dMRI scans were acquired using a single-shot echo planar imaging sequence (EPI, TR=8500ms, TE=85ms, FOV=244x244 mm², voxel size=2x2x2 mm³, 68 slices, TA=9.14min). For every patient, 62 diffusion-weighted images were acquired, comprising 60 images with b = 800 s/mm² and two b0 images, using 30 non-colinear gradient-directions (2 averages).

A Magstim Rapid² Plus¹ magnetic stimulator (Magstim Company Limited, Wales, UK) connected to an active or sham figure-of-eight shaped coil (Magstim 70mm double air film (sham) coil) was used to respectively apply the active and sham stimulation. The left DLPFC, defined as the center part of the midprefrontal gyrus (Brodmann area 9/46) based on anatomical MRI of each individual (Peleman et al., 2010), was stimulated at 110% of the resting motor threshold. Positioning of the coil (45° anterolateral) was maintained with the BrainSight neuronavigation system (BrainsightTM, Rogue Resolutions, Inc). According to the accelerated protocol, five stimulation sessions a day were administered

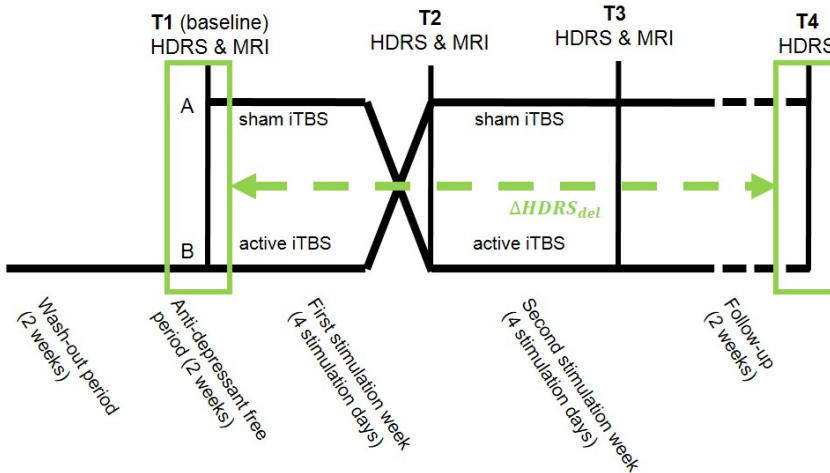


Figure 6.1 — *Design of the aiTBS treatment procedure. After a wash-out period, all patients were at least two weeks anti-depressant free before they were randomized to receive active and sham aiTBS treatment. The green squares represent the parts of the study design that were used for analysis. At T1, T2, T3 and additionally 2 weeks after the last stimulation (T4), depression severity was assessed using the 17-item HDRS questionnaire (Hamilton, 1967) by an experienced psychiatrist not related to the study. Clinical data from T1 and T4 are used to determine the clinical effect of aiTBS. Clinical effects were correlated with baseline (T1) dMRI data.*

on four consecutive days (day 2 to 5, and day 9 to 12). One iTBS session consisted of 54 trains of two seconds of stimulation given in an 8 second cycling period. During these two seconds, 10 bursts of 3 stimuli were given. This adds up to 1620 stimuli per session with a total number of 32,400 stimuli during the four-day treatment. Between sessions there were breaks of approximately 15 minutes. During the stimulation, patients were blindfolded, wore earplugs, and were kept unaware of the type of stimulation (sham or active) they received.

6.2.3 Analysis pipeline

First, MRICron was used to loop through the raw diffusion weighted MRI data, in different orthogonal views, to investigate the existence of obvious artefacts (e.g. large signal dropouts, geometric distortions, zebra artefacts). The quality assessment toolbox from Freesurfer (<https://surfer.nmr.mgh.harvard.edu/fswiki/QATools>) was used to check the quality of the (sub)cortical segmentation of the MPAGE data and Freeview was used to loop through the image maps in multiple planes.

The dMRI datasets were analyzed with ExploreDTI (Leemans et al., 2009) (v4.8.6). First, the FreeSurfer (<http://surfer.nmr.mgh.harvard.edu>) T1 datasets were masked with ExploreDTI (kernel size of morphological operators of 5 and an intensity threshold of 5%). Subsequently, the dMRI data were corrected for signal drift, subject motion, eddy current-induced distortions, and susceptibility artefacts (Irfanoglu et al., 2012; Leemans

and Jones, 2009; Vos et al., 2017), with the masked T1 datasets as undistorted (target) scans. Quality assessment of the corrected dMRI data was performed for every subject. The color-coded FA maps of the pre-processed data and the residuals maps were checked. Data was marked as 'low quality' when the FA colors were incorrect or scattered or when the average residuals showed low fit of the diffusion tensor and when the outliers had high peaks. Also, the diffusion dataset was excluded from further analysis if the translational motion exceeded the voxel size (2 mm^3). More detailed information can be found in Caeyenberghs et al. (2018; 2011).

The diffusion tensor was estimated from the corrected images with the robust fitting routine REKINDLE (Tax et al., 2015; Veraart et al., 2013) before whole brain tractography was applied (Basser et al., 2000) with a uniform seed point resolution of 2 mm^2 , step size of 1 mm, angle threshold of 30° , and fractional anisotropy (FA) threshold of 0.2.

6.2.4 Fiber paths of interest

Freesurfer (v6.0.0), was used to parcellate the anatomical datasets according to the Desikan-Killiany parcellation scheme (Tzourio-Mazoyer et al., 2002) in 68 cortical and 19 subcortical nodes (cerebellum, thalamus, caudate, putamen, pallidum, hippocampus, amygdala, accumbens area, and ventral diencephalon bilaterally, and the brainstem). Additionally, two nodes were added representing the patient-specific stimulation site and the subgenual anterior cingulate (sgACC). The node representing the patient-specific stimulation site was defined as the gray matter part of a circular ROI with radius 12 mm that was placed over the patient-specific stimulation site, as saved in the BrainSight neuronavigation system. The radius is derived from the linear decay of metabolic changes seen in animal TMS experiments (Fox, Liu, and Pascual-Leone, 2013; Valero-Cabré et al., 2005). Of note, one voxel cannot belong to multiple nodes. So, voxels within the stimulation-site node are subtracted from the Desikan-Killiany node they originally belonged to. The sgACC node was defined as the gray matter parts of a circular ROI at MNI position [6 16 -10] (converted to the subject's native space using inverse normalization matrices) with a radius of 10 mm, as used by Fox et al. (2012). This resulted in 89 nodes for structural connectivity analysis.

ExploreDTI was used to calculate connectivity matrices between the 89 nodes. Specifically, only the tracts that actually end within the nodes are taken into account. Manual inspection was performed to confirm that there are no loose fibers in our tracts. Examples of fiber tracts between specific sets of nodes can be seen in Figure 6.4. The label file was derived from the Desikan-Killiany label template as provided by ExploreDTI (FS_cvs_avg35_inMNI152_aparc+aseg_E-DTI_label_names.txt).

According to our hypothesis, parts of the cingulate cortex are responsible for the actual clinical efficacy of brain stimulation treatment. The Desikan-Killiany atlas splits the cingulate cortex into four parts bilaterally: the rostral, caudal, posterior parts, and the isthmus (Figure 6.3). Note that the rostral and caudal parts refer to the anterior cingulate cortex. Together with the sgACC, nine regions, further referred to as regions of interest (ROIs), were used in this study.

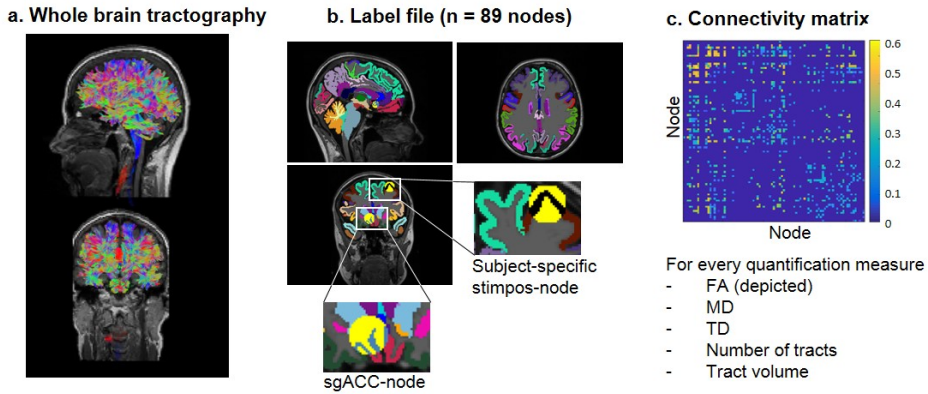


Figure 6.2 — Whole brain tractography results, obtained using ExploreDTI (a). Figure b. shows the label file, containing 89 nodes. Two circular ROIs surrounding the subject-specific stimulation position and the sgACC were manually added (yellow nodes). The gray matter parts of these ROIs were used as the subject-specific stimulation node and the sgACC node (shown in black and gray respectively). Connectivity matrices were computed using multiple quantification measures (c).

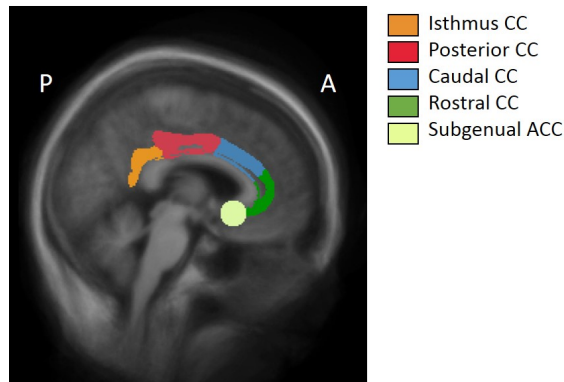


Figure 6.3 — Nine ROIs in the cingulate cortex (CC): the rostral, caudal, posterior, and isthmus (bilaterally) are derived from the Desikan-Killiany atlas. The sgACC was added manually.

Firstly, we investigated the existence of a direct structural connection between the stimulated position within the left DLPFC and any of ROIs. Besides direct connections, potential indirect pathways were investigated. The focus here was on indirect pathways with one or two nodes that connect the stimulation site in the DLPFC to either one of the ROIs in the cingulate cortex, further referred to as internodes.

6.2.5 Quantification of structural connectivity

Various metrics were used to quantify structural connectivity between the stimulation position within the left DLPFC and the predefined ROIs: the number of tracts, volume of tracts, tract density (TD), fractional anisotropy (FA), and mean diffusivity (MD). The number of tracts, between nodes u and v for example, represents the number of tracts starting in u and ending in v (or vice versa). The total volume of these tracts is calculated as the volumes (voxels) intersected by these streamlines. The tract density (Hagmann et al., 2008) is the number of connections per unit surface (i.e. mean area node u and node v). The FA and MD values (Basser et al., 2000) are measures of anisotropy and trace of the diffusion tensor respectively.

Pathways between the stimulation site and the ROIs are quantified according to a formula derived from the definition of path length from graph theory. Path length is a measure of integration and defined as the shortest path (distance, d) between two nodes (Rubinov and Sporns, 2010; Watts and Strogatz, 1998).

$$dPath_{DLPFC-ROI} = \sum a_{uv} \in g_{DLPFC \leftrightarrow ROI}^w f(SC_{uv}) \quad (6.1)$$

$$f(SC_{uv}) = \frac{1}{SC_{uv}} \quad (6.2)$$

In Formula 6.1, the operator f represents the inverse transformation from weight to 'distance', as described by the various structural connectivity (SC) metrics. The stronger the structural connection, the shorter the distance. The undirected, weighted path from the DLPFC to a ROI is represented by $g_{DLPFC \leftrightarrow target}^w$. Since $g_{DLPFC \leftrightarrow target}^w$ represents an indirect pathway, it is quantified by summing the structural characteristics of the sub-paths between the DLPFC and the ROI, a_{uv} . Specifically, in case of one internode, there are two sub-paths: from the DLPFC to the internode ($u = \text{DLPFC}$, $v = \text{internode}$), and from the internode to the ROI ($u = \text{internode}$, $v = \text{ROI}$). Note that there are 3 steps in case of 2 internodes. Beyond the single (shortest) pathway between two nodes that is currently defined as the path length, here all possible pathways between the DLPFC and the ROIs were averaged under the assumption that neuronal communication is not restricted to a single pathway. The final metric to quantify the structural connection between the DLPFC and the ROI is therefore defined as:

$$dTot_{DLPFC-ROI} = \frac{1}{nrpathways} \sum_{i=1}^{nrpathways} dPath_{DLPFC-ROI_{pathway_i}} \quad (6.3)$$

Note that this general measure can be derived from 5 different SC quantification measures: namely the number of tracts, volume of tracts, tract density, FA, and MD.

6.2.6 Specificity to frontocingulate structural connectivity

To investigate if, according to our hypothesis, the specific structural connectivity between the stimulation position and the cingulate cortex is important for the prediction of the clinical response to aiTBS, and not the overall whole-brain structural connectivity strength, three additional measures were derived from the baseline whole brain tractography re-

sults. The total number of tracts and whole brain FA and MD values were correlated with the changes in HDRS. Whole brain FA and MD values were calculated as the sum of the average FA or MD values in every tract.

Also, nodal structural connectivity measures were computed for the stimulation region. The average FA and MD values were calculated within the stimulation node and average FA and MD values were computed for the connections from the stimulation node to all other nodes in the brain. Additionally, the total number of tracts starting from the stimulation region was computed, together with the total volume of these tracts. Nodal structural connectivity measures were correlated with the clinical responses.

6.2.7 Group analysis

To investigate if the specific individual structural characteristics are important for the correlations with clinical responses the analysis was repeated using a group connectome derived from data of our 40 depressed patients. Since the subject-specific stimulation sites were added as nodes in this analysis, it was not possible to average the connectivity matrices over all subjects to obtain an average structural group connectivity matrix. Therefore, an individual subject's specific stimulation site was coregistered to the native space of all other subjects. These results were subsequently averaged to create a 89x89 'patient-specific average connectivity matrix'. This was repeated for each subject, resulting in 40 patient-specific average connectivity matrices, each differing in only one node; the respective stimulation site for the individual subject (see supplementary materials for more details). The sgACC was not taken into account for the group analysis since only nine patients showed indirect structural connections, using two internodes, from the stimulation position in the left DLPFC to the sgACC.

6.2.8 Statistics

Because our previous results (Duprat et al., 2016) clearly showed that the clinical effects of aiTBS treatment have a delayed onset we focused here on the clinical outcome at T4, defined as $\Delta HDRS_{del} = HDRS_{T4} - HDRS_{T1}$. These $\Delta HDRS$ scores were correlated with the $dTot_{DLPFC-ROI}$ values, derived from different structural connectivity metrics based on the individual data and on the group connectome data. Significance level was set to $p < 0.05$, two-tailed.

Of note, also the prediction of the immediate effect (three days after the first 20 sessions, T2) of the sham and active aiTBS was computed. The immediate clinical effects were measured by the change in HDRS before and directly after the sham and active stimulation ($\Delta HDRS_{imm/sham} = HDRS_{T2} - HDRS_{T1}$), respectively arm A and arm B in Figure 6.1). To avoid potential carry-over effects only data between T1 and T2 was considered for the calculation of the immediate stimulation effects. The statistical approach was similar as described for the prediction of the delayed effects.

6.3 Results

Four patients dropped out of the study and one patient retrospectively received an altered diagnosis. Furthermore, in two subjects the stimulation position was not saved, restricting the performance of this method. In the remaining 43 datasets, poor data quality was observed due to severe head motion in one patient (exceeding the size of 1 voxel), and due to artefacts in two other patients. Finally, 40 dMRI data sets were included for analysis.

6.3.1 Structural pathways between the left DLPFC and the cingulate cortices

Given that we found no direct structural connections between the stimulated left DLPFC and any of the ROIs in the cingulate cortex, and less than half of the subjects showed indirect connections with one internode to any of the ROIs, we focused on pathways with up to two internodes. Twenty nodes were detected as first internodes, with the left superior frontal cortex being the most common one (mean number of subjects showing left superior frontal cortex as the first internode in the indirect pathway to any of the ROIs in the cingulate cortex = 15.56, std = 5.66). Distribution of the second internode was slightly more widespread (n=28). The most common observed second internodes are the superior frontal cortex (left: mean = 9.78, std = 7.10, right: mean = 12.44, std = 8.76) and the precuneus bilaterally (left: mean = 8.67, std = 7.43, right: mean = 7.33, std = 5.69). A full overview of the distribution of the first and second internodes can be found in the supplementary material. An example of the pathway between the stimulation position and the caudal part of the cingulate cortex in the left hemisphere in a single random patient is shown in Figure 6.4.

6.3.2 Significant correlations between structural connectivity and clinical response

Data from all patients (n=40, arm A and arm B) were used to calculate the potential of structural connectivity to predict clinical response to aiTBS. Even when two internodes were considered, not all subjects showed indirect structural connections between the stimulated left DLPFC and different ROIs in the cingulate cortex. The results in this section are based on the subgroup of patients that showed structural pathways between the stimulated area in the left DLPFC and the ROIs in the cingulate cortex (see Table 6.1 and supplementary material for more detailed information).

Table 6.1 — Overview of the number of subjects (out of 40) showing indirect structural connections, with up to two internodes, between the stimulation site in the left DLPFC and ROIs in the cingulate cortex. (rost = rostral, caud = caudal, post = posterior, ist = isthmus, part of the cingulate cortex).

	Left cingulate cortex					Right cingulate cortex			
	sgACC	Rost	Caud	Post	Ist	Rost	Caud	Post	Ist
Number of patients	9	20	34	34	38	24	33	33	37

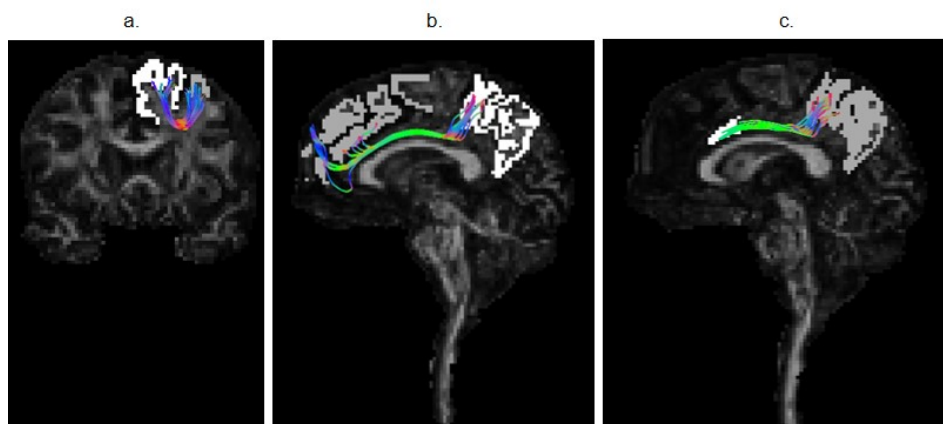


Figure 6.4 — Example of a pathway between the stimulation position and the left caudal part of the cingulate cortex via the left superior frontal cortex. Figure 4a depicts the structural connection between the subject-specific stimulation site in the left DLPFC and the first internode, in this case the superior frontal cortex. In Figure 4b, the connection between the first and second internode is visualized and Figure 4c, shows the connection between the second internode and the caudal part of the cingulate cortex. The FA map is used as template and the nodes are shown in gray and white. Note that in every panel, the pathway is from the gray to the white node. So, the white node in panel a is the gray node in panel b. The same holds for b and c. Different colors represent different directions of neuronal pathways: green = anterior-posterior; red = left-right, blue = inferior-superior.

Structural connectivity, described by three out of five metrics (number of tracts, volume of tracts, MD), between the left DLPFC and the right caudal part of the cingulate cortex showed a significant correlation ($p < 0.05$, uncorrected) with the clinical response to aiTBS. Also, the number of tracts between the stimulation position and the left posterior part of the cingulate showed predictive value. An overview is provided in Figure 6.5, and additional statistical details can be found in Table 6.2. In all cases, positive correlations indicate that lower dTot- values (so stronger structural connections) result in better clinical responses.

6.3.3 Clinical response prediction based on whole brain and nodal structural connectivity metrics

Whole brain structural connectivity metrics, total number of tracts, FA, and MD, did not show significant correlation ($p < 0.05$, uncorrected) with the clinical response to aiTBS. Neither significant correlations were found between the nodal structural connectivity measures and the clinical response. More detailed results can be found in the supplementary material.

6.3.4 Results using group depression connectome

Using group connectome data, derived from 40 dMRI datasets of depressed subjects, no significant correlations ($p < 0.05$, uncorrected) were found between the baseline structural

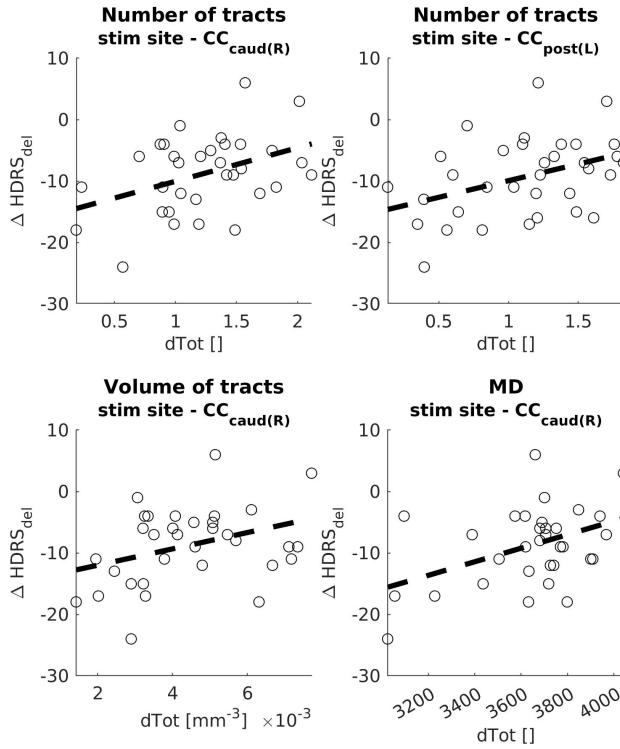


Figure 6.5 — Overview of the significant ($p < 0.05$, uncorrected) correlations between the baseline structural connectivity between the stimulation position in the left DLPFC and different parts of the cingulate cortex and the delayed clinical response to aiTBS, measured at T4 (ΔHRS_{del}). $dTot$, calculated using the number of tracts, volume of tracts, and MD, between the stimulation site and the right caudal cingulate cortex region were significantly correlated with the clinical response. $dTot$, derived from the number of tracts, between stimulation site and left posterior cingulate cortex, was furthermore also significantly correlated. Statistical details can be found in Table 6.2. SC = structural connectivity, CC_{caud(R)} = right caudal cingulate cortex, CC_{post(L)} = left posterior cingulate cortex, MD = mean diffusivity.

connectivity between the stimulation area in the left DLPFC and any of the ROIs in the cingulate cortex and the clinical responses to aiTBS.

6.4 Discussion

This is the first study which uses dMRI data to predict the clinical efficacy of an aiTBS treatment protocol in MDD patients. Baseline structural connectivity between the patient-specific stimulation site in the left DLPFC and the right caudal and left posterior parts of the cingulate cortex showed predictive value for the clinical response to the aiTBS treatment.

Table 6.2 — Significant correlations ($p < 0.05$, uncorrected) between clinical response ($\Delta HDRS_{del}$) and structural connectivity between the stimulation position in the left DLPFC and the ROIs in the cingulate cortex, represented by dTot, including p-values and slope (belonging to Figure 6.5). Note that not all subjects showed indirect connections between the stimulation site and the cingulate cortex. $CC_{caud}(R)$ = right caudal cingulate cortex, $CC_{post}(L)$ = left posterior cingulate cortex, MD = mean diffusivity.

	Correlation coefficient	<i>p</i> -value	slope
Number of tracts			
$CC_{caud}(R)$	0.41	0.02	5.46
$CC_{post}(L)$	0.40	0.02	5.42
Volume of tracts			
$CC_{caud}(R)$	0.35	0.04	1329
Mean diffusivity			
$CC_{caud}(R)$	0.43	0.01	0.013

One of the major findings was the absence of direct structural pathways between the stimulated area in the left DLPFC and any of the cingulate cortices. Although various neuroimaging techniques have shown functional crosstalk between the DLPFC and the cingulate cortex (Baeken et al., 2009; Fox et al., 2012a; Lozano et al., 2008; Weigand et al., 2017; Langguth et al., 2007), indeed functional connections are not always represented by direct structural connections. Honey et al. (2009) reasoned that this unambiguity might be explained by indirect connections, mediated via a third additional brain region. Also, Roge et al. (2017) and Deligianni et al. (2011) demonstrated that functional connections can be predicted by indirect structural connections up to the second order, i.e. indirect pathways with two internodes. In line with these earlier findings, we investigated structural pathways between the left DLPFC and the cingulate cortex with up to two internodes. Here our analyses showed that the stimulation position displayed more indirect structural connections, bilaterally to the caudal and posterior parts of the cingulate cortex and to the isthmus, as compared to the rostral parts (see supplementary material). Especially the structural connections to the caudal and posterior parts of the cingulate cortex showed predictive value for the clinical response to aiTBS. These findings could not be caused by overall structural connectivity strengths, since the whole brain structural connectivity metrics were not significantly correlated with the clinical response.

Clinical outcome was related to structural connections from the left DLPFC to the right caudal part of the cingulate cortex, derived from the number of tracts, volume of tracts, and MD. Also, positive correlations were found between dTot, derived from the MD, between the DLPFC and the left posterior cingulate cortex. The MD is a measure of overall diffusivity (Le Bihann, 2013), and can be interpreted as an inverse measure of membrane density (Alexander et al., 2012): the more membranes within a voxel, the lower the diffusion and consequently the lower the MD. The positive correlation indicates that lower dTot values (resulting from higher MD values, more tracts, and a higher volume of tracts) result in better clinical response. Here, one can speculate that because of higher values, the effect of stimulation can propagate easier to deeper structures, in this case the right caudal and left posterior cingulate cortex.

The caudal and posterior parts of the cingulate cortex have earlier been linked to response to MDD treatment. For example Baeken et al. (2009) showed that higher baseline metabolic activities in the DLPFC and the entire anterior cingulate cortex, including the caudal part, were associated with better clinical outcome. More specifically, the metabolic activity in the right caudal part of the cingulate cortex has been linked to clinical effectiveness of rTMS in a SPECT study (Langguth et al., 2007). Lozano et al. (2008) showed increased metabolism in the posterior cingulate after deep brain stimulation to the subgenual cingulate region in eight responders.

6.4.1 Biomarkers derived from individual data vs group connectome data

The fact that no significant correlations were found between baseline structural connectivity and clinical effects of aiTBS when the group connectome was investigated may emphasize the importance of the use of the individual's structural connectivity data. Even though tractography permits the reconstruction of white matter tract pathways in vivo, the accuracy of these trajectories is limited due to suboptimal acquisition (see Study limitations). Validation of the trajectories is hard due to missing knowledge about the true structural connections in individuals. Tracer studies have been used as gold standard and showed high resemblance of big white matter tracts within macaque monkeys (Schmahmann et al., 2007). However, especially on individual level, the accuracy of small fiber bundles is limited (Thomas et al., 2014).

6.4.2 Study limitations

A limitation about TMS studies in general is the lack of knowledge about the optimal stimulation parameters (Klooster et al., 2016) and the prolongation and durability of the clinical effects (Senova et al., 2019). Patients showing little clinical response at T4, two weeks after the stimulation protocol, might be slow responders. Indeed, previous studies (McDonald et al., 2011; Stubbeman, Ragland, and Khairkhah, 2018) have shown that longer stimulation protocols might lead to delayed remission in subjects that did not remit initially. Since we have no information about the timing of the propagation of the TMS effects via structural connections to potentially cause clinical effects, the findings in this study might be different when clinical data was recorded at different time points.

In the statistical analysis, the stimulation order (sham-active versus active-sham) was not explicitly taken into account. Therefore, time between real TMS stimulation and assessment of the delayed clinical effects is different based on which arm of the study the patients were in.

In this study, the diffusion tensor was used to perform tractography due to the limited ($n=30$) number of diffusion gradients and the low b-value (single shell, 800 s/mm^2). A well-known limitation of the diffusion tensor is the problem to resolve the voxels containing multiple fiber directions, i.e. kissing or crossing fibers (Jeurissen et al., 2013; Jones, Knösche, and Turner, 2013; Jones and Leemans, 2011). This might have been a reason

that some connections are missing in some subjects. In future studies, it is recommended to use multi-shell data with a higher range of b-values (Jeurissen et al., 2014) and a large number of gradient directions to achieve high angular resolution diffusion imaging (Mori and Tournier, 2013), which however also puts a pressure on the study participants as the scanning time can increase drastically. Longer scans tend to increase the presence of artifacts, like notable subject motion (Yendiki et al., 2014) and signal drift (Vos et al., 2017) due to gradient temperature changes. Recent developments in tractography suggest that more advanced models than DTI, like diffusional kurtosis imaging (DKI) (Umesh Rudrapatna et al., 2014; Szczepankiewicz et al., 2013), constrained spherical deconvolution (CSD) (Sinke et al., 2018; Tournier, Mori, and Leemans, 2011) or diffusion spectrum imaging (DSI) (Wedeen et al., 2008) should be taken into consideration (David et al., 2019).

We used five different metrics to quantify the structural connectivity strengths between the stimulated left DLPFC and nine ROIs in the cingulate cortex. This approach induces a multiple comparison issue. However, since this is the first study investigating the potential of dMRI data to predict clinical response to aiTBS, it is considered to be exploratory and all findings with $p < 0.05$ are reported.

Some patients without structural connections between the stimulation site and the ROIs in the cingulate cortex showed clinical improvement. This might indicate that the clinical effects of aiTBS are at least not solely related to the structural connectivity between the stimulation position and the cingulate cortex. Potentially also other limbic structures can be involved in the relief of depressive symptoms (Greicius et al., 2003; Liu, 2017).

Furthermore, the exact $dTot_{DLPFC-ROI}$ measure to quantify the structural connectivity between the DLPFC and any of the ROIs in the cingulate cortex is derived from the path-length formula (Rubinov and Sporns, 2010) but has never been used before in this exact form. Validation of this measure in replication studies is therefore highly recommended. In accordance with Roge et al. (2017) and Deligianni et al. (2011) pathways up to two internodes were studied. Considering more internodes results in more potential pathways. The direction of neuronal communication (orthodromic versus antidromic) cannot be derived from dMRI data. Therefore, this method has a high potential of including false pathways in the analysis pipeline.

The actual activation of neuronal white matter tracts by TMS depends on multiple factors such as the TMS coil position and orientation and on the distance between the coil and the white matter tracts. For neuronal activation, there should be a component of the TMS induced electric field that aligns with the white matter tract and exceeds an activation threshold (Klooster et al., 2016; Wagner, Valero-Cabre, and Pascual-Leone, 2007). Previous studies have demonstrated preferred sites of activation in the sulcal walls, where pyramidal cells bend and create high electric field gradients (Nummenmaa et al., 2014). Future studies might benefit from combining electric field simulations with tractography to determine the actual activated neuronal pathways in the brain more accurately (De Geeter et al., 2012; De Geeter et al., 2015).

6.5 Conclusion

This was the first study in which the biomarker-potential of dMRI data to predict the clinical response to aiTBS is investigated. Structural connections between the patient-specific stimulation area in the left DLPFC and the right caudal and the left posterior part of the cingulate cortex were predictive for clinical outcome. These findings were in line with our hypothesis: baseline structural connectivity may be of essence for the clinical response to aiTBS in some patients, although the aiTBS protocol also induced positive clinical effects in patients not showing these structural connections. Future research is necessary including larger patient samples to confirm these results. After validation of the potential of this dMRI-based prognostic biomarker, dMRI data might in the future be used to optimize and personalize stimulation protocols.

6.6 Supplementary materials

6.6.1 Group connectome generation

As stated before, it was not possible to average the connectivity matrices over all subjects to obtain an average structural group connectome, because all connectivity matrices contain a node representing the patient-specific stimulation site in the left DLPFC (a). Therefore, the subject-specific stimulation sites were coregistered to the native space of all other subjects. Coregistration was done by converting the MNI coordinates from the coil position in patient X to native coordinates in all other patients, using the 4x4 positioning matrix from any other patient (b). So the specific coil position from patient X is mapped onto the brains of all other patients. In c, specific label files are made for all patients and connectivity matrices are derived in d. In the final step, the connectivity matrices are averaged to obtain a 'patient-specific average connectivity matrix'. This procedure was repeated for every patient.

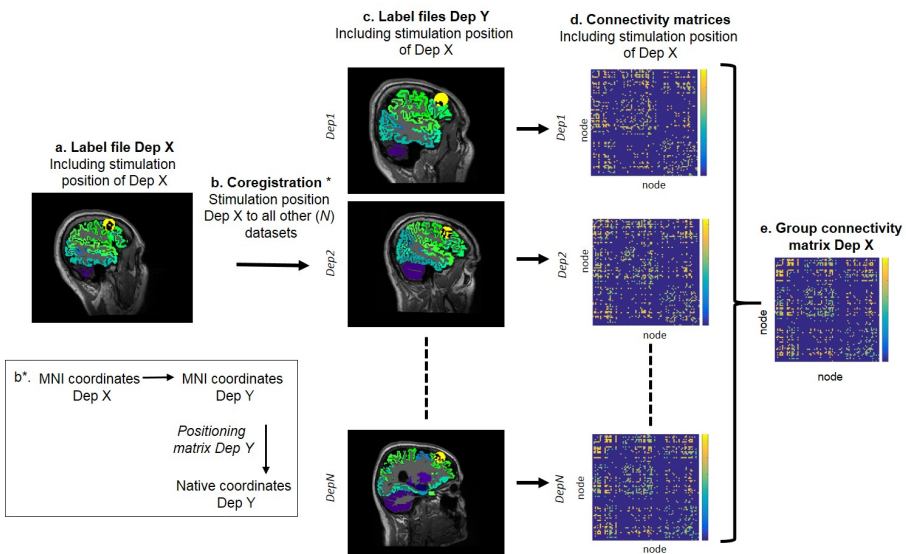


Figure 6.6 — Stepwise overview of the generation of patient-specific average connectivity matrices. Dep = depressed subject.

6.6.2 Distribution of internodes connecting the stimulation position in the left DLPFC to any of the ROIs in the cingulate cortex

Figure 6.7 and 6.8 represent an overview of the internodes that are part of the indirect connections, with two internodes, between the stimulated left DLPFC and any of the ROIs in the cingulate cortex. Figure 6.7 shows the distribution of the first internodes, whereas Figure 6.8 shows the distribution of the second internodes.

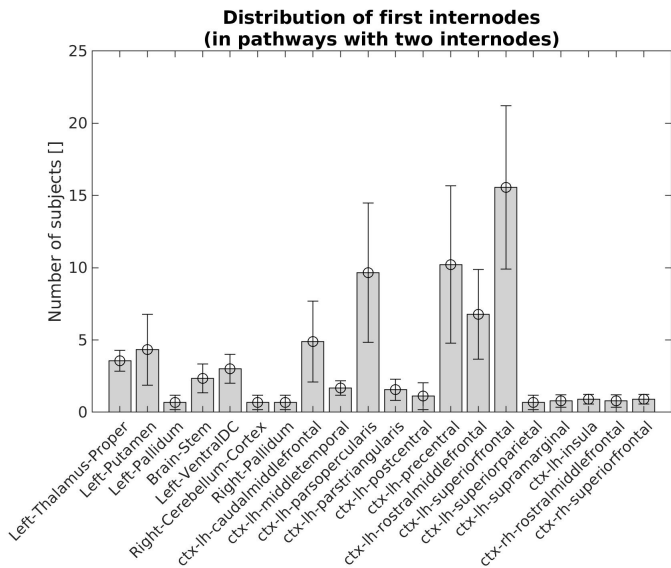


Figure 6.7 — *Distribution of the first internodes. The first internodes are directly connected to the subject-specific stimulation node in the left DLPFC. The mean and standard deviation of the number of subjects using these nodes as first internode to connect the stimulation position to any of the ROIs are depicted. The nodes that are not shown in the figure were not included in any of the pathways between the stimulation node and the ROIs.*

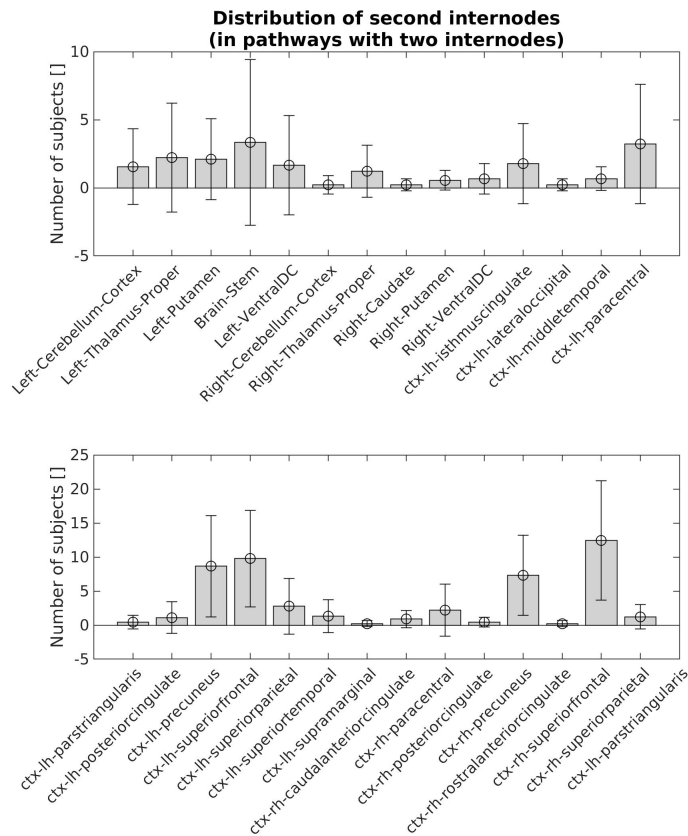


Figure 6.8 — *Distribution of the second internodes. The second internodes are directly connected to any of the ROIs in the cingulate cortex. The mean and standard deviation of the number of subjects using these nodes as second internode to connect the stimulation position to any of the ROIs are depicted. The nodes that are not shown in the figure were not included in any of the pathways between the stimulation node and the ROIs.*

6.6.3 Direct versus indirect structural connections between the stimulated area in the left DLPFC and the cingulate cortex

A. Direct connections

Table 6.3 — Overview of the number of patients with direct structural connections between the stimulated left DLPFC and any of the ROIs in the cingulate cortex. (parts of the cingulate cortex: rost = rostral, caud = caudal, post = posterior, ist = isthmus)

	Left cingulate cortex					Right cingulate cortex			
	sgACC	Rost	Caud	Post	Ist	Rost	Caud	Post	Ist
Number of patients	0	0	0	0	0	0	0	0	0

B. One internode

Table 6.4 — Overview of the number of patients with indirect structural connections, with one internode, between the stimulated left DLPFC and any of the ROIs in the cingulate cortex. Also the mean and median number of connections are shown. (parts of the cingulate cortex: rost = rostral, caud = caudal, post = posterior, ist = isthmus)

	Left cingulate cortex					Right cingulate cortex			
	sgACC	Rost	Caud	Post	Ist	Rost	Caud	Post	Ist
Number of patients	0	4	13	11	16	4	9	3	6
Mean number of connections	-	1	1	1.18	1.25	1	1	1	1.33
Median number of connections	-	1	1	1	1	1	1	1	1

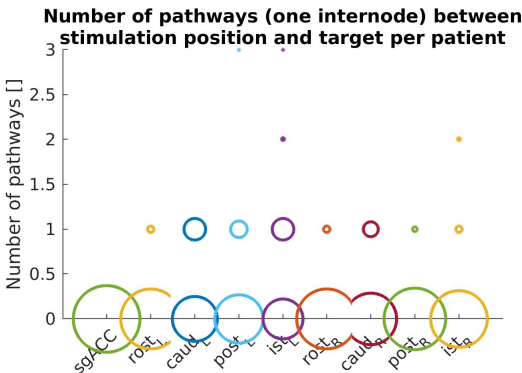


Figure 6.9 — The number of pathways between the stimulated left DLPFC and any of the ROIs in the cingulate cortex. The size of the circles is proportional to the number of patients having that number of connections. Together with Table 6.4, this figure shows that only few patients have indirect structural connections between the specific stimulation site in the left DLPFC and any of the ROIs in the cingulate cortex via one internode.

C. Two internodes

Table 6.5 — Overview of the number of patients with indirect structural connections, with two internodes, between the stimulated left DLPFC and any of the ROIs in the cingulate cortex. Also the mean and median number of connections are shown. (parts of the cingulate cortex: rost = rostral, caud = caudal, post = posterior, ist = isthmus)

	Left cingulate cortex					Right cingulate cortex			
	sgACC	Rost	Caud	Post	Ist	Rost	Caud	Post	Ist
Number of patients	9	20	34	34	38	24	33	33	37
Mean number of connections	1.56	3.25	4.15	4.74	7.74	3.13	3.12	3.91	6.86
Median number of connections	1	3	3	3	6	2	2	3	4

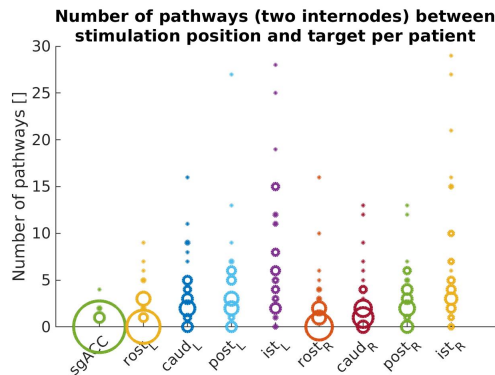


Figure 6.10 — The number of pathways with two internodes between the stimulated left DLPFC and any of the ROIs in the cingulate cortex. The size of the circles is proportional to the number of patients having that number of connections. This figure, and also Table 6.5, shows that most patients have indirect structural connections between the specific stimulation site in the left DLPFC and any of the ROIs in the cingulate cortex, when two internodes are considered.

6.6.4 Prediction of the immediate clinical effects

A. Prediction of sham effects

The data from patients from arm A ($n = 21$) were used to calculate the potential of baseline structural connectivity to predict the immediate response to sham stimulation (red blocks in Figure 6.11). No significant correlations were found between changes in HDRS scores, after sham stimulation with respect to baseline, and any of the structural connectivity metrics. Even though no significant correlations were found, clinical responses were found after sham aiTBS (Duprat et al., 2016). This might be caused by an active placebo effect. A recent meta-analysis showed a high sham response to rTMS (Razza et al., 2018) which is in accordance to sham responses to pharmacological treatments (Meister et al., 2017).

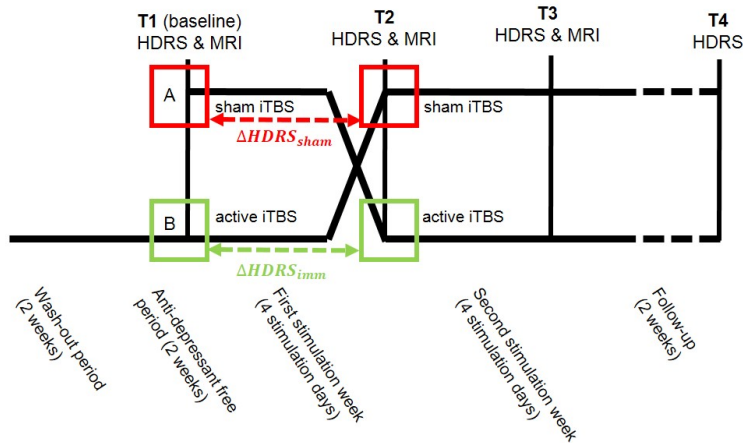


Figure 6.11 — Overview of the stimulation protocol. Parts of the data that are used to compute the predictive effects of baseline structural connectivity on sham and active immediate clinical responses are marked in red and green respectively.

B. Prediction of immediate effects of active aiTBS

The data from patients from arm B ($n=19$) were used to calculate the potential of baseline structural connectivity to predict the immediate clinical response to active aiTBS (green blocks in Figure 6.11). The baseline MD of the connection between the stimulation position and the left caudal and posterior part of the cingulate cortex and the left isthmus was significantly correlated with the change in depression severity. Higher baseline MD values here indicate better clinical response. Also, the FA of the connection to the right posterior part and the isthmus of the cingulate cortex predicted the immediate response to aiTBS (Figure 6.12, Table 6.6). However, these correlations have opposite sign.

Table 6.6 — Correlations, p -values, and slope of the significant results (belonging to Figure 6.12).

	Correlation coefficient	p -value	slopes
Mean diffusivity			
Caud (L)	0.73	<0.01	0.02
Post (L)	0.51	0.04	0.01
Ist (L)	0.48	0.04	0.02
Fractional anisotropy			
Post (R)	-0.66	<0.01	-11.49
Ist (R)	-0.51	0.03	-13.09

The structural connectivity between the patient-specific stimulation site and the left caudal and posterior part and the isthmus of the cingulate cortex, derived from the MD, was positively correlated with the immediate change in HDRS scores. The positive correlation indicates that lower dTot values (resulting from higher MD values) result in better clinical response. So, it might be speculated that higher MD values cause the effect of stimulation

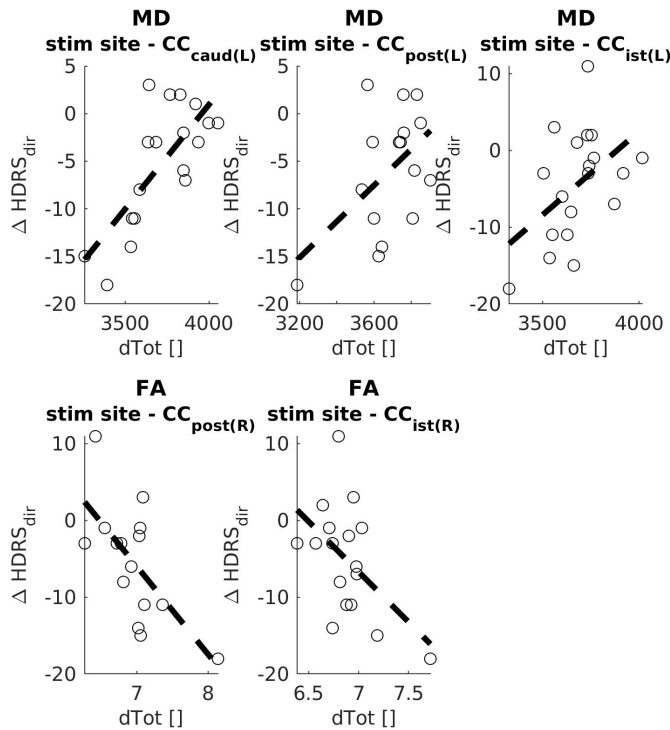


Figure 6.12 — Overview of the correlations showing a significant predictive potential of the immediate clinical effects of aiTBS. Statistical details can be found in Table 6.6.

to propagate easier to deeper structures, in this case the left caudal and posterior parts and isthmus of the cingulate cortex, thereby inducing clinical effects.

Also, clinical outcome was found to be significantly correlated with the structural connections to the right posterior part and right isthmus of the cingulate cortex, described by the dTot derived from the FA metric. This correlation is opposite to the MD findings and suggests that lower baseline FA values in the structural pathway result in better clinical response. FA is a measure of anisotropy. Low FA values might be associated with high MD values. Besides, previous studies have shown that decreased FA is a predictor of long-term motor outcome after stroke (Puig et al., 2013).

C. Prediction of immediate versus delayed clinical response

Significant findings differ when predicting the immediate and the delayed effects. This might indicate that the propagation of the TMS effect via structural connections progress over time and suggests the involvement of the corpus callosum since also structural connectivity to right sided ROIs in the cingulate cortex showed predictive potential (Voineskos et al., 2010). The role of the corpus callosum in the pathophysiology of depression is still

unclear and might also depend on the exact type of depression (Lacerda et al., 2005). Indeed, previous work has shown that TMS alters structural brain connections (Abe, Fukuyama, and Mima, 2014; Kozel et al., 2011). Specifically in this cohort of patients, Caeyenberghs et al. (2018) showed that active aiTBS induces decreases in modularity, a graph measure in this case derived from structural connections, after four days of stimulation treatment. Potentially, these progressive changes in structural connectivity cause changing structural pathways between the stimulated left DLPFC and the cingulate cortex over time, thereby also potentially changing the clinical effectiveness of aiTBS over time. This might, at least partly, explain the different findings of structural connections to predict the immediate versus delayed clinical effects.

6.6.5 Specificity to frontocingulate structural connectivity

The results of correlation between overall baseline structural connectivity measures, derived from whole brain data, and clinical outcome can be found in Figure 6.13. The whole brain FA and MD measures were calculated by averaging these values in every tract, and subsequently these values were summed over the whole brain. No significant correlations were found. Neither significant correlations were found between baseline nodal structural connectivity measures, derived from the stimulation node, and clinical response to aiTBS (Figure 6.14).

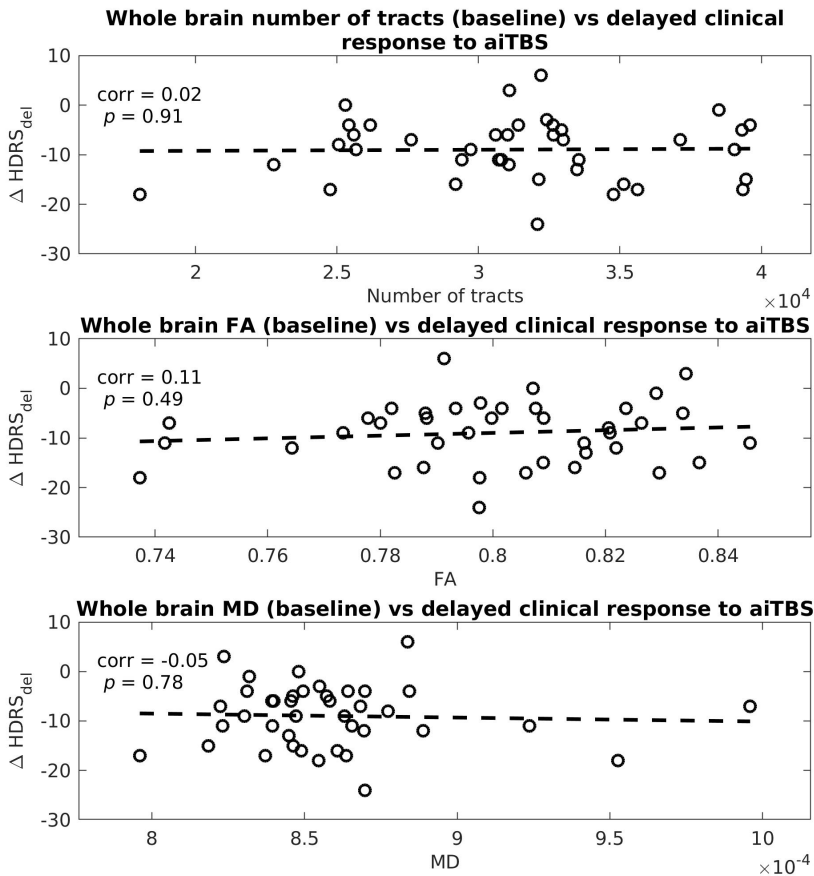


Figure 6.13 — Correlation between baseline whole brain structural connectivity measures, number of tracts, FA, and MD, and clinical response to aiTBS.

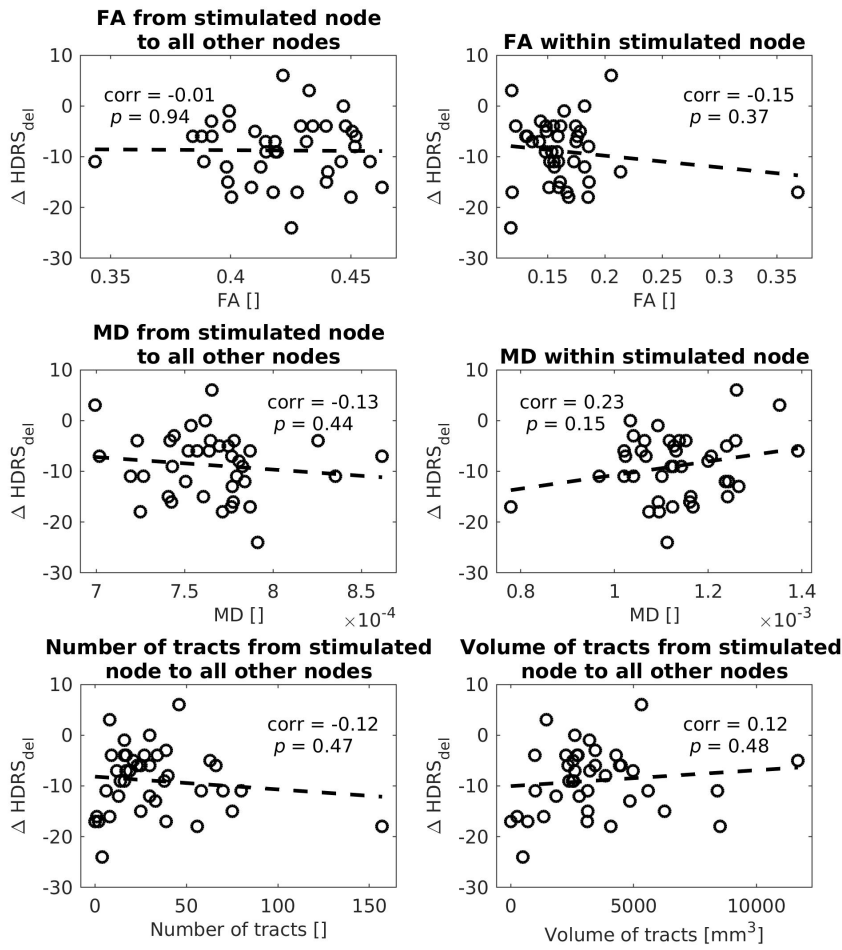


Figure 6.14 — Correlation between baseline nodal structural connectivity measures, FA and MD in and from the stimulation node, and the number and volume of tracts, and clinical response to aiTBS.

*"If you really want to understand something, try
to change it."*

Kurt Lewin

CHAPTER **7**

Stimulation propagation versus functional connectivity

D.C.W. Klooster, J.J. Vink, P. van Mierlo, P.A.J.M. Boon, D. Cooke, T. Gedankien, A. Roberts, P. Boucher, A. Pascual-Leone, M.D. Fox, M.M. Shafi

in preparation

Abstract

Transcranial magnetic stimulation (TMS) is a non-invasive brain stimulation technique that is used to induce changes in neuronal activity. Besides local TMS effects under the stimulation coil, overall effects of stimulation have been found in distributed areas throughout the brain. The aim of this study was to quantify the propagation of TMS effects in terms of the brain's resting-state MR functional connectivity (rsFC).

TMS-EEG recordings were performed in ten healthy subjects. Single-pulse TMS was applied to six stimulation sites (dorsolateral prefrontal cortex (DLPFC), motor cortex, and parietal cortex bilaterally) at 120% resting motor threshold. EEGlab and custom matlab scripts were used to compute the TMS-evoked potentials (TEPs). EEG source imaging was performed to convert the TEPs to source space using subject-specific head models. The parcellation scheme from Power (Power et al. 2011) was used to parcellate the brain into 240 nodes. TEP sizes in every node were quantified using root-mean-square values in different time-intervals after the stimulation (15-75ms, 15-400ms). For every subject and for every stimulation site, rsFC maps were derived from the functional group connectome data ($n=1000$), using the individual stimulation positions as seed. Correlations between the TEP sizes and FC were computed on individual level and also group analysis was performed.

Significant ($p<0.0016$, Bonferroni corrected) correlations between quantified TEPs and rsFC were found when stimulation was applied to the motor areas. There is a large inter-individual variability in the dependence of the propagation from rsFC. This might be caused by differences in TEP distributions or as a result of correlating individual TEP data with group FC maps.

Future studies, including appropriate sham stimulation to all stimulation positions and controlling for the possible effects of brain state, are suggested to better characterize the propagation of single pulse TMS effects in terms of rsFC and validate the results.

7.1 Introduction

Transcranial magnetic stimulation (TMS) is a non-invasive brain stimulation technique that is able to modulate neuronal activity in targeted cortical regions (Wagner, Valero-Cabre, and Pascual-Leone, 2007). A varying current is sent through a stimulation coil, placed tangentially to the scalp, which induces a magnetic field perpendicular to the coil, into the brain. The areas that are directly affected by TMS are located in the cortex, due to the physiological properties of the magnetic field. In the brain, a small electric field is induced that is able to depolarize neurons and cause action potentials. The effects of repetitive administration of magnetic pulses (rTMS) outlast the period of stimulation, making rTMS a potential treatment option. Even though rTMS is investigated to treat a large variety of neuropsychiatric disorders (Klooster et al., 2016), the mechanism of action remains incompletely understood (Hoogendam, Ramakers, and Di Lazzaro, 2010).

It is nowadays known that normal brain functions are organized in robust and efficient networks: brain regions that each have their own task and function that are continuously exchanging information with each other (Bullmore and Sporns, 2012; Heuvel and Hulshoff Pol, 2010). Functional networks are defined as anatomically separated regions that show temporal dependency between spatially remote neurophysiological events (Friston, 1994). These temporal dependencies can be found in either task based functional MRI (fMRI) or resting-state fMRI studies (Biswal et al., 1995). Resting-state fMRI studies on group level have shown the existence of strongly functionally linked sub-networks during rest, also called resting-state networks (Damoiseaux et al., 2006; Fox et al., 2005; Fox and Raichle, 2007; Smith et al., 2009; Smith et al., 2011; Yeo et al., 2011).

Taking into account the properties of TMS and the current knowledge about the brain's network organization, it is not surprising that effects of TMS have been found in distributed areas throughout the brain (Dunlop et al., 2015; Salomons et al., 2014; Wang et al., 2014). The effects of TMS are assumed to propagate via either functional and/or structural connections. Fox et al. (2014) showed that successful cortical targets used for non-invasive brain stimulation treatments are functionally connected to deeper structures, used as target for invasive brain stimulation treatments, in a variety of pathologies. This suggests propagation of the TMS pulses via functional connections. Also earlier studies in depression have suggested to use the information about functional connectivity to define the optimal stimulation site (Fox et al., 2012a; Fox, Liu, and Pascual-Leone, 2013; Weigand et al., 2017).

An example of the propagation of the effect of a TMS pulse is the induction of motor evoked potentials (MEPs) when stimulating the motor cortex. With the development of more advanced amplifier systems (Ilmoniemi and Kicić, 2010; Veniero, Bortoletto, and Miniussi, 2009), simultaneous recording of TMS and EEG became possible, giving the opportunity to study the causal response of TMS applied to brain areas other than the motor cortex. Generally, TMS induces specific perturbations in the EEG, further referred to as TMS-evoked potentials (TEPs). TEPs can be negative (N) and positive (P) potentials at specific latencies relative to the magnetic pulse: N15, P30, N45, P55, N100, P180, and N280 (Farzan et al., 2016; Komssi and Kähkönen, 2006) and have shown to be highly

reproducible within subjects (Lioumis et al., 2009). However, there is inter-individual variability and moreover, TEPs depend on the stimulation location and orientation, state of the cortex, and vigilance of the subject. Diagnostic potential of TEPs, shape and latency, have been shown in the comparison between epilepsy patients and healthy subjects (Shafi et al., 2015; Braack, Koopman, and Putten, 2016).

The ms temporal resolution of EEG can provide information about the temporal pattern of the response to a TMS pulse. However, the spatial resolution of EEG systems is limited to the number of EEG electrodes. With EEG source imaging (ESI) techniques, the location of the brain areas generating the neuronal activity measured with the EEG can be derived (Michel and Brunet, 2019; Hallez et al., 2007; Michel et al., 2004). ESI uses a forward model to subsequently solve the inverse problem. The forward model is built from the EEG electrode positions, a head model containing tissue specific electrical properties, and a source model which is based from multiple source building-blocks such as simple dipoles. The inverse problem, caused by the fact that the number of possible sources within the brain is much larger than the number of EEG electrodes, can be solved using a priori boundary constraints such that the most probable active regions in the brain can be found at every time-point in the EEG data. ESI is often used in the field of epilepsy (Plummer, Harvey, and Cook, 2008) to find the epileptic foci (Boon et al., 2002; Koessler et al., 2010; VanHaerents et al., 2015) or to study the active regions in the brain that cause interictal epileptiform activity (Brodbeck et al., 2009).

In 1997, Ilmoniemi et al. (1997) was the first to describe the propagation of TMS pulses using TMS-EEG data combined with source localization techniques. Initially (3-4 ms after the stimulus), the strongest EEG activity was found below the figure-of-eight coil positioned either at the left somatosensory area or the left visual cortex. Activation in the contralateral hemisphere was found in higher latencies (>10 ms). The spatial propagation of the effect of the TMS was suggested to be related to anatomical connections within the brain (Valero-Cabré et al., 2005). More recently, attempts have been made to quantify this propagation in terms of network knowledge. Amico et al. (2017) aimed to couple the stimulus propagation to properties derived from the structural connectome, derived from diffusion MRI data. Direct functional connectivity was extracted from TMS-EEG data, recorded in fourteen healthy subjects. After conversion to source space, functional connectivity was correlated with complex measures of structural connectivity derived from dMRI data. Different stimulation sites, in this case the left premotor area and the left superior parietal cortex, showed highest correlation with the natural frequency bands (β 2/ γ and β respectively). Bodart et al. (2017) used a comparable approach to study the correlation between the perturbation complexity index (PCI), a TMS derived marker of effective connectivity, and the structural connectivity. In this case, structural connectivity measures were derived from the fractional anisotropy, a diffusion metric, in a subset of 24 patients with disorders of consciousness. The effective connectivity was shown to correlate with the structural integrity of the brain-injured patients.

In this work, we investigated if TEP propagation is also correlated with resting-state MR functional connectivity (rsFC), using a comparable approach as in Vink et al. (2019). We hypothesized that, due to the large-scale neuronal communication (Heuvel and Hulshoff

Pol, 2010), the TMS propagation is correlated with the brain's intrinsic functional connectivity. The ability to predict the propagation of the TMS pulses using these functional connections would have a large clinical implication. Firstly, there will be a clearer hypotheses regarding the determination of stimulation position when the actual target is a structure deep in the brain. Secondly, the overall effects of TMS can be interpreted easier in terms of the effect that occur within areas that are connected to the stimulation site.

7.2 Methods

Simultaneous TMS-EEG data was collected in 11 right-handed healthy volunteers. Written informed consent was given by all subjects and the procedure was approved by the committee for clinical investigation of Beth Israel Deaconess Medical Center (Boston, United States). FC maps were derived from group connectome data to link the propagation of the effects of single TMS pulses to the brain's intrinsic rsFC.

7.2.1 TMS-EEG protocol

Biphasic single pulse TMS was administered (Nexstim eXimia, Nexstim LTD) using a figure-of-eight coil (mean diameter 59 mm, outer diameter 70 mm). Stimulation was applied bilaterally at the dorsolateral prefrontal cortex (DLPFC), primary motor cortex (M1), and the angular gyrus within the parietal cortex (Par) using MRI-guided neuronavigation with the subject's individual anatomical MRI data. The DLPFC target was anatomically defined as a point on the superior aspect of the middle frontal gyrus, 1-2 cm anterior to the premotor gyrus. The M1 target was the motor hotspot, defined as the point that produced the largest motor evoked potential (MEP) in the first dorsal interosseous (FDI) muscle. The parietal target was the posterior half of the angular gyrus, 1-2 cm below the intraparietal sulcus. Additionally, sham stimulation was applied to the left M1, with the coil tilted 90 degrees such that the magnetic field does not penetrate into the brain, to control for the somatosensory and auditory effects induced by TMS. The coil orientation was perpendicular to the underlying target gyrus, with the handle pointing posterolaterally. Stimulation intensity was set to 120% of the resting motor threshold (RMT) defined as the lowest intensity at which TMS, applied to the M1 target, induced a MEP in the contralateral FDI of more than 50 μ V in 5 out of 10 trials. Participants received between 80 and 110 single pulses to each site, with the inter stimulus interval jittered between 4-6s to avoid conditioning. All subjects wore earplugs and were seated comfortably in a reclining chair with their eyes open and were asked to look straight ahead at a fixation point.

During the stimulation, EEG was recorded using a 60 channel TMS-compatible cap (eXimia EEG, Nexstim). The electrode locations were digitized in the neuronavigation system. The sample-frequency was 1450 Hz and data was recorded with a 16-bit resolution and band-pass filtered between 0.1 and 500 Hz. For more detailed information about the subjects and the TMS-EEG setup, please see Vink et al. (2019).

A. EEG analysis

EEGlab (version 12.0.2.4b) and custom Matlab scripts (R2014a, Mathworks Inc., USA) were used for preprocessing of the EEG data. Epochs were defined from 0.5s before till 1s after every stimulation. Bad electrode channels and epochs were manually classified by visual inspection and excluded from further analysis. Independent component analysis (ICA) was used to remove artifacts (Rogasch et al., 2014). Data from missing electrode channels were interpolated. For every subject and for every stimulation position this led to a TEP-scalp matrix [number of remaining epochs x number of channels (60) x number of timepoints (2175)]. A more detailed description of the EEG-preprocessing steps can be found in Vink et al. (2019). The global mean field potentials (GMFP) were calculated to compare the TEPs in scalp space per subject, using Formula 7.1 (Shafi et al., 2015).

$$GMFP(t) = \sqrt{\frac{\sum_i^K (V_i(t) - V_{mean}(t))^2}{K}} \quad (7.1)$$

where K is the number of electrodes, $V_i(t)$ the voltage measured at electrode i at time t , and $V_{mean}(t)$ is the mean voltage across electrodes at time t .

B. EEG source imaging

ESI has been performed to convert the TEP-scalp matrix from scalp space to source space using BrainStorm (Tadel et al., 2011) open source software. Individual head models were generated using the subject's individual anatomical MRI data. For the forward model (Mosher, Leahy, and Lewis, 1999) the brain was split into three layers with different conductivity values (scalp and brain, $\sigma_{scalp} = \sigma_{brain} = 1$, $\sigma_{skull} = 0.0125$). A current dipole was assigned to the vertices in the cortical surface (downsampled to $n = 15,000$, as a compromise between computational load and capturing the individual brain geometry). These dipoles are oriented perpendicular to the cortical surface, so that they align with the cortical pyramidal neurons which are presumed to generate most of the EEG activity. Information about the subject-specific electrode positions was merged with the headmodels. OpenMEEG (Alexandre Gramfort et al., 2009), based on a symmetric boundary element method, was used to compute the leadfield matrix.

The noise covariance matrix was computed based on the TEP-scalp matrix, containing the TEPs per epoch. Consequently, dynamical Statistical Parametric Mapping (dSPM) (Dale et al., 2000) was used to solve the ill-posed inverse problem. The result is a TEP-source matrix [number of vertices (15000) x number of timepoints (2175)].

7.2.2 rsFC maps

For every subject and for every stimulation site a rsFC map was derived using the functional group connectome data. The connectome was obtained using data from 1,000 healthy volunteers who were scanned in a 3T Siemens MRI scanner as part of the superstructure project (<http://neuroinformatics.harvard.edu/gsp>). The seed regions for functional connectivity analysis was based on the cone-model, as previously described by Fox et al. (2013), centered at the normalized subject-specific stimulation location. The

cone-model is a rough approximation of the TMS induced electric fields induced by a figure-of-eight coil (Pascual-Leone et al., 2002), built using concentric spheres with different radii (2, 4, 7, 9, 12 mm). The seed time-series for functional connectivity analysis is defined by the weighted sum of the time-series of the voxels within the cone, masked with a gray- and white-matter mask. Functional connections from each stimulation site were determined by calculating the correlations between the subject-specific seed time-series and time-series of all other voxels. The correlation maps from 1,000 healthy subjects were combined to define final T-maps, for every subject and for every stimulation position (Darby et al., 2017).

7.2.3 Brain parcellation

The parcellation scheme as proposed by Power et al. (2011) was used to investigate the whole brain propagation of TMS pulses in terms of the brain's rsFC. The parcellation scheme is derived from a meta-analysis of resting-state fMRI studies and consists of 264 circular parcels, further referred to as nodes, with a radius of 1 cm. Subcortical nodes were left out for analysis, leaving 240 nodes (see Figure 7.1).

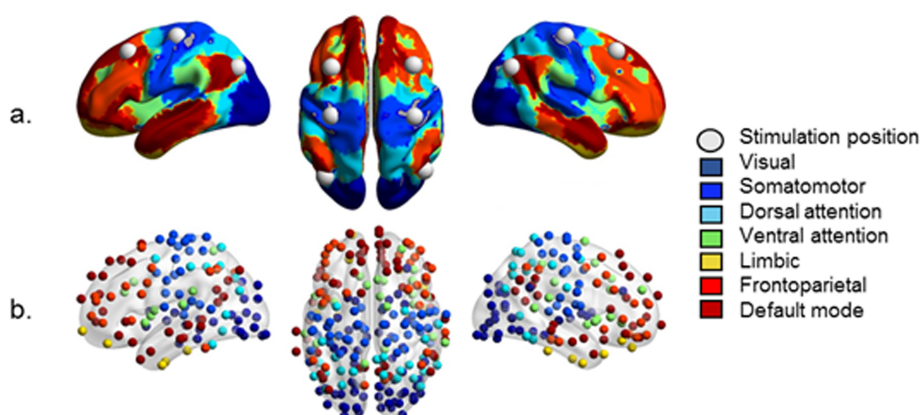


Figure 7.1 — Overview of the nodes used in this study ($n=240$). These nodes are derived from the parcellation scheme proposed by Power et al. (2011), with the exclusion of the subcortical nodes. The nodes are color-coded according to the resting-state network they belong to (Yeo et al., 2011).

To apply the parcellation scheme to the TEP-source matrix, a mask with these nodes was made and loaded into BrainStorm. BrainStorm automatically assigned a subset of vertices (dipoles) to every node. For every node, the TEPs of the dipoles within the node were averaged, resulting in a TEP-source-node matrix [number of nodes (240) x number of timepoints (2175)]. Consequently, TEP size was quantified (qTEP) using the root-mean-square value, calculated within two different time-intervals after the stimulation. The 15-400 ms time-interval was investigated since this interval encompasses the whole TEP. Additionally, the interval between 15-75 ms was specifically investigated since this interval is assumed to be less corroborated by sham artefacts (Gordon et al., 2018). A

similar approach was used to quantify the rsFC in every node. For every nodes, the T-values of the voxels within the node are averaged.

7.2.4 Statistics

On the nodal level, for every subject, for every stimulation position, and for every time-interval the partial correlation was calculated between the qTEP size and the rsFC, thereby correcting for the size of the qTEP-sham. Statistical significance was determined via bootstrapping. The node order of the rsFC was randomly permuted 5,000 times and correlated with the qTEP. Later, the 95th and 99.96th percentiles of the distributions of 5,000 randomly generated correlation coefficients were used as a statistical threshold to determine significance for alpha levels of 0.05 and 0.00042 (Bonferroni corrected for multiple comparisons: 10 subjects, 6 stimulation positions, and 2 different time-intervals), respectively.

A. Group level analysis

For the group analysis a similar approach was used as for the individual analysis. However now, the qTEP data and rsFC data of subjects were merged for every stimulation position and time-interval. After the bootstrapping procedure the 95th and 99.59th percentiles of the distributions of 5,000 randomly generated correlation coefficients were used as a statistical threshold to determine significance for alpha levels of 0.05 and 0.0041 (Bonferroni corrected for multiple comparisons: 6 stimulation positions, and 5 different time-intervals).

7.3 Results

Due to one dropout subject (one subject experienced excessive discomfort from TMS-induced scalp muscle contractions), data of 10 subjects (mean age 38 years, 9 males, 1 female, all right-handed) were analyzed in this study. Figures 7.2 and 7.3 show the variability in coil position and scalp space global mean field potentials (GMFP) between subjects.

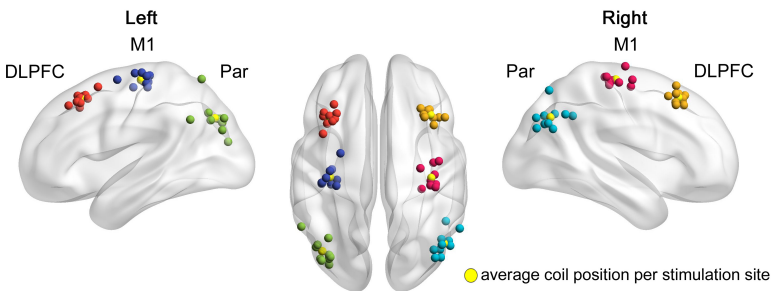


Figure 7.2 — Overview of the actual coil positioning per stimulation site for all 10 subjects. Per stimulation site, the average coil position is represented in yellow.

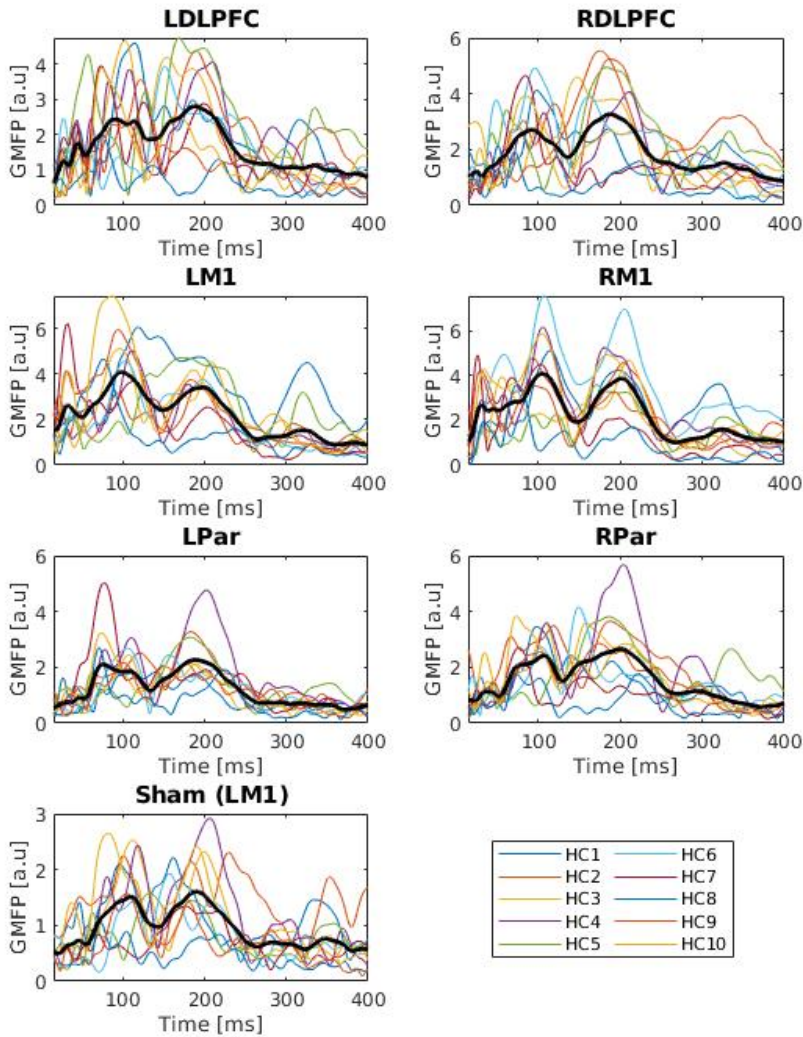


Figure 7.3 — Variability of the scalp space GMFP per stimulation position, including sham stimulation at LM1, for every subject. The mean GMFP was shown in black.

7.3.1 EEG source localization

EEG source localization was performed for every subject and for every stimulation position. Results of sham and verum LM1 stimulation in a random subject are shown in Figure 7.4 and 7.5 respectively. For the sham stimulation, the auditory N100-P180 complex can be clearly detected.

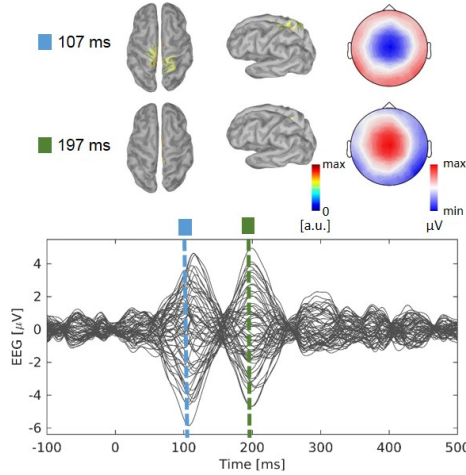


Figure 7.4 — *Example of the results of source localization in a random subject who received sham stimulation at LM1. The bottom figure shows the TEPs in scalp space for all channels, averaged over all epochs. Source localization results of the auditory peaks, at latencies of 107 and 197 ms, are shown, together with the EEG topoplot at these time-points (derived from scalp space).*

Active LM1 stimulation clearly induced evoked potentials. The response peaks are in line with earlier findings in which six peaks were described after stimulation of M1. Even though our time interval of interest did not start before 15 seconds after the stimulation, we found comparable peaks later after the stimulus, at 33, 44, 57, 112, and 193 ms.

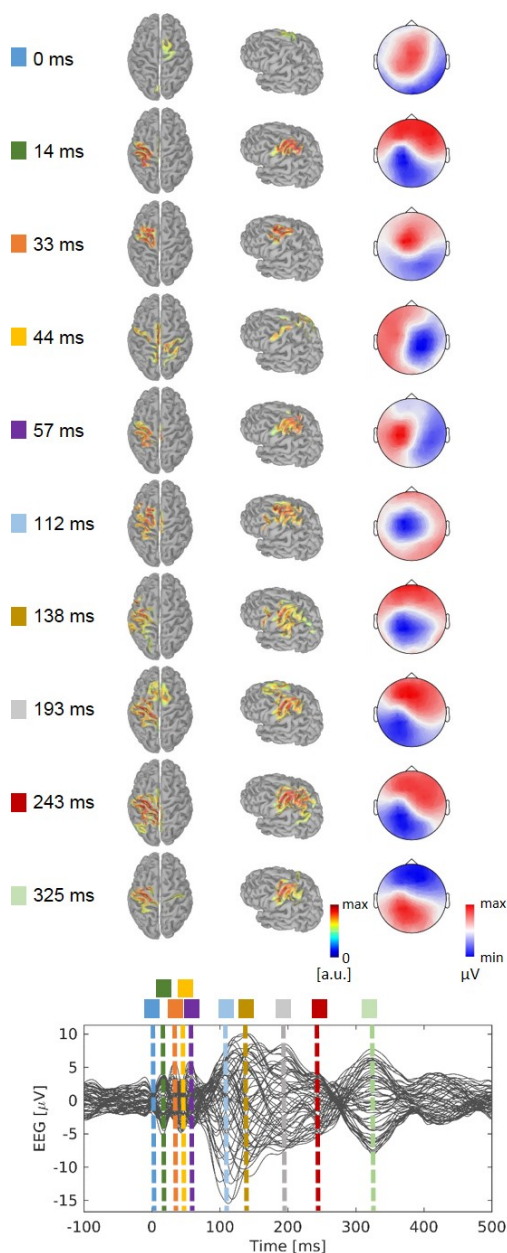


Figure 7.5 — Example of the results of source localization in a random subject stimulated at LM1. The bottom figure shows the TEPs in scalp space for all channels (averaged over epochs). Source localization results are shown for the peak-moments of the TEPs, together with the EEG topoplot (derived from scalp space).

The results of the correlations of the full time-interval (15-400ms) and the first time-interval (15-75ms) are shown in Table 7.1 and 7.2. Significant correlations are marked with * at the 0.05 level and ** for significance after Bonferroni correction.

Table 7.1 — Overview of the correlations between the quantified TEPs in source space and the rsFC in the full time interval (15-400ms). * : $p < 0.05$, ** : $p < 0.00016$ or $p < 0.00016$ Bonferroni corrected for individual or group analysis respectively.

	LDLPFC	RDLPFC	LM1	RM1	LPar	RPar
HC1	0,16*	0,11	0,20*	0,08	0,06	-0,04
HC2	0,05	0,07	0,20*	0,31**	-0,09	-0,11
HC3	0,10	0,11*	0,23*	0,14*	-0,09	-0,01
HC4	0,09	0,16*	0,06	0,04	-0,07	-0,10
HC5	0,04	-0,06	0,12*	0,14*	-0,05	-0,03
HC6	0,11	0,19*	0,09	0,14*	-0,10	-0,04
HC7	0,07	-0,06	0,26**	0,26**	0,10	0,02
HC8	-0,15	-0,17	0,16*	0,06	-0,10	-0,14
HC9	0,10*	0,05	0,28**	0,12*	-0,11	0,01
HC10	-0,08	0,11*	0,31**	0,31**	-0,03	0,08
Group average	0,03	0,03	0,15**	0,12**	-0,02	-0,06

Table 7.2 — Overview of the correlations between the quantified TEPs in source space and the rsFC in the first time interval (15-75ms). * : $p < 0.05$, ** : $p < 0.00016$ or $p < 0.00016$ Bonferroni corrected for individual or group analysis respectively.

	LDLPFC	RDLPFC	LM1	RM1	LPar	RPar
HC1	0,2**	0,13*	0,36**	0,18*	0,06	0,07
HC2	0,02	0,20*	0,21*	0,17*	0,13*	0,04
HC3	0,25**	0,10	0,25**	0,14*	0,01	0,06
HC4	0,21**	0,15*	0,09	0,01	-0,17	-0,06
HC5	0,23*	0,07	0,01	0,16*	-0,10	0,14*
HC6	0,17*	0,13*	0,14*	0,14*	-0,05	-0,11
HC7	0,26**	0,01	0,30**	0,25**	0,05	0,04
HC8	-0,08	-0,02	0,10	0,10	-0,06	-0,18
HC9	0,06	0,09	0,27**	0,04	0,09	0,10
HC10	-0,03	0,06	0,30**	0,31**	-0,07	0,08
Group average	0,09**	0,06	0,14**	0,13**	0	0

7.4 Discussion

This study showed the link between the propagation of the effect of single TMS pulses through the brain and rsFC. Especially when stimulating the motor areas, the brain's intrinsic rsFC was significantly correlated with the TEPs in source space, quantified using the RMS in different time-intervals. This is the first study aiming to investigate the possibility to predict the distribution of TMS effects in terms of rsFC. Earlier, it was already

shown that the brain's intrinsic functional architecture can predict the responses to electrical stimulation (Keller et al., 2011). Cortico-cortical evoked potential (CCEP) mapping was performed in six epilepsy subjects with subdural electrodes implanted (for the purpose of seizure localization). The spatial pattern and magnitude of evoked activity in response to direct cortical stimulation was significantly correlated to rsFC.

7.4.1 Clinical interpretation

The three bilateral stimulation locations are part of different intrinsic rsFC networks. According to the classification of Yeo et al. (2011) (see Figure 7.1), the DLPFC belongs to the frontoparietal network, the M1 is within the somatomotor network, and the Par stimulation sites are part of the default mode network. In this study we showed that propagation of the effects of single TMS pulses applied to the M1 areas could be predicted in terms rsFC, derived from normalized group connectome data. This might suggest that the motor network is a stable network with little variability. However in general, rsFC has a dynamic character which means that connectivity strengths change over time (Chang and Glover, 2010; Handwerker et al., 2012). Using the posterior cingulate cortex within the DMN as seed region, the functional connectivity to other brain areas, especially regions that are involved in higher-level cognitive function such as attention and salience processing, has shown high temporal variability (Chang and Glover, 2010).

7.4.2 Inter-individual variability

As can be seen in Table 7.1 and 7.2, there is a large inter-individual variability when correlating the qTEPs with the rsFC. The strongest correlations were found in subjects 2, 7, 9, and 10. The inter-individual variability can mostly be explained by the variations in the amplitude and latency of the TEP peaks (Figure 7.3). Even though TEPs are described to be highly reproducible within subjects (Lioumis et al., 2009), we here saw clear inter-individual differences in latencies and peak amplitudes. Coil positions per stimulation site did not vary much between our subjects, resulting in relatively similar rsFC maps.

At least part of the inter-individual variability might be explained by the dynamics in a subject's brain state (Silvanto and Pascual-Leone, 2008): the response to external stimulation such as TMS depends on the brain state at the time of stimulation. In this case, for every subject and for every stimulation position, all clean epochs were averaged to obtain one matrix as input for source localization. The state of the brain of these epochs was not taken into account, potentially increasing the inter-individual variability. Ongoing neuronal activity such as brain oscillations and their fluctuations can be recorded by EEG. The brain stimulation protocols can be tailored to specifically interact with the ongoing brain oscillations (Thut et al., 2017). This method is also referred to as brain-state-dependent-brain-stimulation (Bergmann, 2018) and might help to reduce inter-individual variability. For future studies, it is suggested to apply more single pulses, so that retrospectively a subset of pulses during a certain state can be considered for analysis, or to stimulate solely during a certain brain state using real-time brain state information derived from EEG.

Previously, using the same dataset as in this study, Vink et al. (2019) assessed the relationship between EEG rsFC and propagation of TEPs. In this case, pre-stimulation EEG data was used to compute the rsFC. So one can say that the subject-specific brain state was at least partly taken into account. RsFC measures correlated significantly with propagation of the TEPs, with Pearson's correlation-based FC being the best predictor of the TEP propagation. These findings confirm that the brain state during stimulation might contain valuable information about the propagation of TEPs.

7.4.3 Methodological considerations

TEPs do not solely reflect neuronal activity induced by transcranial neuronal excitation. TMS can also activate nerves that innervate cranial muscles (Mutanen, Mäki, and Ilmoniemi, 2013). These twitches in the cranial muscles can cause muscle potentials and electrode movement artefacts and also twitch-induced sensory input in the brain. Moreover, the electrical discharge in the stimulation coil produces a loud 'click' sound which causes auditory evoked potentials. These somatosensory and auditory components overlap substantially with the truly transcranial components. Recently, a 'state-of-the-art' sham method was proposed by Conde et al. (2019) mimicking the multisensory stimulation caused by real TMS as closely as possible. This setup includes placement of a foam layer underneath the coil and auditory noise masking. However, both temporal and spatial distributions of the TEP showed a significant similarity when comparing the real TMS with the realistic sham method. Specifically, the spatial similarity of cortical responses evoked by real and sham stimulation was significant in almost the whole post-stimulus time interval (20-410 ms).

The quantity and quality of somatosensory and auditory co-activation varies from site to site and depends on stimulation intensity and coil design. It is therefore warranted to do a sham stimulation for every active TMS stimulation condition. In this study, sham stimulation was only applied to LM1 by tilting the coil 90 degrees. This way the auditory sound was preserved and transmission of the mechanical vibration via both air- and bone- conduction was still possible (Du et al., 2017; Nikouline, Ruohonen, and Ilmoniemi, 1999). The vibration sensation between real and sham stimulation are different, making it difficult to correct for the non-neural somatosensory effects of TMS. The fact that no sham stimulation was applied to the DLPFC and Par stimulation sites might be related to the non-significant correlations in these areas.

Here, the subject-specific qTEPs were correlated with group level connectome data, instead of subject-specific rsFC data. One advantage of using connectome data over individual data is the robustness. Especially regarding rsFC data, the test-retest reliability of individual datasets is low. A disadvantage however, is that individual information that can affect the functional connections are not taken into account.

7.5 Conclusion

The brain's intrinsic functional connectivity can provide information about the distribution of the effects of single pulse TMS. The size of TEPs, quantified by the RMS over two

time-intervals after the stimulus, was significantly correlated with the rsFC, derived from group connectome data when stimulation was applied to the motor areas. Clinically, the knowledge about the propagation of TMS effects might be incorporated in personalized brain stimulation protocols. Future studies, including appropriate sham stimulation to all stimulation positions and controlling for the possible effects of brain state, are warranted to better characterize the propagation of single pulse TMS effects in terms of rsFC and validate the results.

*"All that is valuable in human society depends
upon the opportunity for development accorded
the individual."*

Albert Einstein

CHAPTER 8

General discussion: The route towards personalized rTMS protocols for depression

Based in part on manuscript:
'The route towards personalized rTMS protocols for depression'
D.C.W. Klooster, M.A.F. Ferguson, P.A.J.M. Boon, C. Baeken

in preparation

8.1 General discussion

Repetitive transcranial magnetic stimulation (rTMS) is an FDA approved brain stimulation technique for the treatment of major depressive disorder (MDD). The clinical application of different rTMS protocols has preceded the knowledge about the actual mechanism of action. In this thesis, we have used various neuroimaging methods to investigate the effects of TMS. We have given an overview of the current options for brain stimulation, beyond TMS (**Chapter 3**). We have used rs-fMRI data to show that accelerated iTBS affects functional connectivity, represented by graph measures (**Chapter 4**). Furthermore, we have shown that baseline brain characteristics, e.g. graph measures derived from rs-fMRI (**Chapter 4**) or structural connections (**Chapter 6**) have predictive value for the response to aiTBS. To quantify the propagation of effects of TMS, we have performed a more fundamental study in which the direct responses to single pulses, as measured in simultaneous TMS-EEG experiments, could be linked to functional brain connectivity (**Chapter 7**).

In line with most of the literature, the studies in this thesis show effects on the group level. Heterogeneous effects across individuals are very common. This probably causes the moderate overall response and remission rates of rTMS treatment in MDD. This could partly be explained by the lack of knowledge about the exact mechanisms of action and this could also be attributed to the application of too general 'one-fits-all' rTMS protocols for a broad patient-population. We therefore hypothesize that individual brain characteristics should be taken into account when administering TMS. These personalized rTMS protocols might reduce the variability in outcome measures and potentially increase the clinical efficacy.

The knowledge about the potential of rs-fMRI (**Chapter 4** and **Chapter 7**) and dMRI (**Chapter 6**) data to predict the outcome of the clinical efficacy of rTMS might be translated to personalized optimal coil positioning. Besides, also the stimulation intensity and the stimulation timing and frequency might be subject for personalization. In the next paragraphs, we discuss our work in the light of new developments, highlight possible improvements, and give potential recommendations for development of future personalized brain stimulation protocols. Thereby, we focus mainly on the stimulation parameters that might become subject-specific and contribute to personalized stimulation protocols.

It is important to emphasize that the further development and improvement of clinical efficacy of TMS treatment does not only require improved knowledge about the mechanism of action of the stimulation technique. It will be equally important to learn more about the patient and the pathology that needs to be treated. Overall improvement of the clinical efficacy of brain stimulation techniques is an iterative process, as shown in Figure 8.1. More knowledge about stimulation techniques can improve the knowledge about pathologies and vice versa. Besides, efficiency of brain stimulation might be increased by combining stimulation treatment with other types of treatment, such as for example psychotherapy. For a review of the potential added value combining psychotherapy with non-invasive brain stimulation, see Sathappan et al. (2019).

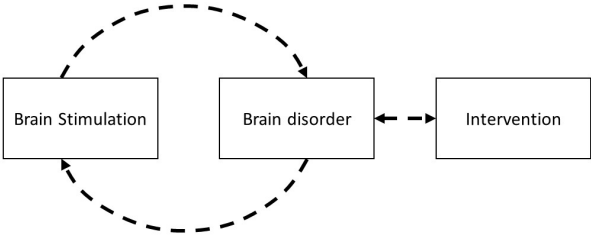


Figure 8.1 — *Development of more effective brain stimulation protocols in an iterative process: gaining more knowledge about brain stimulation techniques will improve the knowledge of the brain disorders and learning more about the brain disorders might lead to more effective stimulation protocols. Besides brain stimulation, also combinations with other interventions such as psychotherapy might help to improve treatment efficacy.*

8.1.1 TMS targeting

Together with the coil shape and the underlying brain geometry, the coil position at the scalp determines which parts of the brain are being stimulated. Previous work has shown that the effects of TMS propagate through the brain via functional and structural connections (Fox et al., 2014; Amico et al., 2017). Therefore, it is very likely that deeper brain structures involved in the clinical response are rather indirectly stimulated when a figure-of-eight coil is used. In this section, a distinction has been made between the direct targets, mostly referred to as the cortical targets, and the indirect targets, the region in the brain that (indirectly) needs to be reached to obtain clinical effects.

A. Cortical target definition

Neuroanatomical correlates of depression have been studied using various techniques. Hypoactivity in the left DLPFC was initially shown in PET studies (Drevets et al., 1992). Recovery of depression was furthermore accompanied by changes in DLPFC activity. These findings eventually led to the selection of this region as a target for rTMS in the first randomized clinical trial for depression (Pascual-Leone et al., 1996). Opposite changes in activity were found in the right DLPFC in depression patients. Presumably excitatory protocols to the left (i.e. high frequency rTMS or iTBS) (O’Reardon et al., 2007) and inhibitory protocols to the right (i.e. low frequency rTMS or cTBS) (Yadollahpour, Hosseini, and Shakeri, 2016), or a combination of both have aimed to normalize these abnormal activities (Fitzgerald et al., 2009b).

Besides the DLPFC, other novel targets in the prefrontal cortex have been suggested (Downar and Daskalakis, 2013). The dorsomedial part of the prefrontal cortex (DMPFC) was defined as the dorsal nexus in depression. Specific resting-state networks that play

a role in depression, the cognitive control network, the affective network, and the default mode network, all show increased functional connectivity with this dorsal nexus (Sheline et al., 2010). Causal relations between the DMPFC and depression have been shown by lesions. DMPFC lesions confer a very high risk ($\sim 80\%$) of severe depression. Bakker et al. (2015) reviewed the effectiveness of 10Hz vs iTBS to the DMPFC. Response and remission rates were 50.6%/38.5% and 48.5%/27.9% for the 10Hz and iTBS protocols, based on the Hamilton scores.

Furthermore, the frontopolar cortex (FPC), and ventromedial (VMPFC) and ventrolateral (VLPFC) parts of the prefrontal cortex might also be successful targets for rTMS treatment for depression. The FPC, also known as Brodmann area 10, showed higher rsFC in MDD patients (Fitzgerald et al., 2008a). Lesions in the VMPFC have shown to be strongly protective against depression mood (Koenigs et al., 2008). The VMPFC is located too deep ($\sim 7\text{cm}$) within the brain and therefore cannot be reached by conventional stimulation coils. The VLPFC reverses the standard dampening pattern of the amygdala response in depression patients. In depression, greater VLPFC activity correlates with higher (instead of dampened) amygdala activity and stronger sympathetic response (Johnstone et al., 2007). The VLPFC is also located outside the reach of the conventional coils. Furthermore, even stimulation of the superficial parts of the VLPFC is problematic due to the proximity of the extraocular and temporalis muscles.

B. Coil positioning in clinical practice

Even though various targets have been proposed to be suitable for stimulation treatment in depression patients (Downar and Daskalakis, 2013), the left DLPFC is by far the most used one in clinical practice. When stimulating the DLPFC as a treatment for depression, the 5-cm rule is often used to position the stimulation coil. This requires identification of the motor cortex and from there moving the coil 5 cm in rostral direction, as derived from the Talairach atlas. This 5-cm rule does not take inter-individual differences, such as head size and shape, into account, making this method suboptimal. This is also the main reason why the 5-cm rule is not suggested anymore to locate the DLPFC. Herbsman et al. (2009) compared stimulation positions from responders to non-responders and showed that more lateral and anterior prefrontal coil locations are beneficial to obtain clinical response. Furthermore, Herwig et al. (2001) showed that in some cases the 5-cm rule results in stimulation of the premotor cortex instead of the DLPFC. These findings led to deviations from the standard 5-cm rule into the 5.5-cm (Weigand et al., 2017) or even the 6-cm rule (Johnson et al., 2013).

Therefore, also other methods have been proposed to localize the DLPFC. The desired TMS coil position can be translated to the 10-20 system in the field of EEG. This 10-20 system accounts for variability in skull size by using certain percentages of the circumference and distances between four basic anatomical landmarks. According to this 10-20 system, the F3 electrode location corresponds to the DLPFC (Herwig, Satrapi, and Schönfeldt-lecuona, 2003). The beam-F3 method (Beam et al., 2009) only uses three skull measurements, the distance from nasion toinion, the distance from left to right tragus, and the head circumference making it easier to localize the DLPFC without losing

accuracy compared to the 10-20 system method (Mir-Moghtadaei et al., 2015).

MRI-guided, preferably maybe even functional MRI-guided might become the most accurate, but also most expensive, method to determine the stimulation target in the DLPFC (Peleman et al., 2010). Anatomical landmarks, such as the junction between Brodmann Area 9 and 46 can be used to define the specific cortical target location (Mylus et al., 2013; Pommier et al., 2017).

C. Targeting symptoms versus pathology

Optimal cortical stimulation targets might differ between subjects with the same pathology. As explained in the introduction of this thesis, MDD is a very heterogeneous disorder. Weigand et al. (2017) investigated the potential of rsFC between the DLPFC and the sgACC to predict the clinical response to rTMS in subgroups of subjects with cognitive, affective, and somatic symptoms. Subgenual connectivity was a significant predictor of improvement in subjects with cognitive and affective symptoms. Moreover, studying the 21 individual symptoms of the Beck Depression Inventory questionnaire separately, subgenual connectivity was associated with improvement in sadness, loss of pleasure, self-dislike, self-criticalness, suicidal thoughts, loss of interest, and worthlessness. Also Siddiqi et al. (2019) has shown distinct targets for depression patients suffering from melancholic versus anxiosomatic symptoms. Based on functional connectivity patterns from group connectome data it was shown that the former group responds best to TMS sites anti-correlated to limbic structures (i.e. the subgenual cingulate) and positively correlated with the insula and the anterior cingulate. Stimulation efficacy in the latter group was highest when the stimulation position was positively correlated to limbic areas and anti-correlated to the anterior cingulate. Note that it remains to be investigated if these different symptoms can also be linked to different optimal indirect stimulation targets deeper within the brain.

D. Personalizing the coil position

D. 1 Based on information about the indirect target

There is ample evidence that the cingulate cortex is involved in the release of depressive symptoms. However, the exact region of the cingulate that shows the highest predictive power between studies is ambiguous. A recently introduced lesion network mapping technique (Fox, 2018) might shed more light into the optimal exact deep brain structure, potentially a region within the cingulate cortex, that causes the best clinical efficacy of rTMS treatment. If the optimal (indirect) target within the brain is known, the optimal cortical target might vary between subjects based on their individual intrinsic brain connections. Neuroimaging techniques can be used to create individual connectivity maps and might be useful in determining the optimal subject-specific cortical target (Luber et al., 2017).

Many studies have suggested that parts of the cingulate cortex should be the indirect target for successful stimulation treatment. The functional anti-correlation between the DLPFC and the subgenual part of the anterior cingulate cortex has shown to correlate with the

clinical outcome of rTMS in depression patients (Fox, Liu, and Pascual-Leone, 2013; Weigand et al., 2017), suggesting that the spot with the highest functional anti-correlation is the optimal stimulation position (MNI = [-42; 44; 30]). Though, both Fox and Weigand used a normative group connectome to come to these findings. These results do not automatically translate into the individual patient. Baeken et al. (2014; 2017) used individual rs-fMRI data to show that the functional connection between the subgenual and parts of the superior medial frontal cortex were stronger in responders to 10Hz left DLPFC rTMS (Baeken et al., 2014). Similar findings were reported in an accelerated iTBS trial (Baeken et al., 2017a).

A potential disadvantage of using rs-fMRI to derive the cortical stimulation position is the limited test-retest reliability (Braun et al., 2012). Specifically, Ning et al. (2019) investigated this test-retest reliability of rs-fMRI guided DLPFC targets. Anatomical variation between simulation sites surpassed the spatial resolution of TMS. Also Santarnecchi et al. (2018) investigated the test-retest reliability of TMS targets derived from rsFC maps. Especially prefrontal brain areas showed strong variability in stimulation position, derived from different rs-fMRI datasets.

Limitations of rs-fMRI might be overcome by using dMRI data. Even though it has been hypothesized that the effects of TMS propagate via structural connections, the use of structural connectivity maps to determine the optimal stimulation position has only been studied in our group (see **Chapter 6**). Compared to rs-fMRI, dMRI is more biologically stable and might therefore be more suitable for the extraction of stimulation targets. Results of our study showed that indirect connections between the stimulation site in the left DLPFC and the caudal and posterior parts of the cingulate cortex were correlated to the clinical response to aiTBS. However, it must be noted that especially on the individual level, the accuracy of small fiber bundles is limited (Thomas et al., 2014). Future studies should explore if personalized target definition, derived from dMRI data, leads to improved clinical efficacy.

Besides MRI, an alternative personalized TMS cortical-targeting method based on heart rate was proposed by Iseger et al. (2017). This, so-called Neuro-Cardiac Guided TMS is based on the hypothesis that the influence of stimulation on parasympathetic activity can be used to target the DLPFC-sgACC network. The parasympathetic activity was quantified by the heart rate deceleration, which reflects activity within the DLPFC-sgACC network. On the group level, F3 and F4 stimulation positions resulted in the largest suppression of heart rate. However, some individuals showed most pronounced decreases in heart rate when stimulating FC3 and FC4.

D. 2 The potential role for computational modeling

Computational electric field modeling has shown that the individual brain geometry can substantially impact the strength and distribution of the TMS-induced electric field (Cocchi and Zalesky, 2018). Individual head models can be derived from anatomical MRI data. These head models are segmented in different tissue types and specific conductivity values are assigned to every tissue type. DMRI data can be used for accurate, orientation-specific conductivity mapping (Opitz et al., 2011; Thielscher, Opitz, and

Windhoff, 2011; Tuch et al., 1999; Tuch et al., 2001). Solving Maxwell's equations can lead to TMS-induced electric field distributions. The region in the brain that is stimulation is not necessarily located underneath the stimulation coil. Instead of calculating the TMS-induced electric field given the coil position and the subject-specific head model, an inverse method might be useful to calculate the optimal coil position given a certain cortical target. Optimal coil positioning might furthermore benefit from studies in which TMS-induced electric field distributions are combined with structural connectivity maps, derived from dMRI data. Neuronal activation will only be induced if the spatial derivative of the electric field along the neuron exceeds a threshold (Walsch and Pascual-Leone, 2003). Therefore, the neuron must either be bent across a uniform electric field or a non-uniform field must traverse an unbent neuron. Combining these techniques might therefore result in an 'effective' TMS-induced electric field.

In **Chapter 5**, we described limited added value to derive seeds for rsFC analyses from TMS-induced electric field simulations. Here, we state that computational modeling might help to determine the optimal coil position on the scalp. However, no studies have yet been performed to prove this assumption.

8.1.2 Stimulation intensity

To date, the stimulation intensity is the only stimulation parameter that is derived from subject-specific characteristics. The stimulation intensity is most often expressed as a percentage of one's resting motor threshold (rMT), defined as the minimal stimulation intensity that induces a reliable motor evoked potential (MEP) of minimal amplitude in the targeted muscle (Rossini et al., 2015). According to this gold standard, individual adjustment for stimulation intensity is purely based on responsivity of the primary motor cortex. There is no evidence so far that other brain regions, such as the DLPFC, show the same excitability as the motor cortex. Actually it was shown that the prefrontal and the motor cortices respond differently to TMS (Kähkönen et al., 2005). Using a simultaneous TMS-EEG setup, it was shown that TMS-evoked potentials (TEPs) after prefrontal stimulation were smaller compared to TEPs after motor cortex stimulation. Greater distance from the coil to the cortex is an indication of reduced intensity within the brain since the magnetic field strength reduces quadratically with distance from the stimulation coil (Barker, 1991). Variation between coil-cortex distance in the motor cortex and other stimulation regions might therefore cause a deviation in effective stimulation intensity. In 2013, Stokes et al. (2013) proposed a method to derive a 'corrected' rMT for distinct stimulation sites, thereby incorporating differences in the coil-cortex distance. Coil-cortex distances can be extracted from anatomical MRI data.

Reliable TMS dose calculation is unavailable (Peterchev et al., 2012). In the future, simultaneous TMS-fMRI or TMS-EEG might help to further optimize subject-specific stimulation intensities, and to validate the correction method proposed by Stokes et al. (2013). Using these combined techniques, the effect of stimulation can be recorded in terms of BOLD activity or TEPs, as a function of intensity. Optimal quantification of these outcome measures needs to be further investigated.

The optimal percentage of rMT to obtain the best clinical response is also not known. At least there is support of a relationship between stimulation intensity and anti-depressant efficacy. A 30%-33% reduction in depression scores was found after 10Hz rTMS at rMT whereas only little improvement was found after subthreshold stimulation and no effects were found after sham stimulation (Padberg et al., 2002). Though this study gives some insight, stimulation intensities in current clinical trials for depression treatment are usually supra-threshold.

8.1.3 Stimulation timing and frequency

The effects of TMS do not only differ between subjects but also within subjects, across and even within sessions (Ziemann and Siebner, 2015). Even though animal studies already suggested that this variability might reflect dynamics in brain state (Huerta and Usman, 1993; Huerta and Lisman, 1995), this phenomenon was long time mostly ignored in human research. In 2008, Silvanto and Pascual-Leone described the potential importance of the baseline cortical activation state when applying TMS (Silvanto and Pascual-Leone, 2008). One of the clearest proves of the importance of brain state is the fact that the active motor threshold is lower compared to the rMT (Hallett, 2007).

Ongoing brain oscillations can reveal information about the brain's excitability state (Buzsaki and Draguhn, 2004). This information is currently not incorporated in brain stimulation protocols, which might add to the heterogeneous outcomes (Mansouri et al., 2018). The neuron's excitability state during the application of stimuli is an essential factor that determine the capabilities of the induction of synaptic plasticity within neuronal networks. Based on this fact, it can be hypothesized that the efficacy of non-invasive brain stimulation, e.g. TMS, can be enhanced when the stimulation is tuned to high excitability states of the ongoing brain oscillations (Thut et al., 2017). This method is also referred to as brain-state-dependent-brain-stimulation (Bergmann, 2018).

Ongoing neuronal activity such as brain oscillations and their fluctuations can be recorded by EEG or MEG. Interaction between stimulation and ongoing brain activity can be achieved in three approaches according to Thut et al. (2017).

- Triggering TMS to instantaneous phase- or power-values of ongoing EEG/MEG that reflect states of heightened excitability. The phase of the oscillation reflects the current excitability state, whereas the amplitude reflects the current degree of local neuronal synchronization. This method requires real-time EEG/MEG analysis, including an algorithm that can forecast the phase or power so that the stimulation can be administered at the preferred timing (Mansouri et al., 2018). Such a system is also referred to as a closed loop system. In a closed loop system, the activity of the target region is recorded and used to inform about the optimal timing of the stimulation. Zrenner et al. (2018) used such a real-time TMS-EEG setup to investigate the effects of stimulation at different phases of the endogenous sensorimotor μ -rhythm in healthy subjects. The negative peak of the μ -rhythm, extracted from EEG data of C3 and surrounding electrodes, was associated with the high excitability state whereas the positive peak represented low excitability. Ap-

plication of 100Hz triplets during the high excitability state resulted in long-term potentiation effects, as measured by increased MEP size. Stimulation during low excitability state or at random μ -rhythm did not show effectiveness.

- Tuning TMS to the known frequencies of specific task-relevant brain oscillations in order to entrain these oscillations and promote the functions of the associated network. Since every individual has different rhythmic firing patterns it can be hypothesized that also the frequency is important for the clinical efficacy of TMS. Chung et al. (2018) highlighted the importance of the stimulation frequency in iTBS protocols by comparing 30Hz bursts repeated at 6Hz, 50Hz bursts at 5Hz, or individualized frequency. The specific individual frequency information was based on the theta-gamma coupling during a 3-back task. In contrast to the two standard protocols, individual iTBS significantly increased the amplitude of the TEPs at specific latencies (increase after 60ms, and decreases after 100 and 200ms).
- Triggering TMS to phase- or power-values, with a certain frequency (i.e. combining the first two options). If the first two options enhance the effects of TMS, it can be hypothesized that combining these methods gives even further improvements. However, no studies have been performed to prove this assumption.

Importantly, closed-loop stimulation requires knowledge of target parameters (such as the optimal choice of phase) that may come from an a priori hypothesis, or can be determined empirically by open-loop stimulation. However, optimal stimulation parameters are not yet known and are probably pathology, potentially even symptom, specific. Especially alpha and gamma oscillations have been related to depression. More specifically, increased left and decreased right prefrontal alpha has been linked to depression (Saletu and Anderer, 2010) and mid-frontal theta activity could predict responses to anti-depressant medication (Mitchell et al., 2008). TMS has shown to interfere with these brain oscillations. Gamma activity in the fronto-parietal network was modulated after 10Hz rTMS (Kito et al., 2014). In depression patients who responded to rTMS treatment, high baseline low-theta power in the subgenual cingulate normalized after rTMS. Changes in low-theta power were furthermore correlated with the clinical response (Narushima et al., 2010).

In the future, EEG-triggered approaches that synchronize each stimulus with the individual patient's instantaneous brain state, probably to certain power of the alpha or gamma oscillations in case of depression treatment, and consider the individual frequency of the patient's brain oscillations might help to reduce the inter- and intra-individual variability in the outcome of brain stimulation treatment.

8.2 Personalized brain stimulation protocols

At the end of this thesis we would like to come back to our initial Figure 1.3 in the Introduction. At some point in time, we hope that the knowledge about the mechanism of action of TMS, and also other brain stimulation techniques, will be fully unraveled. Optimal use of this knowledge will most likely be translated into personalized brain stimulation protocols. Multimodal neuroimaging can help in various ways to obtain these

personalized TMS parameters.

For example, we hypothesized that the findings regarding the potential of baseline functional and structural connections to predict the clinical efficacy of rTMS treatment in MDD patients could be translated to individualized optimal cortical target positions. If the indirect deep brain stimulation target is known, the specific cortical target might be derived from the subject's intrinsic brain architecture, derived from rs-fMRI and dMRI data. Furthermore, anatomical MRI data is key to obtain accurate individual head models for computational modeling of the TMS-induced electric fields. Additionally, dMRI data can be used in this regard to derive orientation-dependent connectivity values. The optimal coil position at the scalp can be computed if the cortical target is known, using a reversed TMS-induced electric field computation, involving the individual head model. Moreover, anatomical MRI data can be used to measure the differences in coil-cortex distances between the motor cortex and the stimulation position in the prefrontal area. This would lead to more accurate personalized stimulation intensities. Future studies need to be performed to investigate if these patient-specific stimulation parameters improve the clinical efficacy.

Besides MRI, future TMS protocols might use EEG or MEG information to focus more on the timing of the stimulation with respect to the ongoing brain oscillations. These brain oscillations represent the excitability state. Optimal and consistent timing of stimulation might therefore further reduce the inter-individual variability. The individual stimulation frequency might be derived from off-line EEG recordings. However, optimizing timing of the stimulation might require real-time EEG or MEG recordings during every stimulation procedure. This is clinically not feasible so alternative methods to optimize timing of the stimulation should therefore be investigated.

So, as can be seen in Figure 8.2, the obtrusiveness of the application of TMS will not return to fully unobtrusive after the knowledge about the mechanism of action is complete. Baseline measures are necessary to create the personalized brain stimulation protocols. Importantly, we think that the clinical efficacy will improve when using these personalized brain stimulation protocol, as represented in orange in Figure 8.2.

8.2.1 Future efficient TMS treatment

Figure 8.3 gives an overview of a possible future situation in which the potential of TMS is fully exploited. If a patient is known to have neurological or psychiatric complaints, the patient will be assessed by a medical doctor. This doctor will diagnose the patient and will decide about a suitable treatment approach: psychotherapy, psychopharmacotherapy, or non-invasive brain stimulation, i.e. rTMS. If rTMS is considered, a subject-specific stimulation protocol will be determined. The stimulation target will be derived from the combined knowledge about the pathology, and the subject-specific functional- and structural brain connections. Consecutively, the optimal coil position will be derived from computational models. Potentially, simultaneous EEG measurement can be used to optimize the exact timing of the stimulation. With this subject-specific stimulation protocols the chance of treatment success may be optimized.

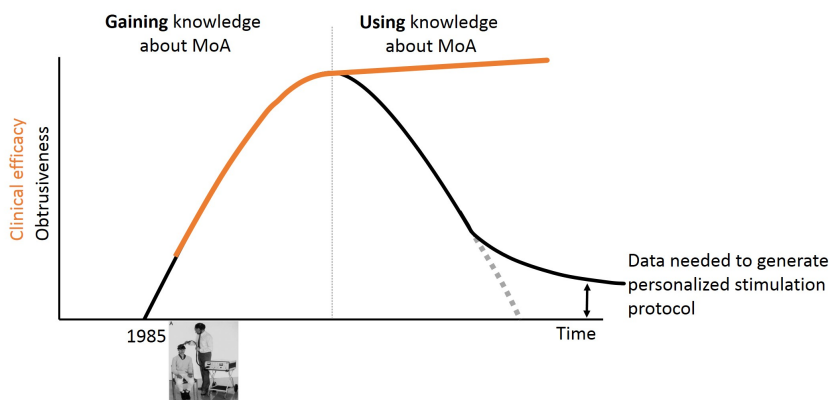


Figure 8.2 — Evolution of the obtrusiveness or complexity of TMS experiments over time including the possible increase of clinical efficacy over time. Baseline subject-specific data is needed to obtain personalized brain stimulation protocols. Hence, the obtrusiveness of TMS will not return to fully unobtrusive after the mechanism of action is known. Optimal use of the knowledge of the mechanism of action (MoA) will lead to increased clinical efficacy.

There are two points in Figure 8.3 that need to be further discussed. Firstly, the option to consider rTMS as a treatment option will hopefully move up in the overall treatment pipeline. Nowadays, rTMS treatment is only considered for a patient after multiple treatment attempts have failed. The STAR*D trial (Rush et al., 2006; Warden et al., 2007) showed increased relapse rates after every additional treatment approach step emphasizing the need to aggressively achieve the desired outcome as soon as possible.

The second point is also related to the relapse rates after rTMS treatment and the sustainability of the rTMS after-effects. A meta-analysis investigating the sustainability of the after-effects of rTMS applied to the left DLPFC in depression subjects showed small anti-depressant effects during follow-up, ranging from 2 to 16 weeks after the stimulation (Kedzior et al., 2015). Another meta-analysis showed sustained response rates of 66.5%, 52.9%, and 46.3% after a longer follow-up periods of 3, 6, and 12 months respectively (Senova et al., 2019). Relapse rates in depression beyond this follow-up period are quite high. Specifically, the STAR*D study (Rush et al., 2006) found relapse rates of 10-45% within a year or less of remission (Greden, 2001).

Maintenance treatment is therefore of high interest and might help to extend the response/remission period. Maintenance treatment can be applied after the initial stimulation protocol by gradually tapering off the amount of stimulation sessions (Richieri et al., 2013) or by applying less frequent clustered stimulation sessions (Fitzgerald et al., 2013). Ideally, these maintenance sessions would be available in home-based setting with a mobile rTMS device. However, it is not likely that home-based TMS devices will become available any time soon. Up til now, the only home based TMS device is used for treatment of migraine but this treatment is based on single pulses instead of rTMS. Hence in

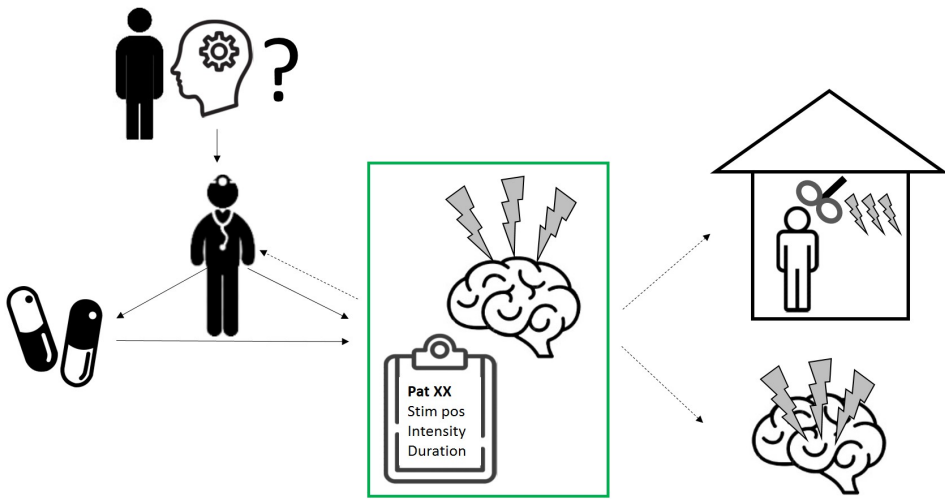


Figure 8.3 — Overview of the potential future application of rTMS treatment. A medical doctor can decide in an early stage whether rTMS would be a feasible treatment approach for the patient. In case it is, baseline MRI and/or EEG data will be recorded to derive a subject-specific stimulation protocol. After successful application of this subject-specific stimulation protocol, maintenance treatment might be necessary to elongate the duration of the rTMS after-effects. Ideally, this maintenance treatment would be possible within a home environment with a mobile device. However, mobile rTMS equipment is not likely to be available any time soon. Therefore, even maintenance treatment might be applied in the clinical setting under medical supervision. The information from successful personalized rTMS protocols might be translated into subject-specific invasive stimulation protocols, for example deep brain stimulation. In that case, personalized rTMS acts as a biomarker for the clinical response to invasive brain stimulation procedures.

the current situation, maintenance treatment will also be applied in a clinical setting.

Of note, decision-making regarding continuation of rTMS protocols should not only be done after the stimulation protocol. Short-term response to treatment might predict the response on longer time scales (Donse et al., 2018). Feffer et al. (2018) showed that clinical response after 2 weeks could predict the overall outcome of 20 sessions administered to the DMPFC. This information would be very helpful in decision making in clinical settings; whether to discontinue or continue the ongoing stimulation protocol and whether to change parameters or not. As a result, this would be beneficial for the cost-to-benefit ratio of TMS.

Another option to proceed with stimulation might be the translation to invasive brain stimulation protocols, for example deep brain stimulation. The information gained from successful personalized rTMS might be translated into a patient-specific treatment plan by means of invasive techniques. Obviously, a pre-requisite for a surgical procedure is a high success-rate. It should be up to the patient if the burden of the surgical procedure outweighs the burden of multiple, potentially life-long repeating, (maintenance) rTMS

session. In these cases, rTMS can be used as a biomarker for the outcome of invasive brain stimulation.

8.3 Conclusion

Overall, the field of brain stimulation is rapidly evolving and has already shown promising therapeutic potential in various neuropsychiatric disorders. However, most results are based on the group level. A high inter- and intra-individual variability exists in the clinical responses to rTMS treatment. In this thesis, we have shown various potential roles of neuroimaging techniques to learn more about the mechanism of action. Pre- and post-stimulation rs-fMRI and dMRI measurements can help to study the effects of stimulation within the brain. Furthermore, biomarkers can be derived from baseline MRI data to predict the clinical response. Potentially, the high inter-individual variability is linked the patient-specific intrinsic brain connections. Using information from neuroimaging to obtain patient-specific brain stimulation protocols might decrease the inter-individual variability and potentially also increase the overall clinical effectiveness.

Bibliography

- Abe, M., H. Fukuyama, and T. Mima (2014). "Water diffusion reveals networks that modulate multiregional morphological plasticity after repetitive brain stimulation". In: *Proceedings of the National Academy of Sciences* 111.12, pp. 4608–4613.
- Abe, O. et al. (2010). "Voxel-based analyses of gray/white matter volume and diffusion tensor data in major depression". In: *Psychiatry Research - Neuroimaging* 181.1, pp. 64–70.
- Abraham, W. C. and M. F. Bear (1996). "Metaplasticity : plasticity of synaptic". In: *Trends in Neuroscience* 19.4, pp. 126–130.
- Ajilore, O., M. Lamar, A. Leow, A. Zhang, S. S. Yang, and A. Kumar (2014). "Graph theory analysis of cortical-subcortical networks in late-life depression". In: *American Journal of Geriatric Psychiatry* 22.2, pp. 195–206.
- Al-Otaibi, F. A., C. Hamani, and A. M. Lozano (Oct. 2011). "Neuromodulation in epilepsy". In: *Neurosurgery* 69.4, pp. 957–979.
- Alexander, A. L., S. A. Hurlley, A. A. Samsonov, N. Adluru, A. P. Hosseinbor, P. Mossahebi, D. P. Tromp, E. Zakszewski, and A. S. Field (2012). "Characterization of Cerebral White Matter Properties Using Quantitative Magnetic Resonance Imaging Stains". In: *Brain Connectivity* 1.6, pp. 423–446.
- Alexandre Gramfort, Théodore Papadopoulos, Emmanuel Olivi, and Maureen Clerc (2009). "OpenMEEG: open-source software for quasistatic bioelectromagnetics". In: *BioMedical Engineering OnLine* 8.1, p. 1.
- Amar, A. P., M. L. Levy, C. Y. Liu, and M. L. J. Apuzzo (2008). "Vagus Nerve Stimulation". In: *Proceedings of the IEEE* 96.7, pp. 1142–1151.
- Amico, E., O. Bodart, M. Rosanova, O. Gosseries, L. Heine, P. Van Mierlo, C. Martial, M. Massimini, D. Marinazzo, and S. Laureys (2017). "Tracking Dynamic Interactions Between Structural and Functional Connectivity: A TMS/EEG-dMRI Study". In: *Brain Connectivity* 7.2, pp. 84–97.
- Antal, A. and W. Paulus (2013). "Transcranial alternating current stimulation (tACS)." In: *Frontiers in human neuroscience* 7.June, p. 317.
- Antal, A., T. Z. Kincses, M. A. Nitsche, O. Bartfai, I. Demmer, M. Sommer, and W. Paulus (2002). "Pulse configuration-dependent effects of repetitive transcranial magnetic stimulation on visual perception". In: *Neuroreport* 13.17, pp. 2223–2229.
- Appleby, B. S., P. S. Duggan, A. Regenberg, and P. V. Rabins (2007). "Psychiatric and neuropsychiatric adverse events associated with deep brain stimulation: A meta-analysis of ten years' experience". In: *Movement Disorders* 22.12, pp. 1722–1728.
- Arai, N., S. Okabe, T. Furubayashi, Y. Terao, K. Yuasa, and Y. Ugawa (Mar. 2005). "Comparison between short train, monophasic and biphasic repetitive transcranial magnetic stimulation (rTMS) of the human motor cortex." In: *Clinical neurophysiology : official journal of the International Federation of Clinical Neurophysiology* 116.3, pp. 605–13.
- Arai, N., S. Okabe, T. Furubayashi, H. Mochizuki, N. K. Iwata, R. Hanajima, Y. Terao, and Y. Ugawa (Oct. 2007). "Differences in after-effect between monophasic and biphasic high-frequency rTMS of the human motor cortex." In: *Clinical neurophysiology : official journal of the International Federation of Clinical Neurophysiology* 118.10, pp. 2227–33.
- Asconapé, J. J. (Aug. 2013). "Epilepsy: new drug targets and neurostimulation." In: *Neurologic clinics* 31.3, pp. 785–798.
- Åström, M., J.-J. Lemaire, and K. Wårdell (Jan. 2012). "Influence of heterogeneous and anisotropic tissue conductivity on electric field distribution in deep brain stimulation." In: *Medical & biological engineering & computing* 50.1, pp. 23–32.

- Åström, M. et al. (2014). "Relationship between Neural Activation and Electric Field Distribution during Deep Brain Stimulation". In: *IEEE Transactions on Biomedical Engineering* 62, February 2015, pp. 664–672.
- Aydin-Abidin, S., V. Moliadze, U. T. Eysel, and K. Funke (July 2006). "Effects of repetitive TMS on visually evoked potentials and EEG in the anaesthetized cat: dependence on stimulus frequency and train duration." In: *The Journal of physiology* 574, Pt 2, pp. 443–55.
- Bae, E. H., L. M. Schrader, K. Machii, M. Alonso-Alonso, J. J. Rivielo, A. Pascual-Leone, and A. Rotenberg (June 2007). "Safety and tolerability of repetitive transcranial magnetic stimulation in patients with epilepsy: a review of the literature." In: *Epilepsy & behavior : E&B* 10.4, pp. 521–8.
- Baeken, C and R De Raedt (2011). "Neurobiological mechanisms of repetitive transcranial magnetic stimulation on the underlying neurocircuitry in unipolar depression". In: *Dialogues Clin Neurosci* 13.1, pp. 139–145.
- Baeken, C., R. De Raedt, L. Santermans, D. Zeeuws, M. A. Vanderhasselt, M. Meers, and N. Vanderbruggen (2010a). "HF-rTMS treatment decreases psychomotor retardation in medication-resistant melancholic depression". In: *Progress in Neuro-Psychopharmacology and Biological Psychiatry* 34.4, pp. 684–687.
- Baeken, C. et al. (2010b). "Right prefrontal HF-rTMS attenuates right amygdala processing of negatively valenced emotional stimuli in healthy females". In: *Behavioral Brain Research* 214.2, pp. 450–455.
- Baeken, C., R. De Raedt, C. Van Hove, P. Clerinx, J. De Mey, and A. Bossuyt (2009). "HF-rTMS Treatment in Medication-Resistant Melancholic Depression: Results from 18FDG-PET Brain Imaging". In: *CNS spectrums* 14.8, pp. 439–448.
- Baeken, C., M. A. Vanderhasselt, J. Remue, S. Herremans, N. Vanderbruggen, D. Zeeuws, L. Santermans, and R. De Raedt (2013). "Intensive HF-rTMS treatment in refractory medication-resistant unipolar depressed patients". In: *Journal of Affective Disorders* 151.2, pp. 625–631.
- Baeken, C., D. Marinazzo, G.-R. Wu, P. Van Schuerbeek, J. De Mey, I. Marchetti, M.-A. Vanderhasselt, J. Remue, R. Luyckaert, and R. De Raedt (2014). "Accelerated HF-rTMS in treatment-resistant unipolar depression : insights from subgenual anterior cingulate functional connectivity". In: *World journal of biological psychiatry* 15.4, pp. 286–297.
- Baeken, C., D. Marinazzo, H. Everaert, G. R. Wu, C. Van Hove, K. Audenaert, I. Goethals, F. De Vos, K. Peremans, and R. De Raedt (2015). "The impact of accelerated HF-rTMS on the subgenual anterior cingulate cortex in refractory unipolar major depression: Insights from 18FDG PET brain imaging". In: *Brain Stimulation* 8.4, pp. 808–815.
- Baeken, C., J. Remue, M. A. Vanderhasselt, A. R. Brunoni, S. De Witte, R. Duprat, E. H. Koster, R. De Raedt, and G. R. Wu (2017a). "Increased left prefrontal brain perfusion after MRI compatible tDCS attenuates momentary ruminative self-referential thoughts". In: *Brain Stimulation* 10.6, pp. 1088–1095.
- Baeken, C., R. Duprat, G.-R. R. Wu, R. De Raedt, K. Van Heeringen, R. D. Raedt, and K. van Heeringen (2017b). "Subgenual anterior cingulate - medio orbitofrontal functional connectivity in medication-resistant major depression: a neurobiological marker for accelerated intermittent Theta Burst Stimulation treatment?" In: *Biological Psychiatry: Cognitive Neuroscience and Neuroimaging* 2.7, pp. 556–565.
- Baillet, S., J. C. Mosher, and R. M. Leahy (2001). "Sylvain Baillet, John C. Mosher, and Richard M. Leahy". In: *IEEE signal processing magazine*, pp. 14–30.
- Bakker, N., S. Shahab, P. Giacobbe, D. M. Blumberger, Z. J. Daskalakis, S. H. Kennedy, and J. Downar (2015). "RTMS of the dorsomedial prefrontal cortex for major depression: Safety, tolerability, effectiveness, and outcome predictors for 10 Hz versus intermittent theta-burst stimulation". In: *Brain Stimulation* 8.2, pp. 208–215.
- Barker, A. T. (1991). "An introduction to the basic principles of magnetic nerve stimulation". In: *Journal of Clinical Neurophysiology* 8.1, pp. 26–37.
- Barker, A. T., B. H. Brown, and I. L. Freeston (1979). "Determination of the Distribution of Conduction Velocities in Human Nerve Trunks". In: *IEEE Transactions on Biomedical Engineering* BME-26.2, pp. 76–81.
- Barker, A. T., R. Jalinous, and I. L. Freeston (1985). "Non-invasive magnetic stimulation of the human motor cortex". In: *Lancet* 1, pp. 1106–1107.
- Bashir, S., D. Edwards, and A. Pascual-Leone (2011). "Neuronavigation Increases the Physiologic and Behavioral Effects of Low-Frequency rTMS of Primary Motor Cortex in Healthy Subjects". In: *Brain topography* 24.1, pp. 54–64. arXiv: NIHMS150003.
- Basser, P. J. and C. Pierpaoli (1996). "Microstructural and physiological features elucidated by quantitative diffusion tensor MRI". In: *J. Magnetic Resonance, B* 111, pp. 209–219.
- Basser, P. J., S. Pajevic, C. Pierpaoli, J. Duda, and A. Aldroubi (2000). "In vivo fiber tractography using DT-MRI data". In: *Magnetic Resonance in Medicine* 44.4, pp. 625–632.
- Bassett, D. S. and E. T. Bullmore (2009). "Human brain networks in health and disease." In: *Current opinion in neurology* 22, pp. 340–347.
- Basu, I., D. Graupe, D. Tuninetti, P. Shukla, K. V. Slavin, L. V. Metman, and D. M. Corcos (2013). "Pathological tremor prediction using surface electromyogram and acceleration: potential use in 'ON-OFF' demand driven deep brain stimulator design." In: *Journal of neural engineering* 10, p. 036019.
- Batsikadze, G. V. Moliadze, W. Paulus, M.-F. Kuo, and M. A. Nitsche (Apr. 2013). "Partially non-linear stimulation intensity-dependent effects of direct current stimulation on motor cortex excitability in humans." In: *The Journal of physiology* 591, pp. 1987–2000.

- Beam, W., J. J. Borckardt, S. T. Reeves, and M. S. George (2009). "An efficient and accurate new method for locating the F3 position for prefrontal TMS applications". In: *Brain Stimulation* 2.1, pp. 50–54. arXiv: NIHMS150003.
- Beckmann, C. F. and S. M. Smith (2004). "Probabilistic Independent Component Analysis for Functional Magnetic Resonance Imaging". In: *IEEE Transactions on Medical Imaging* 23.2, pp. 137–152. arXiv: 978-0-87893-286-3.
- Belmaker, R. and G. Agam (2008). "Mechanisms of disease: Major depressive disorder". In: *New England Journal of Medicine* 358, pp. 55–68.
- Ben-Haim, S., W. F. Asaad, J. T. Gale, and E. N. Eskandar (Apr. 2009). "Risk factors for hemorrhage during microelectrode-guided deep brain stimulation and the introduction of an improved microelectrode design." In: *Neurosurgery* 64.4, pp. 754–62;
- Ben-Menachem, E (2001). "Vagus nerve stimulation, side effects, and long-term safety". In: *Journal of Clinical Neurophysiology* 18.5, pp. 415–418.
- Ben-menachem, E. (2002). "Vagus-nerve stimulation for the treatment of epilepsy". In: *Lancet neurology* 1.December, pp. 477–482.
- Ben-Menachem, E. (2012). "Neurostimulation-past, present, and beyond". In: *Epilepsy Currents* 12.10, pp. 188–191.
- Benabid, A. L. (2003). "Deep brain stimulation for Parkinson's disease". In: *Current Opinion in Neurobiology* 13.6, pp. 696–706.
- Bergey, G. K., M. J. Morrell, E. M. Mizrahi, A. Cole, S. S. Cash, K. Noe, D. Spencer, M. Smith, and L. J. Hirsch (2015). "Long-term treatment with responsive brain stimulation in adults with refractory partial seizures". In: *Neurology* 84, pp. 810–817.
- Bergmann, T. O. (2018). "Brain State-Dependent Brain Stimulation". In: *Frontiers in Psychology* 9.November, pp. 1–4.
- Berlim, M. T., F. Van Den Eynde, S. Tovar-Perdomo, and Z. J. Daskalakis (2014). "Response, remission and drop-out rates following high-frequency repetitive transcranial magnetic stimulation (rTMS) for treating major depression: A systematic review and meta-analysis of randomized, double-blind and sham-controlled trials". In: *Psychological Medicine* 44.2, pp. 225–239.
- Bermppohl, F., F. Fregni, P. S. Boggio, G. Thut, G. Northoff, P. T. M. Otachi, S. P. Rigonatti, M. A. Marcolin, and A. Pascual-Leone (Jan. 2006). "Effect of low-frequency transcranial magnetic stimulation on an affective go/no-go task in patients with major depression: role of stimulation site and depression severity." In: *Psychiatry research* 141.1, pp. 1–13.
- Besseling, R. M. H., J. F. A. Jansen, G. M. Overvliet, S. J. M. Van Der Kruijs, J. S. H. Vles, S. C. M. Ebus, P. A. M. Hofman, A. D. Louw, A. P. Aldenkamp, and W. H. Backes (2013). "Reduced functional integration of the sensorimotor and language network in rolandic epilepsy". In: *NeuroImage: Clinical* 2, pp. 239–246.
- Bestmann, S., J. Baudewig, and J. Frahm (2003). "On the synchronization of transcranial magnetic stimulation and functional echo-planar imaging". In: *Journal of Magnetic Resonance Imaging* 17.3, pp. 309–316.
- Bestmann, S., J. J. Baudewig, H. R. Siebner, J. C. Rothwell, and J. Frahm (2005). "BOLD MRI responses to repetitive TMS over human dorsal premotor cortex". In: *NeuroImage* 28.1, pp. 22–29.
- Beurrier, C., B. Bioulac, J. Audin, and C. Hammond (2014). "High-Frequency Stimulation Produces a Transient Blockade of Voltage-Gated Currents in Subthalamic Neurons". In: *Journal of physiology* 85, pp. 1351–1356.
- Beuter, A., J.-P. Lefaucheur, and J. Modolo (2014). "Closed-loop cortical neuromodulation in Parkinson's disease: An alternative to deep brain stimulation?" In: *Clinical neurophysiology : official journal of the International Federation of Clinical Neurophysiology* 125.5, pp. 874–85.
- Biswal, B., F. Z. Yetkin, V. M. Haughton, and J. S. Hyde (1995). "Functional connectivity in the motor cortex of resting human brain using". In: *Magn Reson Med* 34.9, pp. 537–541.
- Blumberger, D. M. et al. (2018). "Articles Effectiveness of theta burst versus high-frequency repetitive transcranial magnetic stimulation in patients with depression (THREE-D): a randomised non-inferiority trial". In: *The Lancet* 391.10131, pp. 1683–1692.
- Bodart, O. et al. (2017). "Global structural integrity and effective connectivity in patients with disorders of consciousness". In: *Brain Stimulation*, pp. 1–8.
- Bohning, D. E., A. P. Pecheny, C. M. Epstein, A. M. Speer, D. J. Vincent, W. Dannels, and M. S. George (1997). "Mapping transcranial magnetic stimulation (TMS) fields in vivo with MRI." In: *Neuroreport* 8.11, pp. 2535–8.
- Bohr, I. J. et al. (2013). "Resting-State Functional Connectivity in Late-Life Depression: Higher Global Connectivity and More Long Distance Connections". In: *Frontiers in Psychiatry* 3.January, pp. 1–14.
- Boon, P., K. Vonck, P. Van Walleghem, M. D'Havé, L. Goossens, T. Vandekerckhove, J. Caemaert, and J. De Reuck (2001a). "Programmed and magnet-induced vagus nerve stimulation for refractory epilepsy". In: *Journal of clinical neurophysiology : official publication of the American Electroencephalographic Society* 18.5, pp. 402–7.
- Boon, P., K. Vonck, J. De Reuck, and J. Caemaert (2001b). "Vagus nerve stimulation for refractory epilepsy". In: *Seizure : the journal of the British Epilepsy Association* 10.6, pp. 448–55.
- Boon, P., V. D. Herdt, K. Vonck, and D. V. Roost (2007a). "Clinical experience with vagus nerve stimulation and deep brain stimulation in epilepsy". In: *Acta Neurochirurgica, Supplementum* 97.2, pp. 273–280.

- Boon, P., M. D'Havé, B. Vanrumste, G. Van Hoey, K. Vonck, P. Van Walleghem, J. Caemaert, E. Achten, and J. De Reuck (2002). "Ictal Source Localization in Presurgical Patients With Refractory Epilepsy". In: *Journal of Clinical Neurophysiology* 19.5, pp. 461–468.
- Boon, P. et al. (Mar. 2007b). "Deep Brain Stimulation in Patients with Refractory Temporal Lobe Epilepsy". In: *Epilepsia* 48.8, pp. 1551–1560.
- Boon, P., K. Van Rijckevorsel, R. El Tahry, C. Elger, N. Mullatti, A. Schulze-Bonhage, K. Vonck, L. Wagner, W. Van Grunderbeek, and R. McGuire (2014). "Vagus nerve stimulation triggered by cardiac based seizure detection, a prospective multicenter study". In: *Epilepsy Currents* 14.12, Suppl. 1.
- Bortoletto, M., D. Veniero, G. Thut, and C. Miniussi (2015). "The contribution of TMS-EEG coregistration in the exploration of the human cortical connectome". In: *Neuroscience & Biobehavioral Reviews* 49, pp. 114–124.
- Braack, E. M. ter, A. W. E. Koopman, and M. J. A. M. van Putten (2016). "Early TMS evoked potentials in epilepsy: A pilot study". In: *Clinical Neurophysiology* 127.9, pp. 3025–3032.
- Brasil-Neto, J. P., L. G. Cohen, M. Panizza, J. Nilsson, B. J. Roth, and M. Hallett (1992). *Optimal focal transcranial magnetic activation of the human motor cortex: effects of coil orientation, shape of the induced current pulse, and stimulus intensity*.
- Braun, U. et al. (2012). "Test-retest reliability of resting-state connectivity network characteristics using fMRI and graph theoretical measures". In: *NeuroImage* 59.2, pp. 1404–1412.
- Brodbeck, V., A. M. Lascano, L. Spinelli, M. Seeck, and C. M. Michel (2009). "Accuracy of EEG source imaging of epileptic spikes in patients with large brain lesions". In: *Clinical Neurophysiology* 120.4, pp. 679–685.
- Brozova, H., I. Barnaure, R. L. Alterman, and M. Tagliati (2009). "STN-DBS frequency effects on freezing of gait in advanced Parkinson Disease". In: *Neurology* 72, pp. 770–774.
- Brunoni, A. R. et al. (2013). "Clinical Research with Transcranial Direct Current Stimulation (tDCS): Challenges and Future Directions". In: *Brain stimulation* 5.3, pp. 175–195.
- Brunoni, A. R., J. Amadera, B. Berbel, M. S. Volz, B. G. Rizzerio, and F. Fregni (2011). "A systematic review on reporting and assessment of adverse effects associated with transcranial direct current stimulation". In: *The International Journal of Neuropsychopharmacology* 14.08, pp. 1133–1145.
- Bullmore, E. and O. Sporns (2012). "The economy of brain network organization". In: *Nature reviews. Neuroscience* 13, pp. 336–349.
- Bullmore, E. and O. Sporns (2009). "Complex brain networks: graph theoretical analysis of structural and functional systems." In: *Nature reviews. Neuroscience* 10, pp. 186–98.
- Bunch, S., C. M. DeGiorgio, S. Kralj, J. Britton, P. Green, M. Lancman, J. Murphy, P. Olejniczak, J. Shih, and C. N. Heck (2007). "Vagus nerve stimulation for epilepsy: Is output current correlated with acute response?" In: *Acta Neurologica Scandinavica* 116.4, pp. 217–220.
- Butson, C. R. and C. C. McIntyre (Aug. 2007). "Differences among implanted pulse generator waveforms cause variations in the neural response to deep brain stimulation." In: *Clinical neurophysiology : official journal of the International Federation of Clinical Neurophysiology* 118.8, pp. 1889–94.
- Butson, C. R., S. E. Cooper, J. M. Henderson, and C. C. McIntyre (2006). "Predicting the Effects of Deep Brain Stimulation with Diffusion Tensor Based Electric Field Models". In: *Medical Image Computing and Computer-Assisted Intervention* 9, pp. 429–437.
- Buzsaki, G. and A. Draguhn (2004). "Neuronal Oscillations in Cortical Networks". In: *Science* 304.5679, pp. 1926–1929.
- Cabral-Calderin, Y., K. A. Williams, A. Opitz, P. Dechent, and M. Wilke (2016). "Transcranial alternating current stimulation modulates spontaneous low frequency fluctuations as measured with fMRI". In: *NeuroImage* 141, pp. 88–107.
- Caeyenberghs, K., A. Leemans, J. Coxon, I. Leunissen, D. Drijckoningen, M. Geurts, J. Gooijers, K. Michiels, S. Sunaert, and S. P. Swinnen (2011). "Bimanual Coordination and Corpus Callosum Microstructure in Young Adults with Traumatic Brain Injury: A Diffusion Tensor Imaging Study". In: *Journal of Neurotrauma* 28.6, pp. 897–913.
- Caeyenberghs, K., R. Duprat, A. Leemans, H. Hosseini, D. Klooster, and C. Baeken (2018). "Accelerated intermittent theta burst stimulation in major depression induces decreases in modularity: A connectome analysis". In: *Network Neuroscience* 3.1, pp. 157–172.
- Carrette, S., P. Boon, M. Sprengers, R. Raedt, and K. Vonck (2015). "Responsive neurostimulation in epilepsy". In: *Expert Review of Neurotherapeutics* January 2016, pp. 1–10.
- Cash, R., L. Cocchi, R. Anderson, A. Rogachov, A. Kucyi, A. Barnett, A. Zalesky, and P. Fitzgerald (2019). "Multivariate neuroimaging based prediction of individual outcome to transcranial magnetic stimulation in depression". In: *Brain Stimulation* 12.2, p. 477.
- Casula, E. P., V. Tarantino, D. Basso, G. Arcara, G. Marino, G. M. Toffolo, J. C. Rothwell, and P. S. Bisiacchi (2014). "Low-frequency rTMS inhibitory effects in the primary motor cortex: Insights from TMS-evoked potentials". In: *NeuroImage* 98, pp. 225–232.
- Chang, C. and G. H. Glover (2010). "Time-frequency dynamics of resting-state brain connectivity measured with fMRI". In: *NeuroImage* 50.1, pp. 81–98.

- Chaturvedi, A., C. R. Butson, S. E. Cooper, and C. C. McIntyre (2006). "Subthalamic nucleus deep brain stimulation: accurate axonal threshold prediction with diffusion tensor based electric field models." In: *Conference proceedings : ... Annual International Conference of the IEEE Engineering in Medicine and Biology Society. IEEE Engineering in Medicine and Biology Society. Annual Conference* 1, pp. 1240–3.
- Chen, V. C. H., C. Y. Shen, S. H. Y. Liang, Z. H. Li, Y. S. Tian, Y. T. Liao, Y. C. Huang, Y. Lee, R. S. McIntyre, and J. C. Weng (2016). "Assessment of abnormal brain structures and networks in major depressive disorder using morphometric and connectome analyses". In: *Journal of Affective Disorders* 205, pp. 103–111.
- Chen, X., Y. Xiong, G. Xu, and X. Liu (2012). "Deep Brain Stimulation". In: *Interventional Neurology* 1, pp. 200–212.
- Cheng, W., E. T. Rolls, J. Qiu, W. Liu, and Y. Tang (2016). "Medial reward and lateral non-reward orbitofrontal cortex circuits change in opposite directions in depression". In: *Brain* 139, pp. 3296–3309.
- Chistyakov, A. V., O. Rubicsek, B. Kaplan, M. Zaaroor, and E. Klein (2010). "Safety, tolerability and preliminary evidence for antidepressant efficacy of theta-burst transcranial magnetic stimulation in patients with major depression." In: *The International Journal of Neuropsychopharmacology* 13.3, pp. 387–393.
- Chung, S. W., C. M. Sullivan, N. C. Rogasch, K. E. Hoy, N. W. Bailey, R. F. Cash, and P. B. Fitzgerald (2018). "The effects of individualised intermittent theta burst stimulation in the prefrontal cortex: A TMS-EEG study". In: *Human Brain Mapping* August 2018, pp. 608–627.
- Cif, L., D. Ruge, V. Gonzalez, P. Limousin, X. Vasques, M. I. Hariz, J. Rothwell, and P. Coubes (2013). "The influence of deep brain stimulation intensity and duration on symptoms evolution in an OFF stimulation dystonia study." In: *Brain stimulation* 6.4, pp. 500–5.
- Cincotta, M, F. Giovannelli, A. Borgheresi, F. Balestrieri, G. Zaccara, M. Inghilleri, and A. Berardelli (2006). "Modulatory effects of high-frequency repetitive transcranial magnetic stimulation on the ipsilateral silent period." In: *Experimental brain research* 171.4, pp. 490–6.
- Cocchi, L. and A. Zalesky (2018). "Personalized Transcranial Magnetic Stimulation in Psychiatry". In: *Biological Psychiatry: Cognitive Neuroscience and Neuroimaging* 3.9, pp. 731–741.
- Cocchi, L., M. V. Sale, A. Lord, A. Zalesky, M. Breakspear, and J. B. Mattingley (2015). "Dissociable effects of local inhibitory and excitatory theta-burst stimulation on large-scale brain dynamics." In: *Journal of neurophysiology* 113.9, pp. 3375–3385.
- Coley, E, R. Farhadi, S. Lewis, and I. R. Whittle (2009). "The incidence of seizures following Deep Brain Stimulating electrode implantation for movement disorders, pain and psychiatric conditions." In: *British journal of neurosurgery* 23.2, pp. 179–183.
- Coluccia, D., J. Fandino, L. Schwyzer, R. O. Gorman, L. Remonda, J. Anon, E. Martin, and B. Werner (2014). "First noninvasive thermal ablation of a brain tumor with MR-guided focused ultrasound". In: *Journal of therapeutic ultrasound* 2.17, pp. 1–7.
- Conde, V., L. Tomasevic, I. Akopian, K. Stanek, G. B. Saturnino, A. Thielscher, T. O. Bergmann, and H. R. Siebner (2019). "The non-transcranial TMS-evoked potential is an inherent source of ambiguity in TMS-EEG studies". In: *NeuroImage* 185, pp. 300–312.
- Conforto, A. B., W. J. Z'Graggen, A. S. Kohl, K. M. Rösler, and A. Kaelin-Lang (2004). "Impact of coil position and electrophysiological monitoring on determination of motor thresholds to transcranial magnetic stimulation." In: *Clinical neurophysiology* 115.4, pp. 812–9.
- Conte, A., D. Belvisi, E. Iezzi, F. Mari, M. Inghilleri, and A. Berardelli (Apr. 2008). "Effects of attention on inhibitory and facilitatory phenomena elicited by paired-pulse transcranial magnetic stimulation in healthy subjects." In: *Experimental brain research* 186.3, pp. 393–9.
- Cook, I. A., L. M. Schrader, C. M. DeGiorgio, P. R. Miller, E. R. Maremont, and A. F. Leuchter (2013). "Trigeminal nerve stimulation in major depressive disorder: Acute outcomes in an open pilot study". In: *Epilepsy and Behavior* 28.2, pp. 221–226.
- Craddock, R. C., G. A. James, P. E. H. Iii, X. P. Hu, and H. S. Mayberg (2013). "A whole brain fMRI atlas spatially Generated via Spatially Constrained Spectral Clustering". In: *Human brain mapping* 33.8, pp. 1914–1928.
- Cymerblit-Sabba, A., M. Schiller, and Y. Schiller (2013). "Termination of chemoconvulsant-induced seizures by synchronous and asynchronous electrical stimulation of the hippocampus in-vivo". In: *Brain Stimulation* 6.5, pp. 727–736.
- Dale, A. M., A. K. Liu, B. R. Fischl, R. L. Buckner, J. W. Beldiveau, J. D. Lewine, E. Halgren, and S. Louis (2000). "Neurotechnique Mapping : Combining fMRI and MEG for High-Resolution Imaging of Cortical Activity". In: *Neuron* 26, pp. 55–67.
- Damoiseaux, J. S., S. A. R. B. Rombouts, F. Barkhof, P. Scheltens, C. J. Stam, S. M. Smith, and C. F. Beckmann (2006). "Consistent resting-state networks across healthy subjects." In: *Proceedings of the National Academy of Sciences of the United States of America* 103.37, pp. 13848–13853.
- Danner, N., P. Julkunen, M. Könönen, L. Säisänen, J. Nurkkala, and J. Karhu (2008). "Navigated transcranial magnetic stimulation and computed electric field strength reduce stimulator-dependent differences in the motor threshold." In: *Journal of neuroscience methods* 174.1, pp. 116–122.
- Danner, N., M. Könönen, L. Säisänen, R. Laitinen, E. Mervaala, and P. Julkunen (2012). "Effect of individual anatomy on resting motor threshold-computed electric field as a measure of cortical excitability." In: *Journal of neuroscience methods* 203.2, pp. 298–304.

- Darby, R. R., A. Horn, F. Cushman, and M. D. Fox (2017). "Lesion network localization of criminal behavior". In: *Proceedings of the National Academy of Sciences*, p. 201706587.
- Datta, A., M. Elwassif, F. Battaglia, and M. Bikson (2008). "Transcranial current stimulation focality using disc and ring electrode configurations: FEM analysis." In: *Journal of neural engineering* 5.2, pp. 163–174.
- Datta, A., V. Bansal, J. Diaz, J. Patel, D. Reato, and M. Bikson (2009). "Gyri-precise head model of transcranial direct current stimulation: Improved spatial focality using a ring electrode versus conventional rectangular pad". In: *Brain Stimulation* 2.4, pp. 201–207.
- Davey, C. G., B. J. Harrison, M. Yücel, and N. B. Allen (2012). "Regionally specific alterations in functional connectivity of the anterior cingulate cortex in major depressive disorder". In: *Psychological Medicine* 42.10, pp. 2071–2081.
- Davey, K., C. M. Epstein, M. S. George, and D. E. Bohning (2003). "Modeling the effects of electrical conductivity of the head on the induced electric field in the brain during magnetic stimulation". In: *Clinical Neurophysiology* 114.11, pp. 2204–2209.
- David, S. et al. (2019). "The Superoanterior Fasciculus (SAF): A Novel White Matter Pathway in the Human Brain?" In: *Frontiers in Neuroanatomy* 13, pp. 1–18.
- Day, B. L. et al. (1989). "Electric and magnetic stimulation of human motor cortex: surface EMG and single motor unit responses". In: *Journal of physiology*, pp. 449–473.
- De Geeter, N, G Crevecoeur, L Dupré, W Van Hecke, and A Leemans (2012). "A DTI-based model for TMS using the independent impedance method with frequency-dependent tissue parameters." In: *Physics in medicine and biology* 57.8, pp. 2169–2188.
- De Geeter, N, G Crevecoeur, a Leemans, and L Dupré (2015). "Effective electric fields along realistic DTI-based neural trajectories for modelling the stimulation mechanisms of TMS". In: *Physics in Medicine and Biology* 60, pp. 453–471.
- De Geeter, N. (2015). "A Diffusion Tensor-Based Computational Model for Transcranial Magnetic Stimulation: from Macroscopic Fields to Neuronal Membrane Potentials". PhD thesis, pp. 1–44.
- De Geeter, N., G. Crevecoeur, and L. Dupre (2011). "An Efficient 3-D Eddy-Current Solver Using an Independent Impedance Method for Transcranial Magnetic Stimulation". In: *IEEE transactions on biomedical engineering* 58.2, pp. 310–320.
- De Geeter, N., C. Guillaume, and D. Luc (2011). "Eddy-Current Simulations Using an Independent Impedance Method in Anisotropic Biological Tissues". In: *IEEE transactions on biomedical engineering* 47.10, pp. 3845–3848.
- De Witte, N. A. J. and S. C. Mueller (2016). "White matter integrity in brain networks relevant to anxiety and depression: evidence from the human connectome project dataset". In: *Brain Imaging and Behavior* 11.6, pp. 1–12.
- DeGiorgio, C. M. et al. (2000). "Prospective long-term study of vagus nerve stimulation for the treatment of refractory seizures." In: *Epilepsia* 41.9, pp. 1195–1200.
- DeGiorgio, C. et al. (2005). "Vagus nerve stimulation for epilepsy: Randomized comparison of three stimulation paradigms". In: *Neurology* 65.2 SUPPL. 1, pp. 317–319.
- DeGiorgio, C. M. and S. E. Kralh (2013). "Neurostimulation for drug-resistant epilepsy". In: *CONTINUUM Lifelong Learning in Neurology* 19.3, pp. 743–755.
- DeGiorgio, C. M., D. A. Shewmon, and T. Whitehurst (2003). *Trigeminal nerve stimulation for epilepsy*. Tech. rep., pp. 421–422.
- DeGiorgio, C. M., A. Shewmon, D. Murray, and T. Whitehurst (2006). "Pilot study of trigeminal nerve stimulation (TNS) for epilepsy: a proof-of-concept trial." In: *Epilepsia* 47.7, pp. 1213–5.
- DeGiorgio, C. M., D. Murray, D. Markovix, and T. Whitehurst (2009). "Trigeminal nerve stimulation for epilepsy: Long-term feasibility and efficacy". In: *Neurology* 72, pp. 936–938.
- DeGiorgio, C. M., J. Soss, I. A. Cook, D. Markovic, J. Gornbein, S. Oviedo, and C. P. Kealey (2013). "Randomized controlled trial of trigeminal nerve stimulation for drug-resistant epilepsy". In: *Neurology* 80.9, pp. 786–791.
- Deichmann, R., U. Nöth, and N. Weiskopf (2010). "The Basics of Functional Magnetic Resonance Imaging". In: *EEG-fMRI*, pp. 39–62.
- Deli, G., I. Balas, F. Nagy, E. Balazs, J. Janszky, S. Komoly, and N. Kovacs (Jan. 2011). "Comparison of the efficacy of unipolar and bipolar electrode configuration during subthalamic deep brain stimulation." In: *Parkinsonism & related disorders* 17.1, pp. 50–4.
- Deligianni, F., E. Robinson, C. F. Beckmann, D. Sharp, A. D. Edwards, and D. Dueckert (2011). "Inference of functional connectivity from direct and indirect structural brain connections". In: *2011 IEEE International Symposium on Biomedical Imaging: From Nano to Macro*.
- Delvendahl, I., H. Lindemann, N. H. Jung, A. Pechmann, H. R. Siebner, and V. Mall (2014). "Influence of waveform and current direction on short-interval intracortical facilitation: a paired-pulse TMS study." In: *Brain stimulation* 7.1, pp. 49–58.
- Deng, Z. D., S. M. McClintock, and S. H. Lisanby (2015). "Brain network properties in depressed patients receiving seizure therapy: A graph theoretical analysis of peri-treatment resting EEG. Conf Proc IEEE Eng Med Biol Soc". In: *Annual international conference of the IEEE Engineering in Medicine and Biology Society*, pp. 2203–2206.

- Deng, Z.-D., S. H. Lisanby, and A. V. Peterchev (Jan. 2013). "Electric field depth-focality tradeoff in transcranial magnetic stimulation: simulation comparison of 50 coil designs." In: *Brain stimulation* 6.1, pp. 1–13.
- Denys, D., M. Feenstra, and R. Schuurman (2012). *Deep Brain Stimulation: A New Frontier in Psychiatry*, pp. 1–10.
- Dieckhöfer, A., T. D. Waberski, M. Nitsche, W. Paulus, H. Buchner, and R. Gobbelé (2006). "Transcranial direct current stimulation applied over the somatosensory cortex - differential effect on low and high frequency SEPs." In: *Clinical neurophysiology* 117.10, pp. 2221–7.
- Dinga, R., L. Schmaal, B. W. Penninx, M. J. van Tol, D. J. Veltman, L. van Velzen, M. Mennes, N. J. van der Wee, and A. F. Marquand (2019). "Evaluating the evidence for biotypes of depression: Methodological replication and extension of Drysdale et al. (2017)". In: *NeuroImage: Clinical* 22, p. 101796.
- Disner, S. G., C. G. Beevers, E. A. P. Haigh, and A. T. Beck (2011). "Neural mechanisms of the cognitive model of depression." In: *Nature reviews. Neuroscience* 12.8, pp. 467–477.
- Doeltgen, S. H. and M. C. Ridding (2011). "Modulation of cortical motor networks following primed theta burst transcranial magnetic stimulation". In: *Experimental Brain Research* 215.3-4, pp. 199–206.
- Donse, L., F. Padberg, A. T. Sack, A. J. Rush, and M. Arns (2018). "Simultaneous rTMS and psychotherapy in major depressive disorder: Clinical outcomes and predictors from a large naturalistic study". In: *Brain Stimulation* 11.2, pp. 337–345.
- Downar, J. and Z. J. Daskalakis (2013). "New targets for rTMS in depression: A review of convergent evidence". In: *Brain Stimulation* 6.3, pp. 231–240.
- Downar, J. et al. (2014). "Anhedonia and reward-circuit connectivity distinguish nonresponders from responders to dorsomedial prefrontal repetitive transcranial magnetic stimulation in major depression". In: *Biological Psychiatry* 76.3, pp. 176–185.
- Drevets, W. C., T. O. Videen, J. L. Price, S. H. Preskorn, S. T. Carmichael, and M. E. Raichle (1992). "A Functional Anatomical Study of Unipolar Depression". In: *The Journal of Neuroscience* 12, pp. 3628–3641.
- Drysdale, A. T. et al. (2017). "Resting-state connectivity biomarkers define neurophysiological subtypes of depression". In: *Nature Medicine* 23, pp. 28–38.
- Du, X., F. S. Choa, A. Summerfelt, L. M. Rowland, J. Chiappelli, P. Kochunov, and L. E. Hong (2017). "N100 as a generic cortical electrophysiological marker based on decomposition of TMS-evoked potentials across five anatomic locations". In: *Experimental Brain Research* 235.1, pp. 69–81.
- Dunlop, K., B. Woodside, E. Lam, M. Olmsted, and P. Colton (2015). "Increases in frontostriatal connectivity are associated with response to dorsomedial repetitive transcranial magnetic stimulation in refractory binge / purge behaviors". In: *NeuroImage: Clinical* 8, pp. 611–618.
- Duprat, R. et al. (2016). "Accelerated intermittent theta burst stimulation treatment in medication-resistant major depression: A fast road to remission?" In: *Journal of Affective Disorders* 200, pp. 6–14.
- Duprat, R., G. R. Wu, R. De Raedt, and C. Baeken (2017). "Accelerated iTBS treatment in depressed patients differentially modulates reward system activity based on anhedonia". In: *World Journal of Biological Psychiatry* 19.7, pp. 497–508.
- Earhart, G. M., M. Hong, S. D. Tabbal, and J. S. Perlmutter (2007). "Effects of thalamic stimulation frequency on intention and postural tremor." In: *Experimental Neurology* 208.2, pp. 257–263.
- Eaton, H (1992). "Electric field induced in a spherical volume conductor from arbitrary coils: application to magnetic stimulation and MEG." In: *Medical & biological engineering & computing* 30, pp. 433–440.
- Ellrich, J. (2011). "Transcutaneous vagus nerve stimulation". In: *Eur. Neurol. Rev.* pp. 254–256.
- Eusebio, A., C. C. Chen, C. S. Lu, S. T. Lee, C. H. Tsai, P. Limousin, M. Hariz, and P. Brown (2008). "Effects of low-frequency stimulation of the subthalamic nucleus on movement in Parkinson's disease." In: *Experimental neurology* 209.1, pp. 125–30.
- Fadini, T., L. Matthäus, H. Rothkegel, M. Sommer, F. Tergau, A. Schweikard, W. Paulus, and M. A. Nitsche (2009). "H-coil: Induced electric field properties and input/output curves on healthy volunteers, comparison with a standard figure-of-eight coil". In: *Clinical neurophysiology : official journal of the International Federation of Clinical Neurophysiology* 120.6, pp. 1174–1182.
- Farzan, F., M. Vernet, M. M. D. Shafi, A. Rotenberg, Z. J. Daskalakis, and A. Pascual-Leone (2016). "Characterizing and Modulating Brain Circuitry through Transcranial Magnetic Stimulation Combined with Electroencephalography". In: *Frontiers in Neural Circuits* 10.73.
- Fava, M. and K. S. Kendler (2000). "Major Depressive Disorder Review". In: *Neuron* 28.2, pp. 335–341.
- Feffer, K., H. H. Lee, F. Mansouri, P. Giacobbe, F. Vila-Rodríguez, S. H. Kennedy, Z. J. Daskalakis, D. M. Blumberger, and J. Downar (2018). "Early symptom improvement at 10 sessions as a predictor of rTMS treatment outcome in major depression". In: *Brain Stimulation* 11.1, pp. 181–189.
- Fierro, B., F. Brighina, G. Vitello, A. Piazza, S. Scalia, G. Giglia, O. Daniele, and A. Pascual-Leone (June 2005). "Modulatory effects of low- and high-frequency repetitive transcranial magnetic stimulation on visual cortex of healthy subjects undergoing light deprivation." In: *The Journal of physiology* 565, pp. 659–65.
- Fisher, R. et al. (2010). "Electrical stimulation of the anterior nucleus of thalamus for treatment of refractory epilepsy." In: *Epilepsia* 51.5, pp. 899–908.
- Fisher, R. S. (2011). "Benefits of trigeminal nerve stimulation". In: *Epilepsy & behavior : E&B* 22.4, pp. 615–6.

- Fisher, R. S. and A. L. Velasco (2014). "Electrical brain stimulation for epilepsy." In: *Nature reviews. Neurology* 10.5, pp. 261–70.
- Fitzgerald, P. B., T. L. Brown, Z. J. Daskalakis, R. Chen, and J. Kulkarni (2002). "Intensity-dependent effects of 1 Hz rTMS on human corticospinal excitability". In: *Clinical Neurophysiology* 113, pp. 1136–1141.
- Fitzgerald, P. B., A. R. Laird, J. Maller, and Z. J. Daskalakis (2008a). "A meta-analytic study of changes in brain activation in depression". In: *Human Brain Mapping* 29.6, pp. 683–695.
- Fitzgerald, P. B., K. Hoy, S. McQueen, S. Herring, R. Segrave, G. Been, J. Kulkarni, and Z. J. Daskalakis (2008b). "Priming stimulation enhances the effectiveness of low-frequency right prefrontal cortex transcranial magnetic stimulation in major depression." In: *Journal of clinical psychopharmacology* 28.1, pp. 52–8.
- Fitzgerald, P. B., K. Hoy, S. McQueen, J. J. Maller, S. Herring, R. Segrave, M. Bailey, G. Been, J. Kulkarni, and Z. J. Daskalakis (2009a). "A Randomized Trial of rTMS Targeted with MRI Based Neuro-Navigation in Treatment-Resistant Depression". In: *Neuropsychopharmacology* 34.5, pp. 1255–1262.
- Fitzgerald, P. B., K. Hoy, Z. J. Daskalakis, and J. Kulkarni (Jan. 2009b). "A randomized trial of the antidepressant effects of low- and high-frequency transcranial magnetic stimulation in treatment-resistant depression". In: *Depression and anxiety* 26.3, pp. 229–34.
- Fitzgerald, P. B., N. Grace, K. E. Hoy, M. Bailey, and Z. J. Daskalakis (2013). "An open label trial of clustered maintenance rTMS for patients with refractory depression". In: *Brain Stimulation* 6.3, pp. 292–297.
- Fitzgerald, P. B., K. E. Hoy, D. Elliot, R. N. Susan McQueen, L. E. Wambeek, and Z. J. Daskalakis (2018). "Accelerated repetitive transcranial magnetic stimulation in the treatment of depression". In: *Neuropsychopharmacology* 43.7, pp. 1565–1572.
- Fogelson, N., A. A. Kühn, P. Silberstein, P. D. Limousin, M. Hariz, T. Trottenberg, A. Kupsch, and P. Brown (2005). "Frequency dependent effects of subthalamic nucleus stimulation in Parkinson's disease." In: *Neuroscience letters* 382.1-2, pp. 5–9.
- Fonseka, T. M., G. M. Macqueen, and S. H. Kennedy (2018). "Neuroimaging biomarkers as predictors of treatment outcome in Major Depressive Disorder". In: *Journal of Affective Disorders* 233.May 2017, pp. 21–35.
- Fox, M. D. (2018). "Mapping Symptoms to Brain Networks with the Human Connectome". In: *New England Journal of Medicine* 379.23, pp. 2237–2245.
- Fox, M. D., H. Liu, and A. Pascual-Leone (2013). "Identification of reproducible individualized targets for treatment of depression with TMS based on intrinsic connectivity". In: *NeuroImage* 66, pp. 151–160.
- Fox, M. D. and Michael Greicius (2010). "Clinical applications of resting state functional connectivity". In: *Frontiers in Systems Neuroscience* 4.19, pp. 1–13.
- Fox, M. D. and M. E. Raichle (2007). "Spontaneous fluctuations in brain activity observed with functional magnetic resonance imaging". In: *Nature* 8.9, pp. 700–711. arXiv: arXiv: 1011.1669v3.
- Fox, M. D., A. Z. Snyder, J. L. Vincent, M. Corbetta, D. C. Van Essen, and M. E. Raichle (2005). "The human brain is intrinsically organized into dynamic, anticorrelated functional networks." In: *Proceedings of the National Academy of Sciences of the United States of America* 102.27, pp. 9673–9678. arXiv: NIHMS150003.
- Fox, M. D., D. Zhang, A. Z. Snyder, and M. E. Raichle (2009). "The global signal and observed anticorrelated resting state brain networks." In: *Journal of neurophysiology* 101.6, pp. 3270–3283.
- Fox, M. D., R. L. Buckner, M. P. White, M. D. Greicius, and A. Pascual-Leone (2012a). "Efficacy of TMS targets for depression is related to intrinsic functional connectivity with the subgenual cingulate". In: *Biological Psychiatry* 72.7, pp. 595–603.
- Fox, M. D., M. A. Halko, M. C. Eldaief, and A. Pascual-Leone (2012b). "Measuring and manipulating brain connectivity with resting state functional connectivity magnetic resonance imaging (fcMRI) and transcranial magnetic stimulation (TMS)." In: *NeuroImage* 62.4, pp. 2232–2243.
- Fox, M. D., R. L. Buckner, H. Liu, M. M. Chakravarty, A. M. Lozano, and A. Pascual-Leone (2014). "Resting-state networks link invasive and noninvasive brain stimulation across diverse psychiatric and neurological diseases." In: *Proceedings of the National Academy of Sciences of the United States of America* 111.41, E4367–75.
- Fox, P. T., S. Narayana, N. Tandon, H. Sandoval, S. P. Fox, P. Kochunov, and J. L. Lancaster (2004). "Column-based model of electric field excitation of cerebral cortex." In: *Human brain mapping* 22.1, pp. 1–14.
- Fregni, F. et al. (2014). "Regulatory considerations for the clinical and research use of transcranial direct current stimulation (tDCS): Review and recommendations from an expert panel". In: *Clinical Research and Regulatory Affairs* 1333.1, pp. 1–14.
- Friston, K. J. (1994). "Functional and effective connectivity in neuroimaging: A synthesis". In: *Human Brain Mapping* 2.1-2, pp. 56–78.
- Furman, D. J., J. Paul Hamilton, I. H. Gotlib, J. P. Hamilton, and I. H. Gotlib (2011). "Frontostriatal functional connectivity in major depressive disorder". In: *Biology of Mood & Anxiety Disorders* 11, p. 11.
- Fyttagoridis, A, M Åström, K Wårdell, and P Blomstedt (2013). "Stimulation-induced side effects in the posterior subthalamic area: distribution, characteristics and visualization." In: *Clinical neurology and neurosurgery* 115.1, pp. 65–71.

- Gabbay, V., B. A. Ely, Q. Li, S. D. Bangaru, A. M. Panzer, C. M. Alonso, F. X. Castellanos, and M. P. Milham (2013). "Striatum-based circuitry of adolescent depression and anhedonia". In: *Journal of the American Academy of Child and Adolescent Psychiatry* 52.6, pp. 628–641.
- Gabriel, C., S. Gabriel, and E. Cothout (1996). "Dielectric Properties of Biological Tissues: Literature Survey". In: *Physics in Medicine and Biology* 41, pp. 2231–2249.
- Gambo, O. L., A. Antal, V. Moliadze, and W. Paulus (2010). "Simply longer is not better: Reversal of theta burst after-effect with prolonged stimulation". In: *Experimental Brain Research* 204.2, pp. 181–187.
- Gambo, O. L., A. Antal, B. Laczo, V. Moliadze, M. A. Nitsche, and W. Paulus (2011). "Impact of repetitive theta burst stimulation on motor cortex excitability". In: *Brain Stimulation* 4.3, pp. 145–151.
- Ganguly, K. and M. ming Poo (2013). "Activity-dependent neural plasticity from bench to bedside". In: *Neuron* 80.3, pp. 729–741.
- Garry, M. I. and R. H. S. Thomson (2009). "The effect of test TMS intensity on short-interval intracortical inhibition in different excitability states." In: *Experimental brain research* 193.2, pp. 267–74.
- Gawryluk, J. R., E. L. Mazerolle, and R. C. N. D'Arcy (2014). "Does functional MRI detect activation in white matter? A review of emerging evidence, issues, and future directions". In: *Frontiers in Neuroscience* 8.8, pp. 1–12.
- Gennaro, L. D., M. Bertini, F. Pauri, R. Cristiani, G. Curcio, M. Ferrara, and P. M. Rossini (2004). "Callosal effects of transcranial magnetic stimulation (TMS): the influence of gender and stimulus parameters". In: *Neuroscience Research* 48.2, pp. 129–137.
- Gentner, R., K. Wankerl, C. Reinsberger, D. Zeller, and J. Classen (2008). "Depression of human corticospinal excitability induced by magnetic theta-burst stimulation: Evidence of rapid polarity-reversing metaplasticity". In: *Cerebral Cortex* 18.9, pp. 2046–2053.
- George, M. S. (2010). "Transcranial magnetic stimulation for the treatment of depression." In: *Expert review of neurotherapeutics* 10.11, pp. 1761–1772.
- George, M. S., J. J. Taylor, and E. B. Short (2013). "The expanding evidence base for rTMS treatment of depression." In: *Current opinion in psychiatry* 26.1, pp. 13–18. arXiv: NIHMS150003.
- Ghorbani, P., M. Mohammad-Zadeh, J. Mirnajafi-Zadeh, and Y. Fathollahi (2007). "Effect of different patterns of low-frequency stimulation on piriform cortex kindled seizures." In: *Neuroscience letters* 425.3, pp. 162–6.
- Gigante, P. R. and R. R. Goodman (2011). "Alternative surgical approaches in epilepsy". In: *Current Neurology and Neuroscience Reports* 11.4, pp. 404–408.
- Girvan, M. and M. E. J. Newman (2002). "Community structure in social and biological networks". In: *Proceedings of the National Academy of Sciences* 99.12, pp. 7821–7826. arXiv: 0112110 [cond-mat].
- Gold, P. W. and G. P. Chrousos (2002). "Organization of the stress system and its dysregulation in melancholic and atypical depression : high vs low CRH / NE states". In: *Molecular Psychiatry* 7, pp. 254–275.
- Gordon, P. C., D. Desideri, P. Belardinelli, C. Zrenner, and U. Ziemann (2018). "Comparison of cortical EEG responses to realistic sham versus real TMS of human motor cortex". In: *Brain Stimulation* 11.6, pp. 1322–1330.
- Gorsler, A., T. Bäumer, C. Weiller, A. Münchau, and J. Liepert (2003). "Interhemispheric effects of high and low frequency rTMS in healthy humans". In: *Clinical Neurophysiology* 114.10, pp. 1800–1807.
- Gorzelic, P., S. J. Schiff, and A. Sinha (2013). "Model-based rational feedback controller design for closed-loop deep brain stimulation of Parkinson's disease." In: *Journal of neural engineering* 10.2, p. 026016.
- Goto, T., Y. Saitoh, N. Hashimoto, M. Hirata, H. Kishima, S. Oshino, N. Tani, K. Hosomi, R. Kakigi, and T. Yoshimine (2008). "Diffusion tensor fiber tracking in patients with central post-stroke pain; correlation with efficacy of repetitive transcranial magnetic stimulation". In: *Pain* 140.3, pp. 509–518.
- Grant, P. F. and M. M. Lowery (2009). "Electric field distribution in a finite-volume head model of deep brain stimulation." In: *Medical engineering & physics* 31.9, pp. 1095–103.
- Greden, J. F. (2001). "The Burden of Recurrent Depression : Causes , Consequences , and Future Prospects". In: *Journal of clinical p.*, pp. 5–9.
- Greenberg, B. D., D. A. Malone, G. M. Friehs, A. R. Rezai, C. S. Kubu, P. F. Malloy, S. P. Salloway, M. S. Okun, W. K. Goodman, and S. A. Rasmussen (2006). "Three-Year Outcomes in Deep Brain Stimulation for Highly Resistant Obsessive-Compulsive Disorder". In: *Neuropsychopharmacology* 31, pp. 2384–2393.
- Greicius, M. D., B. Krasnow, A. L. Reiss, and V. Menon (2003). "Functional connectivity in the resting brain: a network analysis of the default mode hypothesis." In: *Proceedings of the National Academy of Sciences of the United States of America* 100.1, pp. 253–258.
- Greicius, M. D., B. H. Flores, V. Menon, G. H. Glover, H. B. Solvason, H. Kenna, A. L. Reiss, and A. F. Schatzberg (2007). "Resting-State Functional Connectivity in Major Depression: Abnormally Increased Contributions from Subgenual Cingulate Cortex and Thalamus". In: *Biological Psychiatry* 62.5, pp. 429–437.
- Grill, W. M. and J. T. Mortimer (1996). "The effect of stimulus pulse duration on selectivity of neural stimulation." In: *IEEE transactions on bio-medical engineering* 43.2, pp. 161–6.
- Grimm, S., J. Beck, D. Schuepbach, D. Hell, P. Boesiger, F. Bormpohl, L. Niehaus, H. Boeker, and G. Northoff (2008). "Imbalance between Left and Right Dorsolateral Prefrontal Cortex in Major Depression Is Linked

- to Negative Emotional Judgment: An fMRI Study in Severe Major Depressive Disorder". In: *Biological Psychiatry* 63.4, pp. 369–376.
- Grossheinrich, N. et al. (2013). "Effects of Low Frequency Prefrontal Repetitive Transcranial Magnetic Stimulation on the N2 Amplitude in a GoNogo Task." In: *PloS one* 8.6, e67136.
- Guerra, A., V. López-Alonso, B. Cheeran, and A. Suppa (2018). "Variability in non-invasive brain stimulation studies: Reasons and results". In: *Neuroscience Letters*, pp. 0–1.
- Gusnard, D. A., E Akbudak, G. L. Shulman, and M. E. Raichle (2001). "Medial prefrontal cortex and self-referential mental activity: relation to a default mode of brain function." In: *Proceedings of the National Academy of Sciences* 98.7, pp. 4259–4264.
- Hagmann, P., L. Cammoun, X. Gigandet, R. Meuli, C. J. Honey, J. Van Welden, and O. Sporns (2008). "Mapping the structural core of human cerebral cortex". In: *PLoS Biology* 6.7, pp. 1479–1493.
- Hallet, M. (2000). "Transcranial magnetic stimulation and the human brain". In: *Nature* 406, pp. 147–150.
- Hallett, M. (2007). "Transcranial Magnetic Stimulation: A Primer". In: *Neuron* 55.2, pp. 187–199.
- Hallez, H. et al. (2007). "Review on solving the forward problem in EEG source analysis." In: *Journal of neuroengineering and rehabilitation* 4.4, p. 46. arXiv: 1501.04621.
- Hamada, M., R. Hanajima, Y. Terao, N. Arai, T. Furubayashi, S. Inomata-Terada, A. Yugeta, H. Matsumoto, Y. Shirota, and Y. Ugawa (2007). "Quadro-pulse stimulation is more effective than paired-pulse stimulation for plasticity induction of the human motor cortex." In: *Clinical neurophysiology* 118.12, pp. 2672–82.
- Hamani, C., M. Diwan, S. Isabella, A. M. Lozano, and J. N. Nobrega (2010). "Effects of different stimulation parameters on the antidepressant-like response of medial prefrontal cortex deep brain stimulation in rats." In: *Journal of Psychiatric Research* 44.11, pp. 683–687.
- Hamilton, M. (1967). "Development of a rating scale for primary depressive illness". In: *British journal of clinical psychology* 6.4, pp. 278–296.
- Hampel, K. G., H. Vatter, C. E. Elger, and R. Surges (2015). "Cardiac-based vagus nerve stimulation reduced seizure duration in a patient with refractory epilepsy". In: *Seizure* 26, pp. 81–85.
- Handforth, A et al. (1998). "Vagus nerve stimulation therapy for partial-onset seizures". In: *Neurology* 51.1, pp. 48–55.
- Handwerker, D. A., V. Roopchansingh, J. Gonzalez-Castillo, and P. A. Bandettini (2012). "Periodic changes in fMRI connectivity". In: *NeuroImage* 63.3, pp. 1712–1719.
- Hassan, A. and K. W. Al-Quliti (2014). "A promising therapeutic option for medically refractory epilepsy". In: *Neurosciences* 19.1, pp. 4–10.
- He, W., X. Jing, X. Wang, P. Rong, L. Li, H. Shi, H. Shang, Y. Wang, J. Zhang, and B. Zhu (2013). "Transcutaneous auricular vagus nerve stimulation as a complementary therapy for pediatric epilepsy: a pilot trial". In: *Epilepsy & behavior* 28.3, pp. 343–6.
- Heck, C., S. L. Helmers, and C. M. DeGiorgio (2002). "Vagus nerve stimulation therapy, epilepsy and device parameters". In: *Neurology* 59, S31–S37.
- Helmers, S. L. et al. (2012). "Application of a computational model of vagus nerve stimulation." In: *Acta neurologica Scandinavica* 126.5, pp. 336–43.
- Hemm, S., G. Mennessier, N. Vayssiere, L. Cif, H. El Fertit, and P. Coubes (2005). "Deep brain stimulation in movement disorders: stereotactic coregistration of two-dimensional electrical field modeling and magnetic resonance imaging". In: *Journal of Neurosurgery* 103, pp. 949–955.
- Herbsman, T., D. Avery, D. Ramsey, P. Holtzheimer, C. Wadjik, F. Hardaway, D. Haynor, M. S. George, and Z. Nahas (2009). "More Lateral and Anterior Prefrontal Coil Location Is Associated with Better Repetitive Transcranial Magnetic Stimulation Antidepressant Response". In: *Biological Psychiatry* 66.5, pp. 509–515.
- Herrmann, C. S., S. Rach, T. Neuling, and D. Strüber (2013). "Transcranial alternating current stimulation: a review of the underlying mechanisms and modulation of cognitive processes". In: *Frontiers in Human Neuroscience* 7, pp. 1–13.
- Herwig, U., P. Satrapi, and C. Schönfeldt-lecuona (2003). "Using the International 10-20 EEG System for Positioning of Transcranial Magnetic Stimulation Using the International 10-20 EEG System for Positioning of Transcranial Magnetic Stimulation". In: *Brain topography* 16.2, pp. 95–99.
- Herwig, U., F. Padberg, J. Unger, M. Spitzer, and C. Schönfeldt-Lecuona (2001). "Transcranial magnetic stimulation in therapy studies: Examination of the reliability of "standard" coil positioning by neuronavigation". In: *Biological Psychiatry* 50.1, pp. 58–61.
- Heuvel, M. P. van den and H. E. Hulshoff Pol (2010). "Exploring the brain network: A review on resting-state fMRI functional connectivity". In: *European Neuropsychopharmacology* 20.8, pp. 519–534. arXiv: 0811.3721.
- Hill, A. T., N. C. Rogasch, P. B. Fitzgerald, and K. E. Hoy (2016). "TMS-EEG: A window into the neurophysiological effects of transcranial electrical stimulation in non-motor brain regions". In: *Neuroscience and Biobehavioral Reviews* 64, pp. 175–184.
- Hoepfner, J., F. Padberg, G. Domes, A. Zinke, S. C. Herpertz, N. Groheinhart, and U. Herwig (2010). "Influence of repetitive transcranial magnetic stimulation on psychomotor symptoms in major depression". In: *European Archives of Psychiatry and Clinical Neuroscience* 260.3, pp. 197–202.

- Hofmann, L., M. Ebert, P. A. Tass, and C. Hauptmann (2011). "Modified pulse shapes for effective neural stimulation." In: *Frontiers in neuroengineering* 4, p. 9.
- Honey, C. J., O. Sporns, L. Cammoun, X. Gigandet, J. P. Thiran, R. Meuli, and P. Hagmann (2009). "Predicting human resting-state functional connectivity". In: *Proc Natl Acad Sci U S A* 106.6, pp. 2035–2040.
- Hoogendam, J. M., G. M. J. Ramakers, and V. Di Lazzaro (2010). "Physiology of repetitive transcranial magnetic stimulation of the human brain". In: *Brain Stimulation* 3.2, pp. 95–118.
- Hosseini, S. M. H., F. Hoefft, and S. R. Kesler (2012). "Gat: A graph-theoretical analysis toolbox for analyzing between-group differences in large-scale structural and functional brain networks". In: *PLoS ONE* 7.7, e40709 1–15.
- Houdayer, E., A. Degardin, F. Cassim, P. Bocquillon, P. Derambure, and H. Devanne (2008). "The effects of low- and high-frequency repetitive TMS on the input/output properties of the human corticospinal pathway." In: *Experimental brain research* 187.2, pp. 207–17.
- Huang, H., R. L. Watts, and E. B. Montgomery (2014). "Effects of deep brain stimulation frequency on bradykinesia of Parkinson's disease." In: *Movement disorders : official journal of the Movement Disorder Society* 29.2, pp. 203–6.
- Huang, Y. Z., M. J. Edwards, E. Rounis, K. P. Bhatia, and J. C. Rothwell (2005). "Theta burst stimulation of the human motor cortex". In: *Neuron* 45.2, pp. 201–206.
- Huerta, P. T. and J. E. Lisman (1995). "Bidirectional synaptic plasticity induced by a single burst during cholinergic theta oscillation in CA1 in vitro". In: *Neuron* 15.5, pp. 1053–1063.
- Huerta, P. T. and J. E. Usman (1993). "Heightened synaptic plasticity of hippocampal CA1 neurons during a cholinergically induced rhythmic state". In: *Nature* 364, pp. 723–725.
- Ilmoniemi, R. J. and D. Kicic (2010). "Methodology for combined TMS and EEG." In: *Brain topography* 22.4, pp. 233–48.
- Ilmoniemi, R. J., J. Virtanen, J. Ruohonen, J. Karhu, H. J. Aronen, R. Näätänen, and T. Katila (1997). "Neuronal responses to magnetic stimulation reveal cortical reactivity and connectivity." In: *NeuroReport* 8.16, pp. 3537–3540.
- Im, C.-H., H.-H. Jung, J.-D. Choi, S. Y. Lee, and K.-Y. Jung (2008). "Determination of optimal electrode positions for transcranial direct current stimulation (tDCS)." In: *Physics in medicine and biology* 53.11, N219–N225.
- Irfanoglu, M. O., L. Walker, J. Sarlls, S. Marengo, and C. Pierpaoli (2012). "Effects of image distortions originating from susceptibility variations and concomitant fields on diffusion MRI tractography results". In: *NeuroImage* 61.1, pp. 275–288. arXiv: NIHMS150003.
- Iseger, T. A., F. Padberg, J. L. Kenemans, R. Gevirtz, and M. Arns (2017). "Neuro-Cardiac-Guided TMS (NCG-TMS): Probing DLPFC-sgACC-vagus nerve connectivity using heart rate - First results". In: *Brain Stimulation* 10.5, pp. 1006–1008.
- Isenberg, K., D. Downs, K. Pierce, D. Svarakic, K. Garcia, M. Jarvis, C. North, and T. C. Kormos (2005). "Low Frequency rTMS Stimulation of the Right Frontal Cortex Is as Effective as High Frequency rTMS Stimulation of the Left Frontal Cortex for Antidepressant-Free, Treatment-Resistant Depressed Patients". In: *Annals of Clinical Psychiatry* 17.3, pp. 153–159.
- Iyer, M. B., N. Schleper, and E. M. Wassermann (2003). "Priming Stimulation Enhances the Depressant Effect of Low-Frequency Repetitive Transcranial Magnetic Stimulation". In: *Journal of neuroscience* 23.34, pp. 10867–10872.
- Jagannathan, J., N. T. Sanghvi, L. A. Crum, C. P. Yen, R. Medel, A. S. Dumont, J. P. Sheehan, L. Steiner, F. Jolesz, and N. F. Kassell (2009). "High-intensity focused ultrasound surgery of the brain: Part 1-A historical perspective with modern applications". In: *Neurosurgery* 64.2, pp. 201–210.
- Jannati, A., G. Block, L. M. Oberman, A. Rotenberg, and A. Pascual-Leone (2017). "Interindividual variability in response to continuous theta-burst stimulation in healthy adults". In: *Clinical Neurophysiology* 128.11, pp. 2268–2278.
- Janssen, A. M., T. F. Oostendorp, and D. F. Stegeman (2014). "The effect of local anatomy on the electric field induced by TMS: evaluation at 14 different target sites." In: *Medical & biological engineering & computing* 52.10, pp. 873–883.
- Jeurissen, B., A. Leemans, J. D. Tournier, D. K. Jones, and J. Sijbers (2013). "Investigating the prevalence of complex fiber configurations in white matter tissue with diffusion magnetic resonance imaging". In: *Human Brain Mapping* 34.11, pp. 2747–2766.
- Jeurissen, B., J. D. Tournier, T. Dhollander, A. Connelly, and J. Sijbers (2014). "Multi-tissue constrained spherical deconvolution for improved analysis of multi-shell diffusion MRI data". In: *NeuroImage* 103, pp. 411–426.
- Jin, Y., S. G. Potkin, A. S. Kemp, S. T. Huerta, G. Alva, T. M. Thai, D. Carreon, and W. E. Bunney (2006). "Therapeutic effects of individualized alpha frequency transcranial magnetic stimulation (alphaTMS) on the negative symptoms of schizophrenia." In: *Schizophrenia bulletin* 32.3, pp. 556–61.
- Johnson, K. A. et al. (2013). "Prefrontal rTMS for treating depression: Location and intensity results from the OPT-TMS multi-site clinical trial". In: *Brain Stimulation* 6.2, pp. 108–117.

- Johnstone, T., C. M. van Reekum, H. L. Urry, N. H. Kalin, and R. J. Davidson (2007). "Failure to Regulate: Counterproductive Recruitment of Top-Down Prefrontal-Subcortical Circuitry in Major Depression". In: *Journal of Neuroscience* 27.33, pp. 8877–8884.
- Jones, D. K. (2010). "Challenges and limitations of quantifying brain connectivity". In: *Imaging Med* 2.3, pp. 341–355.
- Jones, D. K., T. R. Knösche, and R. Turner (2013). "White matter integrity, fiber count, and other fallacies: The do's and don'ts of diffusion MRI". In: *NeuroImage* 73, pp. 239–254.
- Jones, D. K. and A. Leemans (2011). "Diffusion tensor imaging". In: *Methods in molecular biology* 711, pp. 127–144.
- Joo, E. Y., S. J. Han, S.-H. Chung, J.-W. Cho, D. W. Seo, and S. B. Hong (2007). "Antiepileptic effects of low-frequency repetitive transcranial magnetic stimulation by different stimulation durations and locations." In: *Clinical neurophysiology* 118.3, pp. 702–8.
- Julkunen, P., L. Säisänen, N. Danner, F. Awiszus, and M. Könönen (2012). "Within-subject effect of coil-to-cortex distance on cortical electric field threshold and motor evoked potentials in transcranial magnetic stimulation." In: *Journal of neuroscience methods* 206.2, pp. 158–164.
- Jung, N. H., I. Delyvendahl, A. Pechmann, B. Gleich, N. Gatteringer, H. R. Siebner, and V. Mall (2012). "Transcranial magnetic stimulation with a half-sine wave pulse elicits direction-specific effects in human motor cortex." In: *BMC neuroscience* 13.1, pp. 139–147.
- Kadosh, R. C. (2014). *The stimulated brain*. 1st. Academic Press, p. 568.
- Kähkönen, S., S. Komssi, J. Wilenius, and R. J. Ilmoniemi (2005). "Prefrontal TMS produces smaller EEG responses than motor-cortex TMS: Implications for rTMS treatment in depression". In: *Psychopharmacology* 181.1, pp. 16–20.
- Kaiser, M. and C. C. Hilgetag (2006). "Nonoptimal component placement, but short processing paths, due to long-distance projections in neural systems". In: *PLoS Computational Biology* 2.7, pp. 805–815. arXiv: 0607034 [q-bio].
- Kaneko, K., S. Kawai, Y. Fuchigami, H. Morita, and A. Ofuji (1996). "The effect of current direction induced by transcranial magnetic stimulation on the corticospinal excitability in human brain". In: *Electroencephalography and Clinical Neurophysiology/Neurophysiology and Motor Control* 101.6, pp. 478–482.
- Kang, J. I., H. Lee, K. Jhung, K. R. Kim, S. K. An, K. J. Yoon, S. I. Kim, K. Namkoong, and E. Lee (2016). "Frontostriatal connectivity changes in major depressive disorder after repetitive transcranial magnetic stimulation: A randomized Sham-Controlled study". In: *Journal of Clinical Psychiatry* 77.9, e1137–e1143.
- Kayser, S., B. H. Bewernick, C. Grubert, B. L. Hadrysiewicz, N. Axmacher, and T. E. Schlaepfer (2011). "Antidepressant effects of magnetic seizure therapy and electroconvulsive therapy, in treatment-resistant depression". In: *Journal of Psychiatric Research* 45.5, pp. 569–576.
- Kedzior, K. K., S. K. Reitz, V. Azorina, and C. Loo (2015). "Durability of the antidepressant effect of the high-frequency repetitive transcranial magnetic stimulation (rTMS) in the absence of maintenance treatment in major depression: A systematic review and meta-analysis of 16 double-blind, randomized, sham-controlled". In: *Depression and Anxiety* 32.3, pp. 193–203.
- Keller, C. J., S. Bickel, L. Entz, I. Ulbert, M. P. Milham, C. Kelly, and A. D. Mehta (2011). "Intrinsic functional architecture predicts electrically evoked responses in the human brain". In: *Proceedings of the National Academy of Sciences* 108.25, pp. 10308–10313.
- Keltner, N. L. and D. J. Boschini (2009). "Electroconvulsive therapy". In: *Perspectives of Psychiatric Care* 45.1, pp. 66–70.
- Kent, A. R. and W. M. Grill (2014). "Analysis of deep brain stimulation electrode characteristics for neural recording." In: *Journal of neural engineering* 11.4, p. 046010.
- Kerestes, R., B. J. Harrison, O. Dandash, K. Stephanou, S. Whittle, J. Pujol, and C. G. Davey (2015). "Specific functional connectivity alterations of the dorsal striatum in young people with depression". In: *NeuroImage: Clinical* 7, pp. 266–272.
- Kim, J.-H., D.-W. Kim, W. H. Chang, Y.-H. Kim, K. Kim, and C.-H. Im (2014). "Inconsistent outcomes of transcranial direct current stimulation may originate from anatomical differences among individuals: electric field simulation using individual MRI data." In: *Neuroscience letters* 564, pp. 6–10.
- King, R. L., J. R. Brown, W. T. Newsome, and K. B. Pauly (2013). "Effective parameters for ultrasound-induced in vivo neurostimulation." In: *Ultrasound in medicine & biology* 39.2, pp. 312–31.
- Kito, S., R. D. Pascual-Marqui, T. Hasegawa, and Y. Koga (2014). "High-frequency left prefrontal transcranial magnetic stimulation modulates resting EEG functional connectivity for gamma band between the left dorsolateral prefrontal cortex and precuneus in depression". In: *Brain Stimulation* 7.1, pp. 145–146.
- Klem, G. H., H. O. Lüders, H. Jasper, and C. Elger (1999). "The ten-twenty electrode system of the International Federation". In: *Journal of the Neurological Sciences*, pp. 3–6.
- Klomjai, W., R. Katz, and A. Lackmy-Vallée (2015). "Basic principles of transcranial magnetic stimulation (TMS) and repetitive TMS (rTMS)". In: *Annals of Physical and Rehabilitation Medicine* 58.4, pp. 208–213.
- Klooster, D. C. W. et al. (2016). "Technical aspects of neurostimulation: Focus on equipment, electric field modeling, and stimulation protocols". In: *Neuroscience and Biobehavioral Reviews* 65, pp. 113–141.

- Klooster, D. C., S. L. Franklin, R. M. Besseling, J. F. Jansen, K. Caeyenberghs, R. Duprat, A. P. Aldenkamp, A. J. de Louw, P. A. Boon, and C. Baeken (2019). "Focal application of accelerated iTBS results in global changes in graph measures". In: *Human Brain Mapping* 40.2, pp. 432–450.
- Knoch, D., V. Treyer, M. Regard, R. M. Müri, A. Buck, and B. Weber (2006). "Lateralized and frequency-dependent effects of prefrontal rTMS on regional cerebral blood flow." In: *NeuroImage* 31.2, pp. 641–8.
- Knoch, D., P. Brugger, and M. Regard (2005). "Suppressing versus releasing a habit: frequency-dependent effects of prefrontal transcranial magnetic stimulation." In: *Cerebral Cortex* 15.7, pp. 885–887.
- Kobayashi, M. and A. Pascual-leone (2003). "Transcranial magnetic stimulation in neurology". In: *Lancet neurology* 2, pp. 145–156.
- Koenigs, M., E. D. Huey, M. Calamia, V. Raymont, D. Tranel, and J. Grafman (2008). "Distinct Regions of Prefrontal Cortex Mediate Resistance and Vulnerability to Depression". In: *Journal of Neuroscience* 28.47, pp. 12341–12348.
- Koenigs, M. and J. Grafman (2009). "The functional neuroanatomy of depression: Distinct roles for ventromedial and dorsolateral prefrontal cortex". In: *Behavioural Brain Research* 201.2, pp. 239–243. arXiv: NIHMS150003.
- Koessler, L., C. Benar, L. Maillard, J. M. Badier, J. P. Vignal, F. Bartolomei, P. Chauvel, and M. Gavaret (2010). "Source localization of ictal epileptic activity investigated by high resolution EEG and validated by SEEG". In: *NeuroImage* 51.2, pp. 642–653.
- Koessler, L., S. Colnat-Coulbois, T. Cecchin, J. Hofmanis, J. P. Dmochowski, A. M. Norcia, and L. G. Maillard (2017). "In-vivo measurements of human brain tissue conductivity using focal electrical current injection through intracerebral multicontact electrodes". In: *Human Brain Mapping* 38.2, pp. 974–986.
- Komssi, S. and S. Kähkönen (2006). "The novelty value of the combined use of electroencephalography and transcranial magnetic stimulation for neuroscience research". In: *Brain Research Reviews* 52.1, pp. 183–192.
- Komssi, S., S. Kähkönen, and R. J. Ilmoniemi (2004). "The effect of stimulus intensity on brain responses evoked by transcranial magnetic stimulation." In: *Human brain mapping* 21.3, pp. 154–64.
- Koo, B. (2001). "EEG Changes With Vagus Nerve Stimulation". In: *Journal of Clinical Neurophysiology* 18.5, pp. 434–441.
- Korgaonkar, M. S., A. Fornito, L. M. Williams, and S. M. Grieve (2014). "Abnormal structural networks characterize major depressive disorder: A connectome analysis". In: *Biological Psychiatry* 76.7, pp. 567–574.
- Koshev, A. R., S. Siggelkow, R. Dengler, and J. D. Rollnik (2003). "Intracortical Inhibition and Facilitation in Paired-Pulse Transcranial Magnetic Stimulation: Effect of Conditioning Stimulus Intensity on Sizes and Latencies of Motor Evoked Potentials". In: *Journal of Clinical Neurophysiology* 20.1, pp. 54–58.
- Kothari, M., P. Svensson, J. F. Nielsen, and L. Baad-Hansen (2014). "Influence of position and stimulation parameters on intracortical inhibition and facilitation in human tongue motor cortex". In: *Brain Research* 1557, pp. 83–89.
- Kozel, F. A., Z. Nahas, C. DeBrux, M. Molloy, J. P. Lorberbaum, D. Bohning, S. C. Risch, and M. S. George (2000). "How coil-cortex distance relates to age, motor threshold, and antidepressant response to repetitive transcranial magnetic stimulation." In: *The Journal of neuropsychiatry and clinical neurosciences* 12, pp. 376–384.
- Kozel, F. A. et al. (2011). "Fractional anisotropy (FA) changes after several weeks of daily left high frequency rTMS of the left prefrontal cortex to treat major depression". In: *Journal ECT* 27.1, pp. 5–10. arXiv: NIHMS150003.
- Krahl, S. E., S. S. Senanayake, and A. Handforth (2001). "Destruction of peripheral C-fibers does not alter subsequent vagus nerve stimulation-induced seizure suppression in rats." In: *Epilepsia* 42.5, pp. 586–9.
- Krahl, S. E. and K. B. Clark (2012). "Vagus nerve stimulation for epilepsy: A review of central mechanisms." In: *Surgical neurology international* 3.Suppl 4, S255–9.
- Krames, E. S., P. Peckham, and A. R. Rezai (2009). *What is neuromodulation (In. Neuromodulation)*. first. Academic Press.
- Krishnan, C., L. Santos, M. D. Peterson, and M. Ehinger (2015). "Safety of Noninvasive Brain Stimulation in Children and Adolescents". In: *Brain Stimulation* 8.1, pp. 76–87.
- Kühn, A. A., N. Fogelson, P. D. Limousin, M. I. Hariz, A. Kupsch, and P. Brown (2009). "Frequency-specific effects of stimulation of the subthalamic area in treated Parkinson's disease patients." In: *Neuroreport* 20.11, pp. 975–8.
- Kujirai, T., M. Caramia, J. Rothwell, B. Day, P. Thompson, A. Ferbert, S. Wroe, P. Asselman, and C. Marsden (1993). "Corticocortical inhibition in human motor cortex". In: *Journal of Physiology* 471, pp. 501–519.
- Kuo, H.-I., M. Bikson, A. Datta, P. Minhas, W. Paulus, M.-F. Kuo, and M. A. Nitsche (2013). "Comparing Cortical Plasticity Induced by Conventional and High-Definition 4x1 Ring tDCS: A Neurophysiological Study". In: *Brain Stimulation* 6.4, pp. 644–648.
- Kupsch, A., S. Klaffke, A. A. Kühn, W. Meissner, G. Arnold, G. H. Schneider, K. Maier-Hauff, and T. Trottenberg (2003). "The effects of frequency in pallidal deep brain stimulation for primary dystonia." In: *Journal of neurology* 250.10, pp. 1201–5.
- Laakso, I. and A. Hirata (2012). "Fast multigrid-based computation of the induced electric field for transcranial magnetic stimulation." In: *Physics in medicine and biology* 57.23, pp. 7753–7765.

- Laakso, I., A. Hirata, and Y. Ugawa (2014). "Effects of coil orientation on the electric field induced by TMS over the hand motor area." In: *Physics in medicine and biology* 59.1, pp. 203–218. arXiv: 0402594v3 [arXiv:cond-mat].
- Labar, D. and A. Dean (2002). "Neurostimulation therapy for epilepsy". In: *Current neurology and neuroscience reports* 2.4, pp. 357–364.
- Lacerda, A. L. T., P. Brambilla, R. B. Sassi, M. A. Nicoletti, A. G. Mallinger, E. Frank, D. J. Kupfer, M. S. Keshavan, and J. C. Soares (2005). "Anatomical MRI study of corpus callosum in unipolar depression". In: *Journal of Psychiatric Research* 39.4, pp. 347–354.
- Lai, H.-Y., L.-D. Liao, C.-T. Lin, J.-H. Hsu, X. He, Y.-Y. Chen, J.-Y. Chang, H.-F. Chen, S. Tsang, and Y.-Y. I. Shih (2012). "Design, simulation and experimental validation of a novel flexible neural probe for deep brain stimulation and multichannel recording." In: *Journal of neural engineering* 9, pp. 1–15.
- LaLumiere, R. T. (2011). "A new technique for controlling the brain: Optogenetics and its potential for use in research and the clinic". In: *Brain Stimulation* 4.1, pp. 1–6.
- Lang, N., J. Harms, T. Weyh, R. N. Lemon, W. Paulus, J. C. Rothwell, and H. R. Siebner (2006). "Stimulus intensity and coil characteristics influence the efficacy of rTMS to suppress cortical excitability." In: *Clinical neurophysiology : official journal of the International Federation of Clinical Neurophysiology* 117.10, pp. 2292–301.
- Langguth, B., R. Wiegand, A. Kharraz, M. Landgrebe, J. Marienhagen, U. Frick, G. Hajak, and P. Eichhammer (2007). "Pre-treatment anterior cingulate activity as a predictor of antidepressant response to repetitive transcranial magnetic stimulation (rTMS)." In: *Neuro Endocrinology Letters* 28.5, pp. 633–638.
- Langguth, B., T. Kleinjung, E. Frank, M. Landgrebe, P. Sand, J. Dvorakova, U. Frick, P. Eichhammer, and G. Hajak (2008). "High-frequency priming stimulation does not enhance the effect of low-frequency rTMS in the treatment of tinnitus." In: *Experimental brain research* 184.4, pp. 587–91.
- Le Bihan, D. (2006). "Looking into the functional architecture of the brain with diffusion MRI". In: *International Congress Series* 1290, pp. 1–24.
- Le Bihan, D., J. F. Mangin, C. Poupon, C. A. Clark, S. Pappata, N. Molko, and H. Chabriat (2001). "Diffusion tensor imaging: concepts and applications." In: *Journal of magnetic resonance imaging : JMRI* 13.4, pp. 534–546.
- Le Bihann, D. (2013). "Apparent Diffusion Coefficient and Beyond: What Diffusion MR Imaging Can Tell Us about Tissue Structure". In: *Radiology* 268.2, pp. 318–322.
- Leemans, A. and D. K. Jones (2009). "The B-matrix must be rotated when correcting for subject motion in DTI data". In: *Magnetic Resonance in Medicine* 61.6, pp. 1336–1349.
- Leemans, A., B. Jeurissen, J. Sijbers, and D. Jones (2009). "ExploreDTI: a graphical toolbox for processing, analyzing, and visualizing diffusion MR data". In: *Proceedings 17th Scientific Meeting, International Society for Magnetic Resonance in Medicine* 17.2, p. 3537.
- Lefaucheur, J. P., X. Drouot, I. Ménard-Lefaucheur, Y. Keravel, and J. P. Nguyen (2006). "Motor cortex rTMS restores defective intracortical inhibition in chronic neuropathic pain". In: *Neurology* 67.9, pp. 1568–1574.
- Lefaucheur, J.-P. et al. (2014). "Evidence-based guidelines on the therapeutic use of repetitive transcranial magnetic stimulation (rTMS)." In: *Clinical Neurophysiology* 125, pp. 1–57.
- Li, C. T. et al. (2014). "Efficacy of prefrontal theta-burst stimulation in refractory depression: A randomized sham-controlled study". In: *Brain* 137.7, pp. 2088–2098.
- Li, W., B. D. Ward, X. Liu, G. Chen, J. L. Jones, P. G. Antuono, S.-J. Li, and J. S. Goveas (2015). "Disrupted Small World Topology and Modular Organization of Functional Networks in Late Life Depression with and without Amnesic Mild Cognitive Impairment". In: *Journal of neurosurgery and psychiatry* 86.10, pp. 1097–1105.
- Lim, H. K., W. S. Jung, and H. J. Aizenstein (2013). "Aberrant topographical organization in gray matter structural network in late life depression: a graph theoretical analysis". In: *Int Psychogeriatr* 25.12, pp. 1929–1940.
- Lin, C.-Y., K. Li, L. Franic, J. Gonzalez-Martinez, V. W. Lin, I. Najm, and Y.-S. Lee (2014). "Frequency-dependent effects of contralateral repetitive transcranial magnetic stimulation on penicillin-induced seizures." In: *Brain research* 1581, pp. 103–16.
- Lioumis, P., D. Kičić, P. Savolainen, J. P. Mäkelä, and S. Kähkönen (2009). "Reproducibility of TMS - Evoked EEG responses". In: *Human Brain Mapping* 30.4, pp. 1387–1396.
- Lipton, R. B. and S. H. Pearlman (2010). "Transcranial Magnetic Stimulation in the Treatment of Migraine". In: *Neurotherapeutics* 7.April, pp. 204–212.
- Liston, C., A. C. Chen, B. D. Zebley, A. T. Drysdale, R. Gordon, B. Leuchter, H. U. Voss, B. J. Casey, A. Etkin, and M. J. Dubin (2014). "Default mode network mechanisms of transcranial magnetic stimulation in depression". In: *Biological Psychiatry* 76.7, pp. 517–526.
- Liu, C., X. W. Wen, Y. Ge, N. Chen, W. H. Hu, T. Zhang, J. G. Zhang, and F. G. Meng (2013). "Responsive neurostimulation for the treatment of medically intractable epilepsy". In: *Brain Research Bulletin* 97.6, pp. 39–47.
- Liu, L. D., I. A. Prescott, J. O. Dostrovsky, M. Hodaie, A. M. Lozano, and W. D. Hutchison (2012). "Frequency-dependent effects of electrical stimulation in the globus pallidus of dystonia patients." In: *Journal of neurophysiology* 108.1, pp. 5–17.

- Liu, T. T. (2017). "Noise contributions to the fMRI signal: An Overview". In: *NeuroImage* 154, pp. 4–14.
- Liu, Z., T. Yin, and X. Guan (2003). "A project of magnetic coils newly designed to restrain the negative value of the intensity of magnetic induced electric field". In: *Journal of biomedical engineering*.
- Loddenkemper, T., A. Pan, S. Neme, K. B. Baker, A. R. Rezai, D. S. Dinner, E. B. Montgomery, and H. O. Luders (2001). "Deep brain stimulation in epilepsy". In: *Journal of Clinical neurophysiology* 18.6, pp. 514–532.
- Lomarev, M., S. Denslow, Z. Nahas, J.-H. Chae, M. S. George, and D. E. Bohning (2002). "Vagus nerve stimulation (VNS) synchronized BOLD fMRI suggests that VNS in depressed adults has frequency/dose dependent effects". In: *Journal of Psychiatric Research* 36.4, pp. 219–227.
- Loo, C., P. Sachdev, W. Hairndl, W. Wen, P. Mitchell, V. Croker, and G. Malhi (2003). "High (15 Hz) and low (1 Hz) frequency transcranial magnetic stimulation have different acute effects on regional cerebral blood flow in depressed patients". In: *Psychological Medicine* 33.6, pp. 997–1006.
- Loo, C. K., T. F. McFarquhar, and P. B. Mitchell (2008). "A review of the safety of repetitive transcranial magnetic stimulation as a clinical treatment for depression." In: *The international journal of neuropsychopharmacology* 11, pp. 131–147.
- Loo, C. K. and P. B. Mitchell (2005). "A review of the efficacy of transcranial magnetic stimulation (TMS) treatment for depression, and current and future strategies to optimize efficacy". In: *Journal of Affective Disorders* 88.3, pp. 255–267.
- López-Alonso, V., B. Cheeran, D. Ríó-Rodríguez, and M. Fernández-Del-Olmo (2014). "Inter-individual variability in response to non-invasive brain stimulation paradigms". In: *Brain Stimulation* 7.3, pp. 372–380.
- Lozano, A. M., H. S. Mayberg, P. Giacobbe, C. Hamani, R. C. Craddock, and S. H. Kennedy (2008). "Subcallosal Cingulate Gyrus Deep Brain Stimulation for Treatment-Resistant Depression". In: *Biological Psychiatry* 64.6, pp. 461–467.
- Luber, B. L., H. Kinnunen, B. C. Rakitin, R. Ellsasser, Y. Stern, and S. H. Lisanby (2007). "Facilitation of performance in a working memory task with rTMS stimulation of the precuneus: frequency- and time-dependent effects." In: *Brain research* 1128.1, pp. 120–9.
- Luber, B. M., S. Davis, E. Bernhardt, A. Neacsu, L. Kwapil, S. H. Lisanby, and T. J. Strauman (2017). "Using neuroimaging to individualize TMS treatment for depression: Toward a new paradigm for imaging-guided intervention". In: *NeuroImage* 148, pp. 1–7.
- Mak, E., S. J. Colloby, A. Thomas, and J. T. O'Brien (2016). "The segregated connectome of late-life depression: a combined cortical thickness and structural covariance analysis". In: *Neurobiology of Aging* 48, pp. 212–221.
- Mallet, L., M. Polosan, and N. Jaafari (2008). "Subthalamic nucleus stimulation in severe obsessive-compulsive disorder". In: *The new England Journal of Medicine* 359, pp. 2121–2134.
- Mansouri, F., P. Fettes, L. Schulze, P. Giacobbe, J. Zariffa, and J. Downar (2018). "A Real-Time Phase-Locking System for Non-invasive Brain Stimulation". In: *Frontiers in Neuroscience* 12, p. 877.
- Martens, H. C. F., E. Toader, M. M. J. Décré, D. J. Anderson, R. Vetter, D. R. Kipke, K. B. Baker, M. D. Johnson, and J. L. Vitek (2011). "Spatial steering of deep brain stimulation volumes using a novel lead design." In: *Clinical neurophysiology* 122.3, pp. 558–66.
- Martin, D. M., R. Liu, A. Alonzo, M. Green, and C. K. Loo (2014). "Use of transcranial direct current stimulation (tDCS) to enhance cognitive training: effect of timing of stimulation." In: *Experimental brain research* 232.10, pp. 3345–51.
- Mayberg, H. S. H. (2003). "Modulating dysfunctional limbic-cortical circuits in depression: Towards development of brain-based algorithms for diagnosis and optimised treatment". In: *British Medical Bulletin* 65, pp. 193–207.
- McDonald, W. M. et al. (2011). "Improving the antidepressant efficacy of transcranial magnetic stimulation: Maximizing the number of stimulations and treatment location in treatment resistant depression". In: *Depression and anxiety* 28.11, pp. 973–980.
- McGough, J. J., S. K. Loo, A. Sturm, J. Cowen, A. F. Leuchter, and I. A. Cook (2015). "Brain Stimulation An Eight-week , Open-trial , Pilot Feasibility Study of Trigeminal Nerve Stimulation in Youth With Attention-deficit / Hyperactivity Disorder". In: *Brain Stimulation* 8.2, pp. 299–304.
- McIntyre, C. C. and P. J. Hahn (2010). "Network perspectives on the mechanisms of deep brain stimulation". In: *Neurobiology of Disease* 38.3, pp. 329–337.
- McIntyre, C. C., W. M. Grill, D. L. Sherman, and N. V. Thakor (2004a). "Cellular effects of deep brain stimulation: model-based analysis of activation and inhibition." In: *Journal of neurophysiology* 91.4, pp. 1457–69.
- McIntyre, C. C., S. Mori, D. L. Sherman, N. V. Thakor, and J. L. Vitek (2004b). "Electric field and stimulating influence generated by deep brain stimulation of the subthalamic nucleus." In: *Clinical neurophysiology* 115.3, pp. 589–95.
- McIntyre, C. C., M. Savasta, L. Kerkerian-Le Goff, and J. L. Vitek (2004c). "Uncovering the mechanism(s) of action of deep brain stimulation: activation, inhibition, or both." In: *Clinical neurophysiology* 115.6, pp. 1239–48.
- Medtronic (1998). *Medtronic implant manual (DBS 3387-3389)*. Tech. rep.

- Meister, R., A. Jansen, M. Härter, Y. Nestoriuc, and L. Kriston (2017). "Placebo and nocebo reactions in randomized trials of pharmacological treatments for persistent depressive disorder. A meta-regression analysis". In: *Journal of Affective Disorders* 215, pp. 288–298.
- Metwally, M. K., Y. S. Cho, H.-J. Park, and T.-S. Kim (2012). "Investigation of the electric field components of tDCS via anisotropically conductive gyri-specific finite element head models." In: *Annual International Conference of the IEEE Engineering in Medicine and Biology Society. IEEE Engineering in Medicine and Biology Society. Annual Conference*, pp. 5514–5517.
- Michel, C. M. and D. Brunet (2019). "EEG source imaging: A practical review of the analysis steps". In: *Frontiers in Neurology* 10.325, pp. 1–18.
- Michel, C. M., M. M. Murray, G. G. Lantz, S. Gonzalez, L. Spinelli, and R. Grave De Peralta (2004). "EEG source imaging". In: *Clinical Neurophysiology* 115.10, pp. 2195–2222. arXiv: arXiv:1011.1669v3.
- Mills, K. R., S. J. Boniface, and M. Schubert (1992). "Magnetic brain stimulation with a double coil: the importance of coil orientation". In: *Electroencephalography and clinical neurophysiology* 85, pp. 17–21.
- Miocinovic, S., S. F. Lempka, G. S. Russo, C. B. Maks, C. R. Butson, K. E. Sakaie, J. L. Vitek, and C. C. McIntyre (2009). "Experimental and theoretical characterization of the voltage distribution generated by deep brain stimulation." In: *Experimental neurology* 216.1, pp. 166–76.
- Mir-Moghtadaei, A., R. Caballero, P. Fried, M. D. Fox, K. Lee, P. Giacobbe, Z. J. Daskalakis, D. M. Blumberger, and J. Downar (2015). "Concordance between BeamF3 and MRI-neuronavigated target sites for repetitive transcranial magnetic stimulation of the left dorsolateral prefrontal cortex". In: *Brain Stimulation* 8.5, pp. 965–973.
- Miranda, P. C., M. Hallett, and P. J. Basser (2003). "The electric field induced in the brain by magnetic stimulation: a 3-D finite-element analysis of the effect of tissue heterogeneity and anisotropy." In: *IEEE transactions on bio-medical engineering* 50.9, pp. 1074–1085.
- Mitchell, D. J., N. McNaughton, D. Flanagan, and I. J. Kirk (2008). "Frontal-midline theta from the perspective of hippocampal theta". In: *Progress in neurobiology* 86, pp. 156–185.
- Mochizuki, H., M. Franca, Y.-Z. Huang, and J. C. Rothwell (2005). "The role of dorsal premotor area in reaction task: comparing the "virtual lesion" effect of paired pulse or theta burst transcranial magnetic stimulation." In: *Experimental brain research* 167.3, pp. 414–21.
- Modolo, J., A. Beuter, A. W. Thomas, and A. Legros (Jan. 2012). "Using "smart stimulators" to treat Parkinson's disease: re-engineering neurostimulation devices." In: *Frontiers in computational neuroscience* 6.September, p. 69.
- Moliadze, V., A. Antal, and W. Paulus (2010). "Electrode-distance dependent after-effects of transcranial direct and random noise stimulation with extracephalic reference electrodes". In: *Clinical Neurophysiology* 121.12, pp. 2165–2171.
- Mollet, L., a Grimonprez, R Raedt, J Delbeke, R El Tahry, V De Herdt, a Meurs, W Wadman, P Boon, and K Vonck (Dec. 2013). "Intensity-dependent modulatory effects of vagus nerve stimulation on cortical excitability." In: *Acta neurologica Scandinavica* 128.6, pp. 391–6.
- Monte-Silva, K., M. F. Kuo, S. Hessesenthaler, S. Fresnoza, D. Liebetanz, W. Paulus, and M. A. Nitsche (2013). "Induction of late LTP-like plasticity in the human motor cortex by repeated non-invasive brain stimulation". In: *Brain Stimulation* 6.3, pp. 424–432.
- Moreau, C., L. Defebvre, A. Destee, S. Bleuse, F. Clement, J. Blatt, P. Krystkowiak, and D. Devos (2008). "STN-DBS frequency effects on freezing of gait in advanced Parkinson disease". In: *Neurology* 71.2, pp. 80–84.
- Mori (2014a). "Basics of Diffusion Measurements by MRI". In: *Introduction to Diffusion Tensor Imaging*, pp. 1–9.
- Mori, S (2014b). "Principle of diffusion tensor imaging". In: *Introduction to Diffusion Tensor Imaging*, pp. 33–40.
- Mori, S. (2014c). "Mathematics of diffusion tensor imaging". In: *Introduction to Diffusion Tensor Imaging*, pp. 41–47.
- Mori, S. and D. Tournier (2013). "Moving Beyond DTI: High Angular Resolution Diffusion Imaging (HARDI)". In: *Introduction to Diffusion Tensor Imaging*, pp. 65–78.
- Morrell, M. (2006). "Brain stimulation for epilepsy: can scheduled or responsive neurostimulation stop seizures?" In: *Current opinion in neurology* 19.2, pp. 164–168.
- Moseley, B. D. and C. M. DeGiorgio (2014). "Refractory status epilepticus treated with trigeminal nerve stimulation". In: *Epilepsy research* 108.3, pp. 600–3.
- Mosher, J. C., R. M. Leahy, and P. S. Lewis (1999). "EEG and MEG: Forward solutions for inverse methods". In: *IEEE Transactions on Biomedical Engineering* 46.3, pp. 245–259.
- Mothersill, O. and G. Donohoe (2016). "Neural effects of social environmental stress- an activation likelihood estimation meta-analysis". In: *Psychological Medicine* 46.10, pp. 2015–2023. arXiv: arXiv:1011.1669v3.
- Mu, Q. et al. (2004). "Acute vagus nerve stimulation using different pulse widths produces varying brain effects." In: *Biological psychiatry* 55.8, pp. 816–25.
- Mulders, P. C., P. F. van Eijndhoven, A. H. Schene, C. F. Beckmann, and I. Tendolkar (2015). "Resting-state functional connectivity in major depressive disorder: A review". In: *Neuroscience & Biobehavioral Reviews* 56, pp. 330–344.

- Murakami, T., F. Müller-Dahlhaus, M.-K. Lu, and U. Ziemann (2012). "Homeostatic metaplasticity of corticospinal excitatory and intracortical inhibitory neural circuits in human motor cortex." In: *The Journal of physiology* 590.22, pp. 5765–5781.
- Murd, C., A. Einberg, and T. Bachmann (2012). "Repetitive TMS over V5/MT shortens the duration of spatially localized motion aftereffect: the effects of pulse intensity and stimulation hemisphere." In: *Vision research* 68, pp. 59–64.
- Murphy, M. L. and T. Frodl (2011). "Meta-analysis of diffusion tensor imaging studies shows altered fractional anisotropy occurring in distinct brain areas in association with depression". In: *Biology of Mood & Anxiety Disorders* 1.1, pp. 1–12.
- Mutanen, T., H. Mäki, and R. J. Ilmoniemi (2013). "The effect of stimulus parameters on TMS-EEG muscle artifacts." In: *Brain stimulation* 6.3, pp. 371–6.
- Mylius, V. et al. (2013). "Definition of DLPFC and M1 according to anatomical landmarks for navigated brain stimulation: Inter-rater reliability, accuracy, and influence of gender and age". In: *NeuroImage* 78, pp. 224–232.
- Nahas, Z. et al. (2001a). "Brain Effects of TMS Delivered Over Prefrontal Cortex in Depressed Adults: Role of Stimulation Frequency and Coil-Cortex Distance". In: *Journal of neuropsychiatry Clin. Neurosci.* 13.4, pp. 459–470.
- Nahas, Z. et al. (2001b). "Unilateral left prefrontal transcranial magnetic stimulation (TMS) produces intensity-dependent bilateral effects as measured by interleaved BOLD fMRI". In: *Biological Psychiatry* 50.9, pp. 712–720.
- Nahas, Z., F. A. Kozel, X. Li, B. Anderson, and M. S. George (2003). "Left prefrontal transcranial magnetic stimulation (TMS) treatment of depression in bipolar affective disorder: A pilot study of acute safety and efficacy". In: *Bipolar Disorders* 5.1, pp. 40–47.
- Narushima, K., L. M. McCormick, T. Yamada, R. W. Thatcher, D Ph, and R. G. Robinson (2010). "Subgenual cingulate theta activity predicts treatment response of repetitive transcranial magnetic stimulation in participants with vascular depression". In: *Journal of neuropsychiatry Clin. Neurosci.* 22.1, pp. 75–84.
- Neuropace (2013). *RNS ® System User Manual*. Tech. rep., pp. 1–91.
- Newman, M. E. J. (2004). "Fast algorithm for detecting community structure in networks". In: *Physical review E* 69.6, p. 66133. arXiv: 0309508v1 [arXiv:cond-mat].
- Niehaus, L, B Meyer, and T Weyh (2000). "Influence of pulse configuration and direction of coil current on excitatory effects of magnetic motor cortex and nerve stimulation". In: *Clinical neurophysiology* 111, pp. 75–80.
- Nikouline, V., J. Ruohonen, and R. J. Ilmoniemi (1999). "The role of the coil click in TMS assessed with simultaneous EEG". In: *Clinical Neurophysiology* 110.8, pp. 1325–1328.
- Ning, L., J. A. Camprodon, N. Makris, and Y. Rathi (2017). "Is resting-state fMRI guided brain target localization for TMS reliable and reproducible?" In: *International Society of Magnetic Resonance in Medicine*, p. 1683.
- Ning, L., N. Makris, J. A. Camprodon, and Y. Rathi (2019). "Limits and reproducibility of resting-state functional MRI definition of DLPFC targets for neuromodulation". In: *Brain Stimulation* 12.1, pp. 129–138.
- Nitsche, M. and S Doemkes (2007). "Shaping the effects of transcranial direct current stimulation of the human motor cortex". In: *Journal of neurophysiol* 97, pp. 3109–3117.
- Nitsche, M. A. et al. (2008). "Transcranial direct current stimulation: State of the art 2008". In: *Brain Stimulation* 1.3, pp. 206–223.
- Noachtar, S. and J. Rémi (2009). "The role of EEG in epilepsy: A critical review". In: *Epilepsy and Behavior* 15.1, pp. 22–33.
- Nojima, K, Y Katayama, and K Iramina (2013). "Predicting rTMS effect for deciding stimulation parameters." In: *Annual International Conference of the IEEE Engineering in Medicine and Biology Society*. Vol. 2013, pp. 6369–72.
- Nummenmaa, A., J. A. McNab, P. Savadjiev, Y. Okada, M. S. Hamalainen, R. Wang, L. L. Wald, A. Pascual-Leone, V. J. Wedeen, and T. Raji (2014). "Targeting of White Matter Tracts With Transcranial Magnetic Stimulation". In: *Brain Stimulation* 7.1, pp. 80–84.
- Oberman, L, D Edwards, M Eldaief, and A Pascual-Leone (2011). "Safety of theta burst transcranial magnetic stimulation: a systematic review of the literature". In: *Journal of Clinical Neurophysiology* 28.1, pp. 67–74.
- Ogiue-Ikeda, M., S. Kawato, and S. Ueno (2003). "The effect of repetitive transcranial magnetic stimulation on long-term potentiation in rat hippocampus depends on stimulus intensity". In: *Brain Research* 993.1-2, pp. 222–226.
- Okun, M. S. and G. Oyama (2013). "Mechanism of action for deep brain stimulation and electrical neuro-network modulation (ENM)". In: *Societas Neurologica Japonica* 53, pp. 691–694.
- Opitz, A., M. Windhoff, R. M. Heidemann, R. Turner, and A. Thielscher (2011). "How the brain tissue shapes the electric field induced by transcranial magnetic stimulation". In: *NeuroImage* 58.3, pp. 849–859.
- Opitz, A., W. Legon, A. Rowlands, W. K. Bickel, W. Paulus, and W. J. Tyler (2013). "Physiological observations validate finite element models for estimating subject-specific electric field distributions induced by transcranial magnetic stimulation of the human motor cortex". In: *NeuroImage* 81, pp. 253–364.

- Opitz, A., M. D. Fox, R. C. Craddock, S. Colcombe, and M. P. Milham (2015a). "An integrated framework for targeting functional networks via transcranial magnetic stimulation." In: *NeuroImage* 190, pp. 443–449.
- Opitz, A., W. Paulus, A. Will, and A. Thielscher (2015b). "Anatomical determinants of the electric field during transcranial direct current stimulation". In: *NeuroImage* 109, p. 2.
- Opitz, A., M. D. Fox, R. C. Craddock, S. Colcombe, and M. P. Milham (2016). "An integrated framework for targeting functional networks via transcranial magnetic stimulation". In: *NeuroImage* 127, pp. 86–96.
- Opitz, A., A. Falchier, G. S. Linn, M. P. Milham, and C. E. Schroeder (2017). "Limitations of ex vivo measurements for in vivo neuroscience". In: *Proceedings of the National Academy of Sciences* 114.20, pp. 5243–5246.
- O'Reardon, J. P. et al. (2007). "Efficacy and Safety of Transcranial Magnetic Stimulation in the Acute Treatment of Major Depression: A Multisite Randomized Controlled Trial". In: *Biological Psychiatry* 62.11, pp. 1208–1216.
- Ostrem, J. L. and P. A. Starr (2008). "Treatment of Dystonia with Deep Brain Stimulation". In: *Neurotherapeutics* 5, pp. 320–330.
- Ostrem, J. L., L. C. Markun, G. A. Glass, C. A. Racine, M. M. Volz, S. L. Heath, C. de Hemptinne, and P. A. Starr (2014). "Effect of frequency on subthalamic nucleus deep brain stimulation in primary dystonia." In: *Parkinsonism & related disorders* 20.4, pp. 432–8.
- Padberg, F. and M. S. George (2009). "Repetitive transcranial magnetic stimulation of the prefrontal cortex in depression". In: *Experimental Neurology* 219.1, pp. 2–13.
- Padberg, F. et al. (2002). "Repetitive transcranial magnetic stimulation (rTMS) in major depression: Relation between efficacy and stimulation intensity". In: *Neuropsychopharmacology* 27.4, pp. 638–645.
- Paek, S. B., H.-K. K. Min, I. Kim, E. J. Knight, J. J. Baek, A. J. Bieber, K. H. Lee, and S.-Y. Y. Chang (2015). "Frequency-dependent functional neuromodulatory effects on the motor network by ventral lateral thalamic deep brain stimulation in swine". In: *NeuroImage* 105, pp. 181–188.
- Pagnin, D., V. de Queiroz, S. Pini, and G. B. Cassano (2004). "Efficacy of ECT in depression: a meta-analytic review." In: *The journal of ECT* 20.1, pp. 13–20.
- Parazzini, M., S. Fiocchi, and P. Ravazzani (2012). "Electric field and current density distribution in an anatomical head model during transcranial direct current stimulation for tinnitus treatment." In: *Bioelectromagnetics* 33.6, pp. 476–487.
- Parazzini, M., S. Fiocchi, E. Rossi, A. Paglialonga, and P. Ravazzani (June 2011). "Transcranial direct current stimulation: estimation of the electric field and of the current density in an anatomical human head model." In: *IEEE transactions on bio-medical engineering* 58.6, pp. 1773–1780.
- Parazzini, M., E. Rossi, R. Ferrucci, I. Lioni, A. Priori, and P. Ravazzani (2014). "Modelling the electric field and the current density generated by cerebellar transcranial DC stimulation in humans." In: *Clinical neurophysiology* 125.3, pp. 577–584.
- Parittotokkaporn, T., D. G. T. Thomas, A. Schneider, E. Huq, B. L. Davies, P. Degenaar, and F. Rodriguez y Baena (2012). "Microtextured surfaces for deep-brain stimulation electrodes: a biologically inspired design to reduce lead migration." In: *World neurosurgery* 77.3-4, pp. 569–76.
- Park, C.-h., W. H. Chang, W.-K. Yoo, Y.-I. Shin, S. T. Kim, and Y.-H. Kim (2014). "Brain topological correlates of motor performance changes after repetitive transcranial magnetic stimulation." In: *Brain connectivity* 4.4, pp. 265–272.
- Pascual-Leone, A., N. Davey, and E. Wasserman (2001). "History and basic principles of magnetic nerve stimulation". In: *Handbook of transcranial magnetic stimulation*, pp. 6–9.
- Pascual-Leone, A., B. Rubio, F. Pallardó, and M. D. Catalá (1996). "Rapid-rate transcranial magnetic stimulation of left dorsolateral prefrontal cortex in drug-resistant depression". In: *The Lancet* 348.9022, pp. 233–237.
- Pascual-Leone, A., N. J. Davey, J. Rothwell, E. M. Wassermann, B. K. Puri, E. Wasserman, and B. K. Puri (2002). *Handbook of Transcranial Magnetic Stimulation*, pp. 3–38.
- Pastrana, E. (2011). "Optogenetics: controlling cell function with light". In: *Nature Methods* 8.1, pp. 24–25.
- Paulus, W. (2011). "Transcranial electrical stimulation (tES-tDCS; tRNS, tACS) methods". In: *Neuropsychological Rehabilitation* 21.5, pp. 602–617.
- Pedoto, G., S. Santaniello, G. Fiengo, L. Glielmo, M. Hallet, P. Zhuang, and S. V. Sarma (2012). "Point process modeling reveals anatomical non-uniform distribution across the subthalamic nucleus in parkinson's disease". In: *IEEE Engineering Medical Biology Society*, pp. 1–11.
- Pedrosa, D. J., M. Auth, C. Eggers, and L. Timmermann (2013). "Effects of low-frequency thalamic deep brain stimulation in essential tremor patients." In: *Experimental neurology* 248, pp. 205–12.
- Peleman, K., P. Van Schuerbeek, R. Luypaert, T. Stadnik, R. De Raedt, J. De Mey, A. Bossuyt, and C. Baeken (2010). "Using 3D-MRI to localize the dorsolateral prefrontal cortex in TMS research". In: *The world journal of biological psychiatry* 11.2, pp. 425–430.
- Pell, G. S., Y. Roth, and A. Zangen (2011). "Modulation of cortical excitability induced by repetitive transcranial magnetic stimulation: influence of timing and geometrical parameters and underlying mechanisms." In: *Progress in neurobiology* 93.1, pp. 59–98.

- Pereira, E. A. C., A. L. Green, R. J. Stacey, and T. Z. Aziz (2012). "Refractory epilepsy and deep brain stimulation." In: *Journal of clinical neuroscience* 19.1, pp. 27–33.
- Perera, T., M. George, G. Grammer, P. Janicak, A. Pascual-leone, and T. Wirecki (2016). "TMS Therapy For Major Depressive Disorder : Evidence Review and Treatment Recommendations for Clinical Practice". In: *Brain Stimulation*.
- Perlman, G. et al. (2012). "Amygdala response and functional connectivity during emotion regulation: A study of 14 depressed adolescents". In: *Journal of affective* 139.1, pp. 75–84.
- Peterchev, A. V., T. A. Wagner, P. C. Miranda, M. A. Nitsche, W. Paulus, S. H. Lisanby, A. Pascual-Leone, and M. Bikson (2012). "Fundamentals of transcranial electric and magnetic stimulation dose: Definition, selection, and reporting practices". In: *Brain Stimulation* 5.4, pp. 435–453.
- Phibbs, F. T., P. G. Arbogast, and T. L. Davis (2013). "60-Hz Frequency Effect on Gait in Parkinson's Disease With Subthalamic Nucleus Deep Brain Stimulation." In: *Neuromodulation* 2013, pp. 1–4.
- Philip, N. S., J. Barredo, M. van 't Wout-Frank, A. R. Tyrka, L. H. Price, and L. L. Carpenter (2017). "Network Mechanisms of Clinical Response to Transcranial Magnetic Stimulation in Posttraumatic Stress Disorder and Major Depressive Disorder". In: *Biological Psychiatry* 21, pp. 1–10.
- Plummer, C., A. S. Harvey, and M. Cook (2008). "EEG source localization in focal epilepsy: Where are we now?" In: *Epilepsia* 49.2, pp. 201–218.
- Polanía, R., W. Paulus, A. Antal, and M. A. Nitsche (2011). "Introducing graph theory to track for neuroplastic alterations in the resting human brain: A transcranial direct current stimulation study". In: *NeuroImage* 54.3, pp. 2287–2296.
- Polson, M., A. Barker, and I. Freeston (1982). "Stimulation of nerve trunks with time-varying magnetic fields". In: *Medical & biological engineering & computing*, pp. 243–244.
- Pommier, B., F. Vassal, C. Boutet, S. Jeannin, R. Peyron, and I. Faillenot (2017). "Easy methods to make the neuronavigated targeting of DLPFC accurate and routinely accessible for rTMS". In: *Neurophysiologie Clinique* 47.1, pp. 35–46.
- Pop, J., D. Murray, D. Markovic, and C. M. DeGiorgio (2011). "Acute and long-term safety of external trigeminal nerve stimulation for drug-resistant epilepsy." In: *Epilepsy & behavior : E&B* 22.3, pp. 574–6.
- Power, J. D. et al. (2011). "Functional Network Organization of the Human Brain". In: *Neuron* 72.4, pp. 665–678.
- Pu, L., Z. Liu, T. Yin, H. An, and S. Li (2010). "Simulation of induced electric field distribution based on five-sphere model used in rTMS." In: *Journal of X-ray science and technology* 18.1, pp. 57–67.
- Puig, J. et al. (2013). "Decreased corticospinal tract fractional anisotropy predicts long-term motor outcome after stroke". In: *Stroke* 44.7, pp. 2016–2018.
- Raghunathan, S., S. K. Gupta, M. P. Ward, R. M. Worth, K. Roy, and P. P. Irazoqui (2009). "The design and hardware implementation of a low-power real-time seizure detection algorithm." In: *Journal of neural engineering* 6.5, p. 056005.
- Rampersad, S., D. Stegeman, and T. Oostendorp (2013). "OP 11. Optimized tDCS electrode configurations for five targets determined via an inverse FE modeling approach". In: *Clinical Neurophysiology* 124.10, e61–e62.
- Ravazzani, P., J. Ruohonen, F. Grandori, and G. Tognola (1996). "Magnetic stimulation of the nervous system: Induced electric field in unbounded, semi-infinite, spherical, and cylindrical media". In: *Annals of Biomedical Engineering* 24, pp. 606–616.
- Ravazzani, P., J. Ruohonen, G. Tognola, F. Anfosso, M. Ollikainen, R. J. Ilmoniemi, and F. Grandori (May 2002). "Frequency-related effects in the optimization of coils for the magnetic stimulation of the nervous system." In: *IEEE transactions on bio-medical engineering* 49.5, pp. 463–71.
- Razza, L. B., A. H. Moffa, M. L. Moreno, A. F. Carvalho, F. Padberg, F. Fregni, and A. R. Brunoni (2018). "A systematic review and meta-analysis on placebo response to repetitive transcranial magnetic stimulation for depression trials". In: *Progress in Neuro-Psychopharmacology and Biological Psychiatry* 81, pp. 105–113.
- Reutens, D. C., R. A. Macdonnell, and S. F. Berkovic (1993). "The Influence of Changes in the Intensity of Magnetic Stimulation on Coil Output". In: *Muscle & nerve* 16.12, pp. 1338–1341.
- Richieri, R., E. Guedj, P. Michel, A. Loundou, P. Auquier, C. Lançon, and L. Boyer (2013). "Maintenance transcranial magnetic stimulation reduces depression relapse : A propensity-adjusted analysis". In: *Journal of Affective Disorders* 151.1, pp. 129–135.
- Rizzone, M., M. Lanotte, B. Bergamasco, A. Tavella, E. Torre, G. Faccani, and A. Melcarne (2001). "Deep brain stimulation of the subthalamic nucleus in Parkinson's disease : effects of variation in stimulation parameters". In: *Journal Neurol Neurosurg Psychiatry* 71, pp. 215–219.
- Rodriguez, F. J., D. Ceballos, M. Schuttler, A. Valero, E. Valderrama, T. Stieglitz, and X. Navarro (2000). "Polyimide cuff electrodes for peripheral nerve stimulation". In: *Journal of neuroscience methods* 98, pp. 105–118.
- Rogasch, N. C., R. H. Thomson, F. Farzan, B. M. Fitzgibbon, N. W. Bailey, J. C. Hernandez-Pavon, Z. J. Daskalakis, and P. B. Fitzgerald (2014). "Removing artefacts from TMS-EEG recordings using independent component analysis: Importance for assessing prefrontal and motor cortex network properties". In: *NeuroImage* 101.1, pp. 425–439.

- Roge, R., K. S. Ambrosen, K. J. Albers, C. T. Eriksen, M. G. Liptrot, M. N. Schmidt, K. H. Madsen, and M. Morup (2017). "Whole brain functional connectivity predicted by indirect structural connections". In: *Pattern Recognition in Neuroimaging (PRNI)*.
- Rong, P et al. (2012). "Transcutaneous vagus nerve stimulation for the treatment of depression: a study protocol for a double blinded randomized clinical trial". In: *BMC complementary and alternative medicine* 12.1, p. 255.
- Rossi, S. et al. (2009). "Safety, ethical considerations, and application guidelines for the use of transcranial magnetic stimulation in clinical practice and research". In: *Clinical Neurophysiology* 120.12, pp. 2008–2039.
- Rossini, D., A. Lucca, L. Magri, A. Malaguti, E. Smeraldi, C. Colombo, and R. Zanardi (2010). "A symptom-specific analysis of the effect of high-frequency left or low-frequency right transcranial magnetic stimulation over the dorsolateral prefrontal cortex in major depression". In: *Neuropsychobiology* 62.2, pp. 91–97.
- Rossini, P. M. et al. (2015). "Non-invasive electrical and magnetic stimulation of the brain, spinal cord, roots and peripheral nerves: Basic principles and procedures for routine clinical and research application. An updated report from an I.F.C.N. Committee". In: *Clinical Neurophysiology* 126.6, pp. 1071–1107.
- Rotem, A., A. Neef, N. E. Neef, A. Agudelo-Toro, D. Rakhmilevitch, W. Paulus, and E. Moses (2014). "Solving the orientation specific constraints in transcranial magnetic stimulation by rotating fields". In: *PLoS ONE* 9.2, e86794.
- Roth, B. J. and P. J. Basser (1990). "a Model of the Stimulation of a Nerve-Fiber By Electromagnetic Induction". In: *IEEE Transactions on Biomedical Engineering* 37.6, pp. 588–597.
- Roth, B. J., J. M. Saypol, M. Hallett, and L. G. Cohen (1991). "A theoretical calculation of the electric field induced in the cortex during magnetic stimulation". In: *Electroencephalography and clinical neurophysiology* 20892, pp. 47–56.
- Roth, Y., G. Pell, and A. Zangen (2013). "Commentary on: Deng et al. Electric field depth-focality tradeoff in transcranial magnetic stimulation: simulation comparison of 50 coil designs". In: *Brain stimulation* 6.1, pp. 14–15.
- Roth, Y., G. S. Pell, and A. Zangen (2010). "Motor evoked potential latency, motor threshold and electric field measurements as indices of transcranial magnetic stimulation depth." In: *Clinical neurophysiology : official journal of the International Federation of Clinical Neurophysiology* 121.2, pp. 255–259.
- Roth, Y., A. Zangen, and M. Hallett (2002). "A coil design for transcranial magnetic stimulation of deep brain regions." In: *Journal of clinical neurophysiology* 19.4, pp. 361–370.
- Roth, Y., A. Amir, Y. Levkovitz, and A. Zangen (2007). "Three-dimensional distribution of the electric field induced in the brain by transcranial magnetic stimulation using figure-8 and deep H-coils." In: *Journal of clinical neurophysiology* 24.1, pp. 31–38.
- Roth, Y., G. S. Pell, A. V. Chistyakov, A. Sinai, A. Zangen, and M. Zaaroor (2014). "Motor cortex activation by H-coil and figure-8 coil at different depths. Combined motor threshold and electric field distribution study." In: *Clinical neurophysiology* 125.2, pp. 336–343.
- Rubinov, M. and O. Sporns (2010). "Complex network measures of brain connectivity: Uses and interpretations". In: *NeuroImage* 52.3, pp. 1059–1069.
- Ruohonen, J., J. Virtanen, and R. J. Ilmoniemi (1997). "Coil optimization for magnetic brain stimulation." In: *Annals of biomedical engineering* 25.5, pp. 840–849.
- Ruohonen, J. (1995). "An analytical model to predict the electric field and excitation zones due to magnetic stimulation of peripheral nerves". In: *IEEE Transactions on Biomedical Engineering* 42.2, pp. 158–161.
- Ruohonen, J., P. Ravazzani, and F. Grandori (1998). "Functional magnetic stimulation: Theory and coil optimization". In: *Bioelectrochemistry and Bioenergetics* 47.2, pp. 213–219.
- Rush, A. J., M. E. Thase, and S. Dube (2003). "Research issues in the study of difficult-to-treat depression". In: *Biological Psychiatry* 53, pp. 743–753.
- Rush, a. J., M. S. George, H. a. Sackeim, L. B. Marangell, M. M. Husain, C. Giller, Z. Nahas, S. Haines, R. K. Simpson, and R. Goodman (2000). "Vagus nerve stimulation (VNS) for treatment-resistant depressions: A multicenter study". In: *Biological Psychiatry* 47.4, pp. 276–286.
- Rush, A. J. et al. (2006). "Acute and Longer-Term Outcomes in Depressed Outpatients Requiring One or Several Treatment Steps : A STAR*D Report". In: *American Journal of Psychiatry* 163, pp. 1905–1917.
- Sacco, P., D. Turner, J. Rothwell, and G. Thickbroom (2009). "Corticomotor responses to triple-pulse transcranial magnetic stimulation: Effects of interstimulus interval and stimulus intensity." In: *Brain stimulation* 2.1, pp. 36–40.
- Sackeim, H. A. et al. (2001). "Vagus nerve stimulation (VNS) for treatment-resistant depression: efficacy, side effects, and predictors of outcome". In: *Neuropsychopharmacology* 25.5, pp. 713–728.
- Sadaghiani, S. and M. D'Esposito (2015). "Functional characterization of the cingulo-opercular network in the maintenance of tonic alertness". In: *Cerebral Cortex* 25.9, pp. 2763–2773.
- Saillet, S., M. Langlois, B. Feddersen, L. Minotti, L. Vercueil, S. Chabardès, O. David, A. Depaulis, C. Deransart, and P. Kahane (2009). "Manipulating the epileptic brain using stimulation: a review of experimental and clinical studies". In: *Epileptic disorders* 11.2, pp. 100–112.
- Saletu, B and P Anderer (2010). "EEG Topography and Tomography (LORETA) in Diagnosis and Pharmacotherapy of Depression". In: *Clinical EEG and Neuroscience* 41.4, pp. 203–210.

- Salinas, F. S. (2009). "3D modeling of the total electric field induced by transcranial magnetic stimulation using the boundary element method". In: *Physics in Medicine and Biology* 54.12, pp. 3631–3647.
- Salinas, F. S., J. L. Lancaster, and P. T. Fox (2007). "Detailed 3D models of the induced electric field of transcranial magnetic stimulation coils." In: *Physics in medicine and biology* 52.10, pp. 2879–2892.
- Salomons, T. V., K. Dunlop, S. H. Kennedy, A. Flint, J. Geraci, P. Giacobbe, and J. Downar (2014). "Resting-State Cortico-Thalamic-Striatal Connectivity Predicts Response to Dorsomedial Prefrontal rTMS in Major Depressive Disorder". In: *Neurops* 39.2, pp. 488–498.
- Salvador, R., A. Mekonnen, G. Ruffini, and P. C. Miranda (2010). "Modeling the electric field induced in a high resolution realistic head model during transcranial current stimulation." In: *Annual International Conference of the IEEE Engineering in Medicine and Biology Society*, pp. 2073–2076.
- Salvador, R., F. Ramirez, M. V'yacheslavovna, and P. C. Miranda (2012). "Effects of tissue dielectric properties on the electric field induced in tDCS: a sensitivity analysis." In: *Conference proceedings : ... Annual International Conference of the IEEE Engineering in Medicine and Biology Society. IEEE Engineering in Medicine and Biology Society. Annual Conference 2012*, pp. 787–790.
- Santarnecchi, E., D. Momi, G. Sprugnoli, F. Neri, A. Pascual-Leone, A. Rossi, and S. Rossi (2018). "Modulation of network-to-network connectivity via spike-timing-dependent noninvasive brain stimulation". In: *Human Brain Mapping* 39.12, pp. 4870–4883.
- Sathappan, A. V., B. M. Luber, and S. H. Lisanby (2019). "The dynamic Duo: Combining noninvasive brain stimulation with cognitive interventions". In: *Progress in Neuro-Psychopharmacology and Biological Psychiatry* 89, pp. 347–360.
- Saturnino, G. B., O. Puonti, J. D. Nielsen, D. Antonenko, K. H. H. Madsen, and A. Thielscher (2018). "SimNIBS 2.1: A Comprehensive Pipeline for Individualized Electric Field Modelling for Transcranial Brain Stimulation". In: *bioRxiv*.
- Schäfer, M., J. Biesecker, A. Schulze-Bonhage, and A. Ferbert (1997). "Transcranial magnetic double stimulation: influence of the intensity of the conditioning stimulus". In: *Electroencephalography and clinical neurophysiology* 105, pp. 462–469.
- Scherrmann, J., C. Hoppe, T. Kral, J. Schramm, and C. E. Elger (2001). "Vagus Nerve Stimulation. Clinical experience in a Large Patient Series". In: *Journal of Clinical Neurophysiology* 18.5, pp. 408–414.
- Schmahmann, J. D., D. N. Pandya, R. Wang, G. Dai, H. E. D'Arceuil, A. J. De Crespigny, and V. J. Wedeen (2007). "Association fibre pathways of the brain: Parallel observations from diffusion spectrum imaging and autoradiography". In: *Brain* 130.3, pp. 630–653.
- Schmidt, C. and U. van Rienen (2012a). "Sensitivity analysis of the field distribution in Deep Brain Stimulation with respect to the anisotropic conductivity of brain tissue." In: *Biomedizinische Technik. Biomedical engineering* 57 Suppl 1, p. 4266.
- Schmidt, C. and U. van Rienen (2012b). "Modeling the field distribution in deep brain stimulation: the influence of anisotropy of brain tissue." In: *IEEE transactions on bio-medical engineering* 59.6, pp. 1583–92.
- Schrader, L. M., J. M. Stern, L. Koski, M. R. Nuwer, and J. Engel (2004). "Seizure incidence during single- and paired-pulse transcranial magnetic stimulation (TMS) in individuals with epilepsy". In: *Clinical Neurophysiology* 115, pp. 2728–2737.
- Schrader, L. M., I. A. Cook, P. R. Miller, E. R. Maremont, and C. M. DeGiorgio (2011). "Trigeminal nerve stimulation in major depressive disorder: First proof of concept in an open pilot trial". In: *Epilepsy & Behavior* 22.3, pp. 475–478.
- Schwarz, A. J. and J. McGonigle (2011). "Negative edges and soft thresholding in complex network analysis of resting state functional connectivity data". In: *NeuroImage* 55.3, pp. 1132–1146.
- Seminowicz, D. A., H. S. Mayberg, A. R. McIntosh, K. Goldapple, S. Kennedy, Z. Segal, and S. Rafi-Tari (2004). "Limbic-frontal circuitry in major depression: A path modeling metanalysis". In: *NeuroImage* 22.1, pp. 409–418.
- Senova, S., G. Cotovio, A. Pascual-leone, and A. J. Oliveira-Maia (2019). "Durability of antidepressant response to repetitive transcranial magnetic stimulation: Systematic review and meta-analysis". In: *Brain Stimulation* 12.1, pp. 119–128.
- Sewerin, S., M. Taubert, H. Vollmann, V. Conde, A. Villringer, and P. Ragert (2011). "Enhancing the effect of repetitive I-wave paired-pulse TMS (iTMS) by adjusting for the individual I-wave periodicity." In: *BMC neuroscience* 12.1, p. 45.
- Shafi, M. M., M. Brandon Westover, L. Oberman, S. S. Cash, and A. Pascual-Leone (2014). "Modulation of EEG functional connectivity networks in subjects undergoing repetitive transcranial magnetic stimulation". In: *Brain Topography* 27.1, pp. 172–191.
- Shafi, M. M. et al. (2015). "Physiological consequences of abnormal connectivity in a developmental epilepsy". In: *Annals of Neurology* 77.3, pp. 487–503.
- Shahid, S., P. Wen, and T. Ahfock (2013). "Assessment of electric field distribution in anisotropic cortical and subcortical regions under the influence of tDCS." In: *Bioelectromagnetics* 57, pp. 41–57.
- Sheehan, D. V., Y. Lecrubier, K. H. Sheehan, P. Amorim, J. Janavs, E. Weiller, T. Hergueta, R. Baker, and G. C. Dunbar (1998). "The Mini-International Neuropsychiatric Interview (M.I.N.I.): The development and validation of a structured diagnostic psychiatric interview for DSM-IV and ICD-10." In: *Journal of Clinical Psychiatry* 59.20, pp. 22–33.

- Sheffield, J. M., S. Kandala, C. A. Tamminga, G. D. Pearson, M. S. Keshavan, J. A. Sweeney, B. A. Clementz, B. Dov, S. K. Hill, and D. M. Barch (2017). "Transdiagnostic Associations Between Functional Brain Network Integrity and Cognition". In: *JAMA Psychiatry* 74.6, pp. 605–613.
- Shekhawat, G. S., C. M. Stinear, and G. D. Searchfield (2013). "Transcranial direct current stimulation intensity and duration effects on tinnitus suppression." In: *Neurorehabilitation and neural repair* 27.2, pp. 164–72.
- Sheline, Y. I., J. L. Price, Z. Yan, and M. A. Mintun (2010). "Resting-state functional MRI in depression unmasks increased connectivity between networks via the dorsal nexus". In: *Proceedings of the National Academy of Sciences* 107.24, pp. 11020–11025.
- Shukla, P., I. Basu, D. Graupe, D. Tuninetti, and K. V. Slavin (2012). "A neural network-based design of an on-off adaptive control for Deep Brain Stimulation in movement disorders." In: *Annual International Conference of the IEEE Engineering in Medicine and Biology Society* 2012, pp. 4140–3.
- Siddiqi, S., S. Taylor, D. Cooke, M. George, and M. Fox (2019). "783: Distinct symptom-specific treatment targets for antidepressant neuromodulation". In: *International Brain Stimulation Conference*, p. 537.
- Silvanto, J. and A. Pascual-Leone (2008). "State-dependency of transcranial magnetic stimulation". In: *Brain topography* 21.1, pp. 1–10.
- Singh, M. K. et al. (2013). "Anomalous gray matter structural networks in major depressive disorder". In: *Biophysical Psychiatry* 74.10, pp. 777–785. arXiv: NIHMS150003.
- Sinke, M. R., W. M. Otte, D. Christiaens, O. Schmitt, A. Leemans, A. van der Toorn, R. A. Sarabdjitsingh, M. Joëls, and R. M. Dijkhuizen (2018). "Diffusion MRI-based cortical connectome reconstruction: dependency on tractography procedures and neuroanatomical characteristics". In: *Brain Structure and Function* 223.5, pp. 2269–2285.
- Skarpaas, T. L. and M. J. Morrell (2009). "Intracranial Stimulation Therapy for Epilepsy". In: *Neurotherapeutics* 6.2, pp. 238–243.
- Smith, S. M. et al. (2009). "Correspondence of the brain's functional architecture during activation and rest." In: *Proceedings of the National Academy of Sciences of the United States of America* 106.31, pp. 13040–13045. arXiv: 0905267106.
- Smith, S. M., K. L. Miller, G. Salimi-Khorshidi, M. Webster, C. F. Beckmann, T. E. Nichols, J. D. Ramsey, and M. W. Woolrich (2011). "Network modelling methods for FMRI". In: *NeuroImage* 54.2, pp. 875–891.
- Sommer, M., N. Lang, F. Tergau, and W. Paulus (2002). "Neuronal tissue polarization induced by repetitive transcranial magnetic stimulation?" In: *Neuroreport* 13.6, pp. 809–811.
- Song, X. W., Z. Y. Dong, X. Y. Long, S. F. Li, X. N. Zuo, C. Z. Zhu, Y. He, C. G. Yan, and Y. F. Zang (2011). "REST: A Toolkit for resting-state functional magnetic resonance imaging data processing". In: *PLoS ONE* 6.9, e25031.
- Sparing, R., F. M. Mottaghy, M. Hungs, M. Brüggmann, H. Foltys, W. Huber, and R. Töpper (2001). "Repetitive Transcranial Magnetic Stimulation Effects on Language Function Depend on the Stimulation Parameters". In: *Journal of clinical neurophysiology* 18.4, pp. 326–330.
- Sparks, O. www.oxfordsparks.ox.ac.uk/mr.
- Speer, A. M., T. A. Kimbrell, E. M. Wassermann, J. D. Repella, M. W. Willis, P. Herscovitch, and R. M. Post (2000). "Opposite effects of high and low frequency rTMS on regional brain activity in depressed patients". In: *Biological Psychiatry* 48.12, pp. 1133–1141.
- Speer, A. M., M. W. Willis, P. Herscovitch, M. Daube-witherspoon, J. R. Shelton, B. E. Benson, R. M. Post, and E. M. Wassermann (2003a). "Intensity-Dependent Regional Cerebral Blood Flow during 1-Hz Repetitive Transcranial Magnetic Stimulation (rTMS) in Healthy Volunteers Studied with H₂¹⁵O Positron Emission Tomography : I. Effects of Primary Motor Cortex rTMS". In:
- Speer, A. M., M. W. Willis, P. Herscovitch, M. Daube-Witherspoon, J. Repella Shelton, B. E. Benson, R. M. Post, and E. M. Wassermann (2003b). "Intensity-dependent regional cerebral blood flow during 1-Hz repetitive transcranial magnetic stimulation (rTMS) in healthy volunteers studied with h215o positron emission tomography: II. effects of prefrontal cortex rTMS". In: *Biological Psychiatry* 54.8, pp. 826–832.
- Sprengers, M, K Vonck, E Carrette, A. Marson, and P Boon (2014). "Deep brain and cortical stimulation for epilepsy (Review)". In: *Cochrane Library* 6.
- Stagg, C. J., M Wylezinska, P. M. Matthews, P Jezzard, J. C. Rothwell, and S Bestmann (2009). "Neurochemical Effects of Theta Burst Stimulation as Assessed by Magnetic Resonance Spectroscopy". In: *Journal of neurophysiology* 101, pp. 2872–2877.
- Stanslaski, S., P. Afshar, P. Cong, J. Giftakis, P. Stypulkowski, D. Carlson, D. Linde, D. Ullestad, A.-T. Avestruz, and T. Denison (2012). "Design and validation of a fully implantable, chronic, closed-loop neuromodulation device with concurrent sensing and stimulation." In: *IEEE transactions on neural systems and rehabilitation engineering* 20.4, pp. 410–21.
- Stefan, H. et al. (2012). "Transcutaneous vagus nerve stimulation (t-VNS) in pharmacoresistant epilepsies: A proof of concept trial". In: *Epilepsia* 53.7, pp. 115–118.
- Stern, W. M., J. M. Tormos, D. Z. Press, C. Pearlman, and A. Pascual-Leone (2007). "Antidepressant Effects of High and Low Frequency Magnetic Stimulation to the Dorsolateral Prefrontal Cortex ." in: *Journal of neuropsychiatry Clin. Neurosci.* 19.2, pp. 179–186.

- Stokes, M. G., A. T. Barker, M. Dervinis, F. Verbruggen, L. Maizey, R. C. Adams, and C. D. Chambers (2013). "Biophysical determinants of transcranial magnetic stimulation: Effects of excitability and depth of targeted area". In: *Journal of neurophysiology* 109, pp. 437–444.
- Stubbeman, W. F., V. Ragland, and R. Khairkhah (2018). "Bilateral neuronavigated 20Hz theta burst TMS for treatment refractory depression : An open label study". In: *Brain Stimulation* 11, pp. 953–955.
- Sturm, V., D. Lenartz, A. Koulousakis, H. Treuer, K. Herholz, J. C. Klein, and J. Klosterkötter (2003). "The nucleus accumbens: a target for deep brain stimulation in obsessive-compulsive- and anxiety-disorders". In: *J Chem Neuroanat* 26.4, pp. 293–299.
- Sun, F. T., M. J. Morrell, and R. E. Wharen (2008). "Responsive cortical stimulation for the treatment of epilepsy." In: *Neurotherapeutics* 5.1, pp. 68–74.
- Sun, W. et al. (2012). "Low-frequency repetitive transcranial magnetic stimulation for the treatment of refractory partial epilepsy: A controlled clinical study". In: *Epilepsia* 53.10, pp. 1782–1789.
- Sylvester, C. M., M. Corbetta, M. E. Raichle, T. L. Rodebaugh, B. L. Schlaggar, Y. I. Sheline, C. F. Zorumski, and E. J. Lenze (2012). "Functional network dysfunction in anxiety and anxiety disorders". In: *Trends in Neurosciences* 35.9, pp. 527–535. arXiv: NIHMS150003.
- Szczepankiewicz, F., J. Lätt, R. Wirestam, A. Leemans, P. Sundgren, D. van Westen, F. Ståhlberg, and M. Nilsson (2013). "Variability in diffusion kurtosis imaging: Impact on study design, statistical power and interpretation". In: *NeuroImage* 76, pp. 145–154.
- Tachas, N. J. and T. Samaras (2014). "The effect of head and coil modeling for the calculation of induced electric field during transcranial magnetic stimulation." In: *International journal of psychophysiology* 93.1, pp. 167–171.
- Tadel, F., S. Baillet, J. C. Mosher, D. Pantazis, and R. M. Leahy (2011). "Brainstorm: A user-friendly application for MEG/EEG analysis". In: *Computational Intelligence and Neuroscience* 2011, pp. 1–13.
- Tatum, W. O. and S. L. Helmers (2009). "Vagus nerve stimulation and magnet use: optimizing benefits". In: *Epilepsy & behavior* 15.3, pp. 299–302.
- Tax, C. M. W., W. M. Otte, M. A. Viergever, R. M. Dijkhuizen, and A. Leemans (2015). "REKINDLE: Robust Extraction of Kurtosis INDices with Linear Estimation". In: *Magnetic Resonance in Medicine* 73.2, pp. 794–808.
- Terney, D., L. Chaieb, V. Moliadze, A. Antal, and W. Paulus (2008). "Increasing human brain excitability by transcranial high-frequency random noise stimulation." In: *The Journal of neuroscience* 28.52, pp. 14147–14155.
- Thielscher, A., A. Antunes, and G. B. Saturnino (2015). "Field modeling for transcranial magnetic stimulation : a useful tool to understand the physiological effects of TMS ?" In: *IEEE Engineering Medical Biology Society*, pp. 2–5.
- Thielscher, A., A. Opitz, and M. Windhoff (2011). "Impact of the gyral geometry on the electric field induced by transcranial magnetic stimulation." In: *NeuroImage* 54.1, pp. 234–43.
- Thomas, C., F. Q. Ye, M. O. Irfanoglu, P. Modi, K. S. Saleem, D. A. Leopold, and C. Pierpaoli (2014). "Anatomical accuracy of brain connections derived from diffusion MRI tractography is inherently limited". In: *Proceedings of the National Academy of Sciences* 111.46, pp. 16574–16579. arXiv: 1408.1149.
- Thomson, R. H., Z. J. Daskalakis, and P. B. Fitzgerald (2011). "A near infra-red spectroscopy study of the effects of pre-frontal single and paired pulse transcranial magnetic stimulation." In: *Clinical neurophysiology* 122.2, pp. 378–82.
- Thordstein, M., K. Saar, G. Pegenius, and M. Elam (2013). "Individual effects of varying stimulation intensity and response criteria on area of activation for different muscles in humans. A study using navigated transcranial magnetic stimulation." In: *Brain stimulation* 6.1, pp. 49–53.
- Thut, G. and A. Pascual-Leone (2010). "A review of combined TMS-EEG studies to characterize lasting effects of repetitive TMS and assess their usefulness in cognitive and clinical neuroscience." In: *Brain topography* 22.4, pp. 219–232.
- Thut, G. et al. (2017). "Guiding transcranial brain stimulation by EEG/MEG to interact with ongoing brain activity and associated functions: A position paper". In: *Clinical Neurophysiology* 128.5, pp. 843–857.
- Tik, M. et al. (2017). "Towards understanding rTMS mechanism of action: Stimulation of the DLPFC causes network-specific increases in functional connectivity". In: *NeuroImage* 15.162, pp. 289–296.
- Toader, E., M. M. J. Decre, and H. C. F. Martens (2010). "Steering deep brain stimulation fields using a high resolution electrode array." In: *Annual International Conference of the IEEE Engineering in Medicine and Biology Society*. Vol. 2010, pp. 2061–2064.
- Todd, G., S. C. Flavel, and M. C. Ridding (2009). "Priming theta-burst repetitive transcranial magnetic stimulation with low- and high-frequency stimulation". In: *Experimental Brain Research* 195.2, pp. 307–315.
- Tofts, P. S. and N. M. Branson (1991). "The measurement of electric field, and the influence of surface charge, in magnetic stimulation." In: *Electroencephalography and clinical neurophysiology* 81, pp. 238–239.
- Tommaso, M. de, C. Serpino, K. Ricci, G. Franco, V. Devitofrancesco, and P. Livrea (2012). "Effects of low and high frequency repetitive transcranial magnetic stimulation of the primary motor cortex on contingent negative variations in normal subjects". In: *Neuroscience Letters* 509.1, pp. 39–43.

- Torii, T, A Sato, M Iwahashi, Y Itoh, and K. I. Member (2012a). "Time-Dependent Effects of Low-Frequency Repetitive Transcranial Magnetic Stimulation of the Supramarginal Gyrus". In: *Annual International Conference of the IEEE Engineering in Medicine and Biology Society*, pp. 3372–3375.
- Torii, T, A. Sato, Y. Nakahara, M. Iwahashi, Y. Itoh, and K. Iramina (2012b). "Frequency-dependent effects of repetitive transcranial magnetic stimulation on the human brain." In: *Neuroreport* 23.18, pp. 1065–70.
- Tournier, J. D., C. H. Yeh, F. Calamante, K. H. Cho, A. Connelly, and C. P. Lin (2008). "Resolving crossing fibres using constrained spherical deconvolution: Validation using diffusion-weighted imaging phantom data". In: *NeuroImage* 42.2, pp. 617–625.
- Tournier, J.-D., S. Mori, and A. Leemans (2011). "Diffusion tensor imaging and beyond". In: *Magnetic Resonance in Medicine* 65.6, pp. 1532–1556.
- Tremblay, S. et al. (2019). "Clinical utility and prospective of TMS-EEG". In: *Clinical Neurophysiology* 130.5, pp. 802–844.
- Tuch, D. S., V. J. Wedeen, a. M. Dale, J. S. George, and J. W. Belliveau (2001). "Conductivity tensor mapping of the human brain using diffusion tensor MRI." In: *Proceedings of the National Academy of Sciences of the United States of America* 98.20, pp. 11697–701.
- Tuch, D. S., V. J. Wedeen, A. M. Dale, J. S. George, and J. W. Belliveau (1999). "Conductivity Mapping of Biological Tissue Using Diffusion MRI". In: *Annals of the New York Academy of Sciences* 888, pp. 314–316.
- Turner, D. A. (2012). "Deep brain stimulation shape and surface characteristics: electrical and mechanical design goals." In: *World neurosurgery* 77.3-4, pp. 468–9.
- Tzourio-Mazoyer, N., B. Landeau, D. Papathanassiou, F. Crivello, O. Etard, N. Delcroix, B. Mazoyer, and M. Joliot (2002). "Automated Anatomical Labeling of Activations in SPM Using a Macroscopic Anatomical Parcellation of the MNI MRI Single-Subject Brain". In: *NeuroImage* 15.1, pp. 273–289.
- Umesh Rudrapatna, S., T. Wieloch, K. Beirup, K. Ruscher, W. Mol, P. Yanev, A. Leemans, A. van der Toorn, and R. M. Dijkhuizen (2014). "Can diffusion kurtosis imaging improve the sensitivity and specificity of detecting microstructural alterations in brain tissue chronically after experimental stroke? Comparisons with diffusion tensor imaging and histology". In: *NeuroImage* 97, pp. 363–373.
- Ushe, M. et al. (2004). "Effect of stimulation frequency on tremor suppression in essential tremor." In: *Movement Disorders* 19.10, pp. 1163–8.
- Vaessen, M. (2012). "The graph ity of cognitive problems in epilepsy". PhD thesis.
- Valero-Cabré, A., B. R. Payne, J. Rushmore, S. G. Lomber, and A. Pascual-Leone (2005). "Impact of repetitive transcranial magnetic stimulation of the parietal cortex on metabolic brain activity: A 14C-2DG tracing study in the cat". In: *Experimental Brain Research* 163.1, pp. 1–12.
- Valero-Cabré, A., J. L. Amengual, C. Stengel, A. Pascual-Leone, and O. A. Coubard (2017). "Transcranial magnetic stimulation in basic and clinical neuroscience: A comprehensive review of fundamental principles and novel insights". In: *Neuroscience and Biobehavioral Reviews* 83, pp. 381–404.
- Van Hartevelt, T. J., J. Cabral, G. Deco, A. Moller, A. L. Green, T. Z. Aziz, and M. L. Kringelbach (2014). "Neural plasticity in human brain connectivity: The effects of long term deep brain stimulation of the subthalamic nucleus in Parkinson's disease". In: *PLoS ONE* 9.1, e86496.
- Van Nieuwenhuijse, B., R. Raedt, J. Delbeke, W. Wadman, P. Boon, and K. Vonck (2015). "In Search of Optimal DBS Paradigms to Treat Epilepsy: Bilateral Versus Unilateral Hippocampal Stimulation in a Rat Model for Temporal Lobe Epilepsy". In: *Brain Stimulation* 8.2, pp. 192–199.
- VanHaerents, S., S. T. Herman, T. Pang, A. Pascual-Leone, and M. M. Shafi (2015). "Repetitive transcranial magnetic stimulation; A cost-effective and beneficial treatment option for refractory focal seizures". In: *Clinical Neurophysiology* 126.9, pp. 1840–1842.
- Vasques, X., L. Cif, O. Hess, S. Gavarini, G. Mennessier, and P. Coubes (2009). "Stereotactic model of the electrical distribution within the internal globus pallidus during deep brain stimulation." In: *Journal of computational neuroscience* 26.1, pp. 109–18.
- Vasques, X., L. Cif, G. Mennessier, and P. Coubes (2010). "A target-specific electrode and lead design for internal globus pallidus deep brain stimulation." In: *Stereotactic and functional neurosurgery* 88.3, pp. 129–37.
- Vecchio, F., R. Di Iorio, F. Miraglia, G. Granata, R. Romanello, P. Bramanti, and P. M. Rossini (2018). "Transcranial direct current stimulation generates a transient increase of small-world in brain connectivity: an EEG graph theoretical analysis". In: *Experimental Brain Research* 236.4, pp. 1117–1127.
- Veer, I. M., C. F. Beckmann, M.-J. van Tol, L. Ferrarini, J. Milles, D. J. Veltman, A. Aleman, M. A. van Buchem, N. J. van der Wee, and S. a.R. B. Rombouts (2010). "Whole brain resting-state analysis reveals decreased functional connectivity in major depression." In: *Frontiers in systems neuroscience* 4, pp. 1–10.
- Velasco, F., J. D. Carrillo-Ruiz, F. Brito, M. Velasco, A. L. Velasco, I. Marquez, and R. Davis (2005). "Double-blind, randomized controlled pilot study of bilateral cerebellar stimulation for treatment of intractable motor seizures." In: *Epilepsia* 46.7, pp. 1071–81.
- Velasco, M, F Velasco, and a. L. Velasco (2001). "Centromedian-thalamic and hippocampal electrical stimulation for the control of intractable epileptic seizures." In: *Journal of Clinical Neurophysiology* 18.6, pp. 495–513.

- Veniero, D., M. Bortoletto, and C. Miniussi (2009). "TMS-EEG co-registration: On TMS-induced artifact". In: *Clinical Neurophysiology* 120.7, pp. 1392–1399.
- Veraart, J., J. Sijbers, S. Sunaert, A. Leemans, and B. Jeurissen (2013). "Weighted linear least squares estimation of diffusion MRI parameters: Strengths, limitations, and pitfalls". In: *NeuroImage* 81, pp. 335–346.
- Vercueil, L. et al. (2007). "Effects of pulse width variations in pallidal stimulation for primary generalized dystonia." In: *Journal of neurology* 254.11, pp. 1533–7.
- Villegier, A., L. Ouchchane, J.-J. Lemaire, and J.-Y. Boire (2006). "Assistance to Planning in Deep Brain Stimulation: Data Fusion Method for Locating Anatomical Targets in MRI". In: *Annual International Conference of the IEEE Engineering in Medicine and Biology Society. IEEE Engineering in Medicine and Biology Society. Annual Conference*, pp. 144–147.
- Vink, J. J. T., D. C. W. Klooster, M. B. Westover, A. Pascual-Leone, and M. M. Shafi (2019). "EEG functional connectivity is predictive of causal brain interactions".
- Voineskos, A. N., F. Farzan, M. S. Barr, N. J. Lobaugh, B. H. Mulsant, R. Chen, P. B. Fitzgerald, and Z. J. Daskalakis (2010). "The role of the corpus callosum in transcranial magnetic stimulation induced interhemispheric signal propagation". In: *Biological Psychiatry* 68.9, pp. 825–831.
- Vonck, K., K. Van Laere, S. Dedeurwaerdere, J. Caemaert, J. De Reuck, and P. Boon (2001). "The mechanism of action of vagus nerve stimulation for refractory epilepsy: the current status". In: *Journal of clinical neurophysiology* 18.5, pp. 394–401.
- Vonck, K., V. D. Herdt, M. Sprengers, and E. Ben-Menachem (2012). "Neurostimulation for epilepsy". In: *Handbook of Clinical Neurology*.
- Vonck, K. and P. Boon (2015). "Epilepsy: Closing the loop for patients with epilepsy". In: *Nature Reviews Neurology* 11, pp. 252–254.
- Vonck, K., P. Boon, E. Achten, J. De Reuck, and J. Caemaert (2002). "Long-term amygdalohippocampal stimulation for refractory temporal lobe epilepsy." In: *Annals of neurology* 52.5, pp. 556–65.
- Vonck, K. et al. (2003). "Neurostimulation for refractory epilepsy". In: *Acta neurologica belgica* 103, pp. 213–217.
- Vonck, K., P. Boon, P. Claeys, S. Dedeurwaerdere, R. Achten, and D. Van Roost (2005). "Long-term deep brain stimulation for refractory temporal lobe epilepsy." In: *Epilepsia* 46, pp. 98–9.
- Vonck, K., V. De Herdt, T. Bosman, S. Dedeurwaerdere, K. Van Laere, and P. Boon (2008). "Thalamic and limbic involvement in the mechanism of action of vagus nerve stimulation, a SPECT study." In: *Seizure : the journal of the British Epilepsy Association* 17.8, pp. 699–706.
- Vos, S. B., C. M. W. Tax, P. R. Luijten, S. Ourselin, A. Leemans, and M. Froeling (2017). "The importance of correcting for signal drift in diffusion MRI". In: *Magnetic Resonance in Medicine* 77.1, pp. 285–299.
- Vries, F. E. de, S. J. de Wit, O. A. van den Heuvel, D. J. Veltman, D. C. Cath, A. J. L. M. van Balkom, and Y. D. van der Werf (2017). "Cognitive control networks in OCD: A resting-state connectivity study in unmedicated patients with obsessive-compulsive disorder and their unaffected relatives". In: *World Journal of Biological Psychiatry* 0.0, pp. 1–13.
- Vucic, S., B. C. Cheah, A. V. Krishnan, D. Burke, and M. C. Kiernan (2009). "The effects of alterations in conditioning stimulus intensity on short interval intracortical inhibition." In: *Brain research* 1273, pp. 39–47.
- Wagner, T., F. Fregni, S. Fecteau, A. Grodzinsky, M. Zahn, and A. Pascual-Leone (2007). "Transcranial direct current stimulation: A computer-based human model study". In: *NeuroImage* 35.3, pp. 1113–1124.
- Wagner, T. et al. (2014). "Impact of brain tissue filtering on neurostimulation fields: a modeling study." In: *NeuroImage* 85, pp. 1048–57.
- Wagner, T., A. Valero-Cabre, and A. Pascual-Leone (2007). "Noninvasive human brain stimulation". In: *Annual Review of Biomedical Engineering* 9.1, pp. 527–565.
- Walckiers, G., B. Fuchs, J.-P. P. Thiran, J. R. Mosig, and C. Pollo (2010). "Influence of the implanted pulse generator as reference electrode in finite element model of monopolar deep brain stimulation." In: *Journal of neuroscience methods* 186.1, pp. 90–96.
- Walsch, V. and A. Pascual-Leone (2003). *Transcranial magnetic stimulation: A neurochronometrics of mind*, pp. 39–63.
- Wang, H.-n., L. Wang, R.-g. Zhang, Y.-c. Chen, L. Liu, F. Gao, H. Nie, W.-g. Hou, Z.-w. Peng, and Q. Tan (2014). "Anti-depressive mechanism of repetitive transcranial magnetic stimulation in rat: The role of the endocannabinoid system". In: *Journal of Psychiatric Research* 51, pp. 79–87.
- Wårdell, K., Z. Kefalopoulou, E. Diczfalussy, M. Andersson, M. Aström, P. Limousin, L. Zrinzo, and M. Hariz (2014). "Deep Brain Stimulation of the Pallidum Internum for Gilles de la Tourette Syndrome: A Patient-Specific Model-Based Simulation Study of the Electric Field." In: *Neuromodulation* 18.2, pp. 90–96.
- Warden, D., A. J. Rush, M. H. Trivedi, M. Fava, and S. R. Wisniewski (2007). "The STAR * D Project Results : A Comprehensive Review of Findings". In: *Current psychiatry reports* 9, pp. 449–459.
- Wassermann, E. M., C. M. Epstein, U. Ziemann, T. Paus, and S. H. Lisanby (2008). *The Oxford Handbook of Transcranial Magnetic Stimulation*. first edit. Oxford University Press, pp. 25–32.
- Watts, D. J. and S. H. Strogatz (1998). "Collective dynamics of 'small-world' networks." In: *Nature* 393.6684, pp. 440–442. arXiv: 0803.0939v1.

- Wedeen, V. J., R. P. Wang, J. D. Schmahmann, T. Benner, W. Y. Tseng, G. Dai, D. N. Pandya, P. Hagmann, H. D'Arceuil, and A. J. de Crespigny (2008). "Diffusion spectrum magnetic resonance imaging (DSI) tractography of crossing fibers". In: *NeuroImage* 41.4, pp. 1267–1277.
- Wei, X. F. and W. M. Grill (2005). "Current density distributions, field distributions and impedance analysis of segmented deep brain stimulation electrodes." In: *Journal of neural engineering* 2.4, pp. 139–47.
- Weigand, A., A. Horn, R. Caballero, D. Cooke, A. P. Stern, S. F. Taylor, D. Press, A. Pascual-Leone, and M. D. Fox (2017). "Prospective validation that subgenual connectivity predicts antidepressant efficacy of transcranial magnetic stimulation sites". In: *Biological Psychiatry* 84.1, pp. 28–37.
- WHO factsheet: Depression (2018).
- Wijk, B. C.M. V., C. J. Stam, A. Daffertshofer, B. C. M. van Wijk, C. J. Stam, and A. Daffertshofer (2010). "Comparing brain networks of different size and connectivity density using graph theory". In: *PLoS ONE* 5.10.
- Windhoff, M., A. Opitz, and A. Thielscher (2013). "Electric field calculations in brain stimulation based on finite elements: an optimized processing pipeline for the generation and usage of accurate individual head models." In: *Human brain mapping* 34.4, pp. 923–935.
- Wongsarnpigoon, A. and W. M. Grill (2011). "Energy-efficient waveform shapes for neural stimulation revealed with genetic algorithm". In: *Journal of neural engineering* 7.4, pp. 1–20.
- Woodbury, D. M. and J. W. Woodbury (1990). "Effects of vagal stimulation on experimentally induced seizures in rats." In: *Epilepsia* 31, S7–19.
- Wu, X., P. Lin, J. J. Yang, H. Song, R. Yang, and J. J. Yang (2016). "Dysfunction of the cingulo-opercular network in first-episode medication-naïve patients with major depressive disorder". In: *Journal of Affective Disorders* 200, pp. 275–283.
- Wyckhuys, T. R. Raedt, K. Vonck, W. Wadman, and P. Boon (2010). "Comparison of hippocampal Deep Brain Stimulation with high (130Hz) and low frequency (5Hz) on afterdischarges in kindled rats." In: *Epilepsy research* 88.2-3, pp. 239–46.
- Xiang Quan, W., X. Lin Zhu, H. Qiao, W. Fang Zhang, S. Ping Tan, D. Z. Feng, and X. Qun Wang (2015). "The effects of high-frequency repetitive transcranial magnetic stimulation (rTMS) on negative symptoms of schizophrenia and the follow-up study." In: *Neuroscience letters* 584, pp. 197–201.
- Xie, T., U. J. Kang, and P. Warnke (2012). "Effect of stimulation frequency on immediate freezing of gait in newly activated STN DBS in Parkinson's disease." In: *Journal of neurology, neurosurgery, and psychiatry* 83.10, pp. 1015–7.
- Yadollahpour, A., S. A. Hosseini, and A. Shakeri (2016). "rTMS for the Treatment of Depression: a Comprehensive Review of Effective Protocols on Right DLPFC". In: *International Journal of Mental Health and Addiction* 14.4, pp. 539–549.
- Yadollahpour, A., S. M. Firouzabadi, M. Shahpari, and J. Mirnajafi-Zadeh (2014). "Repetitive transcranial magnetic stimulation decreases the kindling induced synaptic potentiation: effects of frequency and coil shape." In: *Epilepsy research* 108.2, pp. 190–201.
- Yamamoto, T., Y. Katayama, T. Kano, H. Oshima, and C. Fukaya (2004). "Deep brain stimulation for the treatment of parkinsonian, essential and poststroke tremor: a suitable stimulation method and changes in effective stimulation intensity". In: *Journal of Neurosurgery* 101.2, pp. 201–209.
- Yendiki, A., K. Koldewyn, S. Kakunoori, N. Kanwisher, and B. Fischl (2014). "Spurious group differences due to head motion in a diffusion MRI study". In: *NeuroImage* 88, pp. 79–90.
- Yeo, B. T. T. et al. (2011). "The organization of the human cerebral cortex estimated by intrinsic functional connectivity". In: *Journal of neurophysiology* 106, pp. 1125–1165.
- Yousif, N. and X. Liu (2007). "Modelling the current distribution across the depth electrode- brain interface in deep brain stimulation". In: *Expert Rev Med Devices* 4.5, pp. 623–631.
- Zaghi, S., M. Acar, B. Hultgren, P. S. Boggio, and F. Fregni (2010). "Noninvasive Brain Stimulation with Low-Intensity Electrical Currents: Putative Mechanisms of Action for Direct and Alternating Current Stimulation". In: *The Neuroscientist* 16.3, pp. 285–307.
- Zhang, Q. Z. C. Wu, J. Yu, N. N. Yu, X. L. Zhong, and L. Tan (2012). "Mode-dependent effect of high-frequency electrical stimulation of the anterior thalamic nucleus on amygdala-kindled seizures in rats". In: *Neuroscience*.
- Zheng, J., L. Li, and X. Huo (2005). "Analysis of Electric Field in Real Rat Head Model during Transcranial Magnetic Stimulation." In: *Annual International Conference of the IEEE Engineering in Medicine and Biology Society*. Vol. 2. 2, pp. 1529–1532.
- Ziemann, U. and H. Siebner (2015). "Inter-subject and Inter-session Variability of Plasticity Induction by Non-invasive Brain Stimulation: Boon or Bane?" In: *Brain Stimulation* 8.3, pp. 662–663.
- Zrenner, C., D. Desideri, P. Belardinelli, and U. Ziemann (2018). "Real-time EEG-defined excitability states determine efficacy of TMS-induced plasticity in human motor cortex". In: *Brain Stimulation* 11.2, pp. 374–389.
- Zrinzo, L., T. Foltynie, P. Limousin, and M. I. Hariz (2012). "Reducing hemorrhagic complications in functional neurosurgery: a large case series and systematic literature review." In: 116, pp. 84–94.

- Zyss, T., J. Mamczarz, and J. Vetulani (1999). "The influence of rapid-rate transcranial magnetic stimulation (rTMS) parameters on rTMS effects in Porsolt's forced swimming test". In: *International journal of neuropsychopharmacology*.

Publication List

Journal publications

First author:

1. **D.C.W. Klooster**, I.N. Vos, K. Caeyenberghs, A. Leemans, S. David, R.M.H. Besseling, A.P. Aldenkamp, C. Baeken, Indirect frontocingulate structural connectivity predicts clinical response to accelerated rTMS in major depressive disorder, *Journal of Psychiatry and Neuroscience*, *in press*
2. **D.C.W. Klooster**, S.L. Franklin, R.M.H. Besseling, J.F.A. Jansen, K. Caeyenberghs, R. Duprat, A.P. Aldenkamp, A.J.A. de Louw, P.A.J.M. Boon, C. Baeken, Focal application of accelerated iTBS results in global changes in graph measures, *Human Brain Mapping*, 2019, 40(2):432-450
3. **D.C.W. Klooster**, A.J.A. de Louw, A.P. Aldenkamp, R.M.H. Besseling, R.M.C. Mestrom, S. Carrette, S. Zinger, J.W.M. Bergmans, W.H. Mess, K. Vonck, E. Carrette, L.E.M. Breuer, A. Bernas, A.G. Tijhuis, P.A.J.M. Boon, Technical aspects of neurostimulation: focus on equipment, electric field modeling, and stimulation protocols, *Neuroscience and biobehavioral reviews*, 2016, 65:113-141
4. **D.C.W. Klooster**, R.M.H. Besseling, A.P. Aldenkamp, A. Opitz, M.D. Fox, C. Baeken, Modeling local effects of transcranial magnetic stimulation for functional connectivity analyses, *submitted*
5. **D.C.W. Klooster**, J.J. Vink, P. van Mierlo, P.A.J.M. Boon, D. Cooke, T. Gedankien, A. Roberts, P. Boucher, A. Pascual-Leone, M.D. Fox, M.M. Shafi, Propagation of TMS pulses versus functional brain connectivity, *in preparation*
6. **D.C.W. Klooster**, M.A.F. Ferguson, P.A.J.M. Boon, C. Baeken, The route towards personalized TMS protocols for depression treatment, *in preparation*

Co-authorships:

1. J.J. Vink, **D.C.W. Klooster**, M.B. Westover, A. Pascual-Leone, M.M. Shafi, EEG functional connectivity is a weak predictor of causal brain interactions, *in revision*

2. K. Caeyenberghs, R. Duprat, A. Leemans, H. Hosseidi, P.H. Wilson, **D.C.W. Klooster**, C. Baeken, Accelerated intermittent theta burst stimulation in major depression induces decreases in modularity: A connectome analysis, *Network Neuroscience*, 2019, 3(1):157-172
3. S. de Witte, **D.C.W. Klooster**, J. Dedoncker, R. Duprat, J. Remue, C. Baeken, Left prefrontal neuronavigated electrode localization in tDCS: 10-20 EEG system versus MRI-guided neuronavigation, *Psychiatry Research: Neuroimaging*, 2018, 30(274):1-6
4. L.E.M. Breuer, E. Grevers, P.A.J.M. Boon, A. Bernas, J.W.M. Bergmans, R.M.H. Besseling, **D.C.W. Klooster**, A.J.A. de Louw, R.M.C. Mestrom, K. Vonck, S. Zinger, A.P. Aldenkamp, Cognitive deterioration in adult epilepsy: Clinical characteristics of "Accelerated Cognitive Ageing", *Acta Neurologica Scandinavica*, 2017, 136(1):47-53
5. S. Carrette, P.A.J.M. Boon, C. Dekeyser, **D.C.W. Klooster**, E. Carrette, A. Meurs, R. Raedt, C. Baeken, C. Vanhove, A.P. Aldenkamp, K. Vonck, Repetitive transcranial magnetic stimulation for the treatment of refractory epilepsy, *Expert reviews of Neurotherapeutics*, 2016, 16(9):1093:1110
6. L.E.M. Breuer, P.A.J.M. Boon, J.W.M. Bergmans, W.H. Mess, R.M.H. Besseling, A.J.A. de Louw, A.G. Tijhuis, S. Zinger, A. Bernas, **D.C.W. Klooster**, A.P. Aldenkamp, Cognitive deterioration in adult epilepsy; does Accelerated Cognitive Ageing exist?, *Neuroscience and biobehavioral reviews*, 2016, 64:1-11
7. M.M. Shafi, M. Vernet, **D.C.W. Klooster**, C.J. Chu, K. Boric, M.E. Barnard, K. Romatoski, M.B. Westover, J.A. Christodoulou, J.D. Gabrieli, S. Whitfield-Gabrieli, A. Pascual-Leone, B.S. Chang, Physiological consequences of abnormal connectivity in a developmental epilepsy, *Annals of Neurology*, 2015, 77(3):487-503

Conference contributions

Organized symposia:

1. Symposium title: Multimodal neuroimaging informs mechanism of action for r-TMS in depression (speakers: M.D. Fox, A. Boes, C. Baeken, **D.C.W. Klooster** (organizer), chairs: M.D. Fox, C. Baeken), Third international brain stimulation conference 2019 (Vancouver)
 - Structural connectivity between dorsolateral prefrontal cortex and cingulate cortex predicts clinical response to accelerated iTBS in major depression, **D.C.W. Klooster**, I.N. Vos, K. Caeyenberghs, A. Leemans, S. David, R.M.H. Besseling, A.P. Aldenkamp, C. Baeken
2. Symposium title: The road towards personalized medicine: increasing the effects of brain stimulation using individual characteristics (speakers: **D.C.W. Klooster** (organizer), R. Duprat, R. de Raedt, S. de Witte, chairs: C. Baeken, M.A. Vanderhasselt), 3rd European conference on brain stimulation in psychiatry 2018 (Lyon)

- The potential of graph measures to predict the clinical effect of accelerated iTBS, **D.C.W. Klooster**, S.L. Franklin, R.M.H. Besseling, J.F.A. Janssen, R. Duprat, K. Caeyenberghs, A.P. Aldenkamp, P.A.J.M. Boon, A.J.A. de Louw, C. Baeken

Oral presentations:

1. Dynamic effects of tDCS on functional connectivity, **D.C.W. Klooster**, B. Kalkhoven, G.R. Wu, R.M.C. Mestrom, R. De Raedt, P.A.J.M. Boon, C. Baeken, BrainSTIM 2019 (Rome)
2. Can we use diffusion MRI to determine the optimal stimulation position in the left DLPFC to treat depression? **D.C.W. Klooster**, R.M.H. Besseling, K. Caeyenberghs, A. Leemans, A.P. Aldenkamp, C. Baeken, BrainSTIM 2017 (Vancouver)
3. Global changes in functional connectivity induced by local transcranial magnetic stimulation, **D.C.W. Klooster**, S.L. Franklin, R.M.H. Besseling, R. Duprat, A.P. Aldenkamp, A.J.A. de Louw, P.A.J.M. Boon, C. Baeken, Resting-state conference, Satellite symposium: tackling connectivity using non-invasive brain stimulation 2016 (Vienna).
4. Functional plasticity investigated by TMS in patients with major depressive disorder, **D.C.W. Klooster**, A.J.A. de Louw, S. Zinger, P.A.J.M. Boon, A.P. Aldenkamp, Functional neuroimaging in epilepsy and neuromodulation 2015 (Ghent)
5. Neurostimulation: how can we use the neuromodulatory effects in new areas for clinical use, **D.C.W. Klooster**, A.J.A. de Louw, S. Zinger, P.A.J.M. Boon, A.P. Aldenkamp, Meet the talents session update@Kempenhaghe 2015 (Heeze)
6. The added value of EMG recordings in patients with motor seizures, 2013, **D.C.W. Klooster**, B.U. Kleine, M. van Bussel, M. Lammers, M. Zwarts, in BME2013 (Egmond aan Zee)

Poster presentations (first authorships):

1. Propagation of TMS pulses versus functional brain connectivity, **D.C.W. Klooster**, J.J. Vink, P. van Mierlo, P.A.J.M. Boon, D. Cooke, T. Gedankien, A. Roberts, P. Boucher, A. Pascual-Leone, M.D. Fox, M.M. Shafi, Third international brain stimulation conference 2019 (Vancouver)
2. Influence of seed determination on functional connectivity analyses to study the effects of TMS, **D.C.W. Klooster**, R.M.H. Besseling, M.D. Fox, A.P. Aldenkamp, C. Baeken, 2nd European conference on brain stimulation in psychiatry 2017 (Munich)
3. The effect of accelerated cTBS on functional connectivity in epilepsy patients, **D.C.W. Klooster**, S. Carrette, R.M.H. Besseling, E. Carrette, R. Raedt, C. Baeken, W. Staljanssens, P. van Mierlo, A.J.A. de Louw, A.P. Aldenkamp, P.A.J.M. Boon, K. Vonck, Human Brain Mapping 2017 (Vancouver)

4. Accelerated intermittent theta burst stimulation, applied to the left DLPFC, influences dynamics in depression related networks, **D.C.W. Klooster**, R.M.H. Besseling, S.L. Franklin, A. Bernas, R. Duprat, A.P. Aldenkamp, C. Baeken, International Society of Magnetic Resonance in Medicine 2017 (Honolulu)
5. Graph analysis to explore the effect of transcranial magnetic stimulation on functional connectivity in patients with major depressive disorder. **D.C.W. Klooster**, S.L. Franklin, R.M.H. Besseling, R. Duprat, A.P. Aldenkamp, A.J.A. de Louw, P.A.J.M. Boon, C. Baeken, Resting state conference 2016 (Vienna)
6. Functional connectivity analysis derived from electric field simulations to investigate the effect of TMS, **D.C.W. Klooster**, S.L. Franklin, R.M.H. Besseling, R. Duprat, A.J.A. de Louw, A.P. Aldenkamp, P. Boon, C. Baeken, BrainSTIM 2016 (Geneva)
7. TMS induced functional plasticity investigated in patients with major depressive disorder, 2015, **D.C.W. Klooster**, S.L. Franklin, R.M.H. Besseling, A.J.A. de Louw, A.P. Aldenkamp, P.A.J.M. Boon, A.G. Tijhuis, S. de Haan, C. Baeken, 1st European conference on brain stimulation in psychiatry 2018 (Ghent)
8. Brain stimulation: what is actually happening? **D.C.W. Klooster**, A.J.A. de Louw, S. Zinger, A.P. Aldenkamp, in BME2015 (Egmond aan Zee)
9. The value of simultaneous TMS-EEG recordings for diagnostic purposes in epilepsy patients, **D.C.W. Klooster**, B.U. Kleine, J.P. van Dijk, M. Munneke, D. Stegeman, M. Zwarts, International Conference On Noninvasive Brain Stimulation (Leipzig)
10. Epileptic versus non-epileptic networks underlying generalized epileptic discharges, **D.C.W. Klooster**, P.J. van Houdt, N.A.W. van Riel, P.A.J. Hilbers, P.P.W. Ossenblok, in Science Fair TU/e - Kempenhaeghe 2011 (Eindhoven)
11. Beyond spikes and seizures: detection of interictal EEG asymmetries in focal epilepsy, **D.C.W. Klooster**, S. Vogrin, D.B. Grayden, M.J. Cook, in 29th international epilepsy congress 2011 (Rome)

"Courage is the first virtue that makes all other virtues possible."

Aristotle

Acknowledgements

De eindstreep van het dit promotie-traject is bereikt. Ondanks dat het doen van onderzoek nog steeds vaak gezien wordt als een eenzame bezigheid zijn er ontelbaar veel mensen betrokken geweest bij de verschillende projecten die ik de afgelopen jaren heb uitgevoerd. Een bedankje voor hen is zeker op zijn plaats.

Beste Bert, wat ben ik blij dat ik besloot om naar jouw inauguratie-speech op de TU/e te gaan, inmiddels alweer bijna 6 jaar geleden. Hier leerde ik dat wij een gezamenlijke interesse in neurostimulatie hebben. Na een kennismakingsgesprek was het dan ook snel duidelijk dat ik bij jou wilde gaan promoveren. Jij hebt altijd gezorgd dat de focus van mijn onderzoek op de klinische toepasbaarheid ligt en hebt vele knopen doorgehakt als ik soms weer even twijfelde. Naast onze inhoudelijke discussies heb ik van jou ook veel geleerd over het reilen en zeilen in de wetenschap. Bedankt voor een heel fijne samenwerking.

Beste Paul, na vier jaar ben ik nog altijd onder de indruk van het neurostimulatie-imperium in het UZ Gent. Heel erg bedankt dat ik daar onderdeel van uit mocht (en nog steeds mag) maken. Dankjewel dat je altijd naar mijn nieuwe ideeën wilde luisteren, hoe wild ze ook waren, en dat je me daarin altijd gestimuleerd en (bij)gestuurd hebt. Jouw gedrevenheid, inspirerende presentaties, productieve discussies, en duidelijke feedback zijn voor mij een extra stimulans om een goede wetenschapper te worden.

Beste Chris, het was oorspronkelijk niet gepland maar achteraf helemaal niet onlogisch dat een groot deel van dit onderzoek zich op de afdeling psychiatrie heeft afgespeeld. Het duurde even voordat we elkaar leerden kennen maar inmiddels hebben we helemaal onze eigen wetenschapsbubbel gecreëerd en hebben we aan een half woord genoeg. Bedankt (en sorry...) dat ik echt 24/7 bij jou terecht kan. Ik heb ontzettend veel geleerd binnen de afdeling psychiatrie en genoten van onze discussies (die vaak resulteerden in heuse Picasso-waardige breinschetsen), het maken van (over-ambitieuze?) plannen, en onze gezamenlijke congres bezoeken. Dat er in de toekomst nog maar veel mogen volgen...

Beste Anton, bedankt voor alle klinische lessen die je me hebt geleerd. We hebben, vooral aan het begin, heel wat tijd besteed aan het bladeren door dikke neurologie-boeken om

uit te zoeken hoe stimulatie zou kunnen werken. Deze kennis (of eigenlijk het gebrek daaraan) heeft in grote mate bijgedragen aan onze review en aan de richting die we vervolgens ingeslagen zijn voor dit promotie-traject. Dankjewel daarvoor.

Beste Rene, het was erg fijn om iemand met dezelfde biomedische achtergrond als ik als dagelijkse begeleider te hebben. Doordat jij al veel meer ervaring had op het gebied van medische beeld- en signaalverwerking kon ik altijd bij jou terecht met algemene, maar ook zeer gedetailleerde, vragen. Jij was altijd kritisch en wist precies welk deel van de analyse nog wat verbeterd zou kunnen worden, en had daar ook vaak al meerdere voorstellen voor. Ik vind het heel jammer dat je besloten hebt om je carrière buiten de academische wereld voort te zetten.

Sofie, onze promotietrajecten waren opgezet als twin-studie en het was dan ook zeer leuk om in het begin nauw samen te werken. Jammer dat onze studie niet helemaal via plan is verlopen en dat we ieder onze eigen weg zijn gegaan. Ik mis de wandelende TMS-encyclopedie wel! Daarnaast wil ik ook de overige leden van de dienst neurologie bedanken. Met name Prof. Vonck voor de fijne begeleiding tijdens onze TMS-EEG studie en de waardevolle feedback op onze artikelen en presentaties. Pieter, dankjewel dat je mij een heel stuk wijzer hebt gemaakt over EEG analyses en bronlokalisaties.

Ik wil ook iedereen van het Ghep-lab bedanken. Marie-Anne, jij bent naast Chris de drijvende kracht van het Ghep-lab. Bedankt voor al je opbouwende feedback op mijn presentaties. Dankzij jou zit er zeker meer structuur in! Bedankt ook dat je mij al betrokken hebt in de begeleiding van jouw doctoraat studenten. Ik kijk uit naar een concretere wetenschappelijke samenwerking. Josefen en Sara (@aka kartoffeln sinds München, al zou pizza een geschiktere naam zijn), jullie zijn zeker mijn beste maatjes in het lab. Wij hebben altijd veel lol om wetenschappelijke maar ook niet wetenschappelijke zaken. Heel erg fijn dat jullie mij willen bijstaan als paranimfen. Ik kijk uit naar jullie promoties en zal mijn best doen om jullie daar ook mee te helpen. Daarnaast wil ik ook overige Ghep leden: Gert, Hannelore, Jens, Lars, Linde, Louise, Mattias, de Nele's (vdV en dS), Tasha, Robrecht, Rudi (technisch gezien geen Ghep lid maar toch zeer nauw verbonden met de meeste van onze onderzoeken), Sam, en Stefanie. bedanken voor alle feedback, team-etentjes, en voor de gezellige conferentie bezoeken! Also a big thanks to former Ghep-member Romain. Thank you so much for learning me basically everything about the practicalities of TMS. I am so happy that you found a great postdoc position in Philadelphia but I still hope you will return to Ghent one day. I miss you!

Ook wil ik graag Prof. Rik Achten en overige collega's van GIfMI bedanken. In theorie is scannen niet echt moeilijk, maar in de praktijk blijken er vaak kleine problemen te zijn. Pieter, heel erg bedankt dat je altijd beschikbaar was om ons uit te brand te helpen. Het was ook altijd gezellig als je even bleef hangen nadat de problemen opgelost waren zodat we nog even slap konden ouwehoeren over Budel- en Maldegem-city. Daarnaast ben ik erg blij met wat extra invloeden vanuit de TU/e in het UZ Gent: Pim, bedankt voor al je hulp bij het implementeren van nieuwe scansequenties. Ook dank aan Ben Jeurissen voor de implementatie van het multi-shell diffusie MRI protocol (en de update) op de GIfMI scanner.

Gelukkig was ik de eerste maar niet de enige promovendus binnen het NeuroPlatform. Graag wil ik mijn collega's Stephan, Antoine, Lianne B, Lianne C, Gerald, Maarten, Elles, Edo, en Rolf bedanken voor een heel gezellig tijd. Stephan and Antoine, my former roomies, thanks for the MRI-discussions and fun times when we were (occasionally) all three in the office at the same time. Maarten and Elles, mijn mede TMS-onderzoekers al dan niet vanuit een totaal andere invalshoek, hebben mij zeker andere technische kanten van neurostimulatie laten zien en mijn inzicht vergroot. Daarnaast wil ik ook de senior onderzoekers binnen het NeuroPlatform, Sveta, Rob, en Jaap, bedanken voor hun interesse en waardevolle feedback.

Tijdens mijn promotie had ik ook het genoegen om een aantal master studenten te begeleiden. Suzanne en Iris, heel erg bedankt voor jullie interesse en nauwkeurige uitvoering van onze projecten. Jullie mogen zeker trots zijn op de bijdragen die jullie geleverd hebben aan dit proefschrift.

Ondanks dat ik inmiddels een andere werkplek heb op de TU/e, wil ik ook graag mijn oude VCA collega's bedanken, met Prof. Peter de With als hoofd. Bedankt voor een heel fijne werkomgeving, gezellige lunches en koffie pauzes, quiz-nights, en FIFA competities. Peter, ik vind het extra leuk dat jij mijn verdediging gaat voorzitten. Fons, als iemand het helemaal gaat maken in de wetenschap dan ben jij het! Jij bent naast een goede vriend ook een voorbeeld voor mij. Sander, ik heb ervan genoten om de laatste periode van mijn PhD jouw buurvrouw te zijn in de EM-kamer. Ondanks dat onze onderwerpen totaal verschillen, hebben we veel kunnen delen tijdens de afronding van onze proefschriften en hebben we ontzettend veel gelachen.

Daarnaast ben ik zeker dank verschuldigd aan de office managers: Anja, Marieke, Sunita, en Naomi. Bedankt dat jullie altijd het geduld hebben gehad om de vrijwel onmogelijke afspraken met het hele team toch in iedereen zijn/haar agenda te kunnen passen. En natuurlijk bedankt dat jullie altijd tijd hadden om even gezellig bij te kletsen.

Dank aan de Raad van Bestuur van Kempenhaeghe: Dr. Marlène Chatrou en Drs. Nico Geurts, en de afdeling TriO. Ook wil ik hierbij mijn vroegere mede 'Boondert-bewoners': Dominique, Reina, Geke, Petra, Evelien, en Zita bedanken. Als benjamin van de club heb ik nu ook mijn promotie afgerond. Reina en Doom, ik vind het heel gezellig dat wij nog regelmatig contact hebben.

Dear Mike, dear Mo, thank you so much for the opportunity to return to the BA CNBS during my PhD. It is amazing how much knowledge on brain stimulation is concentrated in the lab. I am amazed by all your brilliant ideas and really appreciate the time that you took (and now still take via Skype) to help me finalizing our projects. I would also very much like to thank all my colleagues from BA CNBS, in alphabetic order: Ali, Anne, Dan, Dani, Davide, Emiliano, Ehsan, Javier, Joyce, Juho, Katy, Mark, Michael, Pete, Ruth, Tamara, and Tim. Davide, thanks for becoming a good friend. We should actually plan our Budel/Sienna vacations! Michael, I am so happy I met you during our exactly one-week-overlap in the center! It is great to have someone with whom you can basically discuss everything. I am looking forward to our shared publication. Thank you all so much for the scientific collaboration but also for the beers in the Yard House, American

bbq's, and fun times exploring Boston. I really had an amazing time and I miss each of you. @aka WorkHarder.

Beste Jord, wat een geluk dat Mo twee Dutchies aan zijn opeenvolgende projecten liet werken! Ik ben blij dat ik jou heb leren kennen en dat we inmiddels een goed team zijn.

Geachte leden van mijn promotie-commissie, prof. Van Ee, prof. Breeuwer, dr. Arns, en dr. Carrette, vriendelijk bedankt voor het lezen en beoordelen van mijn thesis. Evelien, jij bent echt van alle markten thuis en hebt me al met ontelbaar veel dingen geholpen. Van brainstorm-sessies over toekomstige onderzoeksplannen tot het organiseren van een symposium met alles erop en eraan als ik een externe gast mee naar Gent bracht, jij wist overal raad mee. Heel erg bedankt!

Also a big thanks to all my co-authors for their great contributions to our work. Your feedback and ideas were of great value. I could not have done the analysis of the diffusion MRI data without help from Karen, Szabolcs, and Alexander Leemans. Also special thanks to Alex Opitz for the help on the electric field modeling. Furthermore, I am also very grateful to meet fellow researchers from all over the world at conferences. Martin, it is really impossible to visit a brain stimulation related conference without running into you. Thank you for a nice friendship that we developed along the road. Now that we have both finished our theses, I hope we can work on our future collaboration plans together with our c(h)risises team (=Christian + Chris). I would also like to thank researchers that I greatly admire and who have inspired me in conference talks. Big thanks to Jonathan Downar, Axel Thielscher, Hartwig Siebner, Andy Horn, and Aaron Boes.

Ik heb nog nooit een paard in een dankwoord zien staan maar degene die mij een beetje kennen zullen toch niet verbaasd zijn dat ik mijn (voormalige) lieve Zensation hier ook even noem. Veel mensen zullen het niet begrijpen maar paardrijden, of iets leuks doen met je paard, is toch de ultieme vorm van ontspanning (oke, meestal dan toch...). Astrid, dankzij jou kon ik altijd naar het buitenland zonder me ook maar een seconde druk te hoeven maken om Zensi. Ik heb hierdoor de kans gehad om me verder te ontwikkelen als onderzoeker en je hebt daarmee zeker meer bijgedragen aan dit proefschrift dan je zelf waarschijnlijk erg in hebt. Daarnaast wil ik ook nog Pierre en alle stalmeiden van Stoe-terij de Berghoeve (Donna, Elky, Chaline, Mariska, Jaco, en Tamara) bedanken voor de gezellig tijd. Ook wil ik Marleen, Anne, en Marianne bedanken. Ondanks dat we inmiddels geen paard meer hebben ben ik blij dat we nog steeds geregeld afspreken. Inmiddels is Zensi op zijn plek bij zijn nieuwe eigenaresse en ben ik de bijrijder van Dana (Banana). Sanne, bedankt voor het vertrouwen! En meiden van de Hemelrasten, bedankt voor de gezelligheid op stal.

Sommige vriendschappen zijn gelukkig zo hecht dat ze ook lange afstanden en drukke werkschema's doorstaan. Astrid en Tim, gelukkig is het ons gelukt om na de middelbare school contact te blijven houden. Ondanks dat we elkaar weinig zien zijn jullie er op belangrijke momenten altijd voor mij. Ondanks dat Astrid en ik nu een tikkeltje burgerlijk zijn geworden met onze gezinnen, moeten we toch maar eens proberen om Tim zijn nieuwe huis in Hamburg te gaan bekijken.

Het is niet heel verwonderlijk dat Nederlandse studenten elkaar gemakkelijk vinden in het buitenland, maar wel dat er echt een oprechte vriendschap ontstaat en blijft bestaan na terugkeer in Nederland. Fari en Roel, in Melbourne hadden we altijd al de grootste lol en beleefden we de tofste avonturen. Ik ben blij dat we nog geregeld afspreken om te lunchen, shoppen, wandelen, of wat dan ook. Met jullie is er niet veel nodig om een super leuke dag te hebben.

Naast vrienden heb ik gelukkig een heel lieve (schoon)familie die daadwerkelijk altijd voor mij klaar staat voor een heleboel gezelligheid en ontspanning. Bedankt iedereen voor de steun en interesse. Een speciale vermelding ook voor mijn aller grootste fans: mijn lieve opa's. Jammer dat opa Dorplein het bereiken van deze mijlpaal niet meer mee kan maken.

Lieve pap en mam, bedankt dat jullie er altijd voor mij zijn en voor het eeuwige vertrouwen in mijn slagen. Gelukkig wonen we vlak bij elkaar zodat ik geregeld langs kan komen om even te ontspannen en 100% mezelf te zijn. Jullie leven altijd met mij mee, brengen me overal naartoe en halen me (met nog meer plezier) weer op. Zelfs toen ik voor langere tijd op reis ging kwamen jullie mij gewoon achterna. Dit heeft al voor een heleboel onvergetelijke herinneringen gezorgd. Bedankt voor alle gezamenlijke zondagmiddag-lunches met Olaf en Nadja, ontelbare boswandelingen met Belle, en een onmeetbare hoeveelheid liefde. Jullie zijn de beste!

De laatste woorden van dit dankwoord zijn voor mijn mannen. Lieve Rob, het valt vast niet altijd mee om mijn man te zijn. Gelukkig vinden we naast het werk altijd genoeg tijd voor elkaar en anders combineren we werk en privé gewoon. Jouw rust weet mij altijd te temperen en jij houdt mij altijd met twee benen op de grond. Wie had ooit gedacht dat onze kleine Max nog zoveel liefde en warmte zou kunnen toevoegen aan ons gezinnetje? Jullie maken mij heel gelukkig en met jullie kan ik alles aan. Dikke kus!

Curriculum Vitae

Debby Klooster was born on March 14 1988 in Geldrop, The Netherlands. She obtained a Biomedical Engineering bachelor at the Eindhoven University of Technology. During the master Medical Engineering at the same university she went to Melbourne (Australia) for a three month internship at St. Vincent's Hospital and Melbourne University supervised by Mark Cook and David Grayden. The project focused on the relation between EEG-asymmetries and epileptic seizures. Furthermore, she worked on optimizing the imaging pipeline during neurosurgical procedures in the Elisabeth Ziekenhuis in Tilburg, under supervision of Geert-Jan Rutten. Debby completed her master thesis in the group of Peter Hilbers, in close collaboration with epilepsy center Kempenhaeghe. During the graduation project she investigated the added value of independent component analysis to identify epileptic networks.

After graduation in 2012, Debby enrolled in the two year PDEng program Qualified Medical Engineering, again in collaboration with Kempenhaeghe. In 2013 she went to Boston for three months to perform a project in the Berenson-Allen Center for Noninvasive Brain Stimulation, supervised by Alvaro Pascual-Leone and Mouhsin Shafi. Here, she learnt about simultaneous TMS-EEG analyses in a project focused on epilepsy patients with periventricular nodular heterotopia.

In 2014, Debby started as a PhD candidate within the Neu³CA program (current NeuroPlatform) at the department of Electrical Engineering at the Eindhoven University of Technology in close collaboration with the University Hospital in Ghent (Belgium) and Kempenhaeghe. Together with the supervising team (Paul Boon, Chris Baeken, Bert Aldenkamp, René Besseling, Anton de Louw) she focused on the potential of imaging techniques to improve the clinical response to TMS. During this period she returned to Boston for two months to continue collaboration with Mouhsin Shafi and Michael Fox and to extend her knowledge about brain stimulation techniques further. Moreover, she has been actively involved in organizing symposia at international conferences and has given several international scientific talks. The results of the work during her PhD are described in this thesis.

